DEVELOPMENT, CHARACTERIZATION, PROCESSING AND TESTING OF QUANTUM DOTS FOR IMAGING IN VISIBLE AND NEAR INFRARED RANGE

Thesis submitted in fulfillment of the requirements for the Degree of

DOCTOR OF PHILOSOPHY

By

ASHA KUMARI
[Enrollment No. 146955]

Department of Physics and Materials Science

JAYPEE UNIVERSITY OF INFORMATION TECHNOLOGY

WAKNAGHAT, DISTRICT SOLAN, H.P., INDIA

Month August, Year 2018

JAYPEE UNIVERSITY OF INFORMATION TECHNOLOGY

DECLARATION BY THE SCHOLAR

I hereby declare that the work contained in the Ph.D thesis entitled **"Development, characterization, processing and testing of quantum dots for imaging in visible and near infrared range"**, submitted at **Jaypee University of Information Technology at Waknaghat, India** is an authentic record of my work carried out under the supervision of **Dr. Ragini Raj Singh**. I have not submitted this work elsewhere for any other degree or diploma. I am fully responsible for the content of my Ph.D. thesis.

Asha Kumari

Enrollment No.: 146955

Department of Physics and Materials Science,

Jaypee University of Information Technology,

Waknaghat, Solan, HP-173234

Date: 27- 08-2018

ABSTRACT

Quantum dots are fluorescent materials. These are of very interest because of their unique optical properties. Light emitting behavior of these QDs can be tuned because of quantum confinement effect. Fluorescent behavior of QDs make them useful in biological fields like cell, tissue imaging. This thesis includes synthesis, characterization, processing and testing of QDs for imaging in visible and NIR range. We have synthesized visible CdSe, ZnS, CdSe/ZnS and NIR CdTe QDs. After this we have processed surface of these prepared QDs by different polymeric materials and silicates. These prepared materials were tested for their toxic effects toward human kidney cell line (HEK-293).

1st chapter

This chapter introduces about visible, NIR QDs and core shell structures and also includes steps which should be addressed before applying these QDs for bio-applications such as different methods of processing of QDs.

2nd chapter

This chapter provides detailed information about synthesis methodology for QDs and their encapsulated structures and characterization.

3rd chapter

Chapter 3 includes the results obtained for CdSe stabilized by 2-Mercaptoethanol (2-M.E.) and their polymer encapsulated structures.

4th chapter

Chapter involves XRD, TEM, EDX, PL and FTIR results obtained for ZnS1 and ZnS2 and CdSe/ZnS1 and CdSe/ZnS2 structures.

5th chapter

Chapter 5 contains results acquired for CdTe (NIR QDs) stabilized by 3-Mercaptopropionic acid (3-MPA) and their polymer encapsulated structures.

6th chapter

This chapter involves results of toxic effect of CdSe QDs and CdTe QDs and antimicrobial behavior of CdSe and CdTe based nanostructures.

7th chapter

Finally chapter 7 described the overall conclusion of thesis.

SUPERVISOR'S CERTIFICATE

This is to certify that the work reported in the Ph.D. thesis entitled **"Development, characterization, processing and testing of quantum dots for imaging in visible and near infrared range",** submitted by **Asha Kumari** at **Jaypee University of Information Technology at Waknaghat, India,** is a bonafide record of her original work carried out under my supervision. This work has not been submitted elsewhere for any other degree or diploma.

Dr. Ragini Raj Singh
Supervisor
Assistant Professor (senior grade)
Department of Physics and Materials Science
Jaypee University of Information Technology
Waknaghat, Solan, H.P. India-173234
Email: raginirajsingh@gmail.com
Date: 27.08.2018

ACKNOWLEDGEMENTS

CONTENTS

LIST OF TABLES

LIST OF FIGURES

LIST OF SYMBOLS & ABBREVIATIONS

Symbol	Abbreviations
α	Alpha
β	Beta
λ	Lambda
ml	Milliliter
g	Gram
h	Hours
°C	Degree Celsius
µg	Microgram
%	Percent
nm	Nano-meter
QDs	Quantum dots
PEG	Polyethylene glycol
PVA	Poly vinyl alcohal
TEOS	Tetraethyleneorthosilicate
PL	Photoluminescence
PLE	Photoluminescence excitation
TEM	Transmission electron microscopy
XRD	X-ray diffraction
EDX	Energy dispersive X-ray Spectroscopy
UV-vis	Ultraviolet-Visible
FT-IR	Fourier transform infrared spectroscopy

CHAPTER-1

INTRODUCTION TO FLUORESCENT BIOCOMPATIBLE VISIBLE AND NIR QUANTUM DOTS
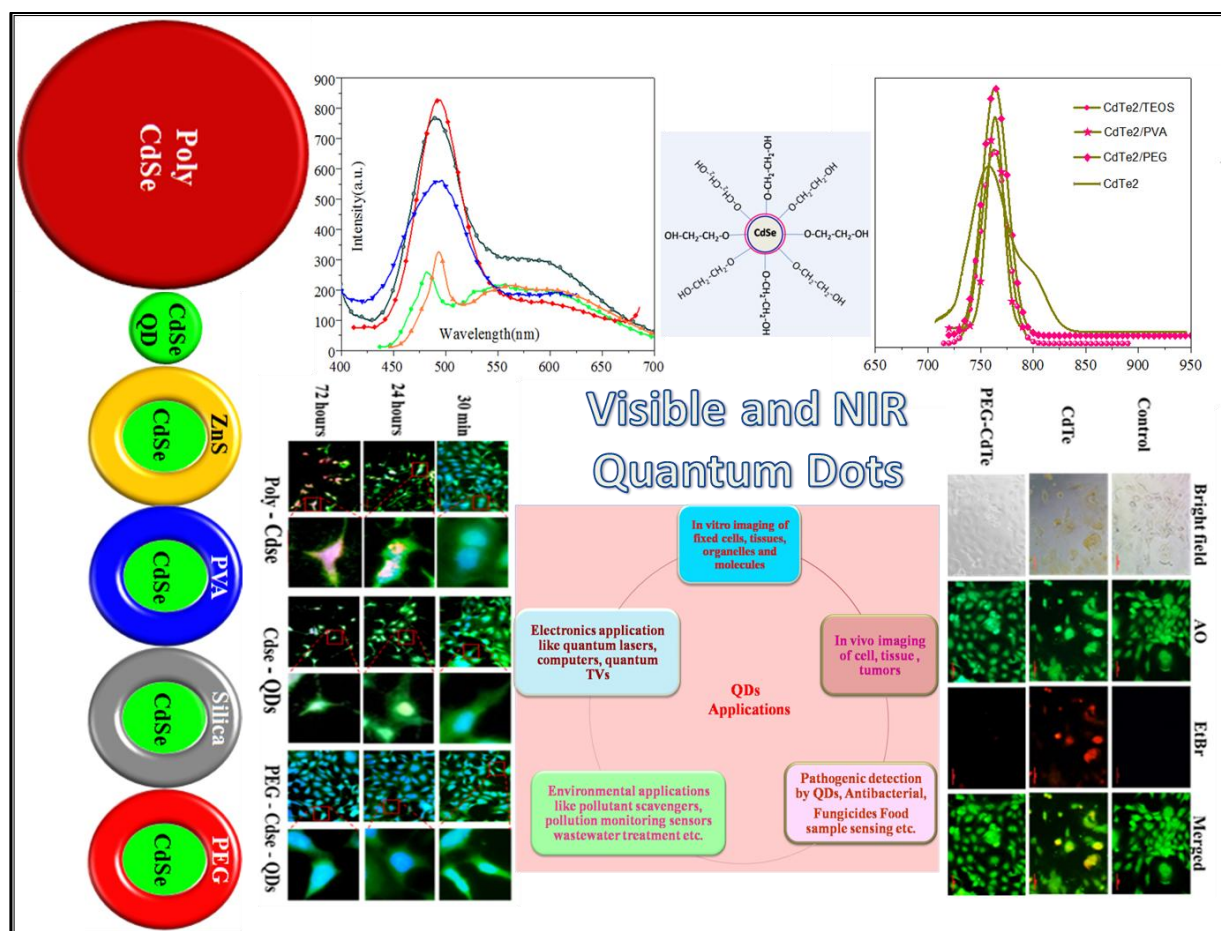
1.1 Introduction

Decisive quality of quantum dots (QDs) such as size, optoelectronic and chemical properties as compared to bulk semiconductor material result in wide spectrum of applications in biological systems especially when compared with organic dyes. In addition to this QDs should be water soluble and should have less toxicity to use them for biological applications. For this purpose we aimed to synthesize hydrophilic visible and near infra red (NIR) QDs using wet chemical aqueous route. After synthesis, studies of structural, elemental and optical properties of QDs give real insights. Based on results specifically optical chattels of these QDs, they can be used as prepared or may need surface modification to overcome expected drawbacks if found such as poor optical properties and toxicity towards biological cells. Therefore, this thesis work devoted to improve optical properties along with stability and to eliminate toxic effects via certain modification processes such as encapsulation with bio friendly agents. However, before all of these studies the basic introduction to QDs, basic science behind QDs, types of QDs, synthesis methods for QDs, applications of QDs, introduction to the problem and aims and objective of the thesis are being presented in this chapter.

1.1.1 Quantum dots: small wonders

QDs are a kind of nanocrystals attracting a great deal of attention due to their confinement based characteristics. In quantum dots electrons and holes are confined three dimensionally with in Bohr exciton radius. The size of QDs is on nanometer scale and as of this tiny size of QDs they comprise discrete electronic energy which results in special optical properties [1]. Key characteristics of QDs such as size, optoelectronic properties as compared to bulk semiconductor material result in wide application in biological system especially when compared with organic dyes. These QDs have advantages over traditional organic dyes because of high quantum yield , narrow and tunable emission spectra, and photostability [2]. Due to all these properties QDs are considered as potential candidates for labeling, tracking and as luminescent probe in biology [3, 4]. These QDs have narrow excitation and tunable emission spectra in wide range of wavelengths, along with narrow Full width at half maximum value (FWHM) [5, 6]. By changing elemental composition of QDs they can emit from the ultraviolet to the NIR region in a quite easy mode. QDs have high fluorescence quantum yields. CdSe QDs have fluorescence intensity

about 20 times than that of rhodamine molecule. The intensity is about 100–10,000 times as compare to standard organic dyes [7, 8]. On the basis of these features QDs tender new prospect in the analysis field. This integrated property of nanomaterials with molecular biology results in development of new research area of nanobiotechnology. Different applications of QDs in biology are the major forerunner of nanotechnology [9].

Generally two major approaches could be used to synthesize QDs. One approach is organometallic route and the one is aqueous route [10-12]. Quantum dots synthesized by organometallic route are hydrophobic in nature and cannot be used directly for biological applications. Thus to use these QDs for biological application they require post treatment with some hydrophilic ligands [13]. This method of post treatment is time consuming, difficult and QDs obtained by this method are often allied with several drawbacks like low quantum emission efficiency and limited stability. However, the aqueous synthesis route for QDs is simpler, cost effective and environment friendly. In earlier reports major drawback related to QDs synthesized by aqueous method was their low luminescence intensity and poor properties. But this limitation of these QDs could be improved by using different strategies like encapsulation by different polymers and silanes [14]. On the basis of optical properties usable in different state of affairs, we are going to discuss about visible and NIR QDs in this section.

1.1.2 Visible quantum dots

Bulk level of material has even physical properties inconsiderate of the size of material. But at nanoscale theory is totally different. Properties of nanomaterials like optical properties changes as size come close to nanoscale. QDs show emission from visible to NIR range. Visible QDs show emission under excitation which is visible to human eyes. This emission wavelength of QDs is not only reliant upon material but also upon size of QDs. Smaller size QDs emit close to blue end while larger size QDs emit close to red end. QDs having emission in the visible region have deprived tendency to transmit visible light through deep tissue in living animal.

Visible II-VI group QDs like CdSe and CdSe/ZnS QDs have been deemed in multipurpose photonic applications like optical fiber amplifiers, solar cells, LED because of their brilliant and exceptional emission profiles. These visible QDs have also been utilized as optical temperature probes as well as in the fields of medicine and biology [15]. In deep tissue imaging

scattering and light absorption tendency of tissues like hemoglobin, proteins, and water reduces the fluorescence signal. This hampers use of visible QDs in biological field [16]. But NIR emitting QDs provides a clear window for animal tissues. Upcoming section provides detailed advantages of NIR QDs.

1.1.3 Near infrared (NIR) quantum dots

Fluorescence is one of the most commanding and flexible tool for biological research. QDs are of great interest in biomedical research for their many extreme features as compared to conventional fluorophores. NIR light having wavelength longer than 650 nm and really escalate the ability of fluorescence in biomedical applications [17, 18]. Organic dyes emitting in NIR found on Alexa, Cyanine fluorophore sequence are available for mark tissues, cells systems *in-vivo* [19]. These fluorescent dyes have some drawbacks such as low quantum yield, rapid photodegradation, broad emission and narrow excitation etc. These drawbacks bound their application in biological field. In comparison to these NIR organic dyes, fluorescent QDs as innovative optical probes have fascinated wide interest in biology and chemistry area. Owing to quantum confinement, these QDs boast numerous divergent optoelectronic characteristics as compared to standard conventional flourophores like high photostability of QDs, and long lifetime excited-state [20, 21].

NIR QDs have more important role in deep tissue detection in contrast to visible QDs Even though NIR QDs have low quantum yield (QY) than visible QDs. But these NIR QDs after surface modification become more fluorescent than other fluorophores like dyes with emission in NIR [22]. These NIR emitting QDs can be utilized for *in-vivo* applications because this is the range of spectrum for negligible absorption of blood and tissue, however still measurable by instrument. Thus NIR QDs emit at 700-1000 nm avoid or minimize problem of endogenous fluorescence of tissue. Here these are few advantages of NIR emitting QDs [23].

1. These NIR emitting QDs are able to absorb visible and near-infrared photons. This feature of QDs helps in improvement of solar cells efficiency.

2. Emission of these QDs can be tuned completely for the telecommunications wavelength.

3. These NIR QDs provide emission in biological diagnostic window (700 to 1100) where scattering of light by tissues is negligible as compared with UV-visible emitting QDs. Thus due to less absorption and minimal autofluorescence these QDs can be utilized for bio-imaging. Figure 1.1 illustrates QDs showing size dependent narrow excitation and broad emission.
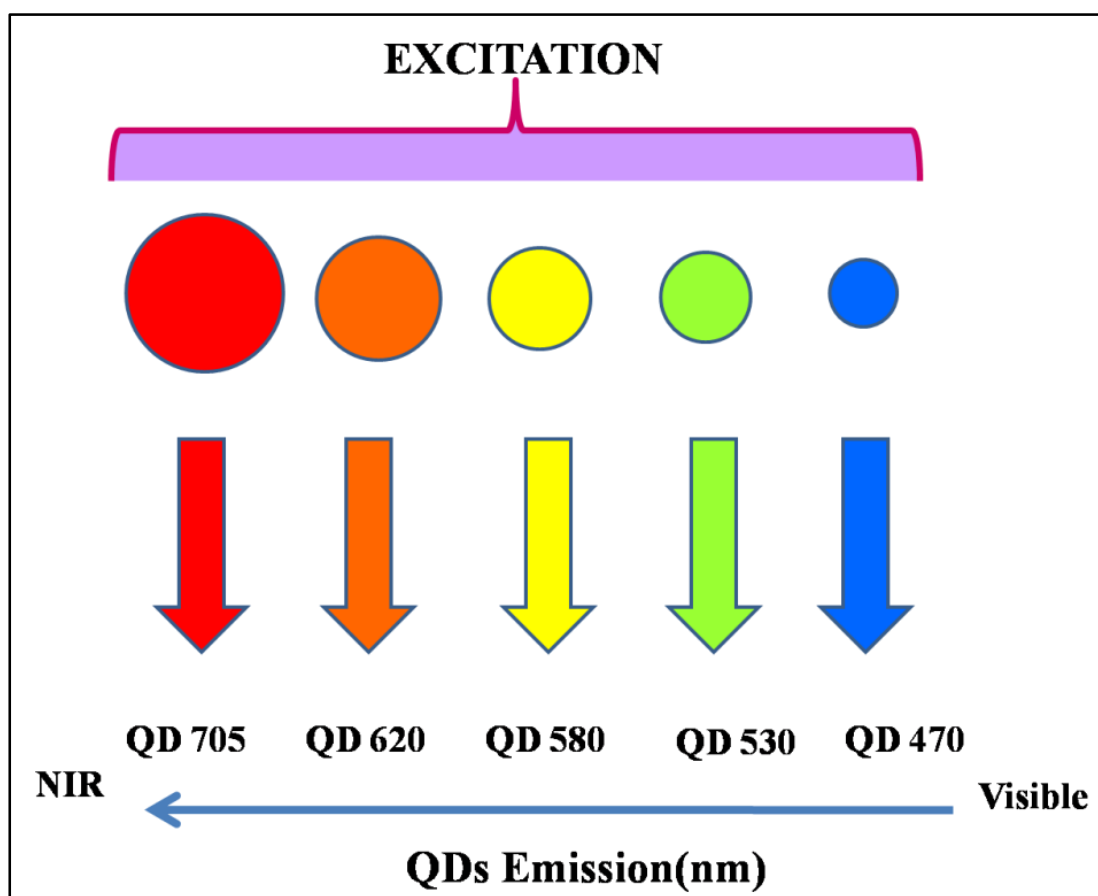
Figure 1.1: Size dependent narrow excitation and broad emission in QDs

1.1.4 Core-shell structures

Core-shell is a biphasic material which is prepared of an inner core and an outer shell component. These particles show inimitable properties arising from the amalgamation of core and shell material. These core-shells are designed in the mode so that the shell material can meliorate the reactivity, thermal stability, or oxidative stability of the core material.

Core-shell structures mostly being synthesized by solution methods. This solution method entails two steps. First step is synthesis of core structure and second step is shell formation. Gas-phase techniques of synthesis subsist and this generally involves chemical vapor deposition (CVD) or pulsed laser deposition (PLD) [24]. Nevertheless, these methods also engross multiple steps. In this method shell material is deposited on previously produced core structure, and this also use substrates [25-27]. Mechanisms of development have been examined for these techniques [28].

QDs have lots of ligand and atoms present on their surface owing to their very eminent surface to volume ratio. These kinds of surface states possibly affect structural and optical behavior of QDs. In literature there are several studies on effect of surface states on optical properties specifically. Optical properties of QDs could be improved by modification of surface of QDs. Surface defects like dangling bonds are the surface related trap states and these cause nonradiative recombination and finally result in new emission band. The outstanding potential behind the formation of core-shell structure was to improve the surface properties of QDs. This surface modification of QDs leads to enhancement in excitonic emission because this leads to blocking of nonradiative e-h pair recombination at traps. These surface modifications also improve the photostability of QDs.

The type of property we require after shell formation totally depend upon the kind of material we selected for shell formation. Here we are discussing two categories of core-shell structures based on alignment of valence band with conduction band [29]. In type-I core-shell structure a given semiconductor material is coated with another kind of semiconductor material and band gap of this coated materials is larger than core material. In type-1 both charge carrier electron-hole pair are confined to core. By formation of type-I core-shell structure we can improve the fluorescence efficiency and prevent the core material by degradation. In type-II core-shell structure electrons and holes are located in core material and shell material respectively. Figure 1.2 represents schematic representation of type-I and type-II core-shell structures.
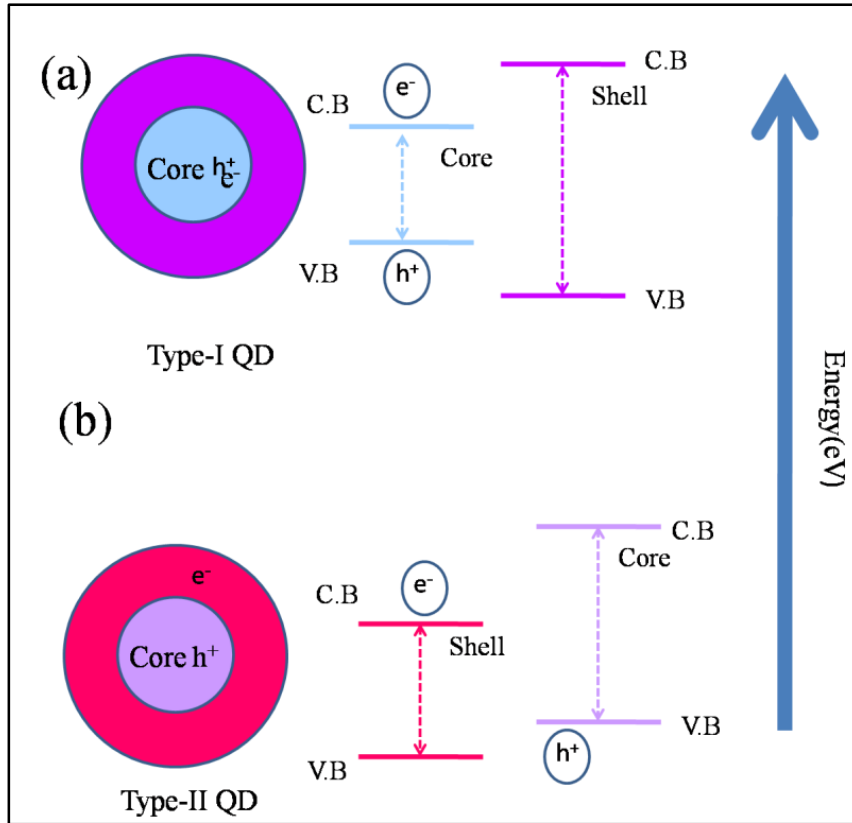
Figure 1.2: Schematic illustration of (a) type-I and (b) type II core-shell structures

1.2 Basics of quantum dots

1.2.1 The exciton

An exciton is bound position in which an electron and a hole are bound together by electrostatic forces. An exciton is formed when a photon incident on a semiconductor, electron get excited and reach the conduction band, this leaves behind a hole in the valence band (Figure 1.3). Electron and hole form a bound state having some less energy than the unbound electron and hole. This bound state is called an "exciton". Effective exciton Bohr radius a_B is the distance between electron and hole pair. If the size of semiconductor QDs is smaller than its Bohr exciton radius evidently confinement effect gets started. Ultimately this confinement effect results in size reliant optical properties of QDs. Electronic parameters of quantum dots used in this thesis have been given in table 1.1.

Table 1.1: Electronic parameters of quantum dots

Material Name	Band gap [E_g (eV)]	Bohr exciton radius (nm)
CdSe	1.74	5.4
CdTe	1.54	6.8
ZnS	3.54	2.8
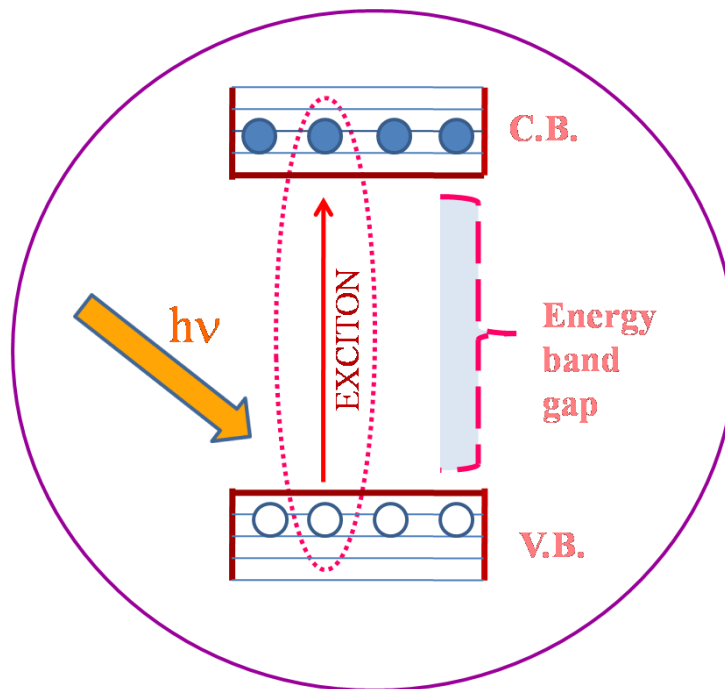
Figure 1.3: Formation of exciton (bound hole-electron pair)

1.2.2 Quantum confinement effect

Quantum confinement is the most admired effect in the nanotechnology. This occurs because of alteration in the atomic structure which directly influences the energy band structure. As the particle sizes of semiconductor is near to or lower than the bulk semiconductor Bohr exciton radius at that time quantization effects become significant. This confinement effect makes material properties size dependent. Figure 1.4 presents schematic representation of quantum confinement and electronic energy states in bulk semiconductors, quantum dots, and molecules.
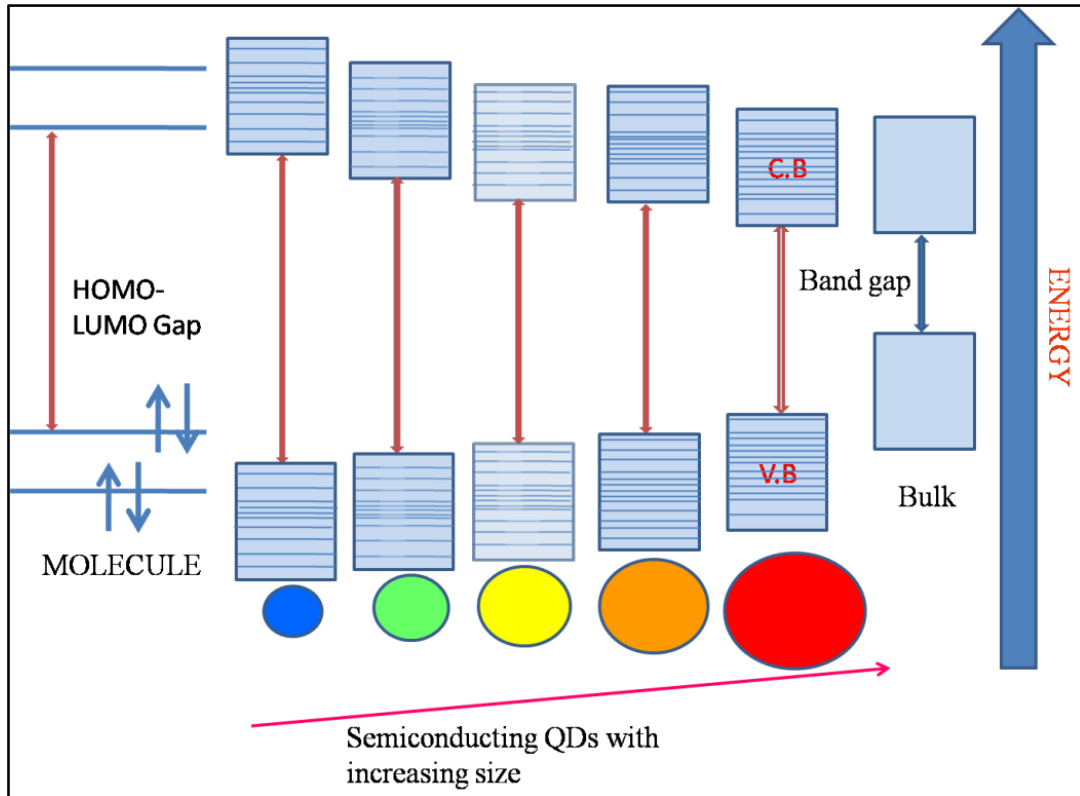
Figure 1.4: Schematic representation of quantum confinement and electronic energy states in bulk semiconductors, quantum dots, and molecules

Bohr radius for a particle is described as

$$a_B = \frac{4\pi\varepsilon_0\varepsilon h^2}{m_r^*.e^2}$$

Where ε is bulk optical dielectric coefficient, ε_0 is permittivity in the vacuum, e is elementary charge and m_r*can calculate as

$$\frac{1}{m_r^*} = \frac{1}{m_e^*} + \frac{1}{m_h^*}$$

Where m_e*and m_h*are electron and hole effective masses.

In small QDs confinement effect originate due to spatial confinement of electrons in the crystallite boundary. Unique optical properties of QDs arise due to quantum confinement effect [30]. Band gap of quantum dots changes with size and this totally depends upon the confinement regime. Confinement regime is how the size of the quantum dot in comparison with the exciton Bohr radius.

If radius of quantum dot is on identical order of magnitude like exciton Bohr radius, then it is in the "weak confinement regime. Quantum dot is said to be in the "strong confinement regime", when it is smaller than the exciton Bohr radius. So it could be said that the inimitable characteristics of quantum dots are due to size regime in which they subsist. These QDs form the continuous valence and conduction bands separated by a forbidden zone in contrast with bulk semiconductor [31].

The confinement of exciton in very smaller space leads to quantized, discrete energy levels in QDs. In case of bigger quantum dots band gap is smaller and continuous its electronic structure is. On the basis of quantum confinement along different dimensions we can divide quantum confined structure into three types quantum well, quantum wire and quantum dots. In QDs, confinement of charge carrier takes place in all the three proportions and the electrons shows a discrete atomic-like energy spectrum (Figure 1.5).

Formation of quantum wires occurs when motion of charge carrier is confined in two dimensions. In quantum wells movement of charge carriers is confined in single plane and movement of these carriers is free in two-dimensions. Density of electronic states is high near to conduction and valence bands edges compared with bulk semiconductors and thus a high concentration of carriers participate in band-edge emission [32]. This concludes that more discrete energy levels arise on the confinement of dimensions. When the size of QDs is larger than it absorb photon of less energy that is closer to red end and as the size of QDs decreases they absorb photon of high energy that is towards blue end. This clarifies how the quantum confinement effect affects the optical properties of QDs.
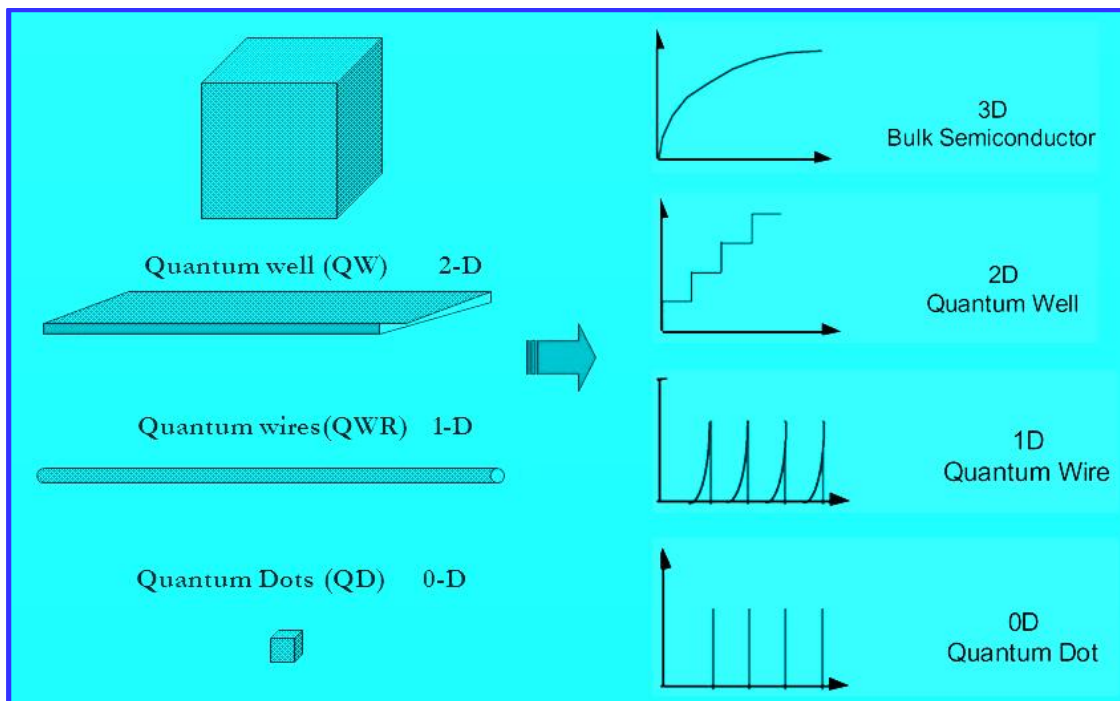
Figure 1.5: A schematic of the degree of confinement for quantum well, quantum wire and quantum dot with comparison to bulk

1.2.3 Fluorescence in QDs

Fluorescence is the emission of light by semiconductors on absorption of light. It is a mode of luminescence. In the majority of the cases, wavelength of emitted light is high as compared to absorption light consequently of lower energy. Excellent optical properties of QDs like broad absorption spectra, narrow or size-tunable emission, high quantum yields and high resistance to photo bleaching make these QDs beneficial over conventional fluorophores for biosensing purposes. These size tunable optical properties of QDs take place due the quantum confinement effect [33]. As the size of QDs decrease band energy gets increased and this results in blue shift in absorption and emission edge. As a result, different sized QDs of same composition can show fluorescence at different wavelengths. Thus it is feasible to alter optical properties from visible to NIR range based upon size. This brilliant optoelectronic feature of QDs makes them useful in highly sensitive bioanalytical assays [3].

Literature survey revealed that colloidal QDs like ZnS, CdTe, CdSe, lead based PbS and PbSe, InAs covers whole range starting from UV to Infrared. Due to broad absorption spectra these QDs emanate a variety of colors e so these QD have great prospective in molecular imaging. As compare to dyes these QDs are highly stable, photoresistant, less photodegradation and better brightness. QDs are greatly brilliant probes in NIR region above 700 nm.

Fluorescent NIR QDs having emission in range 1000–1400 nm are valuable for non-invasive deep-tissue imaging of breast tumor, blood vessels of living mice [34–37]. These NIR QDs act as fluorescent probes to evaluate pathological state of cerebral blood vessels [38]. As we have discussed above quantum dots must emit approximately in NIR range to minimize the problem of tissue endogenous fluorescence. But the major drawback related to these fluorescent QDs is their toxicity and instability and it is tremendously essential to passivate surface of these QDs to make them nontoxic [39].

1.2.4 Defect states in QDs

Defect states of QDs are major root that affects the performance of QDs [40]. In semiconductors defects are introduced due to vacancies created by zinc and sulfur in ZnS, Cd and Se in CdSe etc., impurities, interstitial site defects and dangling bonds present on surface of QDs. These defects originate the energy states within the QDs band gap. These trap states capture charge carriers from electronic states and diminish the mobility of charge carriers across QDs. Non-radiative recombination of photogenerated charge carriers at trap states results in quenching of photoluminescence of QDs [41].

In literature trap emission was also observed in thiol stabilized QDs because of hole scavenging property or hole acceptor property of thiol functionality or sulfide ions and these studies were focused on fluorescence intensity. Trapping of the charge carriers at a defect or surface state (trap states) is a quicker process, which can powerfully contend with radiative recombination and results in quenching of exciton emission [42]. Schematic representation of band edge emission and defect emission is presented in Figure 1.6. These defects originated energy states if lies close to band edge either conduction band or valence band then are called as shallow traps. If energy states lies close to middle of band gap then are named as deep traps.
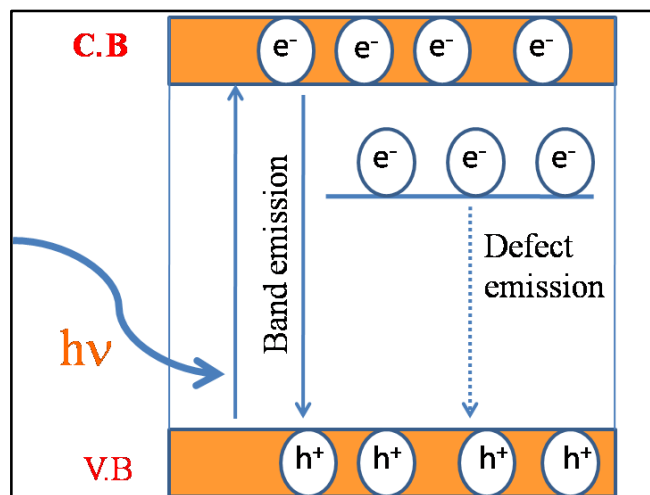
Figure 1.6: Schematic representation of band edge emission and defect emission

1.3 Surface modifications of quantum dots for improved luminescence and viability

1.3.1 Toxicity of QDs

Fluorescent QDs like CdSe, CdTe, PbSe and PbS are made up of toxic cadmium or lead components. Toxicity of QDs is previously reported to get affected by size of QDs and charge of QDs. Concentration of QDs and coating layer of QDs with some other factors like oxidation and stability have been reported as contributing factors which affect toxicity. [43]. Few research groups reported high toxicity of CdSe QDs toward cultured cells under prolonged UV illumination. They find out that uncoated CdSe QDs were toxic due to liberation of Cd^{2+} [44]. This toxicity of QDs is because of lysis of semiconductor particles on UV irradiation. Cadmium and lead ions leached out from the QDs are harmful to cells [45]. Thus coating of these QDs by biocompatible layer is direct way to make them biologically inert and nontoxic. Materials for coating of QDs ought to be nontoxic like some organic molecules and polymers (e.g., PEG). These nontoxic materials may be inorganic layers of ZnS and silica [46-48]. Literature survey exposed that mercaptopropionic acid, mercaptoacetic acid, 2-aminoethanethiol and 11-mercaptoundecanoic encapsulated QDs are more toxic than silica coated QDs. Surface coating of QDs affects the uptake extent and in turn inclined the intracellular cytotoxicity [49]. Use of these

polymer and silica encapsulated QDs in several biomedical detection and imaging applications do not show evidence of toxic effects [50, 51]. Thus to reduce toxicity of QDs their surface passivation is best strategy.

1.3.2 Need for functionalization (solubilization) of QDs

In order to use these fluorescent QDs for biological studies it is necessary that these QDs should be safe, water-soluble and biocompatible. Mostly the QDs are synthesized by organometallic route using organic solvent at high temperature. These QDs synthesized by organometallic route require surface modification to become water soluble. This method is problematic and having several drawbacks. So to avoid this post treatment method it is better to synthesize QDs directly in aqueous route. But literature survey revealed that QDs synthesized by aqueous route posses low luminescence intensity and poor optical properties. Surface passivation of these small QDs by appropriate materials makes them biocompatible along with improved optical properties. Thus surface modification is essential for QDs to utilize them in various biological applications. Here next section important strategies for QDs surface modification for bio related applications are being presented: (1) Silanization of QDs by forming layer of silica on QDs surface (2) Ligand exchange and (3) Amphiphilic polymer encapsulation [52-54]. Figure 1.7 shows graphic depiction of surface functionalization of QDs.
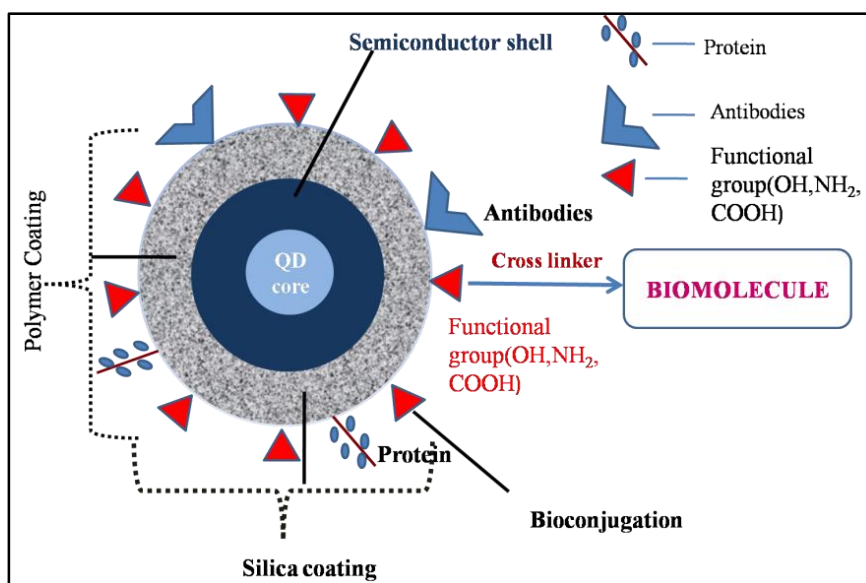
Figure 1.7: Schematic representation of surface functionalization of QDs

1.3.3 Strategies for QDs surface modification

1.3.3.1 Silanization

Covering of QDs surface by silica layer is most preferred approach to make these QDs biocompatible and nontoxic for latent cancer diagnostics and therapeutic allied biomedical applications [55, 56]. This strategy of surface covering is also called surface silanization [57]. In this approach cross linking of trimethoxysilane groups occurs by the arrangement of siloxane bonds. Most regularly employed silanes are polyethylene glycol (PEG)-silane, phosphosilanes and aminopropylsilanes (APS) [58, 59]. These silica encapsulated QDs are very stable as the silica shells be vastly cross-linked. Silanization is favored because of its less toxicity in comparison with other ligands [60, 61]. The majority of information of silica coated process is limited up to the cytotoxicity assessment [62-64].

Numerals of information regarding silica coated nanoparticles have been dedicated to silica coating by aqueous synthesis method [65, 66]. Silica encapsulated systems are also very useful for biosensing and electronic applications. Silica shell formations on core QDs provide good biocompatibility by confiscating the toxic effect of the precursor [67]. Encapsulation of silica on core QDs can be done by two established method one is known as "Stöber" approach. In this method QDs by replacing the native ligands with 3-mercaptopropyltrimethoxysilane (MPS) or 3-aminopropyltrimethoxysilane (APS) are relocated in polar solvents (a mixture of water and ethanol). As prepared QDs possess broad size distribution along with nucleation sites for the nucleation, a good dispersion of QDs into water, and increased quantum yield [68].The second approach is the reverse microemulsion and this approach is able to overcoat hydrophobic QDs directly with a silica layer. This results in enhancement in mechanical stability and photo stability of QDs and prevents them from oxidation [69]. Previously Murase et. Al. synthesizes luminescent CdTe – silica particles by this method [70, 71].

1.3.3.2 Ligand exchange

Ligand exchange approach is applied when a semiconductor nanocrystal is synthesized in solution. Hydrophobic ligands like TOPO make QDs hydrophobic and insoluble in polar solvent. These kinds of nanocrystals are only soluble in non polar solvent. So ligand exchange is an

approach that is developed to address such kind of solubility issue. In ligand exchange method ligands present on QDs surface can be replaced with the ligand of choice. This method mostly involve the functional groups which has high affinity with surface of quantum dots like sulfur and phosphorous. Mostly those functional groups are preferred which have property of interest. Thiol groups are generally preferred due to their high affinity with QDs surface [72]. Previously Puzder et al studied interaction of CdSe QDs surface with phoshphine oxide, phosphine acid and confirmed that interaction was between oxygen atom of ligand and cadmium atom of CdSe QDs [73]. Literature survey also revealed that ligands were helpful in achieving enhanced property of CdSe QDs. More efforts have now concentrated on surface modification of QDs with ligands that incorporate high degree of functionality for biological application.

1.3.3.3 Polymer coating of QDs

Coatings of QDs by polymeric material are unique best methods to promote QDs stability and reduce toxicity. Most of the polymers are biocompatible and are mainly used to sustain long-term colloidal stability of solution dispersed QDs. This polymer coating also results in some additional functional groups on QDs surface which further used in chemical derivatization of the QDs. Polymer coating of QDs is necessary to make them stable; water soluble and biocompatible. This strategy involves hydrophobic –hydrophobic interaction. Here hydrophobic part of QDs surface ligand interacts with hydrophobic ligand of amphiphillic polymer and phospholipid. During polymerization process the reaction takes place between QDs and polymer makes QDs stable. Different kinds of polymeric material were employed in literature to modify QDs such as imidazole modified linear PEG, PAL (poly allyl amine), hyperbranched polyethylene imine (PEI). Chitosan a hydrophilic, nontoxic, biocompatible natural polymer has also been used for coating. The capping method of polymer on QDs generate more compact polymer QD hybrid. With better biocompatibility and lower toxicity polymer is one of the best coating material that make QDs water soluble and provide them biocompatible functionality [74].

1.3.4 Bio-conjugation

To facilitate QDs for biological application it is necessary to link these QDs with some bio-molecules like avidin, peptides, proteins and antibodies. These bio-molecules should be attached to QD's surface without any damage to properties of molecules. Most common method for bio-

conjugation is by mean of cross-linker. Primary amine present on bio-molecule can be linked with –COOH group present on encapsulating layer of QDs using 1-ethyl-3-(3-dimethylaminopropyl)-carbodiimide (EDC) [75] and 4-(N-maleimidomethyl)-cyclohexanecarboxylicacid N-hydroxysuccinimide ester (SMCC) [76]. CdSe, ZnS, CdS and CdTe semiconductor nanocrystal capped by group like mercaptoethanol, mercaptopropionic acid and cysteine residue etc mostly bear –SH contains sulfhydryl. Thus these QDs can be bind to bio-molecules bearing same group [77, 78]. Bio-molecule oligonucleotide gets adsorbed on water soluble QDs. Adsorption depends upon temperature, pH and ionic strength. With broad range of bio-conjugation methods available now it's possible to conjugate nanoparticles with nucleic acid, peptides, carbohydrates, proteins and lipids [79-81]. Thus these bio-conjugated QDs now can be used as fluorescence markers to label structure and molecules in cell.

1.4 Quantum dots synthesis methods

These days to synthesize nanoparticles with great diversity which are made of different materials and are also different in their shape, size and elemental composition is promising. It's also possible to synthesize nanoparticles which have different physical or chemical properties. Synthesis of QDs is possible in solvents like aqueous and non-aqueous solvents. Amphiphilic QDs show dispersion in both kinds of solvents. In general, surfactants which attach to surface of QDs were involved in their synthesis. Surfactant stabilizes nuclei and nanoparticles against agglomeration by a repulsive force. Surfactants are helpful in controlling QDs growth by controlling rate of reaction, final size or geometric shape. Nanoparticle's growth mechanism determines size and shape distribution of nanoparticles. Knowledge of growth mechanism gives opportunity to keep control on preparation of required nanoparticles [82]. Growth mechanism is complex and depends on many factors like temperature, viscosity, pH and concentration of medium etc.)[83]. Conditions determined for QDs growth are changed in accordance with method of preparation [84]. The synthesis of QDs can be achieved mainly by two well known approaches (i) top-down approach and (ii) bottom-up approach using different techniques (Figure 1.8). Both the approaches are beneficial or required depends on diverse targeted outcomes.
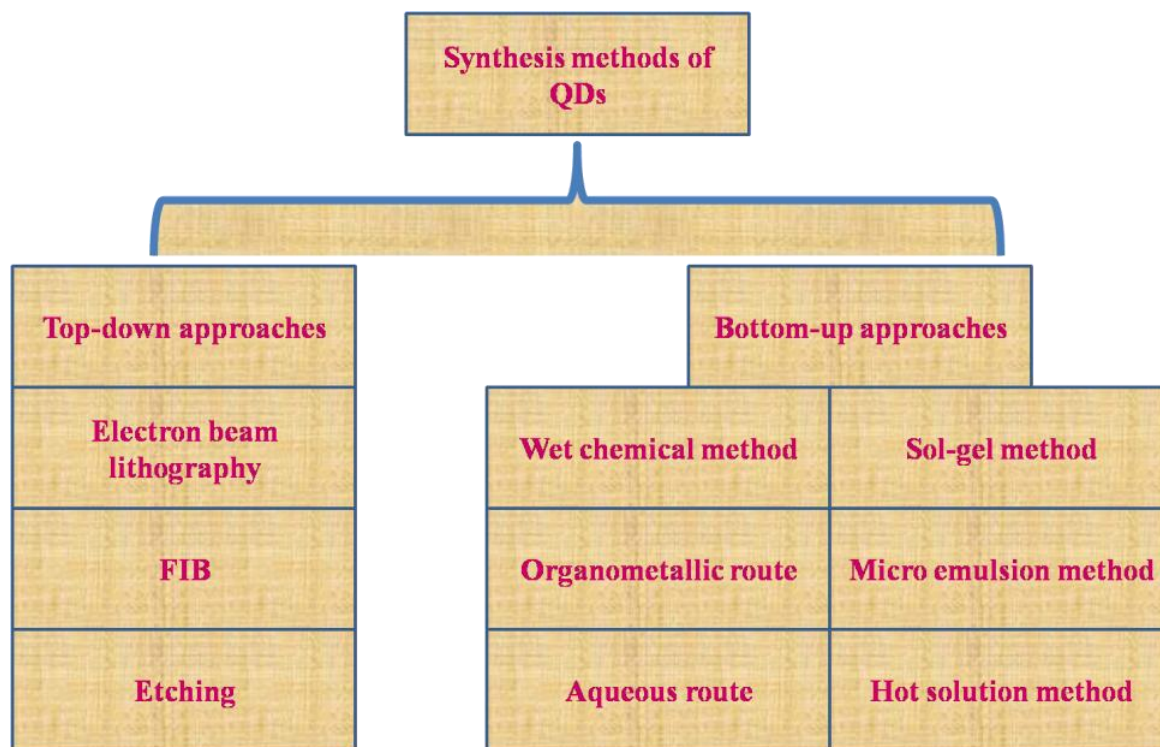
Figure 1.8: Synthesis approaches and methods for QDs

1.4.1 Top-down approaches

As the name suggests top-down approach involves thinning of bulk material or macroscopic initial structure into small QDs. Different kind of lithographic techniques are commonly used to attain QDs of diameter ~30 nm. Some drawbacks are incorporation of impurities into the QDs and structural imperfections.

In this process, quantum dots of size ~ 30 nm are to be formed from bulk semiconductor materials with the help of electron beam lithography, focused ion or laser beams, reactive-ion or wet chemical etching techniques. To obtain quantum dots of specific packing geometries with particular shapes and sizes a series of experiments on quantum confinement effect are required however, these fabrication processes suffers from structural defects and incorporation of various impurities during its long synthetic pathways.

1.4.1.1 Electron beam lithography

In electron beam lithography (EBL) technique scanning of focused beam of electrons is carried out to draw designed shapes on a surface which is covered by an electron sensitive film named as resist. Resist material is made of a polymeric compound. Resist of long chain polymer with high molecular weight (~105 units) is referred as negative tone while small chain polymeric resist are described as positive tone.

Exposure of negative resist to electron beam promotes polymerization of the chain length however chain length reduction takes place in case of positive resist. The electron beam exposure alters the solubility of the resist. This permits the particular elimination of either the bare or enclosed regions of the resist by plunge it in a solvent. This process is developing process.

The purpose of this whole process is to produce very tiny structures in the resist that can afterward be transferred to substrate material by etching. Electron beam sources are hot lanthanum hexaboride for lower-resolution systems while higher-resolution instrument use field electron emission sources like heated W/ZrO_2 for lower energy spread and improved brightness. Main benefit of electron-beam lithography is that it proffers a great degree of flexibility in nanostructured systems (QDs, wires or rings). EBL technique is expensive, complicated as compare to other methods.

1.4.1.2 Etching

Etching is a technique which plays significant role in processes like nanofabrication. In case of dry etching, reactive gas is introduced into an etching chamber. Radio frequency voltage is applied to produce plasma, this lysis of gas molecules to reactive trash.

High kinetic energy fragmented species hit surface and leads to formation of a volatile reaction product. When ions are energetic species, this method is termed reactive ion etching (RIE) [85]. This has also been used for production of close-packed arrays for testing of lasing in QDs [86]. Etching technique has some limitations like some of gases are toxic and corrosive.

1.4.1.3 Focused ion beam

In FIB beam from molten metal source (e.g., Ga, Au/Si/Be, or Pd/As/B) is employed to sputter semiconductor substrate. Size and shape of QDs depends upon size of ion beam. FIB technique is used for material deposition from a precursor gas. But this is a sluggish process requires exclusive equipment and cause damage of surface. Previously III-V and II-VI QDs with particle sizes 30 nm has been synthesized by this approach [87]. The disadvantage of FIB technique is that it leads to extensive damage of substrate.

1.4.2 Bottom-up approach

Bottom up approach as the name suggest is the approach starts from bottom (smaller) and reach to top (up). In this approach material components at atomic level by self assembly lead to formation of nanostructure. To synthesize QDs by this a numeral of diverse self-assembly techniques have been used. We are going to discuss some synthesis methods which come under bottom up approach.

1.4.2.1 Wet-chemical approaches

This method involves synthesis of nanomaterials from polar and nonpolar solvents. It is a kind of conventional precipitation method and nucleation and growth steps are involved in this method. QDs of desired shape, composition and size can be achieved by varying the synthesis parameter like temperature, Ph etc. Nucleation possibly will be classified as homogeneous nucleation, heterogeneous nucleation or secondary nucleation [88]. As solute atoms unite and achieve a decisive size without the help of pre-existing solid line that kind of nucleation referred as homogeneous nucleation. The size, shape and composition of the QDs synthesized by wet chemical method can be varied by varying reaction parameters like temperature, stabilizers, precursor's concentration and solvent. Some common wet chemical methods are briefly discussed below.

1.4.2.2 Sol-Gel process

Sol-gel technique has been utilized to produce nanomaterials include QDs since long time. Synthesis of oxide nanoparticles is well reported by this method. In this method preparation of

sol (dispersion of nanoparticles in solvent by *Brownian* motion) was carried out by using metal as a precursor (usually acetates, nitrates and alkoxides) in acidic and basic media. Main leading step involved in sol-gel method are hydrolysis, condensation and growth. First step is hydrolysis of metal precursor pursue with condensation to form sol and with growth polymerization process to form gel. Low processing temperature, adaptability, and elastic rheology permit simple shaping and embedding. These are main advantages of sol-gel techniques.

Both organic and inorganic kind of materials can be used in this method. Wide size distribution and large number of defects are the main disadvantage of this synthesis technique. Previously II-VI, IV-VI QDs like CdS [89], ZnO [90-93], PbS [94] have been synthesized by sol gel method. As compared to our wet chemical aqueous route this method have drawback like long processing time, high cost of starting materials, complex procedure etc.

1.4.2.3 Microemulsion method

Room temperature synthesis of QDs can be carried out by Microemulsion method. Normal microemulsion (oil-in-water) and reverse microemulsion (water-in-oil) are types of this method. As an alternative of water other polar solvents can be used in this method. The reverse micelle process is popular and can be attained with help of surfactants, like cetyl trimethyl-ammonium bromide (CTAB) and sodium dodecyl sulphate (SDS) to disperse water droplets in n-alkane. Because of the presence of surfactant many minute droplets named as micelles get created in continuous oil medium. Micelles are stable thermodynamically and work as 'nanoreactors'. Vigorous mixing leads to a constant reactant exchange because of dynamic collisions. Major advantage of this method is narrow distribution of size of QDs while low yield, amalgamation of impurities or defects is main disadvantages.

QDs like CdS [95], CdS:Mn/ZnS [96-99], ZnS/CdSe [100], CdSe/ZnSe [101], ZnSe [102] and IV-VI QDs have been prepared by this approach [103]. Microemulsion methods have some limitations over wet chemical aqueous route like high concentrations of surfactant required to stabilize droplet of microemulsion. Environmental parameters like pH and temperature influence stability of microemulsion.

1.4.2.4 Hot-solution decomposition process

Hot solution decomposition process involves synthesis of QDs by high temperature pyrolysis of organometallic compounds and this method was first discussed by *Bawendi* and co-workers in 1993. Procedure involve mixing of starting materials like alkyl, acetatecarbonate, oxides [104,105] of Group II with Group VI elements like phosphene or bis(trimethyl-silyl). Initially coordinating solvent like tri-octyl-phospine oxide (TOPO) at ~ 300 ° C temperatures degassed and dried under vacuum in a three-necked round flask.

After that Cd-precursor and tri-*n*-octyl-phospine selenide is injected with stirring at that temperature, which results in homogeneous nucleation for the formation of quantum dots, with the successive growth through '*Ostwald ripening*'. Stabilization of quantum dot dispersion by coordinating TOPO solvent (purity ~90%) helps in improvement of passivation of the surface, and hand over an adsorption hurdle to slow growth of QDs. Thus purity of coordinating solvent also play role in controlling size and shape. Sufficient thermal energy provided by this method anneals defects and results in mono dispersed QDs. Limitation of this method is its higher cost, high temperature, poor dispersions in water and toxic nature of some of the organometallic precursors. This technique earlier extensively used to produce II-VI [106-108], IV-VI [109] and III-V QDs [110].

1.4.3 Other synthesis method

1.4.3.1 Hydrothermal synthesis

Hydrothermal synthesis method of QDs involves temperature and pressure controlled aqueous solution crystallization of inorganic salts. As the temperature, pressure is decreased inorganic compounds solubility usually reduces leading to crystalline precipitates. By this method QDs of dissimilar shapes and sizes be able to be attained by changing reactants, reaction time, pressure and temperature. CdTe/CdSe quantum dots having luminescence in near-IR region (from 620 to 740 nm) have been prepared by this method. The high-quality quantum dots synthesized by hydrothermal method can be found in CdTe [111-113], CdTe/CdS core/shell [114], CdTe/CdSe core-shell [115], and CdTeS alloyed [116] systems. This synthesis method requires high cost

autoclave and observation of growing crystal is impossible during growth period while aqueous route involves simple beaker chemistry.

1.4.3.2 Organometallic route

Organometallic route is one of the simple synthesis route for the making high-quality nearly monodisperse QDs. In this route hot coordinating solvent TOPO (tri-n-octylphospine oxide) trioctylphosphine (TOP) or hexadecylamine (HDA) ~300ºC injected with organometallic reagents like volatile metal alkyl (dimethylcadmium) or metallic oxide (e.g. CdO) and a chalcogen source say tri-noctylphospine selenide (TOPSe). This process is followed by homogeneous nucleation and growth to form QDs.

Growth of QDs through Ostwald ripening and in Ostwald ripening smaller QDs disappears forming larger QDs because larger QDs are thermodynamically favored. QDs synthesized through organometallic route are hydrophobic but these QDs posses 20-60% quantum yields (QY) in contrast to QDs produced by aqueous route whose yield is below 30 %. Size of QDs is dependent on reaction time and temperature [117-119]. Most complex and tiresome steps are involved for production of high-quality QDs by organic solution route.

To make complex of hydrophobic capping agents with precursor require high temperature (~300˚C) to liquefy the hydrophobic capping agents. Biocompatibility and environment friendly nature of the QDs synthesized by this route is negligible. Thus post treatment of QDs synthesized by organometallic route is must to make them soluble in water and to make them biocompatible (Figure 1.9).

As these water soluble QDs can be used for many applications. These QDs are highly active because of their high surface to volume ratio. This high reactivity of these QDs affects their optical, physical and chemical properties. So surface of QDs should be passivated with different materials having inert chemical properties [120]. To avoid all these steps the most suitable method to synthesize hydrophilic QDs is to synthesize QDs directly in aqueous route and next section is presenting the same in an elaborative way.
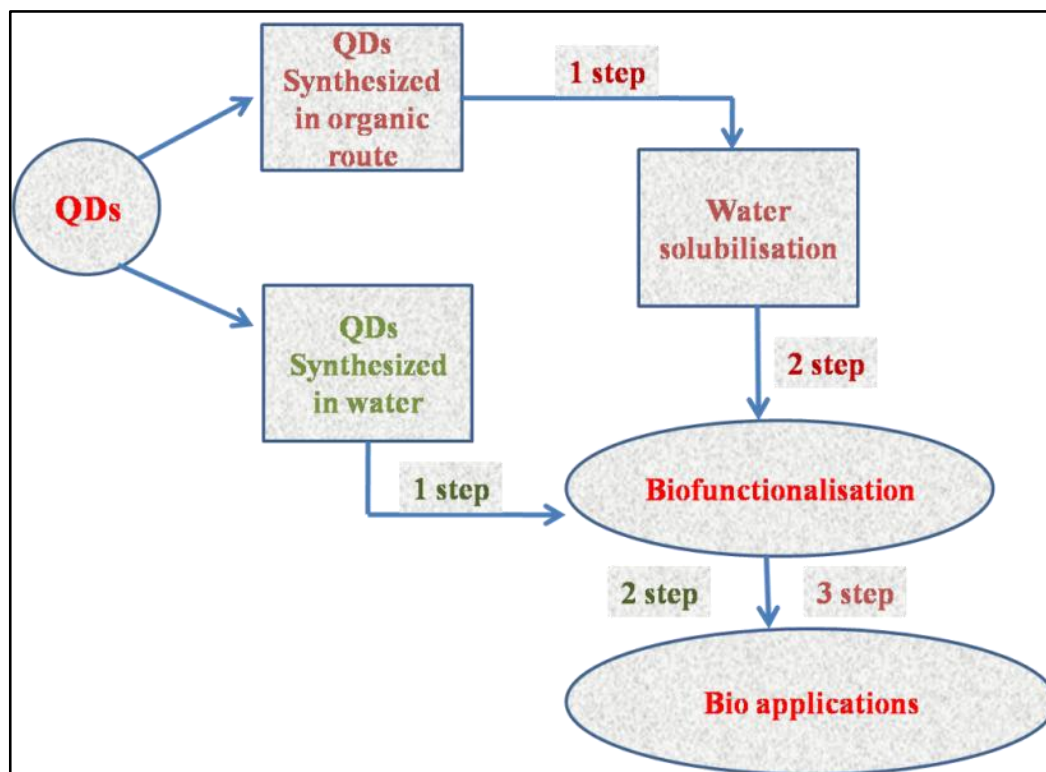
Figure 1.9: Synthesis steps to make QDs structures applicable in biology

1.4.3.3 Aqueous route

QDs synthesize by aqueous route have brilliant biocompatibility, stability (generally more than 2 months) [121-123]. As compare with other synthesis methods QDs synthesized by aqueous route are mostly favored because of their superior reproducibility, cost effectiveness, non toxic and environment friendly nature [124]. Precursors which are easily dissolving in water are used these mostly includes heavy metals nitrates, chlorides and acetates. Chalcogen precursors like NaHSe, Na_2SeO_3 can be freshly synthesized prior to using in reaction procedure [125-127]. Most of these chalcogenide sources are unstable so synthesis could be carried out in inert environment. But Na_2SeO_3 is air-stable and reactions involving this can be performed in air. Capping agent is required in this route to stabilizing size of QDs and capping agent which contains sulfhydryl and carboxyl functional groups are mostly preferred. Thioglycolic acid (TGA) [128], mercaptosucinnic acid (MSA), mercaptopropionic acid (MPA), glutathione (GSH) [129], and L-Cysteine (Cys) are the most commonly used capping agents in aqueous route. [130] Sulfhydryl

group of these capping agents coordinate to QDs, whereas the carboxyl group stabilizes colloidal QDs and also be essential for further surface modification for various applications.

The QDs synthesized in aqueous route are compatible with water and due to biocompatibility these are mainly the centre of attraction for biological applications. As compared to the organic-based synthesis QDs synthesized by aqueous route are less expensive, less toxic and environmental friendly. But regrettably QDs prepared by aqueous route has quite low quantum yield and large size distribution in contrast with QDs synthesized by organic approach. Some different kind of extra post-synthesis treatments like surface modifications, selective photochemical etching can be further use to improve quality of QDs. Here these are few reports about aqueous synthesis of QD in CdSe [131], CdTe [132,133], CdTe/CdS [134], CdTe/ZnTe [135], CdTe/CdSe [136], ZnS [137], ZnSe and Zn1 xCdxSe alloyed [138], and ZnSe(S) alloyed [139] by aqueous route.

1.5 Literature review

1.5.1 CdSe and their core-shell structures

Chuanxin Zhai et al in 2011 reported about biocompatible CdSe, CdSe/CdS core–shell QDs synthesis process. This synthesis was carried out by cost-effective and atmosphere friendly polyol method. Poly (acrylic acid) (PAA) was used as capping ligand and synthesis was carried out at 240°C. PL studies confirmed that peak appeared around 650 nm was due to defect emission was completely removed after formation of CdS layer on CdSe QDs. This enhanced fluorescent quantum yields of band to band emission up to 30%. In addition, the emission peak got tuned from 530 nm to 630 nm for CdSe/CdS. This small size, water soluble QDs with high-quality monodispersity and intense PL emission illustrate elevated attainment as fluorescent cell labels in vitro. MTT assay (3-(4, 5-dimethylthiazol)-2-diphenyltertrazolium bromide) was used to carry out viability testing of QDs-labeled 293T cells. Obtained results show adequate (>80%) biocompatibility [140].

Prashant K Sharma et al in 2010 synthesized CdSe QDs using cytosine as capping agent and found a size reliant blue shifted absorption with superior luminescence. This improved luminescence was attributed to surfactant arbitrated passivation of defects. On the basis of these

results authors were expecting improved bio-compatibility of prepared material QDs for bio-imaging applications. This cytosine capped CdSe QDs may be one of wanted ingredient for imaging in bio and bio-sensors following the bioconjugation of the nanocrystals [141].

Markus Garbolle et al in 2008 explored the relationship between the ZnS shell thickness, QDs stability and fluorescence quantum yield. For measurement of stability they have developed a shell quality test. It was observed that ZnS shell qualitatively control optical properties, stability of CdSe QDs. This research group develops a thiophenol test to evaluate shell quality. To perform this test reaction of CdSe core was carried out with thiophenol radicals produced on exciting thiophenol. Upon UV illumination unshelled CdSe undergoes a total loss of luminescence as compared to shelled CdSe [142].

Viet ha Chu et al (2012) studied optical properties of aqueous soluble CdSe/CdS QDs prepared by using sodium citrate as surfactant through aqueous route. These monodispersed QDs were having strapping luminescent emission intensity. It was concluded that emission peak position of QDs can easily be tunable for a wide range from 555 nm to 615 nm by altering synthesis conditions. PL results clarify that intensity of emission peak was strongest at pH 8 to 8.5. The CdSe/CdS QDs include high photostability and this was nearly unchanged later than several months [143].

S. Mathew et al (2014) described the synthesis of CdSe/ZnS QDs by microemulsion technique. On excitation of 532 nm new emission band appear around 745 nm. This means that there is creation of deep trap in CdSe QDs. In this paper it is clearly explained that surface coating affects optical behavior of QDs in regard of size. From fluorescence studies it was confirmed that as there was increase in shell thickness of ZnS there was increase in trap state. This trap states enhancement indicates distortion in the spherical symmetry of CdSe QDs [144].

Karan Surana et al 2014 reported room temperature and above 200°C synthesis of CdSe QDs by wet-chemical method by using much safer 2-Mercaptoethanol. The prepared CdSe QDs with 2-mercptoethanol were moderately steady for 60 days. After 60 days their color dawn to vary gradually towards red, this change in color happens because of Ostwald ripening [145].

Barik Puspendu and coworkers in 2015 reported synthesis of CdSe and CdSe/ZnS QDs using chemical route. ZnS shell was synthesized using non toxic chemicals and these obtained QDs were found to be non toxic, very stable and bright. Due to non toxic chemical usage for shell formation these kinds of QDs can be used for biological applications without further coating. Coating with shell material was explained on the basis of red shift along with improvement in the PL peak contrast to bare QDs [146].

Samsulida Abd Rahman et al (2017) synthesized thiol capped core-shell QDs and they further use them for glucose detection in aqueous sample. Detection principle of glucose was depending upon quenching of fluorescence signal in presence of glucose. They found that in presence of 0.1 mM glucose fluorescence intensity of bioconjugated QDs quenched about 1200 a.u. Thus it was concluded that quenching of fluorescence intensity was proportional to glucose concentration. Such synthesized QDs are accurate and can be applied as fluorescence nanosensor for detection of glucose [147].

Rekha Dunpall et al (2012) studied cytotoxic effect of cysteine-capped CdSe QDs produced by one-pot solution method. Synthesis of these CdSe QDs was done by varying concentration of the capping agent. After this how CdSe QDs affect DNA stability, blood platelets aggregation and reduce action of iron was estimated *in-vitro*. At 200 μg/mL concentration of QDs DNA damage was seen. In addition, these CdSe nanocrystals posses great reducing power and chelating activity. This concludes that they may injure the activity of haemoglobin by interact with iron. Moreover CdSe QDs prop up blood platelets aggregation of in a dose reliant manner [148].

1.5.2 ZnS based quantum dots

Hua Qu et al (2014) described the production of silica-coated ZnS quantum dots (ZnS/SiO$_2$ QDs) by environmentally friendly method. The prepared ZnS cores were oil soluble and have been productively transfer to water soluble form by the coating of SiO$_2$ shells. The QDs show gratifying dispersion and optical studies confirm good luminescent characteristics in water. These prepared ZnS/SiO$_2$ QDs were used for detection of heavy metal ions without addition of buffer solution. The luminescence property of these QDs was very sensitive to Pb^{2+} ions. This

study confirms that ZnS/SiO$_2$ QDs have immense potentials to be a sensor for Pb^{2+} analysis at low to high concentrations [149].

Bhaskarjyoti Boddo et al (2016) reported that ZnS QDs have been synthesized via chemical bath deposition (CBD) method. TEM images showed the formation of spherical ZnS QDs with the diameter as measured 6.5 nm. According to UV-visible spectra analyses, a large blue shift is observed and this can be accredited to quantum confinement effect in the ZnS QDs. PL spectra measurement indicated the dominant emission bands at 438 nm and 521 nm and are recognized with optical transitions occurs from vacancy and interstitial sites of both Zn and S atoms. Researchers successfully synthesized ZnS QDs using simple CBD method. This method for preparation of light emitting structure is very economical and simple and can be employed on a large scale. X-ray diffraction pattern monitored the structure of ZnS QDs as the zinc-blende structure [150].

Bhaskarjyoti Boddo et al (2012) reported room temperature synthesis of ZnS nanoparticles by co-precipitation method. Prepared material was then characterized for XRD (X-ray Diffraction), TEM, UV-Visible and PL (Photoluminescence) analyses. It was confirmed from XRD that sample prepared were the cubic Zinc blende structure with particle's size in the ranges 5 nm - 12 nm. The TEM analysis revealed the formation of ZnS nanoparticles with almost uniform shape and size. PL measurement showed Zn as well as sulfur vacancy resulting as some crystal defects. In PL analysis, three strong and broad emission bands located at 365 nm, 400 nm and 425 nm have been observed. Peak centered at 365 nm was due to the UV-excitonic emission and other peaks were credited to the sulfur and Zn vacancies [151].

Ranganayak Viswanath et al (2014) reported ZnS and ZnS:Y nanoparticles synthesized by chemical coprecipitation method. EDTA was used as a stabilizing agent. It was concluded from XRD analysis that prepared material was crystalline. UV Visible absorption spectra showed a strong absorption peak at around 322 nm (3.85 eV) for pure ZnS and 332 nm (3.73 eV) for ZnS:Y, which are considerably blue-shifted compared to that of bulk phase ZnS (3.6 eV). This absorption shift indicated quantum confinement effect, representing a change in band gap along with additional features. The doping of Y^{3+} ions has tuned the band gap and photoluminescent properties of ZnS nanocrystallites. Undoped ZnS exhibits an emission maximum at 408 and 432

nm, whereas on doping orange emission band was observed along with the blue emission bands at room temperature. The prepared ZnS:Y^{3+} sample shows efficient emission of orange light with the peak emission 601 nm with the blue emission suppressed. A strong emission in the orange part of the visible spectrum was possible by doping the yttrium ions with zinc sulphide. The photoluminescence studies illustrated that the doping of Y^{3+} ions modifies the emission properties of nanocrystalline ZnS with increase in Y^{3+} ions concentration [152].

This research paper (Ashutosh K Shahi et al) describes synthesis of ZnS nanoparticles by less harmful chemicals by varying the concentration of cationic surfactant CTAB. XRD and TEM measurements show the size of polydispersed ZnS nanoparticles in the range of 2–5 nm with cubic phase structure. The photoluminescence spectrum of ZnS nanoparticles exhibits four fluorescence emission peaks centered at 387 nm, 412 nm, 489 nm and 528 nm showing the application potential for the optical device. PL studies show all electronic transitions from ZnS nanoparticles occur due to surface vacancies and defect states because of large surface to volume ratio. In Raman spectra all the peaks were appeared due to surface optical phonon mode. In Raman spectra of ZnS nanoparticles, the modes around 320, 615 and 700 cm^{-1} are observed [153].

1.5.3 CdTe Quantum Dots

Mengying Li et al in 2008 developed the efficient and simple route for the synthesis of L-cysteine capped CdTe quantum dots in aqueous media. Compared with previous research reports method chosen by this research group have shown advantages like broadened pH range for precursor synthesis and a shortened time period for green QDs and 5 hour for red QDs. The prepared QDs possess good fluorescent properties such as wide absorption, symmetrical emission peaks and high fluorescent intensity. The Cd^{2+} in the QDs solution could be removed by a specified purification process, remaining the fluorescence excellent as before. In addition, a new method for the recovering and maintaining fluorescence of QDs solution was reported, which would be a reference for processing and conserving QDs colloids [154].

Anne S schulze et al studied the effect of reaction temperature, pressure, precursor ratio and surface ligands on optical properties and particle size of CdSe and CdTe QDs synthesized by aqueous solution method. It was concluded from optical studies that one can vary the optical

behavior of QDs by varying chain length of ligand, temperature and so on. These QDs could be flexible tools for biological applications such as cell imaging due to their water solubility and stability. First *in- vitro* studies with mesenchymal stem cells indicated a cell uptake during a period of 1 day by endocytosis, where the nanoparticles started to agglomerate in the cytoplasm and accumulate around the nucleus without penetrating it. Also, no cytotoxicity of the synthesized QDs with and without a protecting ZnS shell was observed [155].

Duan et al 2009 developed one pot microwave irradiation reduction method for synthesis of luminescent CdTe QDs. Influence of temperature, pH value and molar ratio of stabilizer 3-MPA on quantum yield was studied by optical characterization. It was found that QDs synthesized at optimized synthesis condition like time period (10-40 minutes) have high quantum yield. Thus these obtained QDs with high quantum yield can be used as fluorescent probe for detection of mercury ion in aqueous media [156].

Zhang et al in 2009 studied the influence of three different ligands namely mercaptoacetetic acid, L-cysteine and reduced glutathione on optical properties and water phase preparation of QDs. Rate of growth and size distribution of CdTe QDs was dependent upon the type of ligand. Large size nanocrystals with narrow size distribution can be achieved by choosing a proper ligand. In addition to these findings they also studied effect of pH, illumination, heating on spectroscopic properties [157].

Zeng et al in 2009 reported the development of a on synthesis method for CdTe/CdSe core-shell QDs by two step aqueous synthesis method. From PL studies they observed dependency of PL emission peak on thickness of CdSe shell. Emission peak position can be tuned by controlling the thickness of shell. Shell of optimized thickness can help in enhancement in quantum yield from 4% to 40 %. Moreover they coupled these luminescent QDs with folate to utilize them as probe to recognition of tumor cell [158].

Chang et al in 2007 developed a noncoordinating solvent route for synthesis of core-shell CdTe/CdS and CdTe/CdSe. Red shift in PL peaks was observed from optical studies and this confirms the formation of core-shell structures. These results suggested that CdS shell grow more preferentially on CdTe than CdSe, but fast kinetic growth rate of CdS make it difficult to

control epitaxial growth on surface of CdTe core. Basically stepwise increase in concentration of monomer S and Se into CdTe core solution allowed the examination of monomer activity [159].

Weng et al 2006 studied the conjugation of luminescent CdTe QDs with plant lectin (UEA-1) and antibody anti-von Willebr and factors (anti-vWF) as fluorescent probes which were able to particularly attach the corresponding cell membrane receptor and cytoplasm immunogen, respectively. The good quality cell images were achieved in live cells and fixed cells using laser confocal scanning microscopy. From this study they concluded that CdTe QDs prepared in water phase were highly luminescent, water-soluble, stable, and easily conjugated with biomolecules since their surface were coated with MPA containing free carboxyl group. We predicted that QDs prepared in water phase will probably become an attractive alternative probe in cellular imaging and bio-labeling [160].

Saikia 2016 studied the effect of shell formation on photoluminescence quantum yield. It was found that after shell formation CdTe/ZnS found to be very photostable. Only 6.7% of the PL intensity of CdTe/ZnS CS decreased in 100 days whereas for CdTe decrease in PL intensity was 43.6%. Thus the synthesized CdTe/ZnS CS QDs system showed excellent stability as compared with that of the CdTe QDs. The ZnS shell controls the optical properties and the stability of the CdSe/ZnS CS QDs. This excellent stability of CdTe/ZnS makes it a good bioimaging agent [161].

Li Y et al (2015) studied outcome of epitaxial growth of ZnSe shells on CdTe cores. The optical properties of the as-prepared CdTe/ZnSe QDs could be controlled by precisely adjusting the size of CdTe cores, which showed broad emission spectra from 530 to 688 nm. Such QDs have bright future perspectives in the development of biological and nanomedical fields. The ZnSe shell and the several functional groups on glutathione molecules greatly increased the biocompatibility of the original CdTe core. Such QDs could be regarded as nanocrystals with high quality for applications in biological and medical science [162].

Mandal et al (2008) studied pH dependent optical properties of CdTe prepared in aqueous solution by reaction of H_2Te and Cd^{2+}. Effect of pH level on optical properties of different sized QDs was studied and it was found that both luminescence intensity and absorbance changes were reversible when the pH level of the solution was brought back its original value [163].

1.5.4 CdTe, CdSe and their polymer encapsulated structures

Sheng et al (2006) encapsulated QDs in polystyrene microspheres. The chemical amalgamation of the QDs keen on the polymer matrix polystyrene microspheres (PSMS) through chemical bonds formulates a predominantly strong system. These QDs do not pour out of beads yet after high frequency sonication and lengthy shelf period; this builds these beads most important aspirant for a range of applications in callous environments. Optical properties of these entrenched QDs are preserved because of the shield by OP (oligomeric phosphine) ligands. Though, labors to encapsulate elevated concentration of QDs outcome in the aggregation of QDs avert the creation of QD/PSMS. Based on these finding new approaches are consequently required in sort to load extra QDs into microspheres [164].

Jessica Batalla et al (2015) studied the optical properties of carboxyl CdSe/ZnS QDs encapsulated by phospholipids liposome. It makes the QDs water soluble and photo-stable. Fluorescence self quenching of the QDs inside the liposomes was observed. Therefore, encapsulation efficiency of the QDs by the liposomes was studied by the thermal lens microscopy (TLM) and maximum encapsulation efficiency was found around 36%. Furthermore they tested cytotoxicity of encapsulated QDs toward breast cancer cells line MDA-MB-231. The acquired materials were biocompatible present high photothermal conversion efficiency and excellent photostability and nontoxicity towards cells line MDA-MB-231 at low concentration 0.13 nM [165].

Xiaoge Hu et al (2009) developed a new generation approach for synthesizing silica encapsulated single QD. As compare with the earlier traditional sol-gel method, this new CTAB surfactant dependent approach for synthesis of QDs is appreciably simpler, resulting in QDs with size monodispersity, brilliant luminescence and tunable silica shell thickness. A major finding is that in contrast to the previously reported amphiphilic macromolecules, CTAB based surface coating can solubilize QDs into water but significantly trim down their stability. An important finding was that unlike previous reported magnetic and metallic nanoparticles, the QDs coated with only a layer of surfactant molecules were highly unstable and sensitive to the environment. As a consequence, the surfactant stabilized QDs must be prepared fresh and stored in dark before silica coating. The QDs become stable once silica shell formed on their surface and excess

surfactants are removed. Further development of this technology particularly by incorporating drugs into the mesosized silica pores will open exciting opportunities in traceable delivery and controlled release of therapeutic agents [166].

Xiaoge Hu et al (2010) reported unique development of ultra stable QDs by using silica shells and amphiphilic polymers based technology to encapsulate QDs. These encapsulated structures show high resistance toward harsh chemicals like acids. They further demonstrated applications of the ultra stable QDs for pH sensing. In comparison to previous reports, the QDs used here are insensitive to environment changes and only serve as an internal reference. This feature could open new opportunities in sensing applications in complex biological fluids when H^+ and OH^- are not the only solutes. We further reveal the use of these ultra stable QDs as internal references in pH sensing applications. Semiconductor QDs are important fluorescent probes due to their high brightness, multiplexing capability, and photostability. However, applications in quantitative and *in vivo* imaging are hampered by their sensitivity to chemical environments and potential toxicity. We further demonstrate the use of these ultrastable QDs as internal references in pH sensing applications. We expect this work will open exciting opportunities for *in vivo* and quantitative applications, and may help solve the toxicity problem of QDs [167].

Ma et al (2010) compared the commercially available Invitrogen QD605 (carboxylate) with self synthesized silica-coated QDs for in vivo imaging. They synthesized silica-coated QDs by aqueous route without involving any organometallic precursors and high temperature in oxygen-free environment. The as-prepared silica-coated QDs possess high quantum yields and are extremely stable in mouse serum. In addition, the silanization method developed here produces QDs with small sizes that are difficult to achieve via conventional silanization methods. The silica coating helps to prevent the exposure of QD surface to the biological milieu and therefore increases the biocompatibility of QDs for *in-vivo* applications. Interestingly, the silica-coated QDs exhibit a different bio-distribution pattern than commercially available Invitrogen QD605 (carboxylate) with a similar size and emission wavelength. In addition, the silica-coated QDs exhibit a more favorable bio-distribution pattern over the commercially available QDs including low liver and spleen uptakes and prolonged blood circulation, which further enhances their compatibility for *in-vivo* targeting and imaging [168].

Kim et al (2011) reported encapsulation of luminescent near-infrared CdTe/CdSe QDs by poly (lacticco- glycolic acid) (PLGA) nanospheres. Encapsulation of these QDs was done to make them stable and biocompatible for *in-vivo* imaging. Solid dispersion method was used to encapsulate these QDs. The resultant QDs-loaded PLGA nanospheres were characterized by various analytical techniques such as UV–Vis measurement, dynamic light scattering (DLS), fluorescence spectroscopy, and transmission electron microscopy (TEM). This research group further studied toxic effect and stability of QDs loaded in PLGA nanospheres *in-vitro* and *in-vivo*, respectively. It was found that photostability of QDs loaded in PLGA nanospheres was improved than free QDs. From cytotoxicity study they confirmed that QDs entrapped in PLGA nanospheres have many desirable characteristics as imaging agent, delivery vehicles, including water solubility, low cytotoxicity, stability, high cellular uptake and long circulation time *in-vivo*. The internalization and long circulation time of the PLGA nanospheres increases the retention time and amount of the nanoparticles inside the cells. Both of these properties fit very well with the criteria of a molecular target for tumor therapy and imaging [169].

Hector Rodríguez Rodríguez et al (2017) studied photo-brightening and bleaching behaviors of two types of silica-encapsulated QDs excited upon two-photon absorption in an optical trap. The first type consists of alloyed CdSe ZnS QDs covered with a silica shell. The dynamics of these as-prepared architectures are similar to those previously reported for bare surface deposited QDs, where thousands of times smaller irradiances were used. We then analyzed the same quantum dot systems treated with an extra intermediate sulfur passivating shell for the better understanding of the surface traps influence in the temporal evolution of their emission in the optical trap. The concurrence of alloyed QDs with the use of an extra S layer and SiO_2 encapsulation tolerates irradiance doses three orders of magnitude higher than those reported for bare core-shell architectures on solid surfaces, which makes QD systems and trapping scheme suggestive for tracking experiments in biological scenarios. Although photo-oxidation is present in both QD@SiO2and pQD@SiO2 systems, longer PL emission stability is registered for the later, which is associated to the extra passivation S shell that suppresses other light-assisted bleaching mechanisms, in agreement with former qualitative studies with the QDs affixed on a solid surface [170].

Chang et al (2015) presented the synthesis of series of SiO_2 encapsulated semiconductor polymer nanocomposites as photoluminescence phosphors. From optical studies of these nanocomposites it was observed that QDs exhibited multicolor emissions from blue to deep-red region. This emission was reliant on the polymer species. Silica coating of these nanoparticle phosphors illustrate better photostability as compared to pure semiconductor polymer nanoparticles. These consequences indicated that these hybrid nanoparticles show potential for use in solid-state lighting devices [171].

1.5.5 Cytotoxicity of quantum dots

Wei Xu et al (2015) developed a method for cytotoxicity testing of CdTe QDs by means of engineered *Escherichia coli* as a model. Toxicity of CdTe QDs capped with mercaptoacetic acid (MAA), glutathione (GSH), and L-cysteine (Cys) was checked. It was found that MAA capped CdTe QDs were more toxic than GSH CdTe QDs and Cys-CdTe QDs. This method can also be used to test the biological toxicity of other nanoparticles [172].

Muthunayagam Vibin et al in (2009) studied the toxicity of silica coated CdSe QDs toward human cervical cancer cell line *invitro* by Lactate dehydrogenase assay, MTT [3-(4,5-Dimethylthiazol-2-yl)-2,5-Diphenyltetrazolium Bromide] assay, neutral red cell viability assay. Afterward the *in- vivo* fluorescence was also verified by intravenous administration of the QDs in Swiss albino mice. It was concluded that silica coated CdSe QDs were less toxic even at high concentrations. In addition, *in vivo* fluorescence study confirmed that these QDs are very useful for cellular imaging using their relatively stable fluorescence emission under biological conditions [173].

Lin wang et al (2008) studied effect of pH exposure on cytotoxicity of CdSe covered with ZnS QDs covered by PEG (polyethylene glycol). Toxicity of these QDs was tested against caco-2 cell line for 24 hours. It was found that covered CdSe QDs are not toxic or have less toxic effect. But toxicity of these QDs increased on acid treatment demonstrating that route of exposure may be an important factor in QD cytotoxicity [174].

Nanchen et al (2011) studied cytotoxic effects of CdTe, CdTe/ZnS and CdTe/CdS/ZnS structures. It was summarized that release of toxic cadmium ion in CdTe is responsible for

cytotoxicity. Formation of shell on CdTe QDs prevents release of toxic cadmium ions and makes them non-toxic. From their studies on genome-wide gene expression profiling they conclude that cytotoxicity of CdTe QDs not solitary appear from the release of Cadmium ions but also intracellular distribution of QD nanoparticles in cells and the associated nanoscale effects [175].

Yuanyuan et al (2011) methodically deliberate short- and long-term *in vivo* pharmacokinetic, bio-distribution, and toxicity of the QDs with very small hydrodynamic diameters (2.9-4.5 nm). Particularly, the QDs are initially accumulated in liver at short-time (0.5-4 h) post-injection. Afterward, the QDs are increasingly accumulated in the kidney during long-time (15-80 days) blood circulation. Moreover, obvious size-dependent bio-distribution is observed: QDs with smaller sizes are more easily absorbed by the kidney; those with larger sizes are more quickly accumulated in the spleen. On the other hand, *in-vivo* toxicity studies (histology and biochemistry results, body weight measurements) demonstrate that mice intravenous injected with the QDs survived for 80 days without evident toxic effects [176].

1.5.6 Antibacterial properties of quantum dots

Deepika et al (2010) in this report described aqueous synthesis of CdSe QDs. These QDs were capped with different capping agents like thioglycolic acid, 1-thioglycerol, L-cysteine. All these CdSe QDs were tested for antimicrobial activity against S. aureus. It was found from antimicrobial studies that capping agent effect the antimicrobial behavior of CdSe. QDs capped with L-cys demonstrate minimum antimicrobial activity while QDs capped with TGA act as good antimicrobial agent with maximum antimicrobial activity. This difference in antimicrobial activity was explained on the basis of structure of different stabilizing agents. The outlook possibility of the antimicrobial study of QDs is grouping these QDs with bio-molecules and to utilize them as fluorescent probes and biosensors [178].

Najme Parvin et al (2016) present the antibacterial activity of ZnS: Ag evaluated by the disc and well diffusion agar methods against *Pseudomonas aeruginosa, Staphylococcus aureus* and *Salmonella typhi*. It was observed from antimicrobial studies that zone of inhibition increases as concentration of ZnS: Ag increases in wells and discs. The maximum diameter of zone of inhibition was found in case of *S. aureus* [179].

In this work Zhishong Lu et al (2008) presents the mechanism of antimicrobial action of CdTe quantum dots (QDs) towards *Escherichia* coli. Antimicrobial activity of CdTe QDs was tested by colony-forming assay and atomic force microscopy (AFM). Obtained results show that the QDs can efficiently kill the bacteria. Antimicrobial activity of CdTe QDs was in a concentration-dependent mode. Based on these results, the authors proposed that the mechanism of the antimicrobial activity of CdTe QDs involves QDs-bacteria association and a reactive oxygen species-mediated pathway. Thus, CdTe QDs could have the potential to be formulated as a novel antimicrobial material with excellent optical properties [180].

1.6 Applications of quantum dots

The usefulness and application of QDs is continuous to expand and due to their applications QDs are getting much attention. In ODs optoelectronic properties can be tuned by tuning size due to quantum confinement effect. Due to this property these QDs can be applied in various optoelectronic devices and biomedical applications.

1.6.1 Quantum dots in solar cells

Solar cells based on QDs are more cost-effective as compared to their silicon solar cells counterparts. Generally solar cell consists of large silicon p-n junctions. When this solar cell absorb a photon of light having energy greater than band gap of silicon than a single electron get excited with the energy exactly equal to band gap energy. The photon having lesser energy than band gap are transmitted by silicon and these photons do not contribute in power output. But now these days due to increasing demands of energy for human activity it is necessary to pay attention for clean and abundant solar energy. Around $9 \times 10^{22} j$ of energy from the sun reaches the earth everyday and only $9 \times 10^{18} j$ of energy is consumable by mankind per day. Maximum thermodynamic efficiency of solar cell is 31%.Thus there is need of solar cell which exhibit higher conversion efficiency. Quantum dots can offer a significant increase in efficiency, by using dots of varying sizes top of each other with the largest band gaps on top. Incoming photons will be transmitted until reaching a layer with a bandgap smaller than the photon energy. With enough layers each photon will excite an electron with a bandgap close to its own energy and thus waste a small amount of energy. When the number of layers approaches infinity, the

efficiency approaches a theoretical thermodynamic limit of 86%. ZnO, CdSe, PbSe, PbS, CuInS2 and CuInSe2 are the QDs which have been previously used in inorganic-organic hybrid solar cell [181].

1.6.2 Quantum dots in light emitting diode

Quantum dots can be used in light emitting diode due to their luminescent behavior. These QD based LED's replace organic light emitting diodes (OLED) because of their many advantages over OLED. FWHM of QLED is 20-30 nm this low FWHM value is required for fine quality image. In comparison with OLED's these QLED's show high thermal stability. Because of high stability of QLED they have longer life time. OLED usually changes color with time because of difference in life span of red, green and blue pixel but this problem is completely omitted in QDs because all three colors can be obtained from QDs of same composition with different size [182].

1.6.3 Photonic applications of quantum dots

There is need of developing optical signal processor which has better performance and these processor make possible proficient and quick transmit of information. Photonic integrated circuits (PICs) of Chip-scale which are multifunctional are necessary for dropping cost. Chief obstruction to quick development of integrated photonic systems is complexity of integrating high attainment multiple photonic functions on a chip at low price. The majorities of practices are material precise and need exclusive fabrication tackle in addition to unsuited with silicon. Moreover, use of quantum dots as active medium permits researchers to apprehend PICs on silicon stage and cover up broad spectral range. QDs entrenched composites were utilized to exhibit photorefractivity and extra nonlinear optoelectronic properties [183]. In literature PbSe QDs in polymeric host were having great photoconductivity, photorefraction and optical gain [184].

1.6.4 Quantum dots for cancer diagnostic

One of the major health problems in the world is cancer. Diagnosing cancer in its starting stage is a challenge. Molecules which show fluorescent property play major role in cancer detection. Synthesis, development of biocompatible fluorescent QDs is one of the major research areas.

QDs having NIR emission can be used for lymph node mapping to aid biopsy and surgery. In vivo tumors can also be targeted by QDs by conjugate them with peptide and antibodies.

1.6.5 Quantum dots in bioimaging

Most used imaging techniques in biology are nuclear imaging, optical imaging magnetic resonance imaging (MRI) in biological systems [185]. Sensitivity, resolution and operational cost of these techniques are different. On the other hand, many times these imaging technique are identical to each other. Numerous assessments are there based on physical origin of these techniques [186], the instrumentation [187] and problem that influence their working [188]. At present, unique luminescent features of QDs in biological imaging is great area of research [189]. Previously organic dyes were also used for optical bioimaging [190], but there are numerous disadvantages associated with their use.

In visible range cell auto fluorescence results in following effects (1) Signals from organic dye get masked by cell autofluorescence in visible range (2) under photo-irradiation these organic dyes are instable (3) Due to broad emission spectra of organic dyes having long tail at red end cause spectral crossing of different detection channels and generate difficulty to estimate amounts of different probes. As compare to organic dyes QDs have high Quantum yield, less photobleaching, tunable absorbance and emissions spectra. QDs having emission in NIR range are extra acquiescent for deep tissue imaging. From above discussion it is concluded that photostability of inorganic QDs is more as compare to organic molecules, fluorescent feature is also extra saturated [191].

1.6.6 Quantum dots for heavy metal detection

Industrial residue and waste water mainly produce heavy metal pollution. Contamination of heavy metal cause threat to human health and have effect on quality and quality of aquaculture. Thus it's necessary to detect heavy metals in water. Concentration of heavy metal and fluorescence intensity of QDs has a realtion depend on increase in florescence intensity and quenching of fluorescence Intensity. Because of this fluorescent property of these QDs can be used for detection of heavy metals in water. Previously CdTe and CdSe/ZnS QDs are reported for detection of Hg^{2+} and Cu^{2+} [192].

1.6.7 Quantum dots in food science

QDs have important applications in food science. Optical sensor based on CdSe/ZnS QDs have been used for detection of vanillin sensing in food samples. One more group reported detection of melamine sample in milk. In food science these optical QDs can be used for protein and pathogenic detection [193]. Some other applications of Quantum dots are presented in Table 1.2 and figure 1.10.
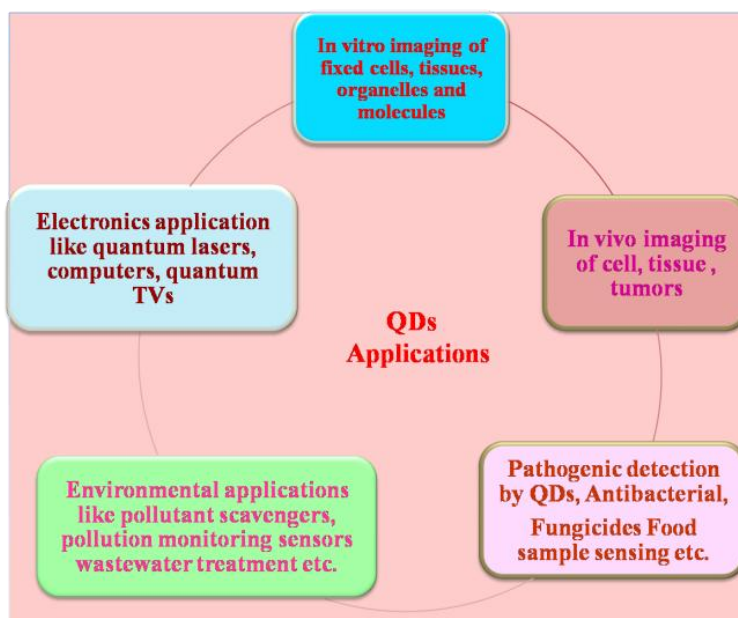
Figure 1.10: Applications of quantum dots in biology and environment

Table 1.2: Different reports on applications of QDs in different fields

	Applications	**Research group**	**References**
CdSe	Identification of bacteria and biochemical process of bacteria	J.A. Kloepfer et al	10.1128/AEM.71.5.2548-2557.2005
CdSe	Free cyanide determination in aqueous solution	Wei Jun Jin et al	10.1039/B414858D

	with high sensitivity		
CdSe	Labeling probe for imaging human mesenchymal stem cells	B.S.Shah et al	https://doi.org/10.1007/978-1-60761-901-7_4
CdSe	Filament tracking and cargo detection	A.Mansson et al	2004 Feb 6;314(2):529-34
CdSe	Deep tissue imaging of vasculature system	D.R.Larson et al	10.1126/science.1083780
CdSe/ZnS	Hela cell labeling	J.K.Jaiswal et al	10.1038/nbt767
CdSe/ZnS	Invitro biosensing	Kim E.Sapsford et al	10.3390/s6080925
CdSe/ZnS	Detection of hepatic cancer	Y.Xuefeng et al	doi.org/10.1117/1.2437744
CdSe/ZnS	Labelling of G-protein coupling receptors	W.Shi et al	10.1088/1748-6041/1/2/005
CdSe/ZnS	QDs based maltose sensor assembly	I.L.Medintz et al	10.1038/nmat961
CdTe	Imaging tool to label salmonella typhimurium cells	Li Hui et al	10.1021/ie060963s
CdTe	Detection of DNA Hybirdisation	S.Mazumder et al	10.1155/2009/815734
CdTe	Sensitive detector for the avian influenza virus subtype A/H5N1	Ung Thi Dieu Thuy et al	10.1088/2043-6262/1/4/045009
CdTe	Determination of	S.M. Brodsky	10.1007/s10512-013-9733-8

	uranium enrichment		
CdTe/Silica	Labelling protein and prevent leakage of toxic cadmium ion	A.Wolcott et al	10.1021/jp057435z
CdTe/PVP	Tool for fluorescent gene delivery reagent	S.Xiaofang	10.1049/mnl.2011.0551
CdTe/polymer nanocomposite	X-ray scintillation and imaging	Z.Kang et al	10.1063/1.3589366
CdTe/Sio2	Technological applications	L.G.Tartuci et al	10.1007/s11051-017-3947-y
Biosilica CdTe QDs	Photocatalytical applications	Marieta L. C. Passos	10.1039/C4RA09748C
CdSe/ZnS/Sio2	Phagokinetic track Imaging	Parak et al	https://doi.org/10.1002/1521-4095

1.7 Motivation behind the work

In past few years visible and NIR fluorescence imaging techniques have emerged that enables the bio imaging. Previously fluorescent organic dyes are used to image, target cell due to their light emitting characteristics. But these organic dyes have some limitations like high FWHM value, low stability, high photodegradation and photobleaching, less fluorescence time and poor signal. So there is need to prepare such a fluorescent material that should be highly stable and have brighter signals. QDs are highly stable and have tunable emission spectra. As compare to dyes these QDs have broad excitation and narrow emission spectra, low FWHM value and high fluorescence time. These outstanding features of QDs over organic dyes motivate us to work on QDs. Visible QDs can be utilized to image cells, tissues etc. But visible QDS cannot be used for deep tissue imaging because light in this range cannot penetrate to depth of tissue. Thus NIR window (700-900 nm) can be explored for sensitive detection. Thus NIR QDs with unique

optical properties can be utilized for deep tissue imaging due to both scattering and autofluorescence are reduced as wavelengths are increased. After surface functionalization of these QDs they show great ability to target and detect specific tissue. These QDs can be used to target specific cells or proteins using peptides, antibodies or ligands and than observed to study the target protein or the behavior of cells. Cell tracking; Fluorescence resonance energy transfer analysis can be achieved by QDs. Pathogen and toxin detection is also possible with these QDs.

1.8 Aims of the thesis

(i) Synthesis of highly luminescent II-VI group CdSe, ZnS, CdSe/ZnS core/shell, polymer (PEG, PVA) and silicates (TEOS) encapsulated structures.

(ii) Synthesis of NIR emitting II-VI group CdTe QDs and their polymer (PEG, PVA) and silicates (TEOS) encapsulated structures.

(ii) Characterization of QDs for structural, morphological, elemental, functional and optical properties using various techniques.

(iv) Biocompatibility and cytotoxicity testing of functionalized nanoparticles along with their photoluminescence studies to make them available for biomedical applications.

(v) Antimicrobial studies of prepared QDs.

1.9 Objectives of the thesis

1. OBJECTIVE-1: Synthesis and encapsulation of cadmium selenide (CdSe) quantum dots confined by 2-mercaptoethanol for defect free, improved and stable fluorescence in visible range.

2. OBJECTIVE-2: Precursor based synthesis of zinc sulfide (ZnS) and CdSe/ZnS nanostructures: Structural, morphological, elemental, optical and functional analysis.

3. OBJECTIVE-3: Synthesis and characterization of near infrared cadmium telluride (CdTe) quantum dots and their polymer encapsulated structures.

4. OBJECTIVE-4: Comprehensive investigation of cytotoxic and antimicrobial behavior of CdSe and CdTe based nanostructures.

1.10 References

1. Mazumder S., Dey R., Mitra M.K., Mukherjee S., Das G.C., *"Biofunctionalized quantum dots in biology and medicine",* Journal of Nanomaterials, pp. 38, Jan. 2009.

2. Xing Y., Rao J., *"Quantum dot bioconjugates for in vitro diagnostics & in vivo imaging",* Cancer Biomarkers, vol. 4(6), pp. 307-319, Jan. 2008.

3. Michalet X., Pinaud F.F., Bentolila L.A., Tsay J.M., Doose S.J.J.L., Li J.J., Weiss S., *"Quantum dots for live cells, in vivo imaging, and diagnostics"* , Science, vol. 307(5709), pp. 538-544, Jan. 2005.

4. Jin S., Hu Y., Gu Z., Liu L., Wu H.C., *"Application of quantum dots in biological imaging",* Journal of Nanomaterials, pp.13, Jan. 2011.

5. Mattoussi H., Mauro J.M., Goldman E.R., Anderson G.P., Sundar V.C., Mikulec F.V., Bawendi, M.G., *"Self-assembly of CdSe− ZnS quantum dot bioconjugates using an engineered recombinant protein",* Journal of the American Chemical Society, vol. 122(49), pp. 12142-12150, Dec. 2000.

6. Bailey R.E., Nie S., *Alloyed semiconductor quantum dots: tuning the optical properties without changing the particle size.* Journal of the American Chemical Society, vol. 125(23), pp. 7100-7106, June 2003.

7. Costa-Fernández J.M., Pereiro R., Sanz-Medel A., *"The use of luminescent quantum dots for optical sensing",* TrAC Trends in Analytical Chemistry, vol. 25(3), pp. 207-218, 2006.

8. Ma Q., Wang C., Su, X., *"Synthesis and application of quantum dot-tagged fluorescent microbeads",* Journal of nanoscience and nanotechnology, vol. 8(3), pp. 1138-1149, Mar. 2008.

9. Gao J., Chen X., Cheng Z., *"Near-infrared quantum dots as optical probes for tumor imaging",* Current topics in medicinal chemistry, vol. 10(12), pp. 1147-1157, Aug. 2010.

10. Murray C., Norris D.J., Bawendi M.G., *"Synthesis and characterization of nearly monodisperse CdE (E= sulfur, selenium, tellurium) semiconductor nanocrystallites",* Journal of the American Chemical Society, vol. 115(19), pp. 8706-8715, Sep. 1993.

11. Peng X., Manna L., Yang W., Wickham J., Scher E., Kadavanich A., Alivisatos A. P., *" Shape control of CdSe nanocrystals",* Nature, vol. 404(6773), pp. 59, Mar. 2000.

12. Chen N., He Y., Su Y., Li X., Huang Q., Wang H., Fan C., *"The cytotoxicity of cadmium-based quantum dots",* Biomaterials, vol. 33(5), pp. 1238-1244, Feb. 2012.

13. Pellegrino T., Manna L., Kudera S., Liedl T., Koktysh D., Rogach A. L., Parak W. J., "*Hydrophobic nanocrystals coated with an amphiphilic polymer shell: a general route to water soluble nanocrystals",* Nano letters, vol. 4(4), pp.703-707, Apr. 2004.

14. Kumari A., Singh R.R., *"Encapsulation of highly confined CdSe quantum dots for defect free luminescence and improved stability",* Physica E: Low-dimensional Systems and Nanostructures, vol. 89, pp. 77-85, May 2017.

15. Mahajan M.R.S., Dubey R.B., Mahajan J., *"Characteristics and properties of CdSe quantum dots",* Int. J. Latest Res. Sci. Tech, vol. 2, pp. 457-459, 2013.

16. Weissleder R., *"A clearer vision for in vivo imaging",* Nature biotechnology, vol.19, pp. 316-317, Apr. 2001.

17. Yang W., Guo W., Gong X., Zhang B., Wang S., Chen N., Chang J., *"Facile synthesis of Gd–Cu–In–S/ZnS bimodal quantum dots with optimized properties for tumor targeted fluorescence/MR in vivo imaging",* ACS applied materials & interfaces, vol. 7(33), pp. 18759-18768, 2015.

18. Guo W., Yang W., Wang Y., Sun X., Liu Z., Zhang B., Chen X., *"Color-tunable Gd-Zn-Cu-In-S/ZnS quantum dots for dual modality magnetic resonance and fluorescence imaging",* Nano research, vol. 7(11), pp. 1581-1591, 2014.

19. Hilger I., Leistner Y., Berndt A., Fritsche C., Haas K.M., Kosmehl H., Kaiser W.A., *"Near-infrared fluorescence imaging of HER-2 protein over-expression in tumour cells",* European radiology, vol. 14(6), pp. 1124-1129, June 2004.

20. Wang F., Tan W.B., Zhang Y., Fan X., Wang M*., "Luminescent nanomaterials for biological labeling",* Nanotechnology, vol. 17(1), Nov. 2005.

21. Jamieson T., Bakhshi R., Petrova D., Pocock R., Imani M., Seifalian A.M., *" Biological applications of quantum dots",* Biomaterials, vol. 28(31), pp. 4717-4732, Nov. 2007.

22. Hyun B.R., Chen H., Rey D.A., Wise F.W., Batt C.A., *"Near-infrared fluorescence imaging with water-soluble lead salt quantum dots"*, The Journal of Physical Chemistry B, vol. 111(20), pp. 5726-5730, May 2007.

23. Kobayashi H., Ogawa M., Alford R., Choyke P.L., Urano Y., *"New strategies for fluorescent probe design in medical diagnostic imaging'*, Chemical reviews, vol. 110(5), pp. 2620-2640, Dec. 2009.

24. Nomoev A.V., Bardakhanov S.P., Schreiber M., Bazarova D.G., Romanov N.A., Baldanov B.B., Syzrantsev V.V., *"Structure and mechanism of the formation of core–shell nanoparticles obtained through a one-step gas-phase synthesis by electron beam evaporation"*, Beilstein journal of nanotechnology, vol. 6, pp. 874, 2015.

25. Sahu G., Wang K., Gordon S.W., Zhou W., Tarr M.A., *"Core-shell Au–TiO 2 nanoarchitectures formed by pulsed laser deposition for enhanced efficiency in dye sensitized solar cells"*, RSC Advances, vol. 2(9), pp. 3791-3800, 2012.

26. Ishii M., Kato H., Hashimoto I., Homma, Y., *"Graphite-encapsulated alumina nanoparticles fabricated by hot-filament chemical vapor deposition"*, Materials Express, vol. 3(4), pp. 355-359, Dec. 2013.

27. Ishii M., Kato H., Hashimoto I., Homma Y., *"Synthesis of sapphire nanoparticles with graphite shells by hot-filament chemical vapor deposition"*, Materials Express, vol. 4(2), pp. 135-143, Apr. 2014.

28. Nomoev A.V., Bardakhanov S.P., Schreiber M., Bazarova D.G., Romanov N.A., Baldanov B.B., Syzrantsev V.V., *"Structure and mechanism of the formation of core–shell nanoparticles obtained through a one-step gas-phase synthesis by electron beam evaporation"*, Beilstein journal of nanotechnology, vol. 6, pp. 874, 2015.

29. Dorfs D., Hickey S., Eychmüller A., *"Type‐I and Type‐II Core–Shell Quantum Dots: Synthesis and Characterization"*, Nanotechnologies for the Life Sciences, Jan. 2011.

30. Rossetti R., Brus, L., *"Electron-hole recombination emission as a probe of surface chemistry in aqueous cadmium sulfide colloids"*, The Journal of Physical Chemistry, vol. 86(23), pp. 4470-4472, Nov. 1982.

31. Smith A.M., Nie S., *"Semiconductor nanocrystals: structure, properties, and band gap engineering",* Accounts of chemical research, vol. 43(2), pp.190-200, Oct. 2009.

32. Gomez D.E., Califano M., Mulvaney P., *"Optical properties of single semiconductor nanocrystals",* Physical Chemistry Chemical Physics, Vol. 8(43), pp. 4989-5011, 2006.

33. Algar W.R., Krull U.J., *"Quantum dots for the development of optical biosensors based on fluorescence",* Biosensing Using Nanomaterials, pp. 199-245, Mar. 2009.

34. Tsukasaki Y., Morimatsu M., Nishimura G., Sakata T., Yasuda H., Komatsuzaki A., Jin T., *"Synthesis and optical properties of emission-tunable PbS/CdS core–shell quantum dots for in vivo fluorescence imaging in the second near-infrared window",* RSC Advances, vol. 4(77), pp. 41164-41171, 2014.

35. Nakane Y., Tsukasaki Y., Sakata T., Yasuda H., Jin T., "Aqueous synthesis of glutathione-coated PbS quantum dots with tunable emission for non-invasive fluorescence imaging in the second near-infrared biological window (1000–1400 nm)", Chemical Communications, vol. 49(69), pp. 7584-7586, 2013.

36. Sasaki A., Tsukasaki Y., Komatsuzaki A., Sakata T., Yasuda H., Jin T., *" Recombinant protein (EGFP-Protein G)-coated PbS quantum dots for in vitro and in vivo dual fluorescence (visible and second-NIR) imaging of breast tumors",* Nanoscale, vol. 7(12), pp. 5115-5119, Mar. 2015.

37. Jin T., Imamura Y., *"Applications of highly bright pbs quantum dots to non-invasive near-infrared fluorescence imaging in the second optical window",* ECS Journal of Solid State Science and Technology, vol. 5(1), pp. R3138-R3145, Jan. 2016.

38. Imamura Y., Murakami Y., Matsumoto N., Matsumoto H., Mitani S., Shimizu K., Jin T., *"In Vivo Imaging of Septic Encephalopathy",* In Sepsis, 2017.

39. Imamura Y., Yamada S., Tsuboi S., Nakane Y., Tsukasaki Y., Komatsuzaki A., Jin T., *"Near-infrared emitting PbS quantum dots for in vivo fluorescence imaging of the thrombotic state in septic mouse Brain",* Molecules, vol. 21(8), pp.1080, Aug.2016.

40. Bozyigit D., Volk S., Yarema O., Wood V., *"Quantification of deep traps in nanocrystal solids, their electronic properties, and their influence on device behavior",* Nano letters, vol. 13(11), pp. 5284-5288, Oct. 2013.

41. Califano M., Franceschetti A., Zunger A., *"Temperature dependence of excitonic radiative decay in CdSe quantum dots: the role of surface hole traps",* Nano Letters, vol. 5(12), pp. 2360-2364, Dec. 2005.

42. Almeida A.J., Sahu A., Riedinger A., Norris D.J., Brandt M.S., Stutzmann M., Pereira R.N., *"Charge Trapping Defects in CdSe Nanocrystal Quantum Dots",* The Journal of Physical Chemistry C, vol. 120(25), pp. 13763-13770, June 2016.

43. Hardman R. *"A toxicologic review of quantum dots: toxicity depends on physicochemical and environmental factors",* Environmental health perspectives, vol. 114 (2), pp.165, Feb. 2006.

44. Derfus A.M., Chan W.C., Bhatia S.N., *"Probing the cytotoxicity of semiconductor quantum dots",* Nano letters, vol. 4(1), pp. 11-18, Jan. 2004.

45. Nguyen K.C., Seligy V.L., Tayabali A.F., *"Cadmium telluride quantum dot nanoparticle cytotoxicity and effects on model immune responses to Pseudomonas aeruginosa",* Nanotoxicology, vol. 7(2), pp. 202-211, 2013.

46. Pinaud F., King D., Moore H.P., Weiss S., *"Bioactivation and cell targeting of semiconductor CdSe/ZnS nanocrystals with phytochelatin-related peptides",* Journal of the American Chemical Society, vol. 126(19), pp. 6115-6123, May 2004.

47. Pellegrino T., Manna L., Kudera S., Liedl T., Koktysh D., Rogach A.L., Parak W.J., *"Hydrophobic nanocrystals coated with an amphiphilic polymer shell: a general route to water soluble nanocrystals",* Nano letters, vol. 4(4), pp. 703-707, 2004.

48. Lin C.A.J., Sperling R.A., Li J.K., Yang T.Y., Li P.Y., Zanella M., Parak W.J., *"Design of an amphiphilic polymer for nanoparticle coating and functionalization",* Small, vol. 4(3), pp. 334-341, Mar. 2008.

49. Correa-Duarte M.A., Giersig M., Liz-Marzan L.M., *"Stabilization of CdS semiconductor nanoparticles against photodegradation by a silica coating procedure",* Chemical Physics Letters, vol. 286(5-6), pp. 497-501, Apr. 1998.

50. Kirchner C., Liedl T., Kudera S., Pellegrino T., Muñoz Javier A., Gaub H.E., Parak W.J.,. *"Cytotoxicity of colloidal CdSe and CdSe/ZnS nanoparticles",* Nano letters, vol. 5(2), pp. 331-338, Feb. 2005.

51. Hoshino A., Fujioka K., Oku T., Suga M., Sasaki Y.F., Ohta T.,Yamamoto K., *"Physicochemical properties and cellular toxicity of nanocrystal quantum dots depend on their surface modification",* Nano Letters, vol.4(11), pp. 2163-2169, Nov. 2004.

52. Alivisatos A.P., Gu W., Larabell C., *"Quantum dots as cellular probes",* Annu. Rev. Biomed, Eng., vol. 7, pp. 55-76, Aug. 2005.

53. Medintz I.L., Uyeda H.T., Goldman E.R., Mattoussi H., *"Quantum dot bioconjugates for imaging, labelling and sensing",* Nature materials, vol. 4(6), pp. 435, June 2005.

54. Klostranec J.M., Chan W.C., *"Quantum dots in biological and biomedical research: recent progress and present challenges",* Advanced Materials, vol. 18 (15), pp. 1953-1964, Aug. 2006.

55. Mulvaney P., Liz-Marzan L.M., Giersig M., Ung T., *"Silica encapsulation of quantum dots and metal clusters",* Journal of Materials Chemistry, vol. 10(6), pp. 1259-1270, 2000.

56. Yang Y., Gao M.Y., *"Preparation of fluorescent SiO2 particles with single CdTe nanocrystal cores by the reverse microemulsion method",* Advanced Materials, vol. 17(19), pp. 2354-2357, Oct. 2005.

57. Bruchez M., Moronne M., Gin P., Weiss S., Alivisatos A.P., *"Semiconductor nanocrystals as fluorescent biological labels",* Science, vol. 281(5385), pp. 2013-2016, Sep.1998.

58. Gerion D., Pinaud F., Williams S.C., Parak W.J., Zanchet D., Weiss S., Alivisatos, A.P., *"Synthesis and properties of biocompatible water-soluble silica-coated CdSe/ZnS semiconductor quantum dots",* The Journal of Physical Chemistry B, vol. 105(37), pp. 8861-8871, Sep. 2001.

59. Parak W.J., Gerion D., Pellegrino T., Zanchet D., Micheel C., Williams S.C., Alivisatos A.P., *"Biological applications of colloidal nanocrystals",* Nanotechnology, vol. 14(7), pp.15, June 2003.

60. Lu J., Liong M., Li Z., Zink J.I., Tamanoi F., *"Biocompatibility, biodistribution, and drug-delivery efficiency of mesoporous silica nanoparticles for cancer therapy in animals",* Small, vol. 6(16), pp.1794-1805, Aug. 2010.

61. Wu S.H., Lin Y.S., Hung Y., Chou Y.H., Hsu Y.H., Chang C., Mou C.Y., *"Multifunctional mesoporous silica nanoparticles for intracellular labeling and animal magnetic resonance imaging studies"*, ChemBioChem, vol. 9(1), pp. 53-57, Jan. 2008.

62. Wang D., Qian J., Cai F., He S., Han S., Mu Y., *"Green'-synthesized near-infrared PbS quantum dots with silica–PEG dual-layer coating: ultrastable and biocompatible optical probes for in vivo animal imaging"*, Nanotechnology, vol. 23(24), pp. 245701, May 2012.

63. Pericleous P., Gazouli M., Lyberopoulou A., Rizos S., Nikiteas N., Efstathopoulos E. P., *"Quantum dots hold promise for early cancer imaging and detection"* International journal of cancer, vol. 131(3), pp. 519-528, Aug. 2012.

64. Richards D., Ivanisevic A., *"Inorganic material coatings and their effect on cytotoxicity"*, Chemical Society Reviews, vol. 41(6), pp. 2052-2060, 2012.

65. Selvan S.T., "Silica-coated quantum dots and magnetic nanoparticles for bioimaging applications (Mini-Review)", Biointerphases, vol. 5(3), pp. FA110-FA115, Sep. 2010.

66. Ohmori M., Matijević E., *"Preparation and properties of uniform coated colloidal particles VII. Silica on hematite"*, Journal of Colloid and Interface Science, vol. 150(2), pp. 594-598, 1992.

67. Yang Y., Gao M.Y., *"Preparation of fluorescent SiO2 particles with single CdTe nanocrystal cores by the reverse microemulsion method"*, Advanced Materials, vol. 17(19), pp. 2354-2357, Oct. 2005.

68. Riassetto D., Ma N., Amador J., Benson B., Briggs A., Mella M., Bartl, M.H., *"Biphasic route to silica-encapsulation of quantum dots"*, Nanoscience and Nanotechnology Letters, vol. 3(5), pp. 655-658, Oct. 2011.

69. Lee A., Wang T., Kim J.H., Yoon H.H., Park, S.J., *"Synthesis of Silica Encapsulated ZnSe Quantum Dots by Microemulsion Method"*, Molecular Crystals and Liquid Crystals, Vol. 564(1), pp. 10-17, Sep. 2012.

70. Selvan S.T., Li C., Ando M., Murase N., *"Formation of luminescent CdTe–Silica nanoparticles through an inverse microemulsion technique"*, Chemistry letters, vol. 33(4), pp. 434-435, Mar. 2004.

71. Dong H., Liu Y., Ye Z., Zhang W., Wang G., Liu Z., Yuan, J., *"Luminescent Nanoparticles of Silica‑Encapsulated Cadmium–Tellurium (CdTe) Quantum Dots with a Core–Shell Structure: Preparation and Characterization"*, Helvetica Chimica Acta, vol. 92(11), pp. 2249-2256, Nov. 2009.

72. Pöselt E., Schmidtke C., Fischer S., Peldschus K., Salamon J., Kloust H., Schumacher U., *"Tailor-made quantum dot and iron oxide based contrast agents for in vitro and in vivo tumor imaging"*, ACS nano, vol. 6(4), pp. 3346-3355, Apr. 2012.

73. Puzder A., Williamson A.J., Zaitseva N., Galli G., Manna L., Alivisatos A.P., *"The effect of organic ligand binding on the growth of CdSe nanoparticles probed by ab initio calculations"*, Nano Letters, vol. 4(12), pp. 2361-2365, 2004.

74. Wang J., Han S., Ke D.,Wang R., *"Semiconductor quantum dots surface modification for potential cancer diagnostic and therapeutic applications"*, Journal of Nanomaterials, pp.1, Jan. 2012.

75. Wu X., Liu H., Liu J., Haley K. N., Treadway J.A., Larson J.P., Bruchez M.P., *"Immunofluorescent labeling of cancer marker Her2 and other cellular targets with semiconductor quantum dots"*, Nature biotechnology, vol. 21(1), pp. 41, Jan. 2003.

76. Xing Y., Rao J., *"Quantum dot bioconjugates for in vitro diagnostics & in vivo imaging"*, Cancer Biomarkers, vol. 4(6), pp. 307-319, Jan. 2008.

77. Pinaud F., King D., Moore H.P., Weiss S., *"Bioactivation and cell targeting of semiconductor CdSe/ZnS nanocrystals with phytochelatin-related peptides"*, Journal of the American Chemical Society, vol. 126(19), pp. 6115-6123, May 2004.

78. Åkerman M.E., Chan W.C., Laakkonen P., Bhatia S.N., Ruoslahti E., *"Nanocrystal targeting in vivo"*, Proceedings of the National Academy of Sciences, vol. 99(20), pp. 12617-12621, Oct. 2002.

79. Slocik J.M., Moore J.T., Wright D.W., *"Monoclonal antibody recognition of histidine-rich peptide encapsulated nanoclusters"*, Nano Letters, vol. 2(3), pp. 169-173, Mar. 2002.

80. Hainfeld J.F., Liu W., Halsey C.M., Freimuth P., Powell, R.D., *"Ni–NTA–gold clusters target His-tagged proteins"*, Journal of structural biology, vol. 127(2), pp. 185-198, 1999.

81. Mattoussi H., Mauro J.M., Goldman E.R., Anderson G.P., Sundar V.C., Mikulec F.V., Bawendi M.G., *"Self-assembly of CdSe− ZnS quantum dot bioconjugates using an engineered recombinant protein",* Journal of the American Chemical Society, vol. 122(49), pp. 12142-12150, 2000.

82. Pal S.L., Jana U., Manna P.K., Mohanta G.P., Manavalan, R., *"Nanoparticle: An overview of preparation and characterization",* pp.2000-2010, 2011.

83. Hasany S.F., Ahmed I., Rajan J., Rehman, A., *"Systematic review of the preparation techniques of iron oxide magnetic nanoparticles",* Nanoscience and Nanotechnology, vol. 2(6), pp. 148-158, 2012.

84. Lue J.T., *"Physical properties of nanomaterials",* Encyclopedia of nanoscience and nanotechnology, vol. 10(1), pp. 1-46, 2007.

85. Tsutsui K., Hu E.L.,Wilkinson, C.D., *"Reactive ion etched II-VI quantum dots: dependence of etched profile on pattern geometry",* Japanese journal of applied physics, vol. 32(12S), pp. 6233, 1993.

86. Scherer A., Craighead H.G., Beebe E.D., *"Gallium arsenide and aluminum gallium arsenide reactive ion etching in boron trichloride/argon mixtures",* Journal of Vacuum Science & Technology B: Microelectronics Processing and Phenomena, vol. 5(6), pp. 1599-1605, 1987.

87. Chason E., Picraux S.T., Poate J.M., Borland J.O., Current M.I., Diaz de La Rubia T., Mayer J.W., *"Ion beams in silicon processing and characterization",* Journal of applied physics, vol. 81(10), pp. 6513-6561, 1997.

88. Burda C., Chen X., Narayanan R., El-Sayed M.A., *"Chemistry and properties of nanocrystals of different shapes",* Chemical reviews, vol. 105(4), pp.1025-1102, Apr. 2005.

89. Spanhel L., Haase M., Weller H., Henglein A., *"Photochemistry of colloidal semiconductors. 20. Surface modification and stability of strong luminescing CdS particles",* Journal of the American Chemical Society, vol. 109(19), pp. 5649-5655, 1987.

90. Bang J., Yang H., Holloway P.H., *"Enhanced and stable green emission of ZnO nanoparticles by surface segregation of Mg",* Nanotechnology, vol. 17(4), pp. 973, Jan. 2006.

91. Bera, D., Qian, L., Sabui, S., Santra, S., Holloway, P. H., *"Photoluminescence of ZnO quantum dots produced by a sol–gel process Optical Materials",* vol. 30 (8), pp. 1233-1239, Apr. 2008.

92. Spanhel L., Anderson M.A., *"Semiconductor clusters in the sol-gel process: quantized aggregation, gelation, and crystal growth in concentrated zinc oxide colloids",* Journal of the American Chemical Society, vol. 113 (8), pp. 2826-2833, Apr. 1991.

93. Bera D., Qian L., Holloway P.H*., "Time-evolution of photoluminescence properties of ZnO/MgO core/shell quantum dots",* Journal of Physics D: Applied Physics, vol. 41(18), pp. 182002, Aug. 2008.

94. Sashchiuk A., Lifshitz E., Reisfeld R., Saraidarov T., Zelner M., Willenz A., *"Optical and conductivity properties of PbS nanocrystals in amorphous zirconia sol-gel films",* Journal of sol-gel science and technology, vol. 24(1), pp. 31-38, May 2002.

95. Colvin V.L., Goldstein A.N., Alivisatos A.P., *"Semiconductor nanocrystals covalently bound to metal surfaces with self-assembled monolayers",* Journal of the American Chemical Society, vol. 114(13), pp. 5221-5230, June 1992.

96. Yang H., Holloway P.H., Cunningham G., Schanze K.S., *"CdS: Mn nanocrystals passivated by ZnS: Synthesis and luminescent properties"* The Journal of chemical physics, vol. 121(20), pp.10233-10240, Nov. 2004.

97. Yang H., Holloway, P.H., *"Efficient and photostable ZnS-passivated CdS: Mn luminescent nanocrystals",* Advanced Functional Materials, vol. 14 (2), pp. 152-156, Feb. 2004.

98. Yang H., Santra S., Holloway P.H*., "Syntheses and applications of Mn-doped II-VI semiconductor nanocrystals"* Journal of nanoscience and nanotechnology, vol. 5(9), pp. 1364-1375, Sep. 2005.

99. Yang H., Holloway, P.H., *"Enhanced photoluminescence from CdS: Mn/ZnS core/shell quantum dots",* Applied Physics Letters, vol. 82(12), pp. 1965-1967, Mar. 2003.

100. Kortan A.R., Hull R., Opila R.L., Bawendi M.G., Steigerwald M.L., Carroll P.J., Brus L.E., *"Nucleation and growth of cadmium selendie on zinc sulfide quantum crystallite seeds, and vice*

versa, in inverse micelle media", Journal of the American Chemical Society, vol. 112(4), pp. 1327-1332, Feb. 1990.

101. Hoener C.F., Allan K.A., Bard A.J., Campion A., Fox M.A., Mallouk T.E., White J.M., *"Demonstration of a shell-core structure in layered cadmium selenide-zinc selenide small particles by x-ray photoelectron and Auger spectroscopies",* The Journal of Physical Chemistry, vol. 96(9), pp. 3812-3817, 1992.

102. Karanikolos G.N., Alexandridis P., Itskos G., Petrou A., Mountziaris T.J., *"Synthesis and Size Control of Luminescent ZnSe Nanocrystals by a Microemulsion− Gas Contacting Technique",* Langmuir, vol. 20(3), pp. 550-553, Feb. 2004.

103. Ogawa S., Hu K., Fan F. R. F., Bard, A. J., *"Photoelectrochemistry of films of quantum size lead sulfide particles incorporated in self-assembled monolayers on gold",* The Journal of Physical Chemistry B, vol. 101(29), pp. 5707-5711, July 1997.

104. Murray C., Norris D.J., Bawendi M.G., *"Synthesis and characterization of nearly monodisperse CdE (E= sulfur, selenium, tellurium) semiconductor nanocrystallites",* Journal of the American Chemical Society, vol. 115(19), pp. 8706-8715, 1993.

105. Qu L., Peng Z.A., Peng X., *"Alternative routes toward high quality CdSe nanocrystals",* Nano Letters, vol. 1(6), pp. 333-337, June 2001.

106. Lee H., Holloway P.H., Yang H., *"Synthesis and characterization of colloidal ternary ZnCdSe semiconductor nanorods",* The Journal of chemical physics, vol. 125(16), pp. 164711, Oct. 2006.

107. Bae Y., Myung N., Bard A.J., *"Electrochemistry and electrogenerated chemiluminescence of CdTe nanoparticles",* Nano Letters, vol. 4 (6), pp. 1153-1161, June 2004.

108. Hines M.A., Guyot-Sionnest P., *"Bright UV-blue luminescent colloidal ZnSe nanocrystals",* The Journal of Physical Chemistry B, vol. 102(19), pp. 3655-3657, May 1998.

109. Bakueva L., Musikhin S., Hines M.A., Chang T.W., Tzolov M., Scholes G.D., Sargent E.H., *"Size-tunable infrared (1000–1600 nm) electroluminescence from PbS quantum-dot nanocrystals in a semiconducting polymer",* Applied physics letters, vol. 82(17), pp. 2895-2897, Apr. 2003.

110. Battaglia D., Peng X., *"Formation of high quality InP and InAs nanocrystals in a noncoordinating solvent",* Nano Letters, vol. 2(9), pp. 1027-1030, Sep. 2202.

111. Zhang H., Wang L.P., Xiong H., Hu L., Yang B., Li W., *"Hydrothermal Synthesis for High‑Quality CdTe Nanocrystals",* Advanced Materials, vol. 15(20), pp. 1712-1715, Oct. 2003.

112. Li M., Ge Y., Chen Q., Xu S., Wang N., Zhang, X., *"Hydrothermal synthesis of highly luminescent CdTe quantum dots by adjusting precursors' concentration and their conjunction with BSA as biological fluorescent probes", Talanta*, vol. 72(1), pp. 89-94, Apr. 2007.

113. Yang W.H., Li W.W., Dou H.J., Sun, K., *"Hydrothermal synthesis for high-quality CdTe quantum dots capped by cysteamine"*, Materials Letters, vol. 62(17-18), pp. 2564-2566, June 2008.

114. Zhao D., He Z., Chan W.H., Choi, M.M., *"Synthesis and characterization of high-quality water-soluble near-infrared-emitting CdTe/CdS quantum dots capped by N-acetyl-L-cysteine via hydrothermal method",* The Journal of Physical Chemistry C, vol. 113(4), pp.1293-1300, Dec. 2008.

115. Wang, J., Han H., *"Hydrothermal synthesis of high-quality type-II CdTe/CdSe quantum dots with near-infrared fluorescence",* Journal of colloid and interface science, vol. 351(1), pp. 83-87, Nov. 2010.

116. Mao W., Guo J., Yang W., Wang C., He J., Chen J., *"Synthesis of high-quality near-infrared-emitting CdTeS alloyed quantum dots via the hydrothermal method",* Nanotechnology, vol. 18(48), pp. 485611, Nov. 2007.

117. Jin T., Fujii F., Komai Y., Seki J., Seiyama A., Yoshioka Y., *"Preparation and characterization of highly fluorescent, glutathione-coated near infrared quantum dots for in vivo fluorescence imaging", International journal of molecular sciences*, vol. 9(10), pp. 2044-2061, Oct. 2008.

118. Peng Z.A., Peng X., *"Formation of high-quality CdTe, CdSe, and CdS nanocrystals using CdO as precursor",* Journal of the American Chemical Society, vol. 123(1), pp. 183-184, Jan. 2001.

119. He R., You X., Tian H., Gao F., Cui D., Gu H., "Synthesis and characterization of monodisperse CdSe quantum dots in different organic solvents", *Frontiers of Chemistry in China*, vol. 1(4), pp. 378-383, Dec. 2006.

120. Zhou X., Kobayashi Y., Romanyuk V., Ochuchi N., Takeda M., Tsunekawa S., Kasuya A., *"Preparation of silica encapsulated CdSe quantum dots in aqueous solution with the improved optical properties",* Applied surface science, vol. 242(3-4), pp. 281-286, Apr. 2005.

121. Liu L., Peng Q., Li Y., *"Preparation of CdSe quantum dots with full color emission based on a room temperature injection technique", Inorganic chemistry*, vol. 47(11), pp. 5022-5028, May 2008.

122. Rogach A.L., Franzl T., Klar T.A., Feldmann J., Gaponik N., Lesnyak V., Donegan J.F., *"Aqueous synthesis of thiol-capped CdTe nanocrystals: state-of-the-art",* The Journal of Physical Chemistry C, vol. 111(40), pp. 14628-14637,Oct. 2007.

123. Li Z., Dong C., Tang L., Zhu X., Chen H., Ren J., *"Aqueous synthesis of CdTe/CdS/ZnS quantum dots and their optical and chemical properties",* Luminescence, vol. 26(6), pp. 439-448, Nov. 2011.

124. Dhar R., *"Synthesis of semiconductor quantum dots and study of their optical electrical property",* 2015.

125. Sun Q., Fu S., Dong T., Liu S., Huang C., "*Aqueous synthesis and characterization of TGA-capped CdSe quantum dots at freezing temperature",* Molecules, vol. 17(7), pp. 8430-8438, July 2012.

126. Ahamed A.J., Ramar K., Kumar, P.V., *"Chemical Synthesis of CdSe Nanoparticles by using Hydrazine Monohydrate as A Reducing Agent",* J. Environ. Nanotechnol, vol. 5(3), pp. 29-33, 2016.

127. Kim D., Mishima T., Tomihira K., Nakayama, M., *"Temperature dependence of photoluminescence dynamics in colloidal CdS quantum dots",* The Journal of Physical Chemistry C, vol. 112(29), pp. 10668-10673, June 2008.

128. Guo J., Yang W., Wang C., *"Systematic study of the photoluminescence dependence of thiol-capped CdTe nanocrystals on the reaction conditions",* The Journal of Physical Chemistry B, vol. 109(37), pp.17467-17473, Sep. 2005.

129. Sobhana S.L., Devi M.V., Sastry T.P., Mandal, A.B., *"CdS quantum dots for measurement of the size-dependent optical properties of thiol capping",* Journal of Nanoparticle Research, vol. 13(4), pp. 1747-1757, Apr. 2011.

130. Ding L., Zhou P.J., Li S.Q., Shi G.Y., Zhong T., Wu M., *"Spectroscopic studies on the thermodynamics of L-cysteine capped CdSe/CdS quantum dots—BSA interactions",* Journal of fluorescence, vol. 21(1), pp. 17-24, Jan. 2011.

131. Kalasad M.N., Rabinal M.K., Mulimani B.G., *"Ambient synthesis and characterization of high-quality CdSe quantum dots by an aqueous route",* Langmuir, vol. 25(21), pp.12729-12735, Aug. 2009.

132. Guo J., Yang W., Wang C., *"Systematic study of the photoluminescence dependence of thiol-capped CdTe nanocrystals on the reaction conditions",* The Journal of Physical Chemistry B, vol. 109(37), pp.17467-17473, Sep. 2005.

133. Zhou L., Gao C., Hu X., Xu W., *"One-pot large-scale synthesis of robust ultrafine silica-hybridized CdTe quantum dots",* ACS applied materials & interfaces, vol. 2(4), pp. 1211-1219, Mar. 2010.

134. Zeng Q., Kong X., Sun Y., Zhang Y., Tu L., Zhao J., Zhang H., *"Synthesis and optical properties of type II CdTe/CdS core/shell quantum dots in aqueous solution via successive ion layer adsorption and reaction",* The Journal of Physical Chemistry C, vol. 112(23), pp.8587-8593, May 2008.

135. Law W. C., Yong K. T., Roy I., Ding H., Hu R., Zhao W., Prasad P.N., *"Aqueous-Phase Synthesis of Highly Luminescent CdTe/ZnTe Core/Shell Quantum Dots Optimized for Targeted Bioimaging",* Small, vol. 5(11), pp. 1302-1310, June 2009.

136. Xia Y., Zhu C., *"Aqueous synthesis of type-II core/shell CdTe/CdSe quantum dots for near-infrared fluorescent sensing of copper (II)",* Analyst, vol. 133(7), pp. 928-932, 2008.

137. Li H., Shih W.Y., Shih W.H., *"Non-heavy-metal ZnS quantum dots with bright blue photoluminescence by a one-step aqueous synthesis",* Nanotechnology, vol. 18(20), pp. 205604, Apr. 2007.

138. Zheng Y., Yang Z., Ying J.Y., *"Aqueous Synthesis of Glutathione-Capped ZnSe and Zn1–xCdxSe Alloyed Quantum Dots",* Advanced Materials, vol. 19(11), pp.1475-1479, June 2007.

139. Zheng Y., Yang Z., Ying J.Y., *"Aqueous Synthesis of Glutathione-Capped ZnSe and Zn1–xCdxSe Alloyed Quantum Dots",* Advanced Materials, vol. 19(11), pp. 1475-1479, June 2007.

140. Zhai C., Zhang H., Du N., Chen B., Huang H., Wu Y., Yang D., *"One-pot synthesis of biocompatible CdSe/CdS quantum dots and their applications as fluorescent biological labels",* Nanoscale Res Lett, vol. 6(1), pp. 31, Dec. 2011.

141. Sharma P.K., Dutta R.K., Liu C.H., Pandey R., Pandey A.C., *"Surfactant mediated optical properties of cytosine capped CdSe quantum dots",* Materials Letters, vol. 64(10), pp.1183-1186, May 2010.

142. Grabolle M., Ziegler J., Merkulov A., Nann T., Resch-Genger U., *"Stability and fluorescence quantum yield of CdSe–ZnS quantum dots—influence of the thickness of the ZnS shell",* Annals of the New York Academy of Sciences, vol. 1130(1), pp. 235-241, May 2008.

143. Chu V.H., Nghiem T.H. L., Le T.H., Vu D.L., Tran H.N., Vu T.K.L., *"Synthesis and optical properties of water soluble CdSe/CdS quantum dots for biological applications",* Advances in natural sciences: nanoscience and nanotechnology, vol. 3(2), pp. 025017, May 2012.

144. Mathew S., Bhardwaj B.S., Saran A.D., Radhakrishnan P., Nampoori V.P.N., Vallabhan C.P.G., Bellare J.R., *"Effect of ZnS shell on optical properties of CdSe–ZnS core–shell quantum dots",* Optical materials, vol. 39, pp. 46-51, Jan. 2015.

145. Surana K., Singh P.K., Rhee H.W., Bhattacharya B., "*Synthesis, characterization and application of CdSe quantum dots",* Journal of Industrial and Engineering Chemistry, vol. 20(6), pp. 4188-4193,Nov. 2015.

146. Barik P., Mandal A.R., Kuznetsov D.V., Godymchuk A.Y., *"Synthesis and Optical Properties of CdSe and CdSe/ZnS Core/Shell Quantum Dots",* In Advanced Materials Research ,vol. 1085, pp. 176-181, 2015.

147. Abd Rahman S., Ariffin N., Yusof N.A., Abdullah J., Mohammad F., Ahmad Zubir Z., Nik Abd Aziz N.M.A., *"Thiolate-Capped CdSe/ZnS Core-Shell Quantum Dots for the Sensitive Detection of Glucose"*, Sensors, vol. 17(7), pp. 1537, July 2017.

148. Dunpall R., Nejo A.A., Pullabhotla V.S.R., Opoku A.R., Revaprasadu N., Shonhai A., *"An in vitro assessment of the interaction of cadmium selenide quantum dots with DNA, iron, and blood platelets"*, IUBMB life, vol. 64(12), pp. 995-1002, 2012.

149. Qu H., Cao L., Su G., Liu W., Gao R., Xia C., Qin J., *"Silica-coated ZnS quantum dots as fluorescent probes for the sensitive detection of Pb 2+ ions"*, Journal of nanoparticle research, Vol. 16(12), pp. 2762, Dec. 2014.

150. Bodo B., Singha R., *"Structural and Optical Properties of ZnS Quantum Dots synthesized by CBD method"* Vol. 6, Aug.2016.

151. Bodo B., Singha R., Das S.C., *"Structural and optical properties of chemically synthesized ZnS nanostructures"*, International Journal of Applied Physics and Mathematics, vol. 2(4), pp. 287, July 2012.

152. Viswanath R., Naik H.S.B., Somalanaik Y.K.G., Neelanjeneallu P.K.P., Harish K.N., Prabhakara M.C., *"Studies on characterization, optical absorption, and photoluminescence of yttrium doped ZnS nanoparticles"*, Journal of Nanotechnology, 2014.

153. Shahi A.K., Pandey B.K., Swarnkar R.K., Gopal, R., *"Surfactant assisted surface studies of zinc sulfide nanoparticles"*, Applied Surface Science, Vol. 257(23), pp. 9846-9851, Sep. 2011.

154. Li M., Zhou H., Zhang H., Sun P., Yi K., Wang M., Xu S., *"Preparation and purification of L-cysteine capped CdTe quantum dots and its self-recovery of degenerate fluorescence"*, Journal of luminescence, vol. 130(10), pp. 1935-1940, Oct. 2010.

155. Schulze A.S., Tavernaro I., Machka F., Dakischew O., Lips K.S., Wickleder M. S., *"Tuning optical properties of water-soluble CdTe quantum dots for biological applications"*, Journal of Nanoparticle Research, vol. 19(2), pp. 70, Feb. 2017.

156. Duan J., Song L., Zhan, J., *"One-pot synthesis of highly luminescent CdTe quantum dots by microwave irradiation reduction and their Hg 2+-sensitive properties"*, Nano Research, vol. 2(1), pp. 61-68, Jan. 2009.

157. Zhang Y.H., Zhang H.S., Ma M., Guo X.F., Wang H., *"The influence of ligands on the preparation and optical properties of water-soluble CdTe quantum dots"*, Applied Surface Science, vol. 255(9), pp. 4747-4753, Feb. 2009.

158. Zeng R., Zhang T., Liu J., Hu S., Wan Q., Liu X., Zou, B., *"Aqueous synthesis of type-II CdTe/CdSe core–shell quantum dots for fluorescent probe labeling tumor cells"*, Nanotechnology, vol. 20(9), pp. 095102, Feb. 2009.

159. Chang J.Y., Wang S.R., Yang C.H., *"Synthesis and characterization of CdTe/CdS and CdTe/CdSe core/shell type-II quantum dots in a noncoordinating solvent"*, Nanotechnology, vol. 18(34), pp. 345602, July 2007.

160. Weng J., Song X., Li L., Qian H., Chen K., Xu X., Ren J., *"Highly luminescent CdTe quantum dots prepared in aqueous phase as an alternative fluorescent probe for cell imaging"*, Talanta, vol. 70(2), pp. 397-402, Sep. 2006.

161. Saikia D., Chakravarty S., Sarma N.S., Bhattacharjee S., Datta P., Adhikary N.C., *"Aqueous synthesis of highly stable CdTe/ZnS Core/Shell quantum dots for bioimaging"*, Luminescence, vol. 32(3), pp. 401-408, May 2017.

162. Li Y., Wang W., Zhao D., Chen P., Du H., Wen Y., Zhang, X., *"Water-Soluble Fluorescent CdTe/ZnSe Core/Shell Quantum Dot: Aqueous Phase Synthesis and Cytotoxicity Assays"*, Journal of nanoscience and nanotechnology, vol. 15(6), pp. 4648-4652, June 2015.

163. Mandal A., Tamai N., *"Influence of acid on luminescence properties of thioglycolic acid-capped CdTe quantum dots"*, The Journal of Physical Chemistry C, vol. 112(22), pp. 8244-8250, May 2008.

164. Sheng W., Kim S., Lee J., Kim S. W., Jensen K., Bawendi M.G., *"In-situ encapsulation of quantum dots into polymer microspheres"*, Langmuir, vol. 22(8), pp. 3782-3790, Apr. 2006.

165. Batalla J., Cabrera H., San Martín-Martínez E., Korte D., Calderón A., Marín E., *"Encapsulation efficiency of CdSe/ZnS quantum dots by liposomes determined by thermal lens microscopy"*, Biomedical optics express, vol. 6(10), pp. 3898-3906, Oct. 2015.

166. Hu X., Zrazhevskiy P., Gao, X., "Encapsulation of single quantum dots with mesoporous silica", Annals of biomedical engineering, vol. 37(10), pp. 1960-1966, Oct. 2009.

167. Hu X., Gao X., *"Silica− Polymer Dual Layer-Encapsulated Quantum Dots with Remarkable Stability"*, Acs Nano, vol. 4(10), pp. 6080-6086, Oct. 2010.

168. Ma N., Marshall A.F., Gambhir S.S., Rao J*., "Facile synthesis, silanization, and biodistribution of biocompatible quantum dots"*, Small, vol. 6(14), pp. 1520-1528, July 2010.

169. Kim J.S., Cho K.J., Tran T.H., Nurunnabi M., Moon T.H., Hong S.M., Lee Y.K., *"In vivo NIR imaging with CdTe/CdSe quantum dots entrapped in PLGA nanospheres"*, Journal of colloid and interface science, vol. 353(2), pp. 363-371, Jan. 2011.

170. Rodríguez-Rodríguez H., Acebrón M., Juárez B.H., Arias-Gonzalez J.R., *"Luminescence Dynamics of Silica-Encapsulated Quantum Dots During Optical Trapping"*, The Journal of Physical Chemistry C, vol. 121(18), pp. 10124-10130, Apr. 2017.

171. Chang K., Men X., Chen H., Liu Z., Yin S., Qin W., Wu C., *"Silica-encapsulated semiconductor polymer dots as stable phosphors for white light-emitting diodes"*, Journal of Materials Chemistry C, vol. 3(28), pp.7281-7285, 2015.

172. Xu W., Du T., Xu C., Han H., Liang J., Xiao S., *"Evaluation of biological toxicity of CdTe quantum dots with different coating reagents according to protein expression of engineering Escherichia coli"*, Journal of Nanomaterials, Jan. 2015.

173. Vibin M., Vinayakan R., John A., Raji V., Rejiya C.S., Vinesh N.S., Abraham A., *"Cytotoxicity and fluorescence studies of silica-coated CdSe quantum dots for bioimaging applications"*, Journal of Nanoparticle Research, vol. 13(6), pp. 2587-2596, June 2011.

174. Wang L., Nagesha D. K., Selvarasah S., Dokmeci M. R., Carrier, R. L., *"Toxicity of CdSe nanoparticles in Caco-2 cell cultures"*, Journal of nanobiotechnology, vol. 6(1), pp. 11, Oct. 2008.

175. Chen N., He Y., Su Y., Li X., Huang Q., Wang H., Fan, C., *"The cytotoxicity of cadmium-based quantum dots"*, Biomaterials, vol. 33(5), pp. 1238-1244, Feb. 2012.

176. Su Y., Peng F., Jiang Z., Zhong Y., Lu Y., Jiang X., He, Y., *"In vivo distribution, pharmacokinetics, and toxicity of aqueous synthesized cadmium-containing quantum dots"*, Biomaterials, vol. 32(25), pp. 5855-5862, Sep. 2011.

177. Su Y., Peng F., Jiang Z., Zhong Y., Lu Y., Jiang X., He Y., *"In vivo distribution, pharmacokinetics, and toxicity of aqueous synthesized cadmium-containing quantum dots"*, Biomaterials, vol. 32(25), pp. 5855-5862, Sep. 2011.

178. Dhar R., Singh S., Kumar, A., *"Effect of capping agents on optical and antibacterial properties of cadmium selenide quantum dots"* Bulletin of Materials Science, vol. 38(5), pp. 1247-1252, 2015.

179. Parvin N., Amiri G., Karbasizadeh V., *"Antibacterial effect assessment of ZnS: Ag nanoparticles"* Nanomedicine Journal, vol.3 (3), pp.191-195, 2016.

180. Lu Z., Li C.M., Bao H., Qiao Y., Toh Y., Yang X., *"Mechanism of antimicrobial activity of CdTe quantum dots"*, Langmuir, vol. 24(10), pp. 5445-5452, Apr. 2008.

181. Nozik A.J., *"Quantum dot solar cells"*, Physica E: Low-dimensional Systems and Nanostructures, vol.14 (1-2), pp.115-1200, Apr. 2002.

182. Bagher A.M., *"Quantum dots applications"*, Sensors & Transducers, vol. 198(3), pp. 37, 2016.

183. Liu B., Li H., Chew C.H., Que W., Lam Y.L., Kam C.H., Xu G.Q., "PbS–polymer nanocomposite with third-order nonlinear optical response in femtosecond regime", Materials Letters, vol. 51(6), pp. 461-469, Dec 2001.

184. Roy Choudhury K., Sahoo Y., Prasad P.N., *"Hybrid Quantum-Dot–Polymer Nanocomposites for Infrared Photorefractivity at an Optical Communication Wavelength"*, Advanced materials, vol. 17(23), pp. 2877-2881, Apr. 2005.

185. Cassidy P.J., Radda G.K., *"Molecular imaging perspectives"*, Journal of the royal society interface, vol. 2(3), pp.133-144, June 2005.

186. Schillaci O., Danieli R., Padovano F., Testa A., Simonetti G., *"Molecular imaging of atheroslerotic plaque with nuclear medicine techniques",* International journal of molecular medicine, vol. 22(1), pp. 3-7, July 2008.

187. Lecchi M., Ottobrini L., Martelli C., Del Sole A., Lucignani G., *"Instrumentation and probes for molecular and cellular imaging",* The Quarterly Journal of Nuclear Medicine and Molecular Imaging, vol. 51(2), pp. 111, June 2007.

188. Levenson R. M., Lynch D. T., Kobayashi H., Backer J. M., Backer M. V., *"Multiplexing with multispectral imaging: from mice to microscopy",* ILAR journal, vol. 49(1), pp.78-88, Jan. 2008.

189. Zrazhevskiy P., Gao X., *"Quantum dots for cancer molecular imaging",* Minerva Biotecnologica, vol. 21(1), pp. 37, Mar. 2009.

190. Luker G.D., Luker K.E., *"Optical imaging: current applications and future directions",* Journal of Nuclear Medicine, vol. 49(1), pp. 1-4, Jan. 2008.

191. Sapsford K.E., Pons T., Medintz I.L., Mattoussi H., *"Biosensing with luminescent semiconductor quantum dots",* Sensors, vol. 6(8), pp. 925-953, Aug. 2006.

192. Chen B., Zou L., Wu Z., Sun M*., "The application of quantum dots in aquaculture pollution detection",* Toxicological & Environmental Chemistry, vol. 98(3-4), pp. 385-394, Mar. 2016.

193. Bonilla J.C., Bozkurt F., Ansari S., Sozer N., Kokini J.L., *"Applications of quantum dots in food science and biology",* Trends in Food Science & Technology, vol. 53, pp. 75-89, July 2016.

CHAPTER-2

SYNTHESIS, CHARACTERIZATION AND EVALUATION TECHNIQUES
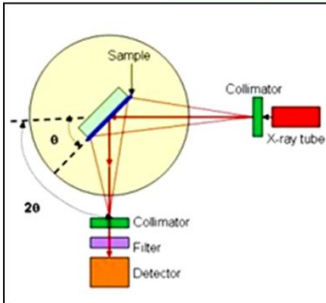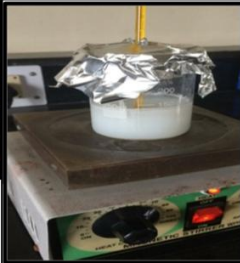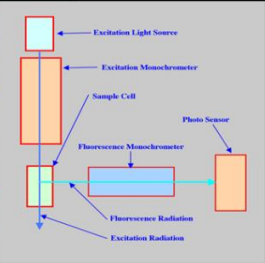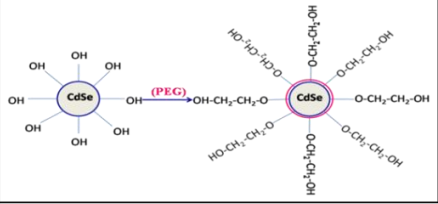
2.1 Introduction

Present chapter provides the detailed information of synthesis procedure of poly CdSe, CdSe QDs, ZnS QDs, CdSe/ZnS structures, poly CdTe, CdTe QDs and polymer, silicates encapsulated structures of CdSe and CdTe QDs. Methods employed to study antimicrobial and cytotoxic behavior of QDs and encapsulated structures have also been discussed. Structural, morphological, and optical properties of QDs were studied by X-ray diffraction (XRD), Transmission Electron Microscope (TEM), UV-Vis absorption spectroscopy (UV-Vis) and photoluminescence (PL) spectroscopy. All the experimental arrangements used in our work have been described in this chapter. Different synthesis methods of QDs have been discussed in chapter 1. Out of all these method we have selected wet chemical aqueous route for synthesis of QDs. On the basis of better reproducibility, cost effectiveness, non toxic and environment friendly nature. This synthesis route requires capping agent to stabilize particle size. Capping agent which have functional groups sulfhydryl and carboxyl are generally preferred.

2.2 Synthesis of poly CdSe and CdSe QDs

2.2.1 Chemicals required for CdSe synthesis

Cadmium chloride monohydrate ($CdCl_2.H_2O$), triethanolamine (TEA) $C_6H_{15}NO_3$, sodiumselenosulphate (Na_2SeSO_3), ammonia solution (25%) (NH_3) and 2-mercaptoethanol ($HOCH_2CH_2SH$). All chemical used in synthesis were procured from Merck India. All the analytical grade chemicals were employed as it is without additional refinement. Ultra-pure distilled water (Milli-Q, Millipore) was employed during the entire conduct test.

2.2.2 Synthesis procedure of poly CdSe

We have attempted the synthesis of several batches of CdSe QDs in order to attain a most suitable synthesis procedure to proceed further. Finalized the synthesis procedure is given here.

Poly CdSe was synthesized at $70^{o}C$ by wet chemical method. 50 ml of distilled water was used as solvent for production of hydrophilic QDs. Two different precursors and complexing agent ($CdCl_2.H_2O$, $C_6H_{15}NO_3$ and Na_2SeSO_3) were used in 3:1.4:1 molar ratio. Selenium reactant Na_2SeSO_3 solution preparation involves dissolution of 0.2 molar of Se in 0.5 molar of Na_2SO_3

solution in water $CdCl_2.H_2O$ was mixed with triethanolamine and was utilized as complexing agent. NH_3 was used to adjust the pH at 11. Now sodiumselenosulphate was added to the reaction mixture. After the synthesis of the products completed, obtained powder was washed and centrifuged several times. Cleaned samples were filtered and allowed to dry at room temperature.

2.2.3 Procedure for synthesis of CdSe1, CdSe2, CdSe4 and CdSe6 QDs

Wet chemical route was used to prepare CdSe QDs at optimized temperature of 70°C. We have used the same precursors in the synthesis of CdSe QDs which were used for poly CdSe. But we have used 5% 2-ME (2-Mercaptoethanol) as stabilizing agent to have a control over the particle size. 1 ml, 2 ml, 4 ml and 6 ml of 5 % 2-ME were used to synthesize CdSe1, CdSe2, CdSe4 and CdSe6 respectively. After the reaction completed the powder was filtered, centrifuged and dried at room temperature. Experimental setup and process flow to synthesize all types of CdSe particle is give in figure 2.1 and figure 2.2 respectively.

Figure 2.1: Experimental setup used to synthesize CdSe QDs

Precursors CdCl$_2$, complexing agent triethanolamine and Se source sodiumselenosulphate were used in 3:1.37:1 molar ratio.

(i) Synthesis of sodium seleno sulphate:

$$Na_2SO_{3(aq)} + Se\,(\text{powder}) \rightarrow Na_2SeSO_3$$

The $CdCl_2$ dissolve in water and release Cd^{2+}:

$$CdCl_2 \rightarrow Cd^{2+} + 2Cl^-$$

The addition of TEA to reaction mixture gives milky colored solution this is an indication of:
$$Cd^{2+} + TEA \rightarrow [Cd(TEA)]^{2+}$$

Ammonia on addition reacts with $[Cd(TEA)]^{2+}$ and forms complex ion as:

$$[Cd(TEA)]^{2+} + 4NH_3 \rightarrow [Cd(NH_3)_4]^{2+} + TEA$$

$$Na_2SeSO_3 + OH^- \rightarrow Na_2SO_4 + HSe^-$$

$$HSe^- + OH^- \rightarrow Se^{2-} + H_2O$$

$$[Cd(NH_3)_4]^{2+} + Se^{2-} \rightarrow CdSe + \text{Waste products}$$
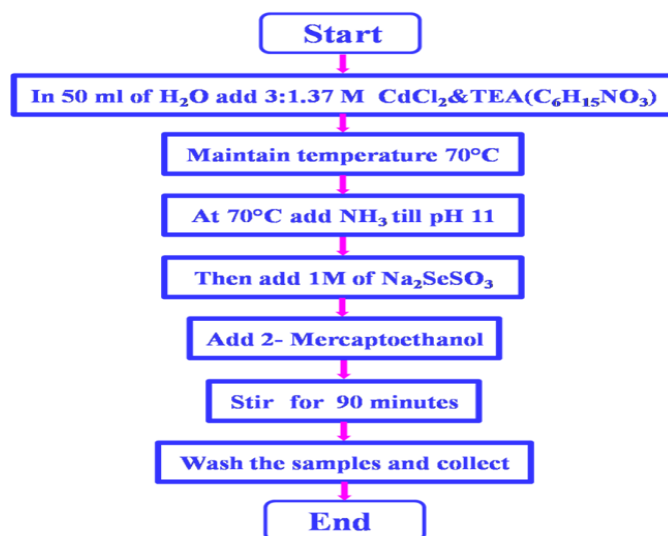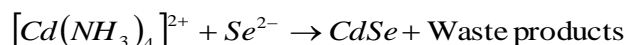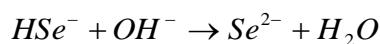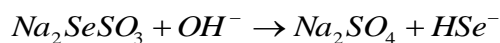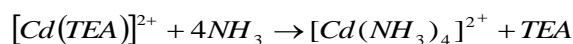
Figure 2.2: Process flow for wet chemical synthesis of CdSe QDs

2.2.4 Encapsulated structures of CdSe4 QDs

Quantum dot surface stability is a major concern while synthesizing small CdSe QDs. To overcome this issue we have encapsulated CdSe QDs by silicate tetraethylorthosilicate (TEOS) and polymers polyethylene glycol (PEG), and poly vinyl alcohal (PVA). This encapsulation helps in preventing QDs from oxidation and chemical degradation. Encapsulated QDs were referred as CdSe/TEOS, CdSe/PVA and CdSe/PEG QD. 0.0012 moles of poly vinyl alcohol (PVA) was dissolved in distilled water to prepare CdSe/PVA QDs. Reaction mixture was continuously put on a shaker for 48 hours. CdSe/TEOS QDs and CdSe/PEG QDs were synthesized by following the same methodology which was used for CdSe/PVA QDs. Polymer encapsulation of QDs schematically presented in Figure 2.3.
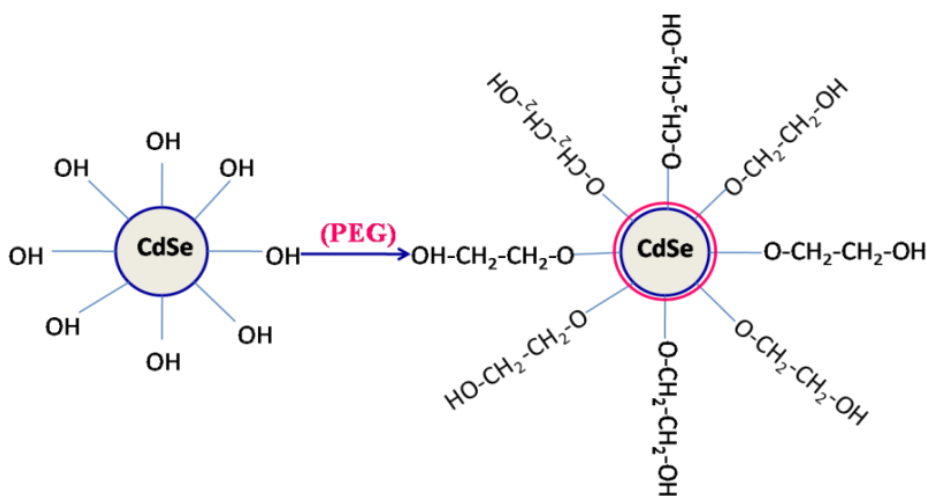
Figure 2.3: Schematic presentation of polymer encapsulation of CdSe (eg PEG)

2.3 Synthesis of ZnS and CdSe/ZnS QDs

2.3.1 Chemicals required

The following chemicals obtained from the suppliers were used without further purification. Cadmium chloride monohydrate, triethanolamine and sodiumselenosulphate, zinc sulphate heptahydrate, dry zinc chloride, hydrazine hydrate and thiourea all from Merck (India).

2.3.2 Synthesis process of ZnS1 and ZnS2 QDs

Two different precursors ($ZnSO_4.7H_2O$ and $ZnCl_2$) as zinc source were utilized to synthesize ZnS QDs. $ZnSO_4.7H_2O$ and $ZnCl_2$ were used as Zn source to synthesize ZnS1 and ZnS2 respectively. Different Zn precursors $ZnSO_4.7H_2O$, $ZnCl_2$ and S precursor $(NH_2)_2CS$ were taken in 0.025:0.035 molar ratios. Wet chemical method was used to synthesize these ZnS QDs at $70^\circ C$ temperature (Figure 2.4). In 70 ml of distilled water N_2H_4 was mixed with $ZnSO_4.7H_2O$ for ZnS1 and $ZnCl_2$ for ZnS2 for the reduction of Zn precursors. This prepared solution was followed by addition of $(NH_2)_2CS$ and continuously stirred for 3 hours. Synthesis was followed by washing of samples about 5 times with distilled water followed by sonication and centrifugation for removing byproducts from mixture. Washed QDs were dried out at room temperature.

Chemical equation for synthesis of ZnS

$$ZnSO_4.7H_2O \rightarrow Zn^{2+} + SO_4^{2-} + 7H_2O$$

$$Zn^{2+} + N_2H_4 \rightarrow [Zn(N_2H_4)_n]^{2+}$$

$$[Zn(N_2H_4)_n]^{2+} \rightarrow Zn^{2+} + nN_2H_4$$

$$SC(NH_2)_2 + OH^- \rightarrow SH^- + CH_2N_2 + H_2O$$

$$Zn^{2+} + S^{2-} \rightarrow ZnS$$
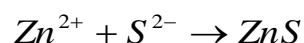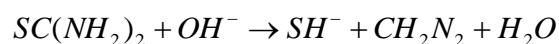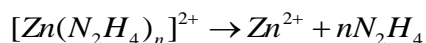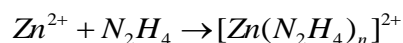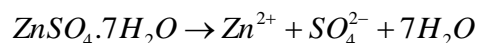
Figure 2.4: Experimental setup used to synthesize ZnS QDs

2.3.3 CdSe/ZnS core/shell synthesis

Core-shell QDs were synthesized by seed growth method. The whole synthesis process for core shell involves two-steps (figure 2.5). First step involves synthesis of monodispersed bare CdSe 4 QDs where these CdSe4 QDs were stabilized with 2-ME capping groups. Second step was synthesis of shell on these bare QDs. $ZnSO_4.7H_2O$ was used as precursor to synthesize CdSe/ZnS1 and $ZnCl_2$ was used to synthesize CdSe/ZnS2 core-shell QDs. Zn precursor i.e $ZnSO_4.7H_2O$ for CdSe/ZnS1 and $ZnCl_2$ for CdSe/ZnS2 (0.49 millimole) was mixed in distilled water and followed by addition of 10 ml hydrazine hydrate. N_2H_4 behave as reducing agent and involves in complexation with Zn^{2+}. 0.8 g of bare CdSe4 QDs in aqueous solution was mixed in the above synthesized mixture at 50°C and pH 9.8. Then to 80 ml of this reaction mixture 0.69 millimole of $(NH_2)_2CS$ was added and continuously stirred for1 hour. Thereafter samples were cleaned with distilled water, dried and stored at room temperature. The process flow for the synthesis of precursor based ZnS and CdSe/ZnS core shell is presented in Figure 2.5.
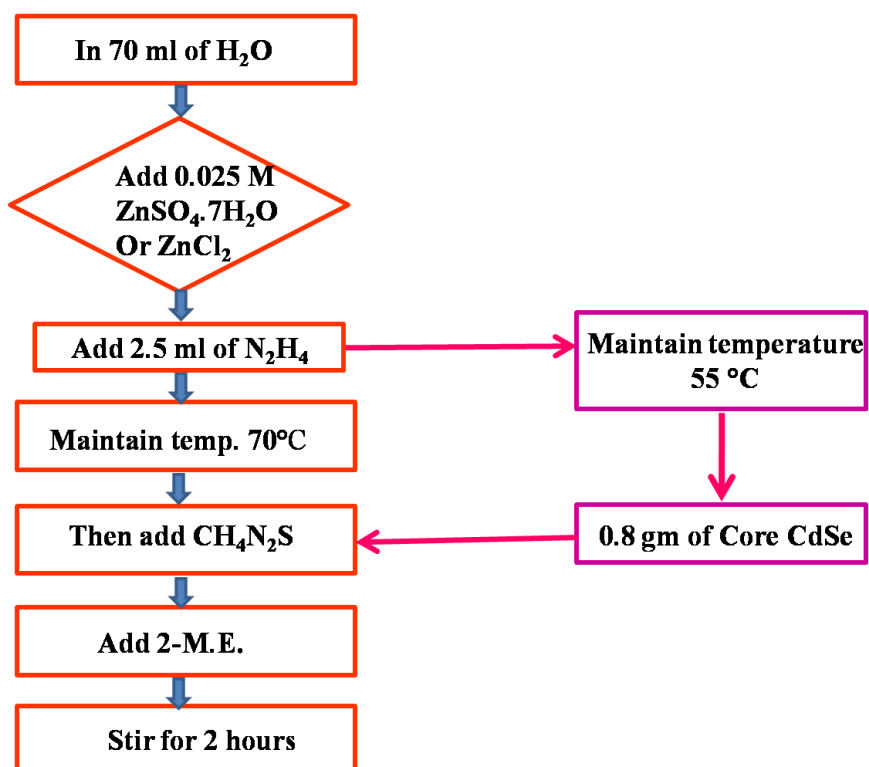
Figure 2.5: A process flow for wet chemical synthesis of ZnS1, ZnS2 and CdSe/ZnS core-shell QDs

2.4 Synthesis of poly CdTe and CdTe QDs

2.4.1 Chemicals required for CdTe synthesis

Cadmium chloride monohydrate ($CdCl_2.H_2O$), triethanolamine (TEA) $C_6H_{15}NO_3$, sodiumthiosulphate pentahydrate ($Na_2S_2O_3.5H_2O$), TeO_2, ammonia solution (25%) (NH_3), 3-and mercaptopropionic acid ($C_3H_6O_2S$) were procured in CdTe poly and CdTe QDs synthesis. All these chemical were purchased from Merck India.

2.4.2 Procedure for synthesis of poly CdTe

To synthesize poly CdTe firstly the Te source Na_2TeO_3 was prepared by dissolving 3.1 g of $Na_2S_2O_3.5H_2O$ in 25 ml of H_2O. In another beaker dissolve 0.31 g of TeO_2 at basic pH 10. Now mix these both solutions and stir for 1 hr at 80°C. Poly CdTe was synthesized at 80°C by wet chemical route. $CdCl_2.H_2O$ precursors, Na_2TeO_3 and $C_6H_{15}NO_3$ were used in 3:1.4:1 molar ratio. NH_3 was used to adjust the pH at 11. Now Te source was added to the reaction mixture. After the synthesis of the products, obtained powder was washed and centrifuged several times. Cleaned samples were filtered and allowed to dry at room temperature.

2.4.3 Procedure for synthesis of CdTe1, CdTe2 and CdTe3

CdTe QDs were synthesized at temperature of 80°C. Same precursors were used for synthesis of CdTe QDs which were used for poly CdTe. To control the particle size we have used 5% 3-mercaptopropionic acid as stabilizing agent. 1 ml, 2 ml, 3 ml of 5% 3-mercaptopropionic acid was used to synthesize CdTe1, CdTe2, and CdTe3 respectively. After the reaction completed the powder was filtered, centrifuged and dried at room temperature. The process flow for all the CdTe related synthesis is presented in figure 2.6.

Chemical equation for synthesis of CdTe
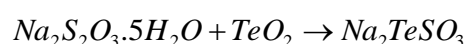
$$Na_2S_2O_3.5H_2O + TeO_2 \rightarrow Na_2TeSO_3$$

The $CdCl_2$ dissolve in water and release Cd^{2+} :

$$CdCl_2 \rightarrow Cd^{2+} + 2Cl^-$$

The addition of TEA to reaction mixture gives milky colored solution this is an indication of:

$$Cd^{2+} + TEA \rightarrow [Cd(TEA)]^{2+}$$

$$[Cd(TEA)]^{2+} + 4NH_3 \rightarrow [Cd(NH_3)_4]^{2+} + TEA$$

$$Na_2TeSO_3 + OH^- \rightarrow Na_2SO_4 + HTe^-$$

$$HTe^- + OH^- \rightarrow Te^{2-} + H_2O$$

$$[Cd(NH_3)_4]^{2+} + Te^{2-} \rightarrow CdTe + \text{Waste products}$$
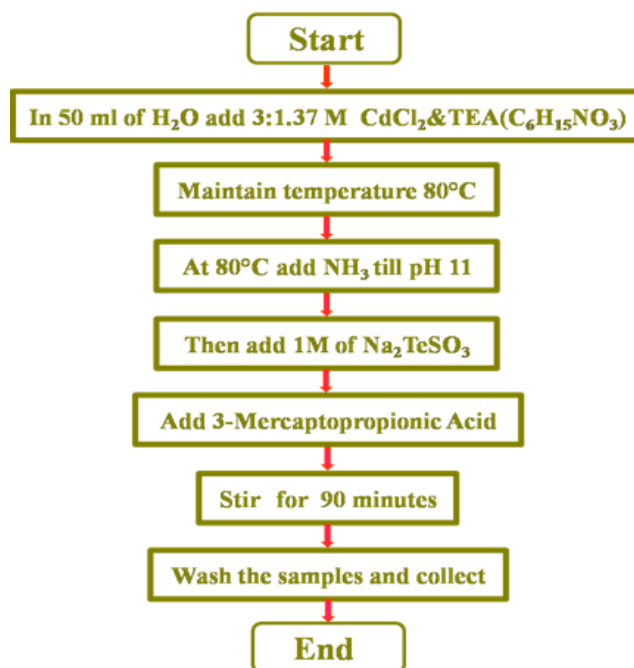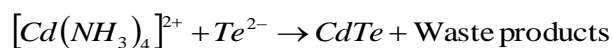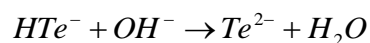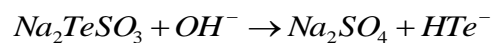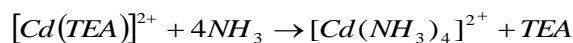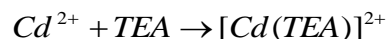
Figure 2.6: A process flow for wet chemical synthesis of poly CdTe and CdTe QDs

2.4.4 Encapsulated structures of CdTe QDs

Quantum dot surface stability and toxicity is a major concern for NIR CdTe QDs also. To rule out this problem CdTe QDs were encapsulated by silicate tetraethylorthosilicate (TEOS) and polymers polyethylene glycol (PEG), and poly vinyl alcohal (PVA). Encapsulated QDs were

named as CdTe/TEOS, CdTe/PEG and CdTe/PVA QD. 0.000125 moles of polyethylene glycol (PEG) was dissolved in distilled water to prepare CdTe/PEG QDs. Reaction mixture was continuously put on a shaker for 48 hours. CdTe/TEOS QDs and CdTe/PVA QDs were synthesized by following the same methodology which was used for CdTe/PEG QDs.

2.5 Bacterial growth and QDs treatment

2.5.1 Material and method of CdSe based nanostructures

Culture media like MacConkey agar, Mueller Hinton agar, Mueller Hinton broth and luria broth were acquired from Hi-Media Pvt. Ltd. (India). Disc of cotrimoxazole (1.25/23.75mcg) and meropenem were also acquired from Hi-Media Pvt. Ltd. (India). The reference strains *Escherichia coli* ATCC 25922 and *Acinetobacter baumannii* ATCC 19606 utilized in antimicrobial studies were received as a gift from Dr. Arti Kapil Head of Bacteriology division department of Microbiology, AIIMS, New Delhi, India.

2.5.2 Antimicrobial susceptibility testing of CdSe based nanostructures

Kirby Bauer's disk diffusion method was used to screen antibacterial activity of QDs and their core/shell structures against potential gram negative pathogens; *Escherichia coli (E.coli)* ATCC 25922 and *Acinetobacter baumannii (A. baumannii*) ATCC 19606 [1]. Standard guidelines of CLSI (Clinical laboratory standard institute) and ICMR (Indian council of medical research) were used to perform these studies [2]. Bacterial cultures were inoculated in Luria broth and then they were incubated overnight at 37°C. 0.5 O.D. McFarland standards bacterial culture was swabbed onto Muller Hinton agar plate and permitted to dry for 15 minutes. Disks of control antibiotics and synthesized compounds were positioned onto agar plates. Plates were transferred in to an incubator for 24 hours and maintained at 37°C and lysis zones around disk were read according to ICMR and CLSI guidelines [3].

2.5.3 Antimicrobial susceptibility testing of CdTe based nanostructures

In-vitro Antibacterial assays: In this study two reference strains gram-negative *E. coli* and gram-positive Staphylococcus aureus (*S.aureus)* were used as model bacterium to evaluate the anti-bacterial activity of surface coated quantum dots.

Quantitative anti-microbial analysis

For qualitative analysis, respective bacterium is cultured on Luria Broth agar plates and assessed for zone of inhibition. Agar well diffusion method was used to check the antimicrobial activity. Briefly, the overnight grown (12hr at 37°C) bacterial suspension (OD=0.5) (100µl) was first spreaded onto the agar plates with the help of a glass spreader. Suitable well were dug in the plate using the cork borer to make the well on the agar plate. All the synthesized QDs were sterilized [UV exposure] for 3 h before they were seeded into the well (100µl) at different concentration [100µg/ml- 62µg/ml]. The plates were then incubated at 37°C for 24 h and the zone of inhibition for each sample on the plate was measured with the scale and was recorded in mm.

2.6 Cytotoxicity testing of synthesized CdSe QDs and their encapsulated structures

All the synthesized QDs were tested against human embryonic kidney cell line (HEK-293 cells) to examine their toxic behavior. These cytotoxicity studies were performed to ensure their utilization towards *in-vivo* imaging [4].

2.6.1 Cell lines and cell culture

HEK-293 cells were obtained from NCCS Pune India. After this cells were cultured in Dulbecco's modified Eagle's medium (DMEM), supplement with 10% heat-inactivated fetal bovine serum (FBS) and antibiotics (100 µg/ml penicillin and 100 µg/ml streptomycin) at 37°C in the humidified atmosphere with 5% CO_2.

2.6.2 Cell cytotoxicity assay of QDs

Toxicity of QDs was studied by colorimetric 3-(4, 5-dimethylthiazol-2-yl)-2, 5-diphenyltetrazolium bromide (MTT) assays. For cytotoxicity testing cells were sub-cultured in 96-well plate (1×10^4/well). Different concentrations (0 to 1000 µg/ml) of QDs were added afterward to each well and incubated for different time periods (12 hrs, 24 hrs, 48 hrs and 72 hrs) at 37°C. Subsequent to specific incubation time, each well was followed by addition of 20 µL MTT (5 mg/ml) and then incubated for 4 h at 37°C. After incubation for dissolving formazan salt

Dimethyl sulfoxide (DMSO) was added to every well. Absorbance (A) values were obtained at 570 nm test wavelength and 630 nm reference wavelengths by help of microplate reader (Bio-Rad). Study was carried out in triplicates and obtained results were as mean ± SD (n=3). The cytotoxicity of cells was evaluated by using the equation given below:

$$\% \text{ cell cytotoxicity} = [\frac{(A)\ Test}{(A)\ Control} \times 100]$$

IC_{50} (Half maximal inhibitory concentration at which 50 % of cell get die) value for every sample was calculated from plot between dose and percent (%) cell cytotoxicity.

Note: Similar procedure for cytotoxicity testing of CdTe based nanomaterials was used. But in this case cells were cultured in 96-well plate (1×10^4 cells/well) and further exposed to QDs for 24 hrs with varying concentrations of QDs ranging from 0 to 500 µg/ml subsequently.

2.6.3 Cellular imaging assay for CdSe based nanostructures

Cellular morphological changes as an effect of QDs incubation were further confirmed through Full form 4', 6-diamidino-2-phenylindole (DAPI), Acridine orange (AO), and propidium iodide (PI), microscopy. Briefly, 1×10^5 cells/well (HEK-293) was seeded in 12 well plate and QDs were added for different time period (0.5 hrs, 24 hrs and 72 hrs). Following end of fixed incubation the medium was detached, and then washing of cell was done by PBS and 5 µL of DAPI (1µg/ml), 5 µL of 10 µg/mL (AO) and 5 µL of 10 µg/mL PI were added to each well for 10 min. Change in cellular morphology was analyzed by capturing fluorescent microscopic images and corrected total cell fluorescence (CTCF) intensity was calculated through Image-J software.

2.6.4 Cellular imaging assay for CdTe based nanostructures

To evaluate the morphological alteration as an effect of QDs exposure, live dead staining was performed by using AO and Ethidium bromide (EtBr) fluorescent dyes. Briefly, 1×10^5 cells/well (HEK-293) was cultured in 12 well plates and afterwards QDs were incubated with uniformly full-fledged cells for 24 hrs. Medium was removed after completing stipulated time peroids, cells

were then washed by using PBS and 5 µL of 10 µg/mL AO and 5 µL of 10 µg/ml EtBr were supplemented to each well for 10 min. Fluorescent microscopic images were captured through fluorescent microscope (Nikon eclipse Ti).

2.7 Characterization techniques

2.7.1 X-ray diffractometer (XRD)

X-ray powder diffraction is technique utilized for structural analysis in material science field. X-ray tube, X-ray detector and sample holder are major parts of XRD. Figure 2.7 shows Shimadzu (XRD 6000) X-Ray diffractrometer employed for XRD experiments. XRD is a prevailing nondestructive method used for characterization of crystalline materials. This technique gives information about crystal structure, atomic spacing, phases, preferred crystal orientations (texture) and some other parameters like crystallite size, strain and some kind of crystal defects. Constructive interference of scattered X-ray beam at specific angles from lattice planes leads to formation of XRD peaks.

XRD graph of samples is blotch of periodic atomic measures in particular material. In this technique cathode ray tube produces X-rays after this these X-rays are filtered to construct monochromatic radiation and then collimated to concentrate in the direction of the sample (Figure 2.8). When interaction takes place between incident bean and sample this produce diffracted rays. Distance among the diffracted atomic planes is acquired by Bragg's law. This law relates electromagnetic radiation wavelength to the diffraction angle and lattice spacing i.e $n\lambda = 2dsin\theta$ where n is an integer; θ is diffraction angle, λ is wavelength, d is interplanar spacing produce the diffraction. After this process these diffracted X-ray are detected by detector. Alterations of diffraction peak to d-spacings permit recognition of the sample as each sample has unique value of d-spacings [5].

Figure 2.7: Shimadzu (XRD 6000) X-Ray diffractrometer employed for XRD experiments
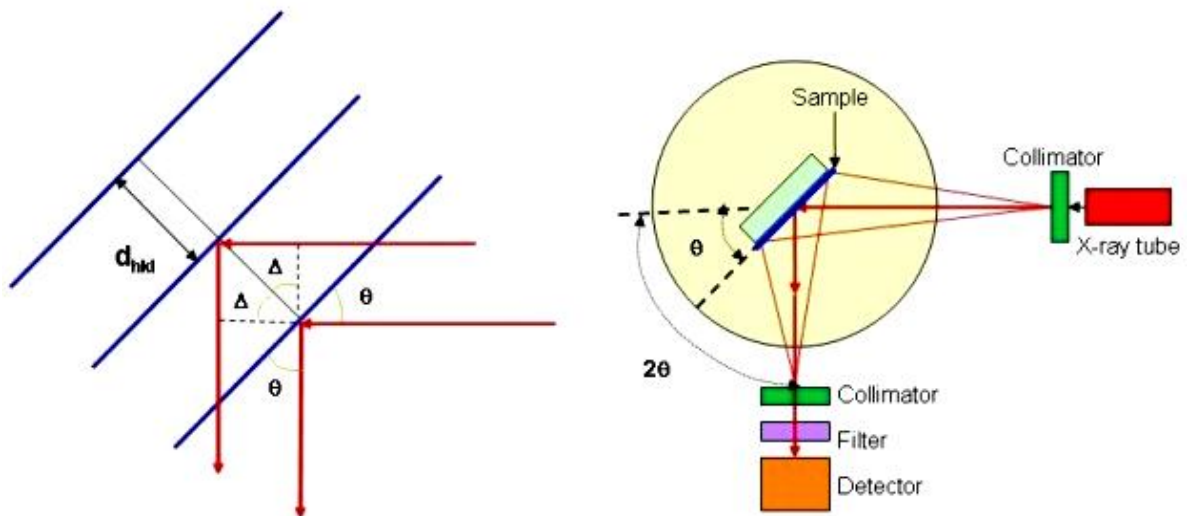
Figure 2.8: Schematic for X-ray diffraction

2.7.2 Transmission electron microscopy (TEM)

Transmission electron microscopy is a technique employ for visualization and analysis of crystal structure and microstructure of specimen. Figure 2.9 shows photograph of Transmission electron microscope (TEM): Hitachi (H-7500) used for characterization [6].In TEM an image is produced

from sample by illuminating sample with electron beam. An image producing system present below sample position consist of objective lens, intermediate and projector lenses and these are responsible for focus the electron to go by the sample to form a highly magnified image on fluorescent screen. These produced electron images are monochromatic and can be digitally stored on computers.

TEM put forward two modes for observation of a sample one is diffraction mode and another is image mode (Figure 2.10). Diffraction mode or dark field mode produces a diffraction pattern for sample which originates by illuminating sample area using electron beam. Such diffraction pattern produced by TEM is totally equivalent to diffraction pattern produced by XRD. Image mode is for producing image from illuminating area of sample.

Figure 2.9: Photograph of Transmission electron microscope (TEM): Hitachi (H-7500)
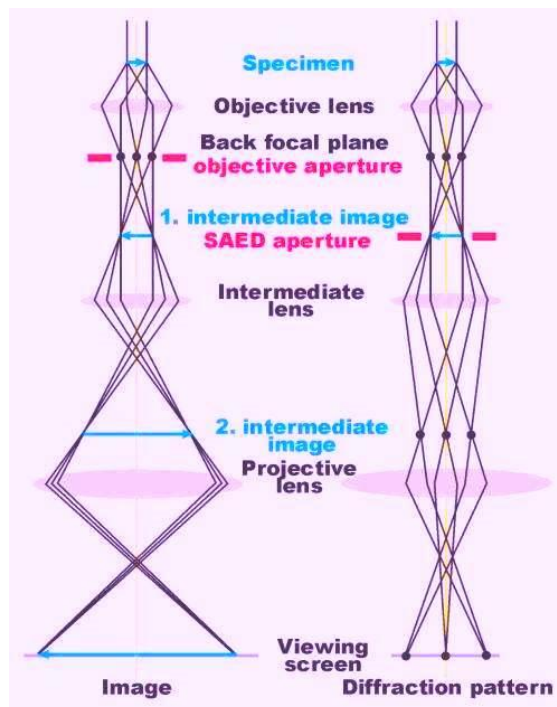
Figure 2.10: The ray diagram of transmission electron microscope

2.7.3 Energy dispersive X-ray spectroscopy (EDX)

EDX is extremely powerful analysis method which is used for analyzing the elements of sample. In EDX X-rays are produced by ionization of an atom with high energy radiation (10-20 KeV) and this process result in vacancy in inner shell. Incident beam excite an electron from inner shell and ejects this electron from shell and produce an electron hole. After this process an higher energy shell electron fill up hole. In this process the energy is produced in form of X-ray. This produced energy equals to disparity in energy of higher-energy shell and lower energy shell. This energy of X-rays released from analyte is then calculated energy dispersive spectrometer. This X-rays is feature of the differentiation in energy among the two shells and this permit the elemental composition of specimen to be deliberate. By investigating the nature of these emitted X-ray we are able to analyze the elements present in specimen [7].

2.7.4 Optical characterization

2.7.4.1 UV-Vis-Spectrophotometer

UV spectroscopy involves absorption of light of ultra-violet region (200-400 nm) by the molecule. UV-Vis-Spectrophotometer: Perkin-Elmer Lambda 750 was employed to record absorption (Figure 2.11). In absorption spectroscopy there is absorption of light takes place and this cause electron excitation from ground to high energy state. The absorption energy is equals to difference in energy between ground state and higher energy states. UV spectroscopy act upon Beer-Lambert law, this law affirm that: while a beam of monochromatic light get passed from solution of absorbing substance, the rate with which there is diminish in intensity of radiation by means of thickness of absorbing solution is proportional to incident radiation and concentration of solution.

$A = \log (I_0/I) = \varepsilon c l$

A= Absorbance

I_0=Incident light intensity

I= Light incident after passing

c= Solute molar concentration

ε= molar absorptivity

l= Sample cell length

This is fundamental law of UV spectroscopy. In Uv-Vis spectroscopy Tungsten filament lamps and Hydrogen-Deuterium lamps are used as source of light because these sources covers whole UV region. Monochromators there in spectrophotometers commonly composed of prisms and slits. Radiation emitted by source gets dispersed with the help of rotating prisms. Various wavelengths of light separated by prism pass through the slits for recording purpose. The beam selected by the slit is monochromatic and further divided into two beams with the help of another prism.

Out of these two divided beams, one passed through the sample solution and second beam pass through the reference solution. Detector contains two photocell. One of the photocell receives the beam from sample cell and second detector receives the beam from the reference. This process results in the generation of pulsating or alternating currents in the photocells. Current generated in the photocells is of very low intensity and amplifiers amplify the signals to obtain clear signals. These amplifiers are connected to the computer. Computer stores all the data

generated and produces the spectrum of the desired compound. Figure 2.12 presents ray diagram of UV-Vis-Spectrophotometer [8].

Figure 2.11: Photograph of UV-Vis-Spectrophotometer made of Perkin-Elmer Lambda 750
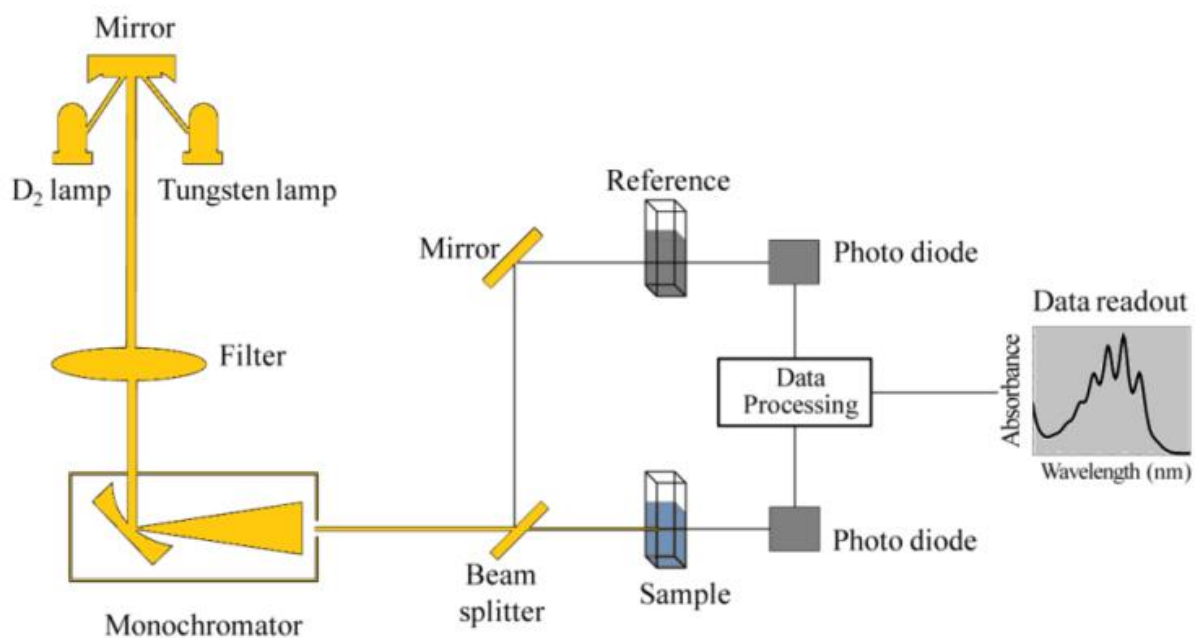
Figure 2.12: Ray diagram of UV-Vis-Spectrophotometer

2.7.4.2 Photoluminescence (PL) and Photoluminescence excitation (PLE) spectroscopy

2.7.4.2.1 Photoluminescence Spectroscopy

A spectrophotometer is an analytical technique which is used to record the luminescent behavior of a sample. Figure 2.13 shows photograph of photoluminescence spectrophotometer LS-55 which was used to record luminescence.

Figure 2.13: Photograph of photoluminescence spectrophotometer LS-55

It's possible to record both excitation wavelength (PLE) and emission spectra (PL). Fluorescence spectrophotometer consists of light source of 150 W ozone free xenon lamp. Light from the lamp is collected by elliptical mirror. This light then focused on entrance slit of the excitation monochromator. Reflective optics of monochromator retains high resolution over the whole spectral range and reduces spherical aberrations. The necessary part of a monochromator is a reflection grating. This grating disperses incident light with help of its vertical grooves. The entrance and exit part of monochromator have constantly adjustable slits. The slit width of excitation monochromator decided the band pass of incident light on the sample. The emission monochromator's slits have power over the intensity of fluorescence signal which finally recorded by detector. An excitation shutter is situated after the excitation monochromator's exit slit. The shutter act as cushion and protect sample from photo bleaching and photo degradation

from prolonged exposure to the light source. An emission shutter is placed just before the emission monochromator's entrance and protects the detector from bright light. The sample compartment hold various optional frills and fiber optic bundles to take the excitation beam to a inaccessible sample and return emission beam to emission monochromator. Detector is a photomultiplier tube, which sends the signal to a photon counting module. Figure 2.14 presents ray diagram of Photo Luminescence-Spectrophotometer [9].
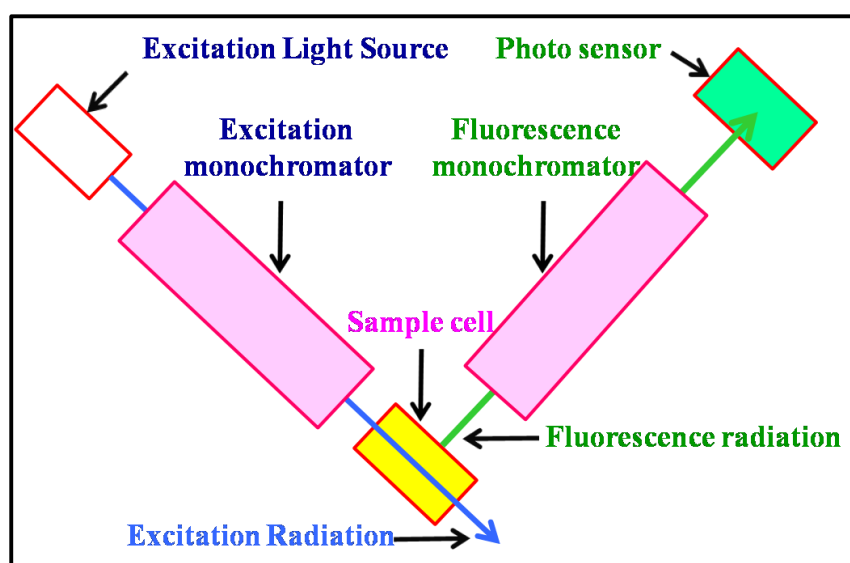
Figure 2.14: Ray diagram of LS-55 Photo Luminescence Spectrophotometer

Photoluminescence is light emitting property of material upon excitation. This spectroscopy is a versatile, nondestructive and powerful optical method. Photo excitation of material leads to excitation of electron from ground to excited state. After these excited electrons get back to equilibrium states and in this process extra energy gets released and this release of energy either takes place in radiative process (luminescence) either via non radiative process. Radiative transition in semiconducting materials takes place between conduction and valence bands. To record PL spectra sample is excited by a laser light which having energy more than that of band gap. After this excited electrons relax by recombining with holes with radiative emission. These kinds of radiative transitions in case of semiconductors might also entail localized impurity and defect states. Thus analysis of PL spectra may also give information about defects and impurities and along with this PL signal magnitude permit determining their concentration. Thus photoluminescence is a process of photon excitation followed by photon

emission and important for determination of purity, crystalline quality and impurity defect levels of semiconducting material. It also helps to understand the physics of the recombination mechanism.

2.7.4.2.2 Photoluminescence excitation spectroscopy

A Photoluminescence excitation (PLE) spectrum is recorded to know about optical window where the absorption value of semiconductors lies. In PLE, emission is fixed and then scanned for excitation. To obtain PLE data emission is fixed on blue edge at different wavelengths.

2.7.4.2.3 Fluorescence Microscopy

Fluorescent microscopic images of QDs were captured through fluorescent microscope NIKON Eclipse-Ti (Figure 2.15).

Figure 2.15: Photograph of NIKON Eclipse-Ti

2.7.5 Fourier transforms infrared spectroscopy (FT-IR)

Figure 2.16 illustrate Photograph of FT-IR spectrophotometer cary-630 used to record FT-IR. Infrared spectroscopy is employed for recognition of functional groups present in a molecule. This technique is also helpful in unique compilation of absorption bands to corroborate the characteristics of a pure compound or to detect the occurrence of precise impurities. Analysis by

infrared spectroscopy is dependent on the verity that molecules have exacting frequencies of internal vibrations.

Frequencies should befall in the IR range that is from ~ 4000 cm^{-1} to ~ 200 cm^{-1}. Sample positioned in sample holder will absorb radiation at frequencies which corresponds to molecular vibrational frequencies, and this will transmit all additional frequencies. Infrared spectrometer measures absorbed frequencies and the plot between absorbed energy vs. frequency is called infrared spectrum for a material. By using FT-IR spectra we can identify substance because different materials have different vibrations and acquiesce special infrared spectra. Moreover, from absorption frequencies it is probable to decide whether diverse chemical groups are there or not in a chemical structure. Figure 2.17 presents block diagram of Fourier transforms infrared spectroscope [10].

Figure 2.16: Photograph of FT-IR spectrophotometer cary-630
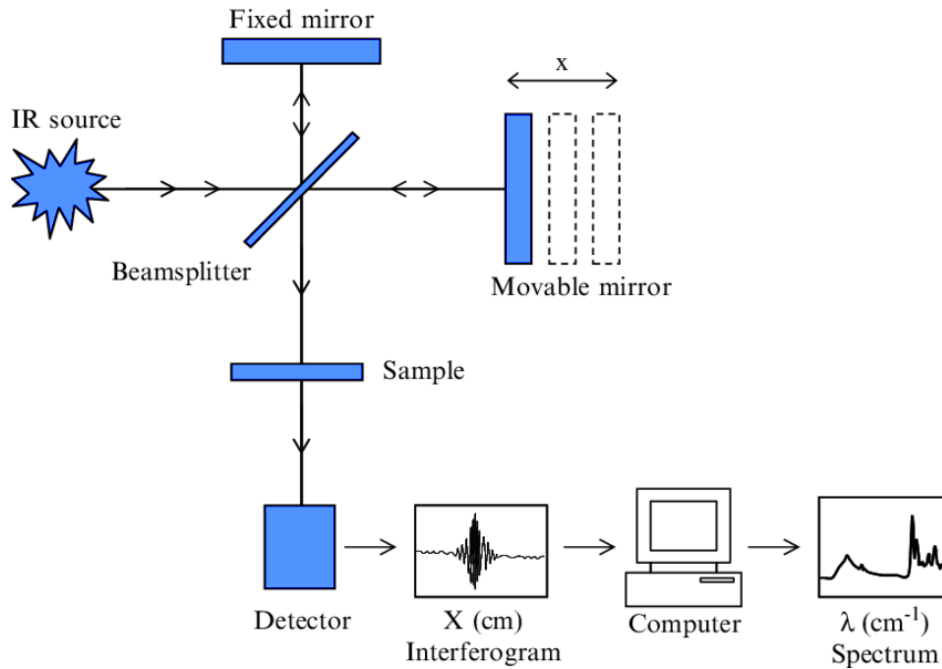
Figure 2.17: Block diagram of Fourier transforms infrared spectroscope

2.8 Formulae used

1. Crystallite size of QDs were obtained by Scherrer's formula

$$D = K\lambda / \beta \, Cos\theta \qquad (1)$$

Where λ = x-rays wavelength used, β = full width at half maximum and θ = Bragg angle.

 2. The *d*-spacing *(d_{hkl})* and lattice constant (a) for samples have been determined by using equation 2 [11] and equation 3 [12] in each case

$$n\lambda = 2d \sin\theta \qquad (2)$$

$$a = d\left(h^2 + k^2 + l^2\right)^{1/2} \qquad (3)$$

3. The microstrain (ε) in all samples has been obtained using the (equation4) [13]

$$\varepsilon = \beta / 4 \tan\theta \qquad (4)$$

4. Surface to volume ratio for QDs was calculated using equation 5

$$SA/V = 3/r \qquad \textbf{(5)}$$

   Where SA =surface area; r =radius

5. The percent of cytotoxicity was evaluated with help of equation 6:

$$\% \text{ cell cytotoxicity} = [\frac{(A)\ \text{Test}}{(A)\ \text{Control}} \times 100] \qquad \textbf{(6)}$$

IC_{50} (Half maximal inhibitory concentration at which 50% of cell get die and for calculating this value a graph was plotted between dose and cell viability.

2.9 References

1. Bauer A.W., Perry D.M., Kirby W.M., *"Single-disk antibiotic-sensitivity testing of staphylococci: An analysis of technique and results",* AMA archives of internal medicine, vol. 104(2), pp. 208-16, Aug. 1959.

2. Patel J.B., Cockerill F.R., Alder J., Bradford P.A., Eliopoulos G.M., Hardy D., Hindler J.A., Jenkins S.G., Lewis J.S., Miller L.A., Powell M., *"Performance standards for antimicrobial susceptibility testing; twenty-fourth informational supplement",* CLSI standards for antimicrobial susceptibility testing, vol. 34(1), pp.1-226, Jan. 2014.

3. www.icmr.nic.in/Publications/SOP/SOP_Bacteriology.pdf

4. Bhanoth S., Kshirsagar A.S., Khanna P.K., Tyagi A., Verma A.K., *"Biotoxicity of CdS/CdSe Core-Shell Nano-Structures",* Advances in Nanoparticles, vol. 5(01):1, Feb. 2016.

5. Bunaciu A.A., UdriŞTioiu E.G., Aboul-Enein H.Y., *"X-ray diffraction: instrumentation and applications",* Critical reviews in analytical chemistry, vol. 45(4), pp. 289-299, Oct. 2015.

6. Wang Z.L., *"Transmission electron microscopy of shape-controlled nanocrystals and their assemblies",* 2000.

7. EDX Hafner B., *"Energy dispersive spectroscopy on the SEM: a primer",* Characterization Facility, University of Minnesota, pp. 1-26, 2006.

8. Gemta A.B., *UV/VIS SPECTROPHOTOMETER* (Doctoral dissertation, Addis Ababa University, 2005.

9. Ye R., Barron A.R., *"Photoluminescence Spectroscopy and its Applications",* Physical methods in chemistry and nano science, OpenStax CNX, June 2011.

10. Doyle W.M., *"Principles and applications of Fourier transform infrared (FTIR) process analysis",* Process control and quality, vol. 2(1), pp. 11-41, 1992.

11. Prabahar S., Dhanam M., *"CdS thin films from two different chemical baths—structural and optical analysis",* Journal of Crystal growth, vol. 285(1-2), pp. 41-48, Nov. 2005.

12. Barman J., Sarma K.C., Sarma M., Sarma K., *"Structural and optical studies of chemically prepared CdS nanocrystalline thin films",* Indian journal of pure and applied physics, vol. 46, pp. 339-343, May 2008.

13. Kumar H., Barman P.B., Singh, R.R., *"Effect of size and shell: enhanced optical and surface properties of CdS, ZnS and CdS/ZnS quantum dots",* Physica E: Low-Dimensional Systems and Nanostructures, vol. 67, pp. 168-177, Mar. 2015.

CHAPTER – 3

SYNTHESIS AND ENCAPSULATION OF CADMIUM SELENIDE (CdSe) QUANTUM DOTS CONFINED BY 2-MERCAPTOETHANOL FOR DEFECT FREE, IMPROVED AND STABLE FLUORESCENCE IN VISIBLE RANGE
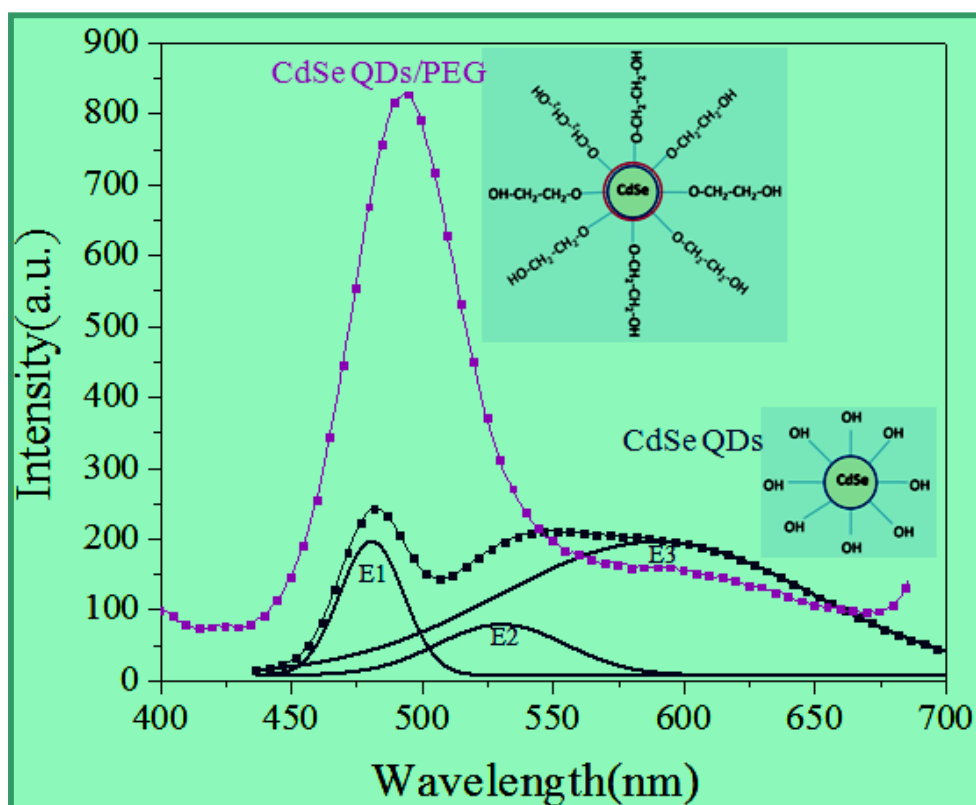
Highlights

- Synthesis of highly confined luminescent CdSe, CdSe1, CdSe2, CdSe4 and CdSe6 QDs, CdSe4/PEG, CdSe4/PVA and CdSe4/TEOS quantum dots by aqueous route.
- Studied Effect of 2-Mercaptoethanol on optical properties.
- Trap state removal by polymer encapsulation was observed for the first time.
- Functionalization of the surface of QDs by biocompatible groups.
- It has been practically confirmed that surface modification of QDs improves optical properties of QDs.

Abstract

This chapter includes results obtained for different sized fluorescent CdSe QDs prepared using 2-mercaptoethanol. Surface modification of QDs was carried out by different polymers and silicates. High concentration of 2-ME was reported to decrease particle size and to increase trap states in QDs. Trap states were removed from CdSe QDs on surface modification. Photoluminescence spectroscopy confirms role of surface modification in improving the optical properties of CdSe QDs.

3.1 Introduction

QDs (quantum dots) have some unique characteristics like size tunable emission spectra, broad absorption and bright luminescence. Because of these features these QDs are appropriate for a variety of applications such as fluorescence imaging and sensing applications [1]. Synthesis of QDs can be carried out by two approaches one is aqueous synthesis and another is organometallic route [2, 3]. It is not possible to use QDs prepared by organometallic route for biological applications because they are hydrophobic in nature. To utilize these QDs biologically there is a need of polymer encapsulation and ligand exchange by means of hydrophilic ligands [4, 5]. Therefore to make these QDs hydrophilic, defect free and biocompatible there is requirement of modification of their surface by using hydrophilic capping agents in aqueous solvent. This strategy is typically problematic and the as prepared QDs are linked with many downsides for instance low emission quantum efficiency and limited stability [6].

Furthermore, as compared to organometallic route, aqueous route of synthesis is simpler, cheaper and more environment friendly. For that reason we chose aqueous route for the synthesis of QDs. In former studies it was described that QDs produced by aqueous route show wide full width at half maxima (FWHM) and low emission efficiency of photoluminescence (PL) ensuing in deprived optical properties attributed to traps on surface of QDs as surface contains atoms which are partially coordinated [7]. In addition to this optical behavior of QDs is also directly correlated to size of QDs. These optical properties can be amazingly refined by optimization of synthetic parameters and encapsulation strategies [8]. Strong confinement results in decrease in particle size and this ultimately causes increase in number of atoms on surface of QDs and impinges optical properties. Atoms found on surface of QDs are partly bonded to crystal lattice, discontinue crystal periodicity and put down other dangling orbitals which project outward from QD surface [9]. Presence of such kinds of surface energy states in band gap of QDs traps charge carrier at surface. This trapping reduces the overlap between electron and holes and finally results in exciton dissociation. Exciton dissociation raises the chances of non-radiative decay and cause traps emission [10- 13]. Previously trap emission was seen in the QDs stabilized by thiol as these thiol functionality or sulfide ions are known for hole scavenging property or hole acceptor property. These studies were paying attention on fluorescence intensity [14-23]. On the

basis of these studies it was concluded that increased quantity of thiol in solution frequently quench the PL emission of QDs and originate surface traps [24, 25]. Detailed literature survey exposed that while the quenching of both band edge emission and trap emission was occurred, trap emission intensity was incessantly growing with respect to band edge emission [26]. Similar trend has been noticed in present work where 2-ME capped CdSe QDs were prepared by using aqueous solvent. A close check of literature reveal band edge emission near 480 nm in CdSe QDs with trap emission was observed in our QDs for the first time. So it is essential to modify surface of these QDs by proper encapsulation method for trap free improved luminescence properties. This surface encapsulation will provide passivation of dangling bonds and defect states. QDs surface passivation with an inorganic and organic ligand molecule can conduct needed passivation of vacancies and [27, 28]. Reduction in toxicity and to improvement luminescence stability of QDs passivation of surface states through encapsulation is an absolutely appropriate way. Lots of attempts have been devoted to refine the spectral properties of aqueous QDs. Out of these several methods polymer capping has been evolved as most suitable method to prepare nanoparticles with high surface stability [29, 30]. Thus to improve intensity of band edge emission and to eliminate trap related emission we carried on for polymer encapsulation of these QDs.

Current chapter involves the aqueous synthesis of poly CdSe and strongly confined CdSe QDs referred as CdSe1, CdSe 2, CdSe4 and CdSe6 which were capped by 2-ME. Capping by 2-ME induce defects in QDs which were further increased with increase in concentration of 2-ME. We demonstrate the removal of trap states from emission spectrum of CdSe4 QDs with increased intensity of band edge emission on polymer encapsulation. In accordance with the aims of the thesis, luminescence properties of the QDs are the key feature. In line with this we have characterized the prepared QDs for luminescence and hence reached to a conclusion that decides about the best QDs for further studies based on discussion given in continuation. Out of all these prepared samples CdSe1, CdSe2, CdSe4 and CdSe6; CdSe4 QDs have been encapsulated by different materials and have been selected for further studies because in CdSe4 QDs intensity of band edge emission is more as compared to trap emission, however, in case of CdSe6 the intensity of trap emission dominates the band edge emission. Moreover, amount of particles formed in CdSe6 (higher 2-ME) was negligible and it was impossible to collect these CdSe6

QDs for application purposes. Furthermore, CdSe4/PEG encapsulated structure is superior then CdSe6/PEG as FWHM value for CdSe6/PEG band edge emission has also been increased and this shows decline in monodispersity. It was also noted from PL spectra that red tail in CdSe6/PEG still shows traces that demonstrate presence of a few trap states whereas in CdSe4/PEG the spectra was clear.

3.2 Experimental details

CdSe QDs of different size were prepared via aqueous chemical route at 70°C temperature with constant stirring using distilled water as solvent. Detailed procedure has already been described in chapter 2 (section 2.2.3). For detailed study of other characteristics which have effect on properties of CdSe QDs like their structure, particle size, elemental composition, luminescence (band edge and defect) and functional groups they were characterized by X-ray diffraction (XRD), Transmission electron microscopy (TEM), energy dispersive analysis by X-rays (EDX), absorbance spectroscopy, photoluminescence spectroscopy and Fourier transform infrared spectroscopy (FTIR). Shimadzu powder x-ray diffractometer using Cu Kα1 radiation was used to know the crystal structure and particle size of prepared sample. Transmission electron microscopy (TEM) was performed by putting a drop of dilute aqueous suspension of QDs on surface of 300 mesh copper grid and then copper grid was dried. TEM images were obtained using HITACHI (H-7500). Samples were characterized by EDX using HRTEM instrument TECNAI G^2 20S-TWIN (FEI Neitherlands) to know elemental composition of samples. Perkin-Elmer Lambda750 UV–Vis spectrophotometer was used to carry out UV-Vis spectroscopy measurements. Luminescent behavior of samples was studied using Perkin Elmer LS55 fluorescence spectrophotometer with an excitation source from Xe lamp within wavelength range of 200-900 nm. For confirmation of functionality found on surface of QDs they were characterize by FTIR spectroscopy. This study was carried out by Cary 630 spectrophotometer (Agilent technology) with wavenumber region between 4000 cm^{-1} - 400 cm^{-1}.

3.3 Results and discussion

CdSe II-VI QDs formation takes place from II and VI group elements of periodic table. CdSe crystallizes in three forms cubic, hexagonal and infrequently observed cubic rocksalt. Cubic

structure of CdSe has two forms sphalerite (cubic) and rock salt cubic. Cubic (sphalerite) form of CdSe is unstable. This form gets converted to wurtzite at moderate temperature. CdSe is n-type semiconducting material having direct band gap. CdSe is common material which is used for viable construct of devices. CdSe nanostructures are being extensively investigated due to their immense potential in biomedical and optoelectronic applications. The cadmium atom is type II; it has two electrons in the valence band in s orbital [31]. CdSe is present in two forms cubic and wurtzite and are presented in figure 3.1.
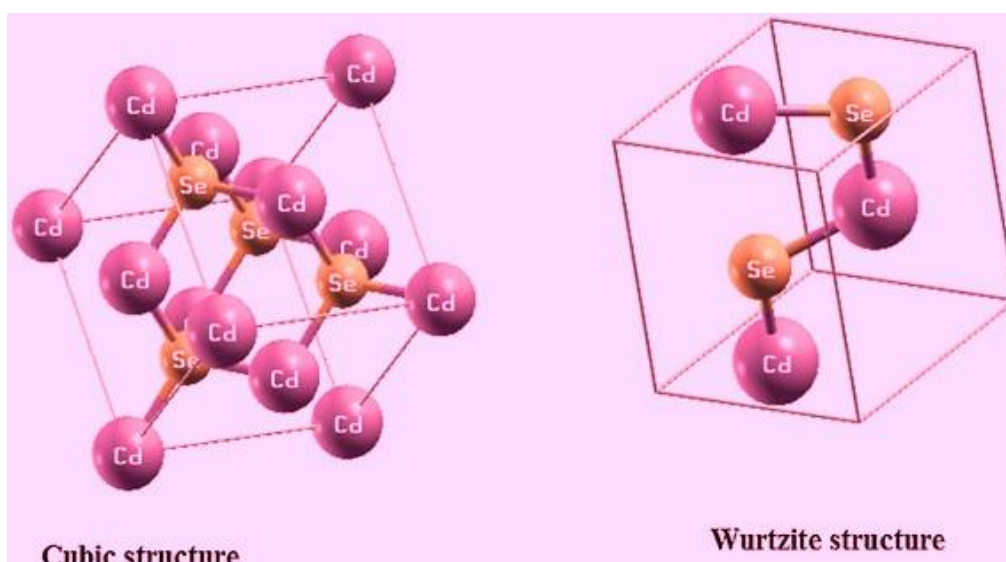
Figure 3.1: Crystal structures of CdSe

3.3.1 Structural analysis of Poly CdSe, CdSe1, CdSe2 and CdSe4 QDs

XRD spectra of poly CdSe, CdSe1, CdSe2 and CdSe4 QDs were recorded to know about structural parameters. Acquired XRD spectra for QDs are presented in figure 3.2. XRD spectra shown in figure revealed that QDs include four main peaks at diffraction angles $2\theta = 25.43^{o}$, 42.12^{o}, 30.63^{o} and 50°. These peaks are attained due to (111), (200), (220) and (311) reflections respectively. These peaks are in a good conformity with cubic phase of CdSe. Figure 3.2 also elucidate that decrease in particle size results into broadening in FWHM. This is a distinctive feature of QDs or nanoparticles. It is important to note that the 2-ME (4 ml) capping provides the smallest grain size (1.9 nm). Width of most prominent peak (111) was employed to calculate crystallite size using the Scherrer's formula (equation 1) in each case [32].

$$D = K\lambda / \beta \, Cos\theta \qquad (1)$$

The d-spacing (d_{hkl}) and lattice constant (a) for samples have been determined by using equation 2 [32] and equation 3 [33] in each case

$$n\lambda = 2d \sin\theta \qquad (2)$$

$$a = d\left(h^2 + k^2 + l^2\right)^{1/2} \qquad (3)$$

The microstrain (ε) in all samples has been obtained using the (equation4) [34]

$$\varepsilon = \beta / 4 \tan\theta \qquad (4)$$

The calculated d-spacing values for different CdSe QDs were ranging between 3.47 Å to 3.49 Å and hence chance of lattice distortion is less. Size of unit cell is indicative of cubic structure. Attained values of corresponding lattice constant to these interplanar spacing are found 6.04 Å, 6.01 Å and 6.02 Å near to standard value 6.05 Å. All the calculated structural parameters along with strain and crystallite size of poly CdSe, CdSe1, CdSe2 and CdSe4 QDs were presented in the table 3.1. It is observed from the table that as crystallite size decreases strain value increases.

TEM analysis confirms spherical shape of QDs therefore surface area of sphere= $4\pi \, r^2$ and volume of sphere = $4/3 \, \pi \, r^3$ and thus surface to volume ratio for QDs was calculated using equation 5 and tabulated in Table [34].

$$SA/V = 3/r \qquad (5)$$

Where SA =surface area; r =radius

Obtained values for surface to volume ratio increases as particle size decreases and this leads to increase in number of dangling bonds or unsatisfactory atoms on surface of small QDs and these dangling bonds are responsible for trap origin in small QDs. Trap origin was further confirmed from PL spectra for small sized QDs.
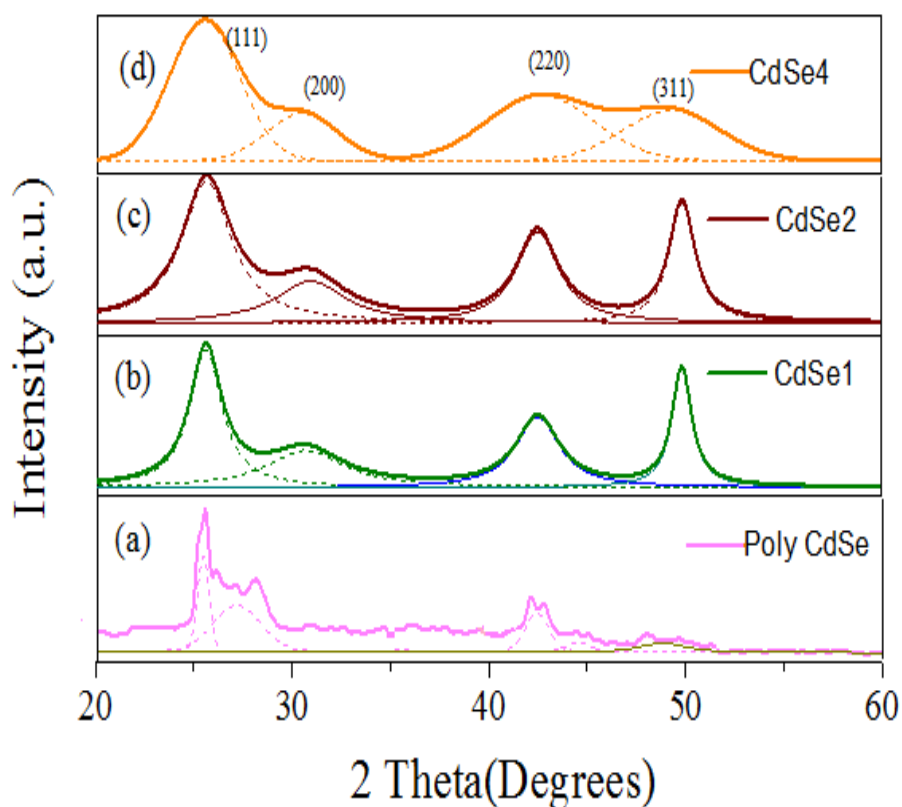
Figure 3.2: XRD spectra of synthesized (a) poly CdSe (b) CdSe1 (c) CdSe2 and (d) CdSe4

Table 3.1: Structural parameters of poly CdSe, CdSe1, CdSe2 and CdSe4 QDs

Sample Name	2θ (^{0})	d(Å)	FWHM (^{0})	Intensity	(hkl)	Size (nm)	Lattice Constant (Å)	Surface/ Volume Ratio (nm^{-1})	Strain
CdSe4	25.46	3.49	4.60	88	111	1.8	6.04	3.15	5.13
CdSe2	25.59	3.47	3.49	258	111	2.5	6.01	2.4	3.85
CdSe1	25.48	3.49	1.82	204	111	3.7	6.02	1.62	2.04
Poly CdSe	25.12	3.51	0.4	315	111	22	6.0	-	0.44

3.3.2 Transmission electron microscopy

TEM analysis for CdSe2, CdSe4, CdSe4/TEOS, CdSe4/PVA, and CdSe4/PEG were performed to obtain the size and shape of QDs. Figure 3.3 (a, b, c, d and e) show the obtained TEM images for QDs and their encapsulated structures. It is clear from TEM images that all the prepared samples are spherical in shape and agglomeration tendency of particle was found negligible. Image J software was used for determination of particle size of QDs. Observed particle size for QDs is tabulated in table 3.4 and it was less than Bohr excitonic radius. Particle size obtained by TEM was found prodigiously close to diameter obtained from X-ray diffraction. TEM image for CdSe2 (figure 3.3(a)) confirms spherical shape of QDs. Figure 3.3(b) shows that CdSe4 QDs have uniform size distribution and are spherical in shape with the average size 1.8 nm. In CdSe4/TEOS (figure 3.3(c)) silica shell is clearly visible (inset of the picture) this also confirms the encapsulation of CdSe by TEOS. Polymer encapsulation did not show any special effect on the morphology and the size of CdSe QDs and it is evidently noticeable in TEM images of CdSe4/PVA QDs (figure 3.3(d)) and CdSe4/PEG QDs (figure 3.3(e)) [35]. Because in polymeric materials electron density is low enough in comparison to semiconducting material. Furthermore, results presented point out that there is no significant variation in size and morphology in all the QD structures. Histograms for the particle size distribution in case of CdSe2, CdSe4, CdSe4/TEOS, CdSe4/PVA and CdSe4/PEG are presented in figure3.3 (a, b, c, d and e).
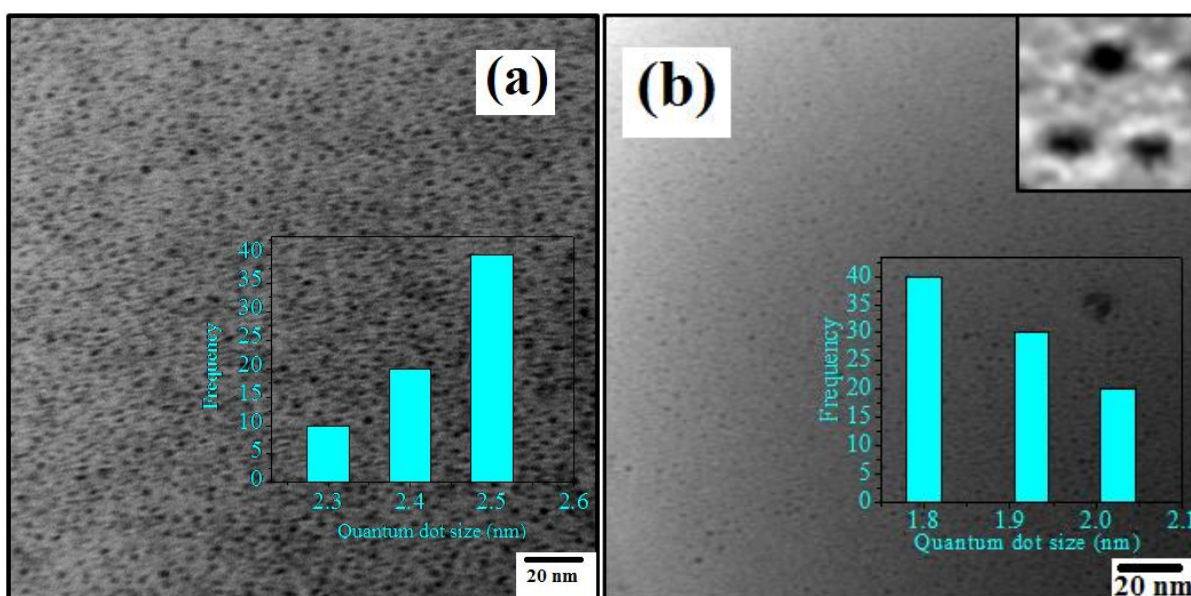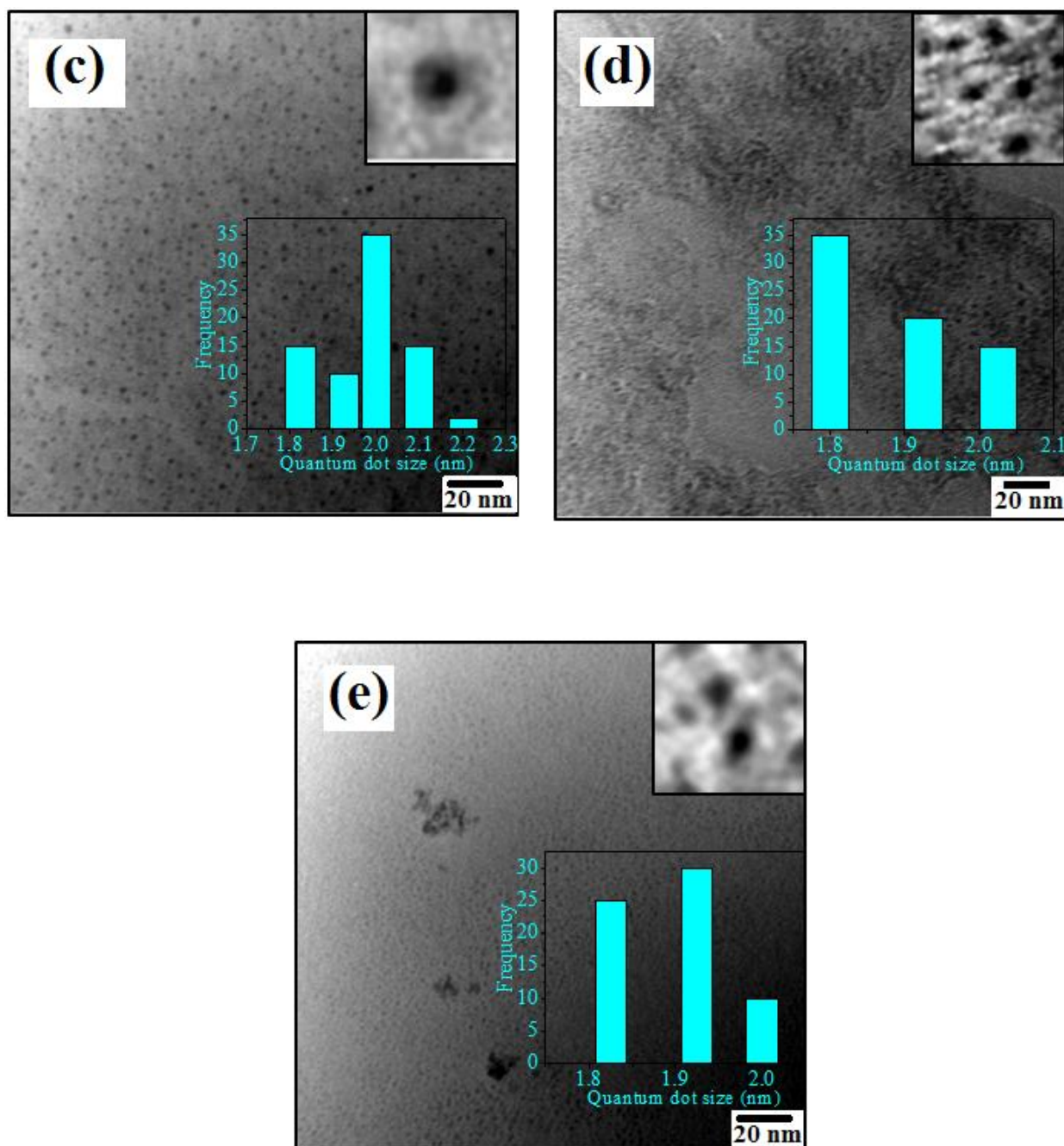
Figure 3.3: (a) TEM image of CdSe2 (b) TEM image of CdSe4 (c) TEM image of CdSe4/TEOS (d) TEM image of CdSe4/PVA and (e) TEM image of CdSe4/PEG

3.3.3 Energy-dispersive X-ray spectra

EDX spectra of QDs and their encapsulated structures were recorded for corroboration of elemental composition and to evaluate the affect of encapsulation of QDs. Atomic percentage for all CdSe QDs and their encapsulated structures was confirmed from EDX. Atomic percentage of Cd and Se in case of CdSe1 was 5.73 %, 5.28% respectively.

Obtained values of atom percentage for CdSe1, CdSe2, CdSe4, CdSe4/TEOS, CdSe4/PVA and CdSe4/PEG are mentioned in table (3.2). Occurrence of sulphur in EDX spectra of CdSe2 and CdSe4 (figure 3.4 b, c) is due to 2-ME and atomic percentage of sulphur in these QDs is in increasing order and tabulated in Table (3.2). The peak of sulphur is intense in CdSe4 as they have high concentration of 2-ME. C and Cu peaks are present in EDX spectra due to carbon coated copper grids used as sample holders for characterization of samples. Existence of oxygen in spectra is due to moisture effect during characterization. Attained stochiometric ratios for Cd:Se with different concentration of 2-ME are mentioned in table 3.3. As we can see in table 3.3 that ratio of Cd: Se is 1:0.63 in CdSe4 this ratio is not in good stochiometry as compared to ratio in case of CdSe1 and CdSe2 as tabulated in table 3.3. From table 3.3 it is also clear that sulphur content also increased on high concentration of 2-ME as it is 0.83 in CdSe4. While in case of polymer encapsulated QDs there is no peak of sulphur. This also confirms that there is no hole scavenging sulfide ions in CdSe4/PEG QDs, CdSe4/PVA and CdSe4/TEOS.

In case of CdSe4/TEOS (figure 3.4 (d)) EDX spectrum shows presence of peaks for cadmium and selenium along with silicon peaks and confirms the encapsulation of CdSe4 QDs by silica. Chemical composition analysis of CdSe4/PVA QDs and CdSe4/PEG QDs (figure 3.4 (e) and (f)) show the peaks of cadmium and selenium due to CdSe4 QDs used for encapsulation. In figure 3.4(e) and 3.4(f) there is no peak that shows the presence of polymers and it is well known that EDX analysis does not provide information for polymeric materials [40]. These encapsulated CdSe4/PEG QDs posses 1.15 atomic percentage of cadmium and 1.14 atomic percentage of selenium. The result obtained through EDX analysis strongly supports the TEM findings and also authenticiate the stoichimetry of as praepared as well as encapsulated structures. In earlier research sulfide ions were reported to act as hole scavenger and hence affect optical properties [26] and will be discussed in the section (3.4.2) of PL spectroscopy.
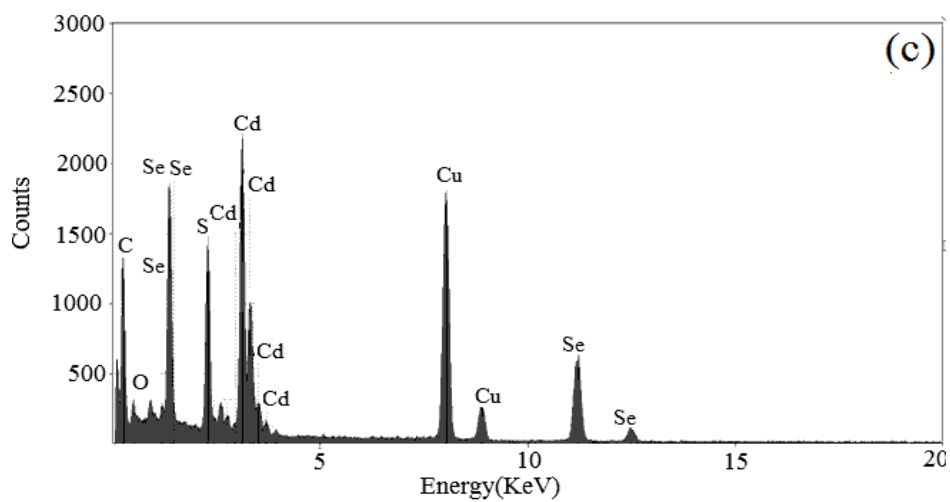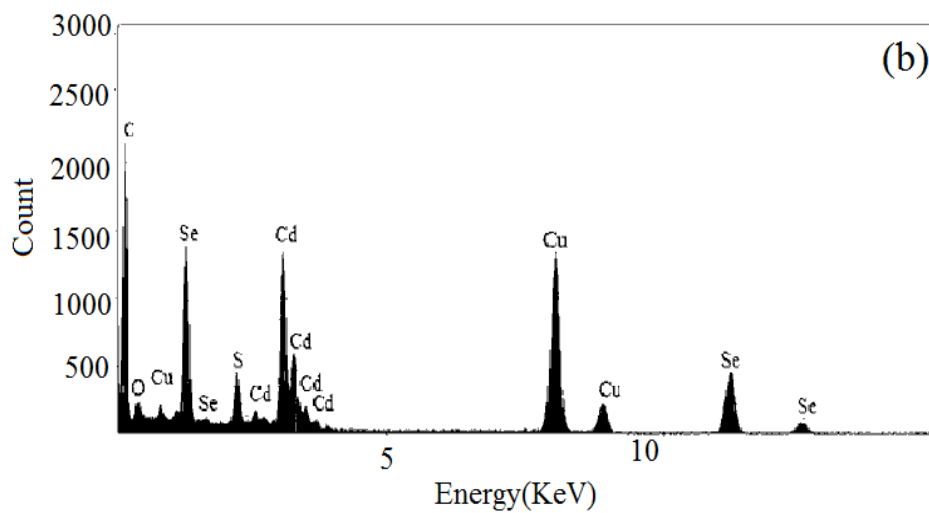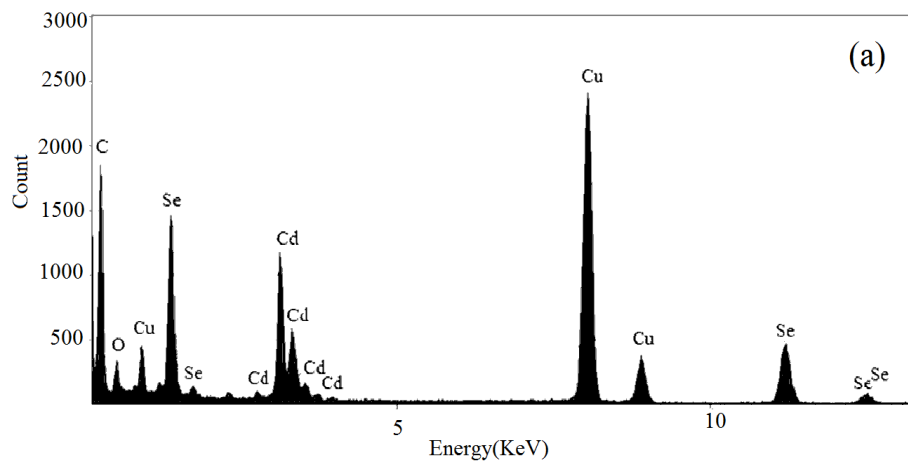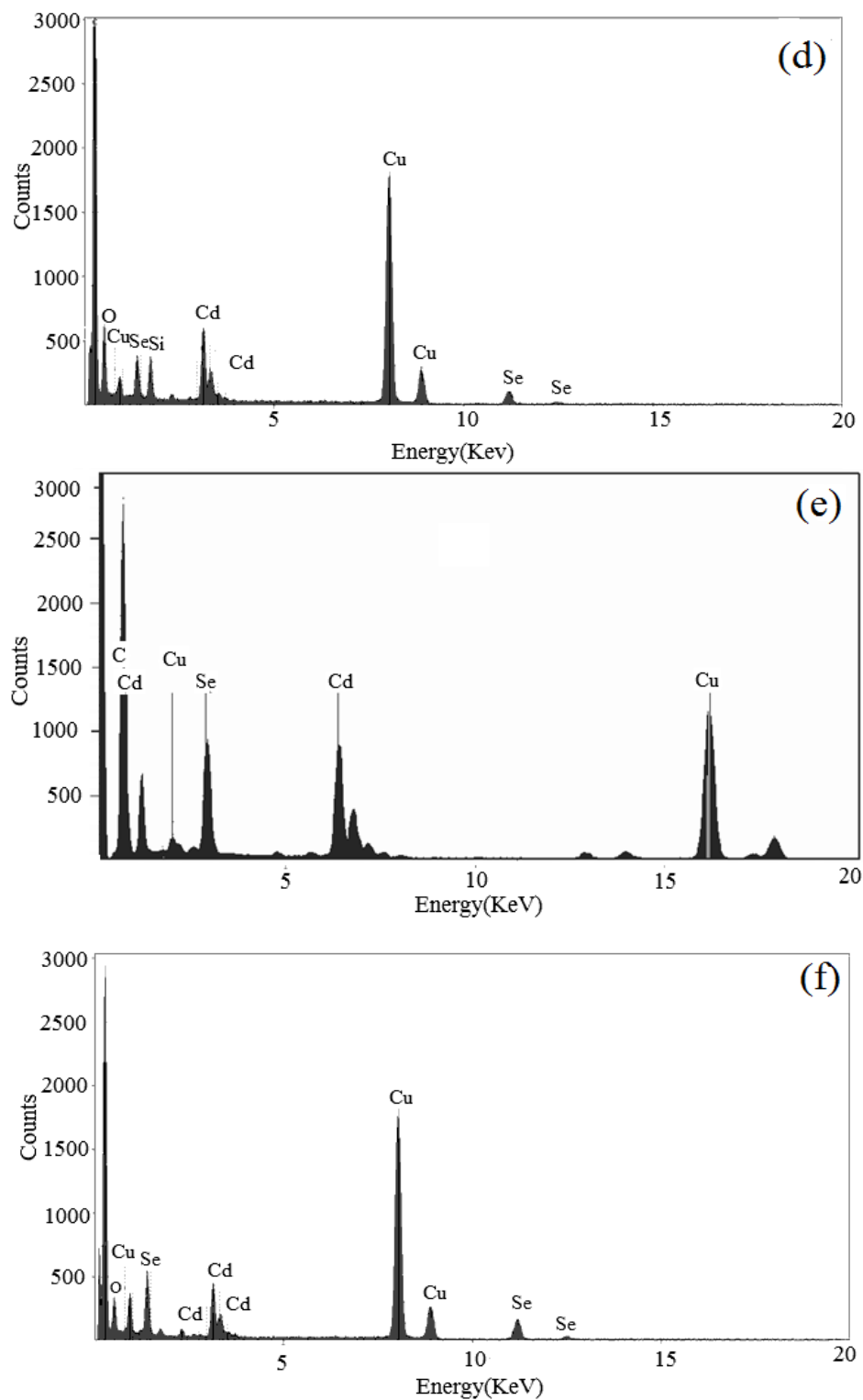
Figure 3.4: EDX spectra of synthesized QDs of (a) CdSe1 (b) CdSe2 (c) CdSe4 (d) CdSe4/TEOS (e) CdSe4/PVA and (f) CdSe4/PEG

Table 3.2: Elemental stochiometric ratio of CdSe1, CdSe2, CdSe4 and CdSe4/PEG QDs

ATOMIC PERCENTAGE (%)						
Elements	CdSe1	CdSe2	CdSe4	CdSe4/PEG	CdSe4/PVA	CdSe4/TEOS
Cd	5.73	5.96	6.04	1.14	1.49	1.32
Se	5.28	4.80	3.87	1.15	1.07	0.63
O	4.11	2.26	1.26	3.58	-	3.92
S/Si	Nil	2.18/Nil	4.99/Nil	Nil	Nil	Nil/0.81 silica

Table 3.3: Elemental stochiometric ratio of Cd:Se, Cd:S and Se:S in CdSe1, CdSe2, CdSe4 and CdSe4/PEG QDs

Sample	Conc. of 2-ME (in 50 ml solvent)	Ratio of Cd:Se	Ratio of Cd:S	Ratio of Se:S
CdSe 1	1:50	1:0.98	1:00	1:00
CdSe2	2:50	1:0.80	1:0.36	1:0.45
CdSe 4	4:50	1:0.63	1:0.83	0.76:1
CdSe4/PEG	PEG capped	1:1	1:00	1:00
CdSe4/PVA	PVA capped	1:0.72	1:00	1:00
CdSe4/TEOS	TEOS capped	1:0.47	1:00	1:00

3.4 Optical studies

3.4.1 Absorbance spectroscopy

The prepared poly CdSe, CdSe4, CdSe4/TEOS, CdSe4/PVA and CdSe4/PEG QDs were characterized by UV-Visible spectroscopy for the as-prepared poly CdSe (Figure 3.5(a)), and CdSe4, CdSe4/TEOS, CdSe4/PVA and CdSe4/PEG QDs (figure 3.5(b)). It is clear from figures that absorption maximum at 688, 415, 436, 431 and 430 nm is due to the transition between electronic state present in conduction band and hole state of valance band for poly CdSe , CdSe4,

CdSe4/TEOS, CdSe4/PVA and CdSe4/PEG QDs respectively. But in case of CdSe4 (figure 3.5 (b)) absorption edge at 520 nm is because of defects. As compared to poly CdSe large blue shift of about 288 nm was observed in CdSe4 QDs. This blue shift in CdSe4 with respect to poly CdSe proves that quantum confinement takes place in QDs. Negligible difference was found between absorbance edge position in CdSe4 and CdSe4/PEG QDs [36].
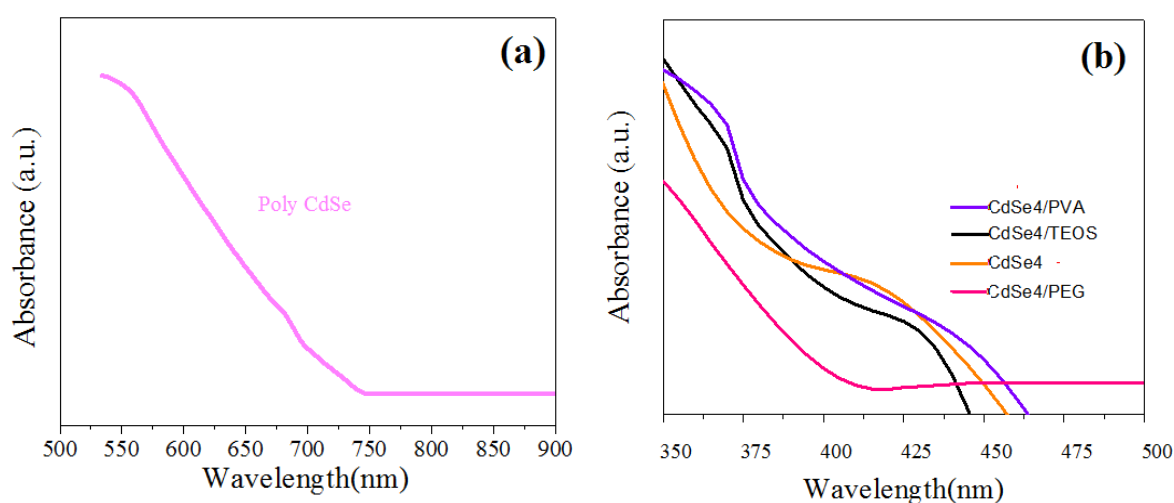
Figure 3.5: Absorbance spectra of (a) Poly CdSe (b) CdSe4, CdSe4/TEOS, CdSe4/PVA and CdSe4/PEG

3.4.2 Photoluminescence spectroscopy

Photoluminescence spectra of CdSe QDs capped with varying concentration of 2-ME (1 ml -6 ml) and polymer encapsulated CdSe QDs are shown in (figure 3.6 (a-d)). A fixed concentration 0.02 mg/ml for all CdSe QDs and encapsulated samples was taken to record room temperature photoluminescence spectra. These QDs were excited at different excitation wavelengths between the range 300 nm - 410 nm just for confirmation whether the emission shown by QDs is band edge emission or generated from several defect states. No variance was observed in emission spectra with respect to excitation wavelength. Emission takes place at same wavelength in every scan. This corroborate that all synthesized samples are emitting only the band edge luminescence or the luminescence due to surface traps. This PL study also confirms that QDs possess broad excitation and narrow emission spectra. It is clear from figure that PL emission peak get blue shifted on increase in concentration of 2-ME. Attained PL results show brilliant capping efficiency of 2-ME. However increase in concentration of 2-ME cause major variation in the

emission spectra of QDs. The emission spectra of as prepared CdSe1 (lower 2-ME concentration i.e; 1ml), CdSe2, CdSe4 and CdSe6 (highest 2-ME concentration i.e; 6 ml) are presented in figure 3.6a. CdSe4 and CdSe6 having high concentrations of 2-ME show (Figure 3.6 (a)) two distinctive features in spectra (1) band edge emission (2) trap emission. Emission peaks with their position and intensity along with ratio of trap emission with respect to band edge emission for comparison from all the samples are tabulated in table 3.4.
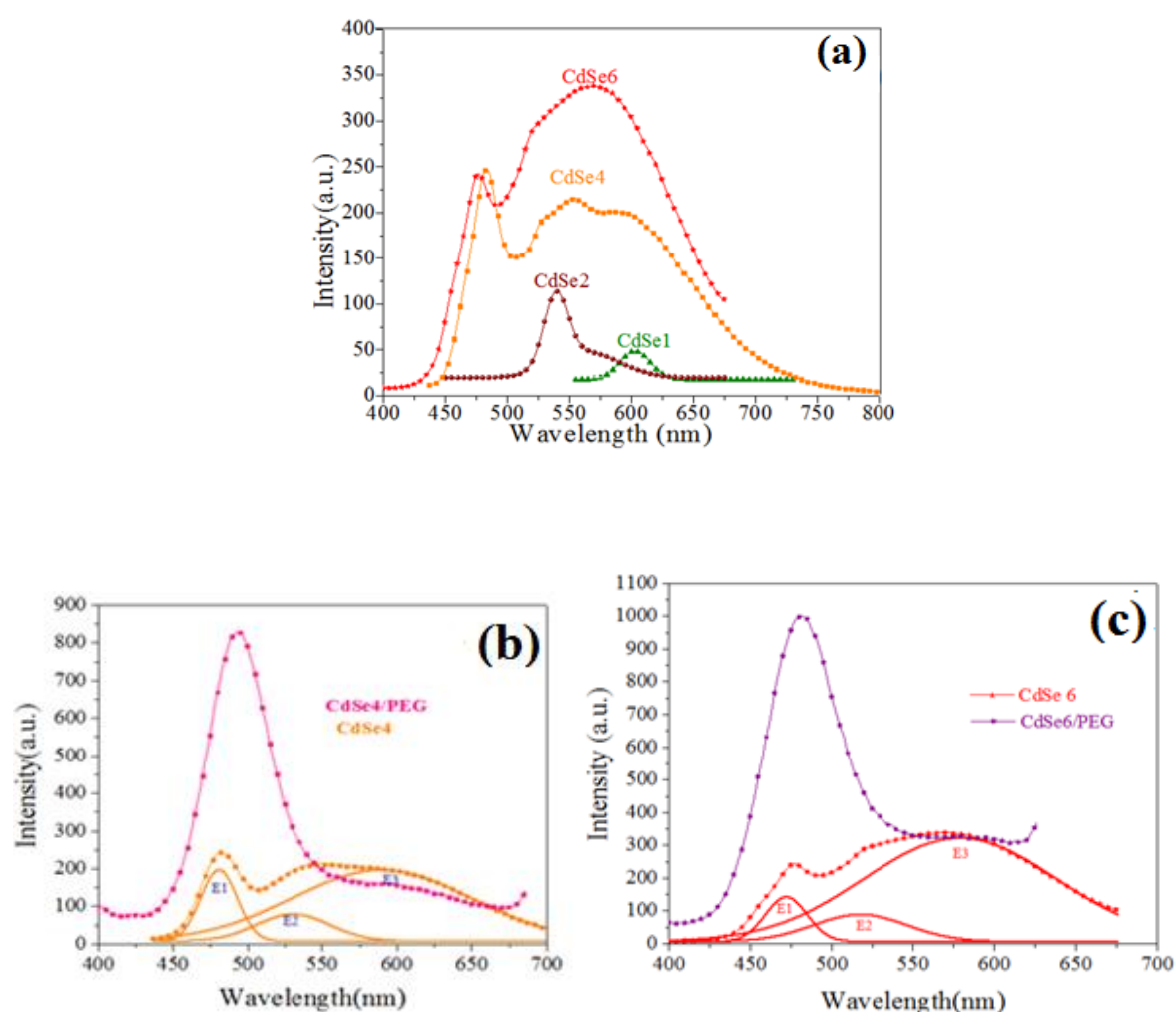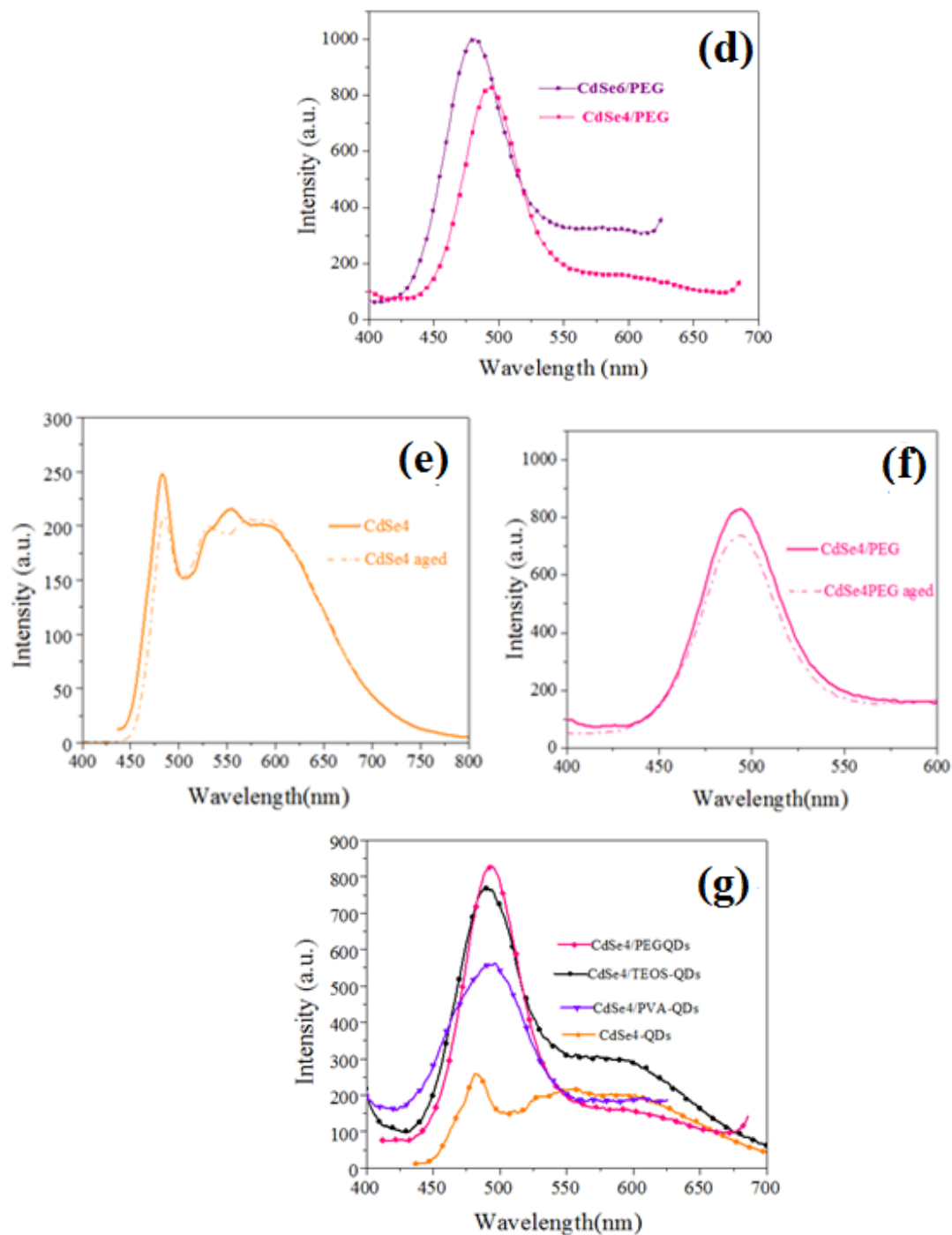
Figure 3.6: (a) Photoluminescence spectra of capped CdSe QDs with different concentration of 2-ME; where ∇-CdSe1; •-CdSe2; □-CdSe4; *-CdSe (b) Photoluminescence spectra of CdSe4 and CdSe4/PEG (c) Photoluminescence spectra of CdSe6 and CdSe6/PEG (d) Comparative photoluminescence spectra of CdSe4/PEG and CdSe6/PEG (e) Photoluminescence spectra of CdSe4 and CdSe4 aged (f) Photoluminescence spectra of CdSe4/PEG and CdSe4 /PEG aged (g) Comparative PL spectra of CdSe4 QDs encapsulated with different polymers

Table 3.4: Summary of photoluminescence peak positions, corresponding FWHM and relative intensities for all CdSe QDs and their polymer encapsulated structures

Sr.No.	Name of Sample	Particle size (TEM) (nm)	PL Emission Peak Position (nm)	FWHM (nm)	Intensity	Ratio of Band edge emission Intensity: Defect Intensity	Ratio comparison to the most intense CdSe4/PEG (in %)
1	CdSe1	-	600	24.26	49	1:0	-
2	CdSe2	2.6	540	25.41	114	1:0.38	-
3	CdSe4	1.8	482	31	259	1:0.86	31
4	CdSe6	-	475	-	241	1:1.40	-
5	CdSe6/PEG	-	481	50	1007	1:0.20	-
6	CdSe4/PEG	1.9	492	47.66	828	1:0	100
7	CdSe4/TEOS	2.0	488	57	765	1:0.25	92
8	CdSe4/PVA	1.8	494	62	560	1:0	67

Table 3.5: Summary of deconvoluted photoluminescence peak positions, corresponding FWHM and relative intensities for CdSe4 and CdSe6 along with the emission intensity after PEG encapsulation

Sample Name	Spectral position of PL emission (nm)			FWHM(nm)			Intensity			Intensity Ratios			Intensity of CdSe/PEG
	E1	E2	E3	E1	E2	E3	E1	E2	E3	E1/E1	E2/E1	E3/E1	
CdSe4	481	529	586	29	57	141	**199**	81	195	1	0.40	0.97	**828** (CdSe4/PEG)
CdSe6	471	515	578	30	64	132	**145**	92	320	1	0.63	2.2	**1007** (CdSe6/PEG)

Defect emission ratio was found high in case of CdSe4 and CdSe6 as they contain high 2-ME as compare to CdSe1, CdSe. In CdSe4 intensity of trap emission peak grow continuously with respect to band edge emission but as we further enhance addition concentration of 2-ME in case of CdSe6 trap emission intensity is totally dominating the band edge emission. For determination of peak positions in the spectra, we deconvoluted the spectra for CdSe4 and CdSe6. After deconvolution of spectra it was fitted to three peaks E1, E2 & E3 as can be perceived from figure 3.6(b) and figure 3.6 (c). Peak at E1 corresponds to band edge emission and E2 and E3 assigned to trap emission peaks in every case.

The peak positions along with the corresponding intensity & half widths have been presented in table 3.5. In previous studies quenching of both band edge emission and trap emission was described. The authors also revealed that intensity of trap emission keep on growing with respect to band edge emission as they increase the quantity of mercaptopropionic acid [26]. Analogous response was observed in our case, in as synthesized CdSe4 QDs band edge emission intensity was more as compare to trap emission (figure 3.6 (b)) but in CdSe6 the trap emission intensity dominate the band edge emission (figure 3.6 (c)). The peak positions along with the corresponding intensity & half widths have been presented in table 3(b). It was concluded from PL studies of all CdSe1, CdSe2, CdSe4 and CdSe6 that trap emission dominates the band edge emission on raising the 2-ME.

Surface defects on QDs surface mainly dangling bonds originate traps and these traps have strong hole acceptor quality. Photo excitation of such kind of QDs causes hole trapping in surface states. Owing to higher possibility of non-radiative relaxation process related with dangling bonds, quantum efficiency of particles emitting from surface states is not very high [9]. As thiols are well-known for their hole scavenging property which cause quenching of band edge emission and boost the tendency of deep trap emission. In bare CdSe QDs trap emission arise due to selenium vacancies because in these QDs leakage chances of selenium are high because of weak bonding of Cd and Se. This study also confirms that surface interaction plays an important role in emission intensity of QDs.

To overcome all these problems like stability, leakage of toxic ions from bare CdSe and to improve luminescence properties we encapsulated CdSe4 QDs with polymer. Firstly we tried

polyethylene glycol (PEG) for encapsulation of CdSe4 and CdSe6 QDs. It was found from its PL studies that luminescence properties get improved because this encapsulation prevents oxidation and chemical degradation of surface atoms. In occurrence of PEG a layer get formed on QDs surface by bonding between ether group in PEG polymer and CdSe QDs which provide strength to the Cd-Se bond in QDs. This bond formation takes place between hydrophilic group of QDs and PEG. Formation of layer reduces the chances of selenium leakage and as well pacifies the surface dangling bonds and decreases the chance of increasing trap emission and stabilizes the QDs.

It is clear from PL spectra of polymer encapsulated QDs (figure 3.6(b) and 3.6(c)) that intensity of band edge emission get 10 fold increased in CdSe4/PEG and CdSe6/PEG as compared to bare CdSe4 and CdSe6 QDs. Traps were completely removed from QDs surface on polymer encapsulation. We are in the position to say that this is the first report ever that reports on the removal of the trap emission and occurrence of only band edge emission with increased intensity. Detailed diagram of probable emissions in as synthesized QDs (with trap states) and PEG encapsulated QDs (trap state free) are presented in figure 3.7(a) and figure 3.7(b).
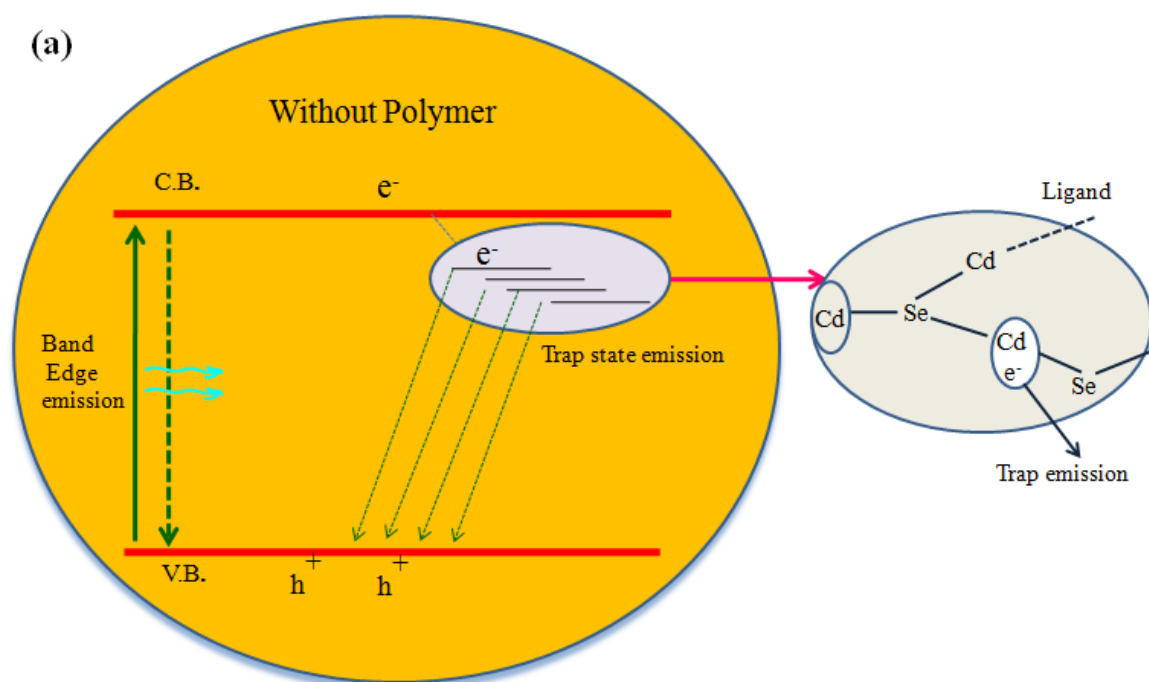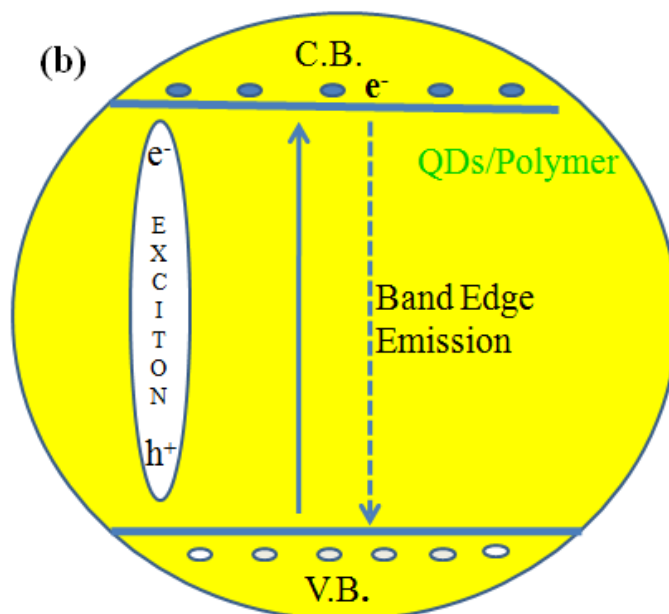
Figure 3.7: (a) Polymer encapsulated QDs without trap states and (b) Polymer encapsulated QDs without trap emission

Comparative intensities for bare CdSe QDs and their polymer encapsulated structures are presented in table 3.3 (a). We have compared CdSe4/PEG and CdSe6/PEG Figure 3.6(d) on comparison it was found that even though there is slight increase in intensity of CdSe6/PEG but the FWHM value for CdSe6/PEG has also been increased and this shows decline in monodispersity. This may be due to clusters formation resulted from agglomeration in small sized CdSe6 QDs. It was also noted that at red tail of spectra in CdSe6/PEG there is still traces that demonstrate presence of a few trap states whereas in CdSe4/PEG the spectra was clear.

Luminescence stability of CdSe4 and CdSe4/PEG QDs was confirmed with a procedure described here. PL spectra of stored samples CdSe4 and CdSe4/PEG have been recorded again after 6 months. These samples were stored at room temperature (temperature varies from 10°C to 35°C). It was clear from spectra that aged samples of CdSe4 (figure 3.6(e)) and CdSe4/PEG (figure 3.6(f)) for six months approximately possesses same luminescence as that of fresh samples with little decrease in intensity. Intensity of band edge luminescence decreased from 249 to 210 in CdSe4 and defects were prominent as they were in fresh CdSe4. In case of CdSe4/PEG aged sample reduction in intensity was from 827 to 733. This confirms that here is no further

subsistence of agglomeration in QDs on ageing. This result also demonstrate that the encapsulation of QDs by polymer prevent release of toxic selenium ions from CdSe QDs.

After confirmation of polymer encapsulation effectiveness in improvement in the stability and luminescence intensity of QDs, we have encapsulated these QDs by another polymer PVA and silicate TEOS. Comparative PL spectra of all CdSe4, CdSe4/TEOS, CdSe4/PVA and CdSe4/PEG presented in (figure 3.6 (g)) clarify that there is 10 fold increments in intensity along with complete exclusion of defects in case of silicate and polymer encapsulated structures. Silicates and different polymers have been used for the encapsulation of QDs and prevent oxidation and chemical degradation of surface atoms and improve luminescence characteristics. Formation of a layer takes place on CdSe4QDs surface on encapsulation. This layer assist in pacifying the dangling bonds present on surface of QDs, as well as decreases the probability of Cd^{2+} and Se^{2-} leakage from QDs and stabilizes the QDs.

Emission peak positions along with their corresponding intensities for CdSe4 QDs, CdSe4/PEG, CdSe4/PVA and CdSe4/TEOS structures are tabulated in Table 3.4. Results in Table 3.4 revealed that PL intensity is low in bare CdSe QDs but on encapsulation intensity get enhanced by many folds. This enhancement in fluorescence intensity by encapsulation is because of smoothening of QDs surface. Finally from these results it was found that we achieved improved and enhanced luminescence in all samples. Therefore, from EDX analysis and optical studies it has been confirmed that increased sulphur content affect optical properties. Now after this confirmation the samples were characterized by FTIR to know about the functional group present on the QD surface and the results are discussed in the next section.

3.5 FTIR analysis

Poly CdSe, CdSe4 QDs, CdSe4/TEOS, CdSe4/PVA and CdSe4/PEG were scanned by FTIR to know different functionalities in range 4000-600 cm^{-1}. FTIR spectra of poly CdSe and CdSe4 (figure 3.8(a and b)) contains intense peak at 3346 cm^{-1} due to presence of OH group. Peak at 1630 cm^{-1} was assigned to NH bending and 1462 cm^{-1} indicates presence of CH_2 bending. Peak which appears around 1100 cm^{-1} is due to CH_2 rocking. Weak band at 2200 cm^{-1} was referred to thiol group. Peak found around 1067-1041 cm^{-1} is due to C-O stretching. Band at 706 -899 cm^{-1}

is due to C-S stretching. Presence of extra peaks in spectra of CdSe4 was due to some impurities. Likewise FTIR spectra of CdSe4/TEOS (figure3.8(c)) demonstrates peak around 3260 cm^{-1} for OH, 1640 cm^{-1} for NH bend, C=O stretching 2100 cm^{-1} for alkynes. Presence of silica peak around 1089 cm^{-1} is accredited to silica encapsulation [41]. In case of CdSe4/PVA (figure3.8 (d)) band for OH is around 3245 cm$^{-1,}$ 2110 cm^{-1} corresponds to alkyne and band at 1640 cm^{-1} is for NH. Table 3.6 summarized all available functional groups on the QD surface. Similarly an FTIR spectrum of CdSe4/PEG (figure 3.8(e)) shows presence of an intense peak at 3257 cm^{-1} for OH group. Peaks appear around 1400 cm^{-1} is due to CH$_2$ bending. Peak around 2121 cm^{-1} and 1640 cm^{-1} are due to characteristic vibrations of NH bends respectively.

From FTIR studies it was concluded that these QDs hold functional groups like NH and OH which formulate them towards hydrophilicity and biocompatibility. Luminescent QDs prepared by aqueous route can be directly affixed to bio molecules due to their hydrophilic nature with great affinity. This is a boon of our technique, because the QDs which are produced by organic routes are all the time contains hydrophobic surfaces and need post treatment for biocompatibility and bioconjugation purposes. There are most commonly found functional groups on biomolecules are-OH, -CHO, -C=O, -NH and –SH [37].

Table 3.6: FTIR most common band positions of CdSe4, CdSe4 encapsulated structures and their assignments

Assingments	Band Position
OH group	3346 cm^{-1}
Alkyne	2100 cm^{-1}
CH$_2$ bending	1462 cm^{-1}
NH bend, C=O stretching	1630 cm^{-1}
C-S Streching	672 cm^{-1}
Silica	1089cm^{-1}
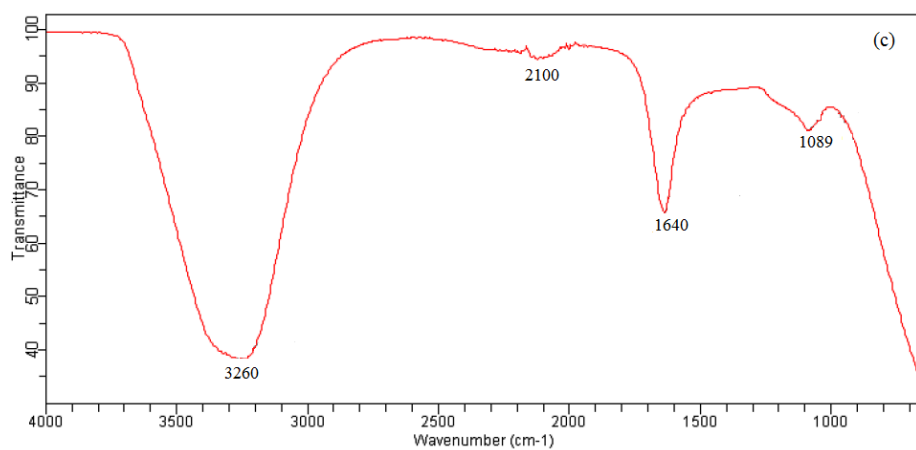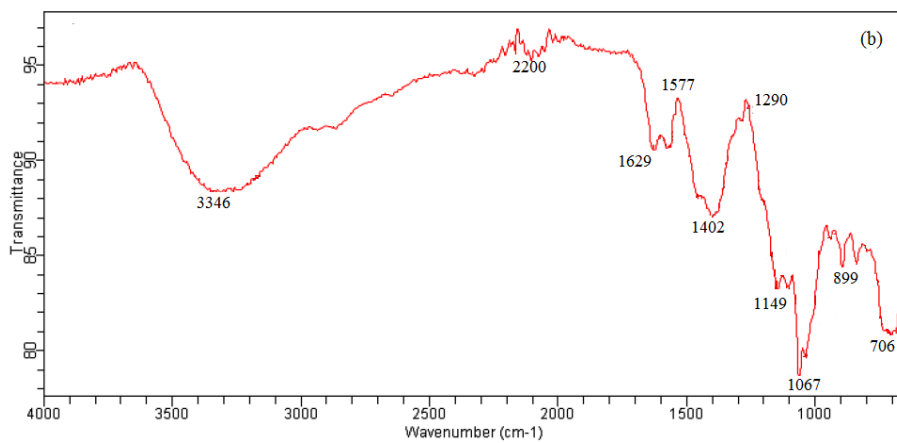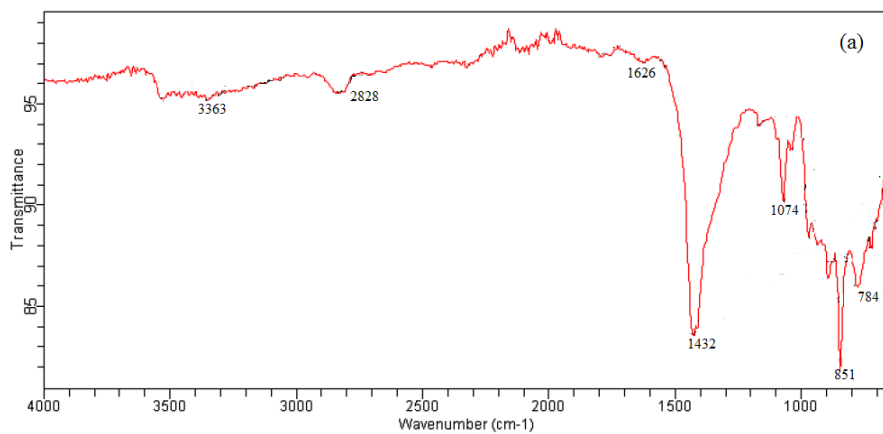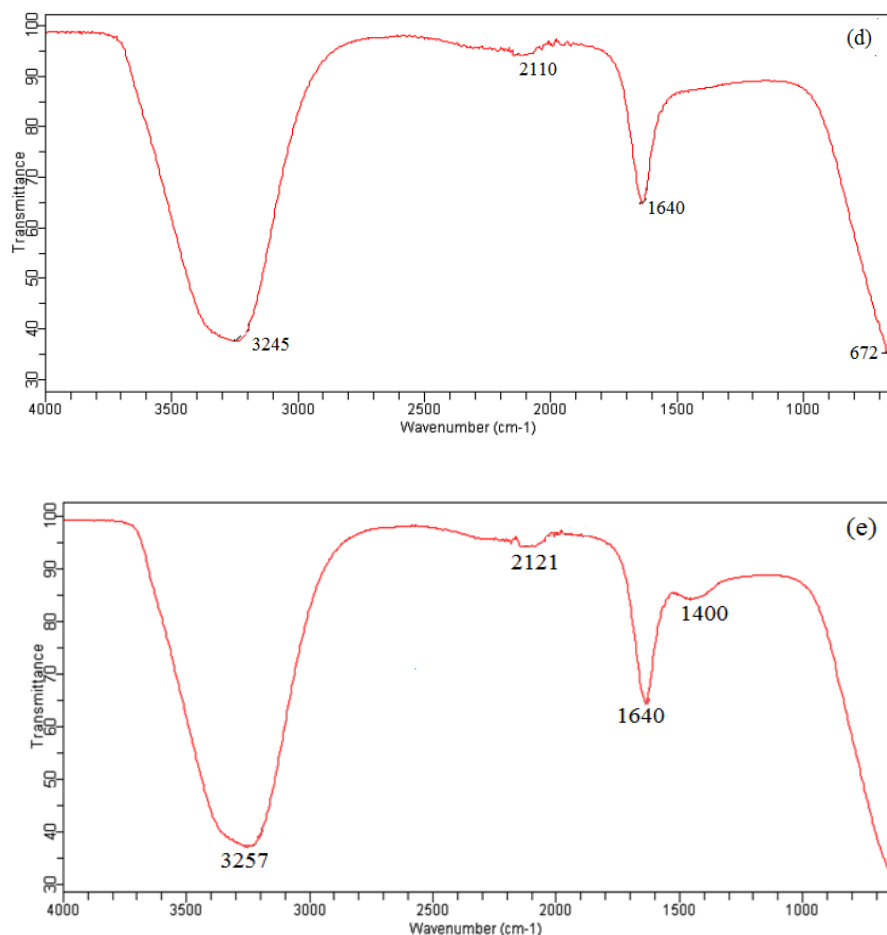
Figure 3.8: (a) FTIR spectra of poly CdSe (b) FTIR spectra of CdSe4 QDs (c) FTIR spectra of CdSe4/TEOS QDs (d) FTIR spectra of CdSe4/PVA QD and (e) FTIR spectra of CdSe4/PEG QD

3.6. Conclusion

Present chapter concludes that increase in concentration of stabilizing agent i.e., 2-ME leads to reduction in particle size as well as formation of trap sites. Trap sites originated due to hole scavenging property of thiol group. Encapsulation of surface of small CdSe4 QDs by polymer and silicates plays a noteworthy role to improve optical properties. The prepared QDs were characterized by XRD, TEM, EDX, absorbance spectroscopy, photoluminescence spectroscopy and FTIR. It has been found from photoluminescence spectroscopy that the QDs are of very small size with emission 480 nm. On rising 2-ME there is increase in surface to volume ratio. This cause increased number of unsatisfactory groups on surface of QDs and leads to defect

origin. This study leads to confirmation that thiol content is responsible for trap emission beyond a particular concentration of 2-ME and this has also been confirmed from EDX analysis. Other probable cause of trap emission was presence of dangling bonds, high surface/volume ratio or moreover may be because of selenium vacancies. To conquer all these setbacks we encapsulated QDs by polymers and silica. PL studies noticeably revealed that QDs encapsulated with polymers show brilliant emission intensity with complete removal of trap emission. Considerably these polymer encapsulated QDs posses outstanding aqueous dispersibility enhanced trap free band edge emission intensity and improved fluorescence stability.

3.7 References

1.Singh M.K., Hassan P.A., Kadam A., *"Hole scavenging and aging effect on the photoluminescence of CdS quantum dots",* Materials Chemistry and Physics, vol. 146(1-2), pp. 136-140, July 2014.

2.Murray C., Norris D.J., Bawendi M.G*., "Synthesis and characterization of nearly monodisperse CdE (E= sulfur, selenium, tellurium) semiconductor nanocrystallites",* Journal of the American Chemical Society, vol. 115(19), pp. 8706-8715, Sep. 1993.

3.Peng X., Manna L., Yang W., Wickham J., Scher E., Kadavanich A., Alivisatos A. P., *"Shape control of CdSe nanocrystals",* Nature, vol. 404(6773), pp. 59, Mar. 2000.

4.Pellegrino T., Manna L., Kudera S., Liedl T., Koktysh D., Rogach A.L., Parak W.J., *"Hydrophobic nanocrystals coated with an amphiphilic polymer shell: a general route to water soluble nanocrystals ",* Nano letters, vol. 4(4), pp.703-707, Apr. 2004.

5.Gerion D., Pinaud F., Williams S.C., Parak W.J., Zanchet D., Weiss S., Alivisatos A.P., *"Synthesis and properties of biocompatible water-soluble silica-coated CdSe/ZnS semiconductor quantum dots",* The Journal of Physical Chemistry B, vol. 105(37), pp. 8861-8871, Sep. 2001.

6.Fei X., Hao Y., Guo J., Jia G., Xie L., Wei F., Hou S., *"Optical properties investigation of core/shell quantum dots by low temperature synthesis"* Int. J. Electrochem. Sci, vol. 9, pp. 3795, July 2014.

7.Gaponik N., Talapin D.V., Rogach A.L., Hoppe K., Shevchenko E.V., Kornowski A., Weller H., *"Thiol-capping of CdTe nanocrystals: an alternative to organometallic synthetic routes"*, The Journal of Physical Chemistry B, vol. 106(29), pp.7177-7185, July 2002.

8.Underwood D.F., Kippeny T., Rosenthal S.J., *"Ultrafast carrier dynamics in CdSe nanocrystals determined by femtosecond fluorescence upconversion spectroscopy"*, The Journal of Physical Chemistry B, vol. 105(2), pp. 436-443, Jan. 2001.

9.Pokrant S., Whaley K.B., *"Tight-binding studies of surface effects on electronic structure of CdSe nanocrystals: the role of organic ligands, surface reconstruction, and inorganic capping shells"*, The European Physical Journal D-Atomic, Molecular, Optical and Plasma Physics, vol. 6(2), pp. 255-267, May 1999.

10. Bawendi M.G., Steigerwald M.L., Brus L.E., *"The quantum mechanics of larger semiconductor clusters (" quantum dots")"*, Annual Review of Physical Chemistry, vol. 41(1), pp. 477-496, Oct. 1990.

11. Califano M., Franceschetti A., Zunger A., *"Temperature dependence of excitonic radiative decay in CdSe quantum dots: the role of surface hole traps "*, Nano Letters, vol. 5(12), pp. 2360-2364, Dec. 2005.

12. Smith A.M., Duan H., Rhyner M.N., Ruan G., Nie S., *"A systematic examination of surface coatings on the optical and chemical properties of semiconductor quantum dots"*, Physical Chemistry Chemical Physics, vol. 8(33), pp. 3895-3903, 2006.

13. Qu L., Peng X., *"Control of photoluminescence properties of CdSe nanocrystals in growth"*, Journal of the American Chemical Society, vol. 124(9), pp. 2049-2055, 2002.

14. Jeong S., Achermann M., Nanda J., Ivanov S., Klimov V.I., Hollingsworth J.A., *"Effect of the thiol− thiolate equilibrium on the photophysical properties of aqueous CdSe/ZnS nanocrystal quantum dots"*, Journal of the American Chemical Society, vol.127(29), pp.10126-10127, July 2005.

15. Fomenko V., Nesbitt D.J., *"Solution control of radiative and nonradiative lifetimes: A novel contribution to quantum dot blinking suppression"*, Nano Letters, vol. 8(1), pp. 287-293, Jan. 2008.

16. Landes C., Burda C., Braun M., El-Sayed M. A., *"Photoluminescence of CdSe nanoparticles in the presence of a hole acceptor: n-butylamine",* The Journal of Physical Chemistry B, vol. 105(15), pp. 2981-2986, Apr. 2001.

17. Kalyuzhny G., Murray R.W., *"Ligand effects on optical properties of CdSe nanocrystals",* The Journal of Physical Chemistry B, vol.109 (15), pp.7012-7021, Apr. 2005.

18. Gaunt J.A., Knight A.E., Windsor S.A., Chechik V., *"Stability and quantum yield effects of small molecule additives on solutions of semiconductor nanoparticles",* Journal of colloid and interface science, vol. 290(2), pp. 437-443, Oct. 2005.

19. Bullen C., Mulvaney P., *"The effects of chemisorption on the luminescence of CdSe quantum dots",* Langmuir, vol. 22(7), pp. 3007-3013, Mar. 2006.

20. Munro A.M., Jen-La Plante I., Ng M.S., Ginger D.S., "*Quantitative study of the effects of surface ligand concentration on CdSe nanocrystal photoluminescence",* The Journal of Physical Chemistry C, vol. 111(17), pp. 6220-6227, May 2007.

21. Gómez D.E., van Embden J., Jasieniak J., Smith T.A., Mulvaney P., *"Blinking and surface chemistry of single CdSe nanocrystals",* Small, vol. 2(2), pp. 204-208, Feb. 2006.

22. Hammer N.I., Early K.T., Sill K., Odoi M.Y., Emrick T., Barnes M.D.*,* "Coverage-mediated suppression of blinking in solid state quantum dot conjugated organic composite nanostructures", The Journal of Physical Chemistry B, vol. 110(29), pp. 14167-14171, July 2006.

23. Odoi M.Y., Hammer N.I., Early K.T., McCarthy K.D., Tangirala R., Emrick T., Barnes M.D., *"Fluorescence lifetimes and correlated photon statistics from single CdSe/oligo (phenylene vinylene) composite nanostructures",* Nano letters, vol.7(9), pp. 2769-2773, Sep. 2007.

24. Wuister S.F., de Mello Donega C., Meijerink A., *"Influence of thiol capping on the exciton luminescence and decay kinetics of CdTe and CdSe quantum dots",* The Journal of Physical Chemistry B, vol. 108(45), pp. 17393-17397, Nov. 2004.

25. Ji X., Copenhaver D., Sichmeller C., Peng X., *"Ligand bonding and dynamics on colloidal nanocrystals at room temperature: the case of alkylamines on CdSe nanocrystals",* Journal of the American Chemical Society, vol. 130(17), pp. 5726-5735, Apr. 2008.

26. Baker D. R., Kamat P.V., *"Tuning the emission of CdSe quantum dots by controlled trap enhancement",* Langmuir, vol. 26(13), pp. 11272-11276, Apr. 2010.

27. Zheng M., Gu M., Jin Y., Jin G., *"Preparation, structure and properties of TiO2–PVP hybrid films",* Materials Science and Engineering: B, vol. 77(1), pp. 55-59, Aug. 2000.

28. Bol A.A., Meijerink A., *"Doped semiconductor nanoparticles–a new class of luminescent materials",* Journal of Luminescence, vol. 87, pp. 315-318, May 2000.

29. Xu S.J., Wang X.C., Chua S.J., Wang C.H., Fan W. J., Jiang J., Xie X. G., *"Effects of rapid thermal annealing on structure and luminescence of self-assembled InAs/GaAs quantum dots",* Applied Physics Letters, vol.72 (25), pp. 3335-3337, June 1998.

30. Manorama S.V., Reddy K.M., Reddy C.G., Narayanan S., Raja P.R., Chatterji P.R. *"Photostabilization of dye on anatase titania nanoparticles by polymer capping",* Journal of Physics and Chemistry of Solids, vol. 63(1), pp.135-143, Jan. 2002.

31. Gao Y., Peng X., *"Crystal structure control of CdSe nanocrystals in growth and nucleation: dominating effects of surface versus interior structure",* Journal of the American Chemical Society, vol. 136(18), pp. 6724-6732, Apr. 2014.

32. Prabahar S., Dhanam M., *"CdS thin films from two different chemical baths—structural and optical analysis",* Journal of Crystal growth, vol. 285(1-2), pp. 41-48, Nov. 2005.

33. Barman J., Sarma K.C., Sarma M., Sarma K., *"Structural and optical studies of chemically prepared CdS nanocrystalline thin films",* Indian journal of pure and applied physics, vol. 46, pp. 339-343, May 2008.

34. Kumar H., Barman P.B., Singh, R.R., *"Effect of size and shell: enhanced optical and surface properties of CdS, ZnS and CdS/ZnS quantum dots",* Physica E: Low-Dimensional Systems and Nanostructures, vol. 67, pp. 168-177, Mar. 2015.

35. Schipper M.L., Iyer G., Koh A.L., Cheng Z., Ebenstein Y., Aharoni A., Chen, X., *"Particle size, surface coating, and PEGylation influence the biodistribution of quantum dots in living mice",* Small, vol. 5(1), pp. 126-134, Jan.2009.

36. SalmanOgli A*., "Nanobio applications of quantum dots in cancer: imaging, sensing, and targeting",* Cancer nanotechnology, vol. 2(1-6), pp.1-19, Dec. 2011.

37. Raven P.h., Johnson G.B., "The chemical building blocks of life", Biology 6th edition.

CHAPTER-4

PRECURSOR BASED SYNTHESIS OF ZINC SULFIDE (ZnS) AND CdSe/ZnS NANOSTRUCTURES: STRUCTURAL, MORPHOLOGICAL, ELEMENTAL, OPTICAL AND FUNCTIONAL ANALYSIS
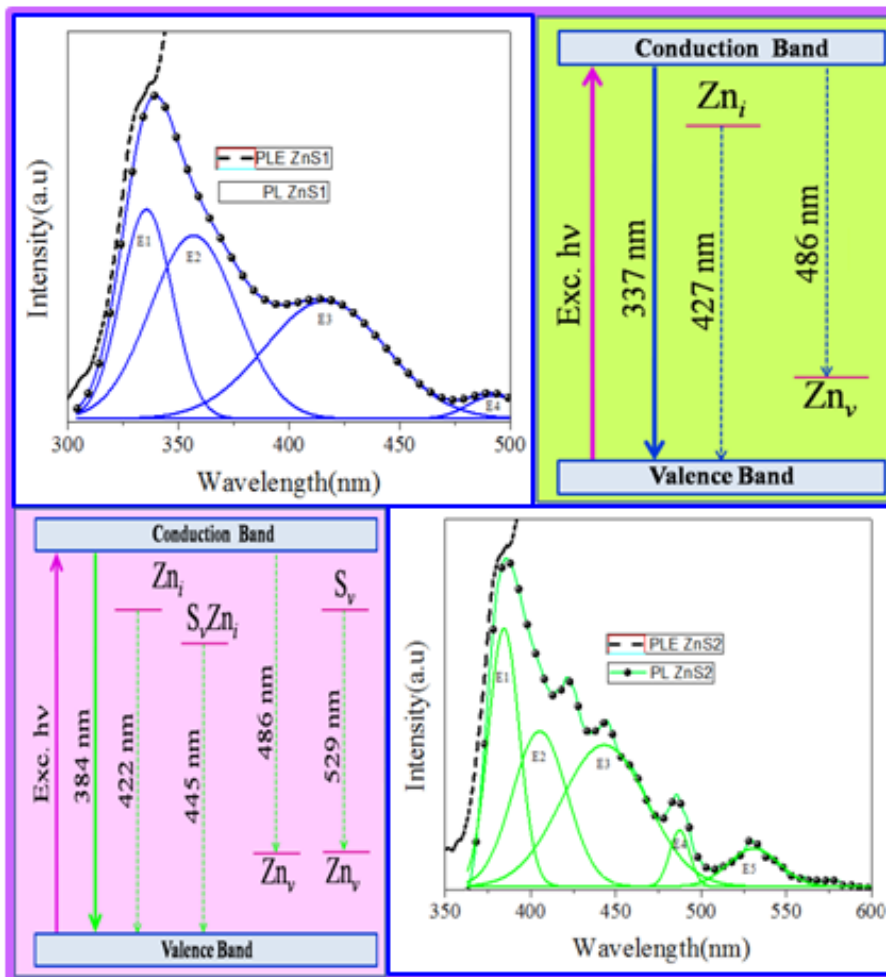
Highlights

- Synthesis of CdSe, ZnS and CdSe/ZnS QDs via aqueous route.

- Evaluated link between precursor reactivity, size of QDs and optical properties.

- Optical studies confirmed that different precursor affects the band edge emission and defect emission profiles in ZnS1 and ZnS2.

Abstract

In this chapter the effect of two different precursors on optical properties of ZnS quantum dots (QDs) and CdSe/ZnS core-shell structures on the basis of their reactivity have been studied. ZnS (precursor based), CdSe and CdSe4/ZnS QDs have been prepared opting aqueous route and have been characterized by XRD, TEM, EDX, PL and FTIR techniques. CdSe/ZnS core-shell QDs structures were prepared using different precursor of shell material i.e. ZnS (with zinc chloride and zinc sulphate as the source of Zn). Photoluminescence spectra of all QDs confirm the effective fluorescence.

4.1 Introduction

In last few decades semiconducting QDs and core-shell nanostructures have gained much attention due to the vast fields of their applicability e.g. in optical amplifier [1], LED [2, 3] and biomedical fields [4]. These core-shell structures have high luminescence quantum yield. This happens because in core-shell, shell confines electron and hole wave functions in core of the particle. This shell also minimizes interaction of wave function with trap states.

Core-shell structures CdSe/ZnS [5] QDs are extensively applied in biomedical application because they have relatively less complex methods of synthesis and tunable luminescent properties [6]. Core-shell structures improve luminescence and surface properties of QDs. These characteristics of core-shell QDs make them fascinating from experimental and a practical point of view [7, 8]. Previously enhancement in photoluminescence quantum yields of CdSe was observed on formation of shell of higher band gap material. Covering of CdSe by shell leads to passivation of nonradiative recombination sites [9]. Core-shell materials are biphasic and mainly synthesized by solution growth method. The reason of the shell formation on the core particle is like surface modification [10]. Shell increase stability and dispersibility by controlled release of the core. Type-1 core-shell exhibit high fluorescence yield with high stability because shell confines electron hole wave functions to core and reduces interactions of the surface defects which can behave as traps and recombination centers [11].

Selection of the shell material depends upon required properties that we desire after coating. Small mismatch between core and shell material leads to favorable formation of core-shell material [12]. Selection of precursors also influences quantity and quality of the obtained products. Particle size, optical properties and other features of QDs get affected by reactivity and conversion rate of precursors. Conversion rate of precursors affect the growth of QDs. Slow reactive precursor leads to generation of few nuclei in nucleation process. This whole process extends the growth time and produce large size particles. Since the nanomaterials come up to frontward with their exceptional size dependent physical and optical properties and this aspect makes them brilliant competitor for biological activities [13-18].

Current chapter is focused in the direction of the synthesis of ZnS1, ZnS2 QDs (with zinc chloride and zinc sulphate as the Zn precursor) and their core-shell structures in aqueous media. Here we purposely studied the effect of various experimental parameters on optical properties. For core-shell synthesis we took CdSe4 QDs as core (as discussed in chapter 3). In this chapter effect of two different precursors (based on their reactivity) on photoluminescence of ZnS and CdSe/ZnS QDs is explained. X-ray diffraction (XRD), photoluminescence spectroscopy (PL), Fourier transform infrared spectroscopy (FTIR) and Transmission electron microscopy (TEM) characterization techniques were used to study their structural, optical, luminescence, surface chemistry properties and size distribution respectively.

4.2 Experimental details

ZnS1 and ZnS2 were synthesized by aqueous chemical method. CdSe4 was taken as core. Synthesis of CdSe/ZnS1 and CdSe/ZnS2 was carried out by seed growth method. Complete methodology for synthesis of is presented in chapter 2 (section 2.3) in detail. To study structural, elemental and optical properties of prepared QDs they were characterized by XRD (Shimadzu powder x-ray diffractometer using Cu $K_{\alpha 1}$ radiation), TEM (HITACHI (H-7500), EDX (TECNAI G^2 20S-TWIN (FEI Neitherlands)) and PL (Perkin Elmer LS55). FTIR spectra of these QDs were recorded using Cary 630 spectrophotometer (Agilent technology).

4.3 Results and discussions

ZnS exists in two crystallite forms hexagonal wurtzite and zinc blende ZnS cubic phase (Figure 4.1). At room temperature the stable structure of ZnS is zinc blende. There were a small number of reports related to stable wurtzite ZnS at room temperature. Band gap of cubic form of ZnS is 3.54 eV at 300 K while hexagonal phase band gap is 3.91 eV. Transition of cubic form of ZnS to the wurtzite form takes place at 1020°C. Moreover, ZnS is a significant phosphor host lattice material employ in electroluminescent devices (ELD) [19].
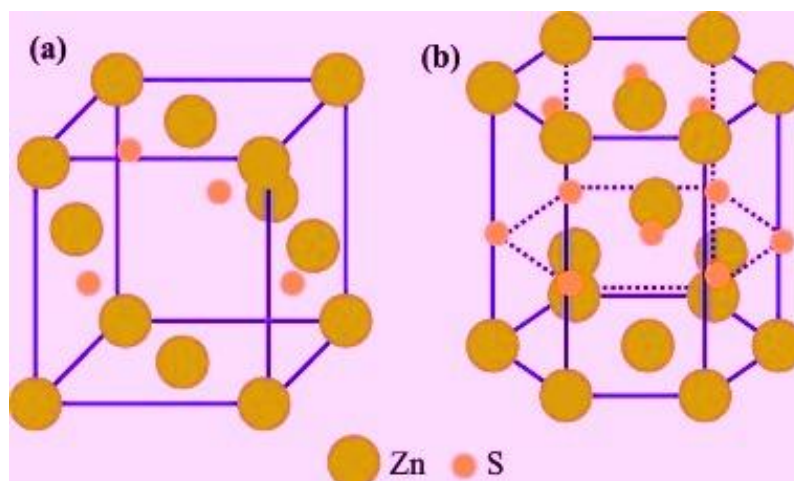
Figure 4.1: Crystal structure of ZnS (a) cubic and (b) Wurtzite

4.3.1 Structural analysis

4.3.2 XRD analysis

Structural characterization of synthesized samples was carried out by XRD and the spectra obtained are arranged in the (Figure 4.2 (a-e)). XRD of core CdSe4 QDs shows cubic phase of CdSe. XRD of CdSe4 (Figure 4.2 (a)) has already been discussed in detail in chapter 3. XRD pattern of ZnS1 (Figure 4.2 (b)), showed four peaks ascribed to pure cubic phase of ZnS1. In case of ZnS2 (Figure 4.2 (c)) there is presence of three prominent diffraction peaks at diffraction angle $2\theta = 28°$, $47°$ and $56°$ corresponds to miller indices (111),(220) and (311) demonstrate cubic structure for ZnS QDs. In addition to these peaks spectra of ZnS2 contains additional peaks at 2θ positions $31°$, $34°$, $36°$, $62°$and $67°$ and (l00), (002), (101), (013) and (112) are the Miller indices linked to these peaks respectively [20,21]. These additional peaks in ZnS2 present the hexagonal phase of ZnO. XRD of ZnS2 clearly reveals partial oxidation of ZnS takes place due to extremely highly hygroscopic nature of zinc chloride. Figure 4.2 (d) and (e) show XRD pattern for core-shell structures CdSe/ZnS1 and CdSe/ZnS2 respectively. Structural parameters calculated from XRD spectra for all samples like 2θ positions, hkl planes, and phase are tabulated in Table 4.1. It is clear from table 4.1 and figure 4.2 ((d) and (e)) that XRD of core-shell QDs contains prominent peaks situated at the centre of both CdSe and ZnS. Shift in 2θ positions in case of core-shell toward high diffraction angle is clear confirmation of core-shell

structure formation. Crystallite size for ZnS1 and ZnS2 were obtained using the Scherrer's formula.

Table 4.1: Structural parameters of core CdSe4, ZnS1, ZnS2, CdSe/ZnS1 and CdSe/ZnS2 QDs

Sample Name	2θ Position	hkl	Size from XRD (nm)	Size from TEM (nm)	Surface/Volume Ratio (nm^{-1})
CdSe4	25.47	111	1.8	1.9	3.15
	30.39	200			
	42.58	220			
	49.11	311			
ZnS1	29.18	111	2.8	3.1	1.93
	33.08	200			
	48.73	220			
	58.13	311			
ZnS2	28.74(ZnS)	111	2.5	2.5	2.4
	31.65(ZnO)	100			
	34.19(ZnO)	002			
	36.05(ZnO)	101			
	47.48((ZnS)	220			
	56.55(ZnS)	311			
CdSe/ZnS1	25.53	111		3.5	1.71
	31.69	200			
	42.78	220			
	49.19	311			
CdSe/ZnS2	25.49	111		3.7	1.61
	31.69	100			
	34.57	002			
	36.19	101			
	42.61	220			
	47.74	220			
	56.69	311			
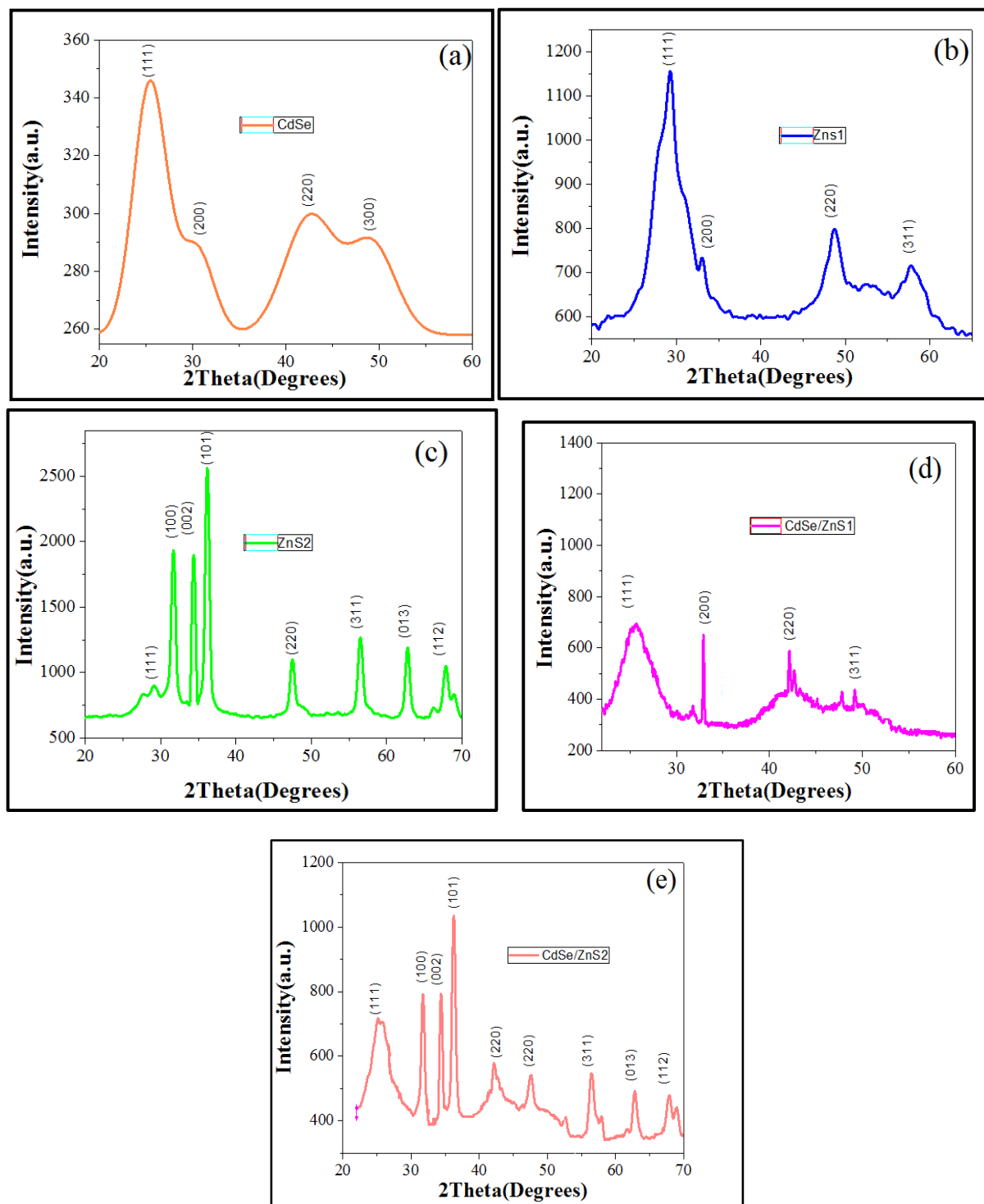
Figure 4.2: XRD spectra of synthesized (a) Core CdSe4 (b) ZnS1(c) ZnS2 (d) CdSe/ZnS1 and (e) CdSe/ZnS2

4.3.3 Transmission electron microscopy

Core CdSe4, ZnS1, ZnS2, CdSe/ZnS1 and CdSe/ZnS2 were also examined by TEM for their morphological behaviors which are shown in figure 4.3(a-e).
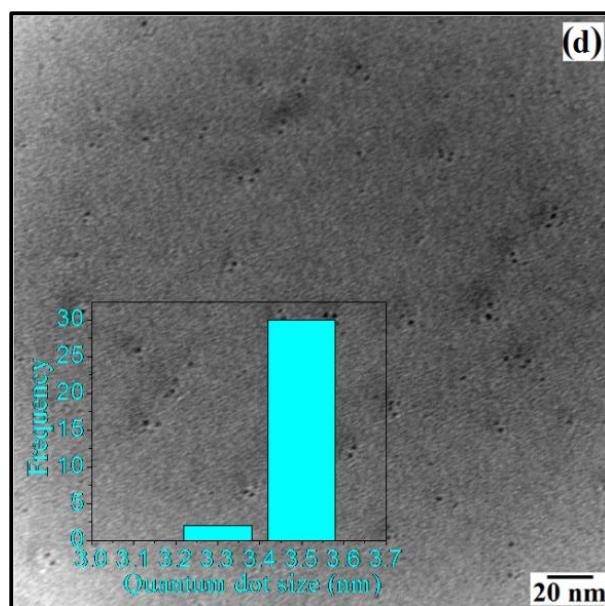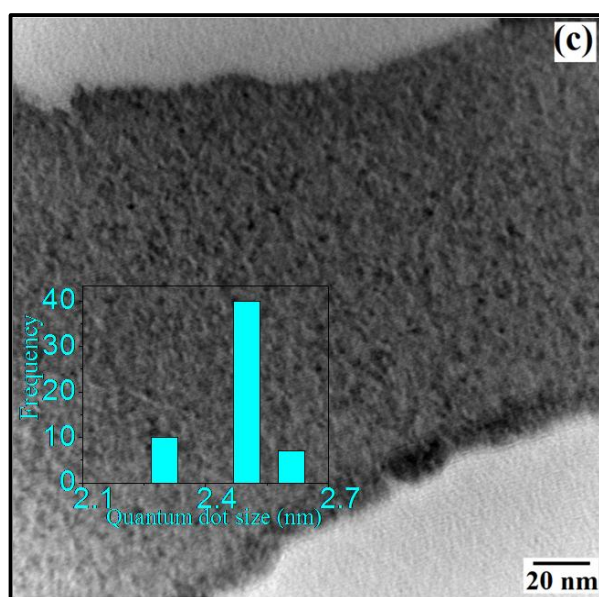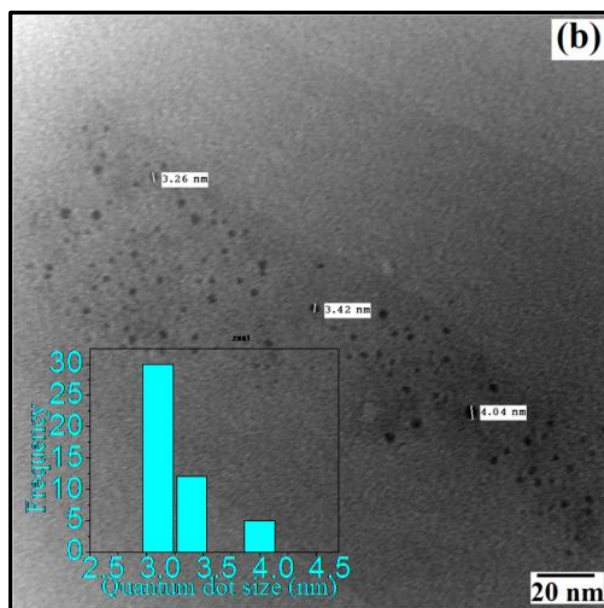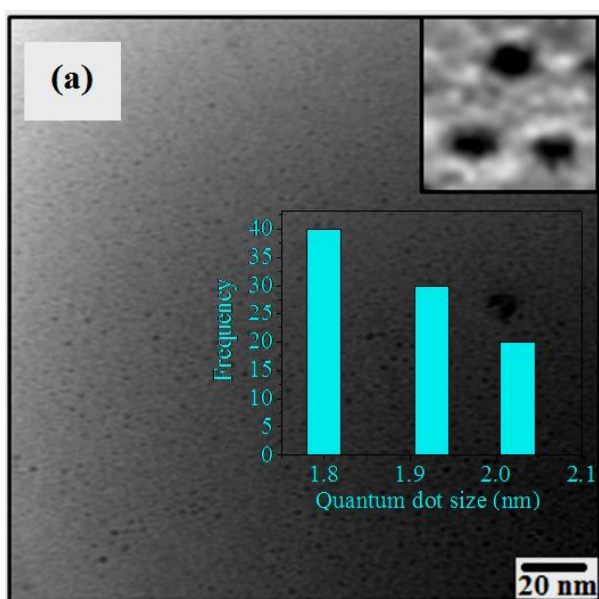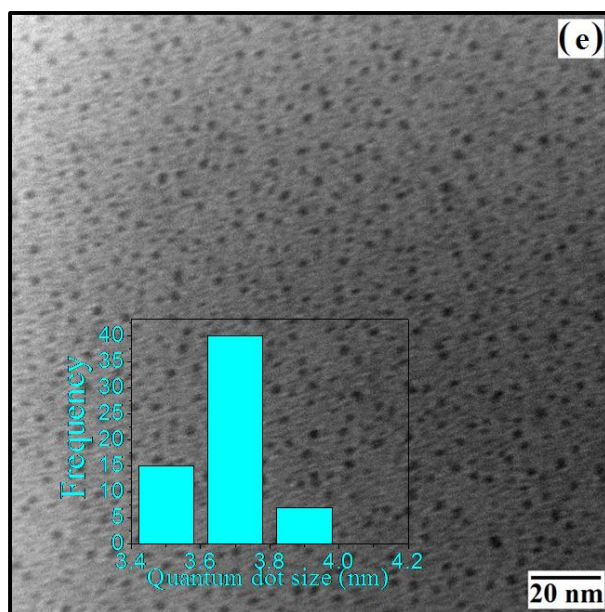
Figure 4.3: TEM images of synthesized (a) Core CdSe4 (b) ZnS1(c) ZnS2 (d) CdSe/ZnS1 and (e) CdSe/ZnS2

Images revealed that particles were in monodispersed phase that denied agglomerate formation. Average diameter of QDs was measured with the help of Image-J software. Figure 4.3 (a) confirms that core CdSe4 QDs are uniformly distributed with particle size 1.8 nm. TEM images of ZnS1 (figure 4.3(b)) and ZnS2 (figure 4.3(c)) showed spherical QDs with uniform size distribution. Particle size of ZnS1 was found larger as compared to ZnS2 due to variation in the precursor reactivity used for synthesis of ZnS1 and ZnS2. Shell formation on CdSe4 core QDs by ZnS was also confirmed by TEM images shown in figure 4.3(d). There is clear presentment of shell on CdSe4 core QDs in this figure. In case of CdSe/ZnS2 no clear presentment of shell. Obtained particle size for all samples has been mentioned in Table 4.1.

4.3.4 Energy-dispersive X-ray spectra

Synthesized QDs and their core-shell structures were analyzed by EDX for verification of elemental composition of samples. EDX spectra of all samples contain peak of carbon and copper and these peaks are because of carbon coated copper grid used during EDX analysis. EDX spectra for core CdSe4 (figure 4.4 (a)) show that the sample was pure CdSe. Figure 4.4 (b)

shows intense peaks of Zn and S due to high concentration of Zn and S precursors. Similarly EDX spectra of ZnS2 have intense peak of Zn and S figure 4.4 (c). Figure 4.4 (d) and 4.4 (e) demonstrate the EDX spectra of core/shell CdSe/ZnS1 and CdSe/ZnS2, peaks of Cd and Se are due to core CdSe4 and peaks of Zn and S are due to ZnS shell. This EDX analysis also leads to confirmation of CdSe/ZnS structure. Stochiometric ratio of Zn:S and CdSe: ZnS for ZnS1, ZnS2, CdSe/ZnS1 and CdSe/ZnS2 QDs are tabulated in Table 4.2.
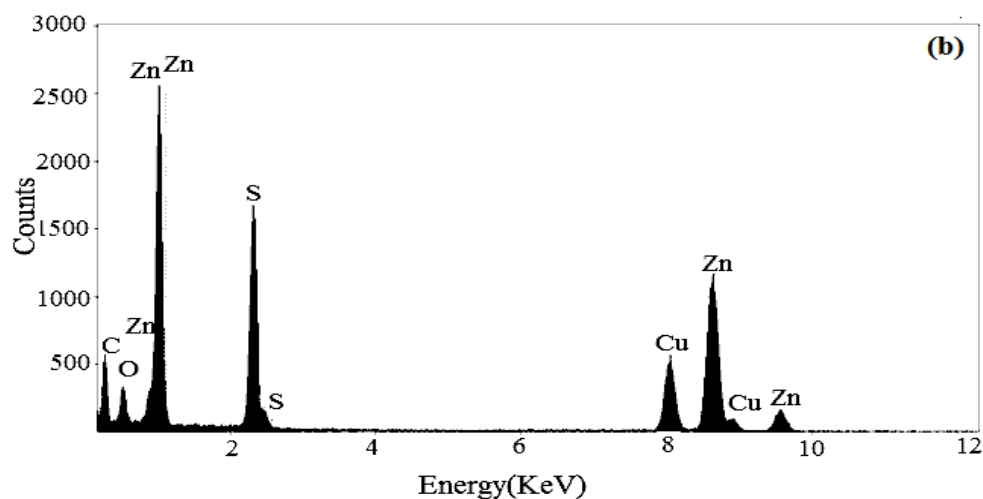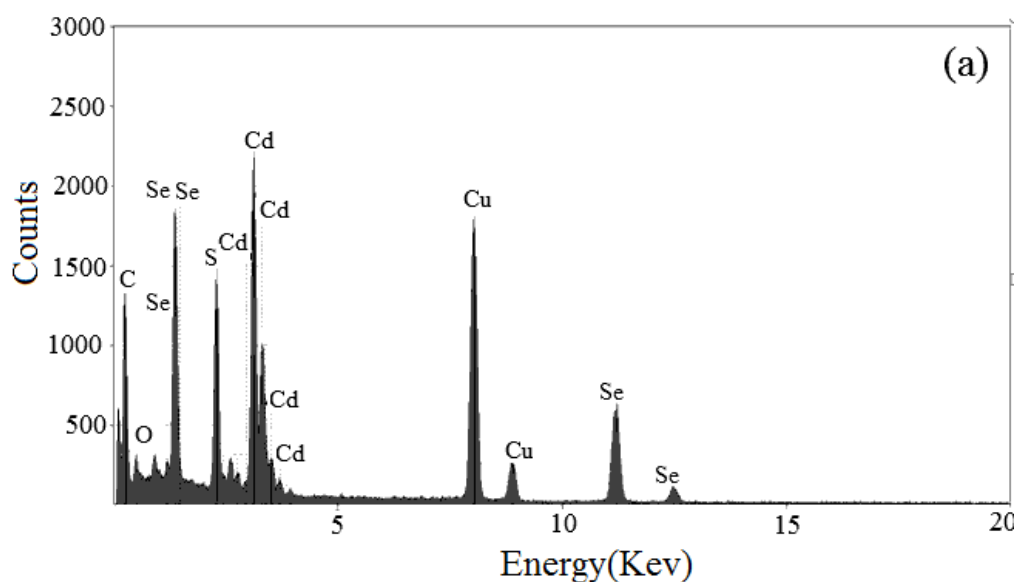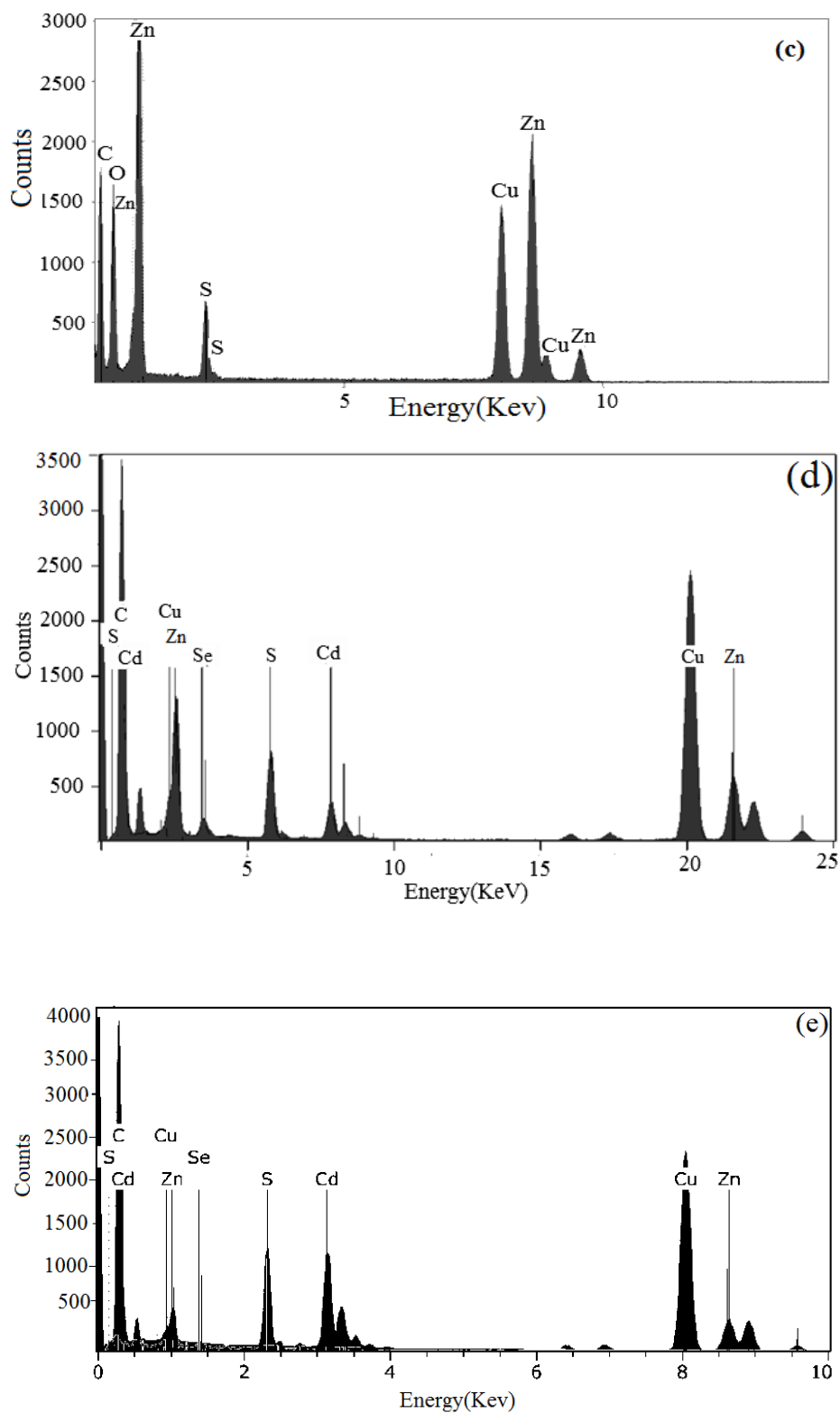
Figure 4.4: EDX spectra of synthesized (a) Core CdSe4 (b) ZnS1(c) ZnS2 (d) CdSe/ZnS1 and (e) CdSe/ZnS2

Table 4.2: Stochiometric ratio of Zn: S and CdSe: ZnS for ZnS1, ZnS2, CdSe/ZnS1 and CdSe/ZnS2 QDs

Sample	Ratio of Zn:S	Ratio of CdSe:ZnS
ZnS 1	1:0.23	-
ZnS2	1:0.95	-
CdSe/ZnS1	-	1:0.5
CdSe/ZnS2	-	1:0.35

4.4 Optical studies

4.4.1 Photoluminescence and photoluminescence excitation (PLE) Studies

Photoluminescence spectra and photoluminescence excitation (PLE) of all the QDs were recorded by using 0.02 mg/ml solution of QDs. This study was carried out at room temperature. Emission of samples was recorded by exciting samples at different excitation wavelengths. Excitation spectra for all QDs were recorded by setting proper emission edge of PL peak. PL and PLE spectra for CdSe4 i.e. core material are presented in figure 4.5(a) this figure concludes that in core CdSe4 QDs band edge transition $1s^e$ and $1s^h$ is around 2.6 eV (476 nm) while emission position is at 481 nm (2.5 eV) respectively. As we have already discussed in chapter 3 that PL spectrum of CdSe4 shows band edge emission along with trap emission. The possible reason of defects in case of these CdSe has been formerly discussed [22]. Hereafter CdSe4 will be considered as CdSe. In case of ZnS1 (Figure 4.5(b)) excitation spectra contain excitation peak at 333 nm which associated to emission at 337, 427, 486 nm where band edge emission for ZnS1 was at 337 nm with defects states at 427 and 486 nm. Schematic illustration of emission transitions in ZnS1 QDs are presented in figure 4.5 (b1). ZnS2 (figure 4.5 (c)) show excitation peak at 380 nm and this excitation peak associated to band emission at 384 and defect emissions at 422, 445, 486 and 529. Schematic depiction of emission transitions in ZnS2 QDs are shown in figure 4.5 (c1). All the emission peak positions and PLE positions are enumerated in table 4.3. For the determination of peak positions and FWHM in PL spectra of CdSe, ZnS1, and ZnS2 deconvulation has been implemented. Deconvulated PL spectra was fitted to different peaks

which can be seen from figure (4.5 (a, b, c)). Deconvulated E1 peak in every case presents band edge emission and other additional peaks present defects. Position of every peak in deconvulated spectra along with FWHM value and intensity are given in table 4.4. In case of ZnS1 and ZnS2 emission peaks between 400-450 nm (figure 4.5 b and 4.5 c) are associated with interstitial zinc and sulfur vacancies. Peaks at 485 nm - 490 nm were assigned to Zn-vacancies [23]. Blue green emission peaks at 525 nm is due to vacancy associated to recombination of electron from energy level of sulfur vacancy to hole on the energy level of Zn vacancy [24]. Vacancy originated because of recombination of electron from energy level of sulfur vacancy to hole on the energy level of Zn were not found in ZnS1. Figure 4.5 (d)) shows excitation peak at 474 nm for CdSe/ZnS1which correspond to emission at 487 nm along with defect emission at 531 nm respectively. Similarly, PLE spectra of CdSe/ZnS2 (Figure 4.5 (e)) contain absorption peak at 472 nm this corresponds to PL emission at 484 nm with defect emission at position 532. Presence of peak at 532 nm even after shell formation may be due to sulfur vacancies. Just for confirmation of effect of shell formation we compared the PL spectra of CdSe with CdSe/ZnS1 (Figure 4.5 (f)) and CdSe/ZnS2 (Figure 4.5 (g)) and improvement in intensity was perceived on shell formation with decline in defects. Defect emission in small QDs generally takes place due to unsatisfactory dangling bonds on their surface. These dangling bonds cause trap generation and these traps have strong hole acceptor tendency. From comparison of bare CdSe4 and core-shell structures it was found that in CdSe4 band edge emission intensity is approximately equivalent to defect luminescence. However, in core-shell structures band edge emission is extended in contrast with defect luminescence. It was confirmed from PL analysis that all QDs are fluorescent and fluorescent behavior of these QDs gets better on shell formation.

Table 4.3: Summary of PLE and emission wavelengths for core CdSe4, ZnS1, ZnS2, CdSe/ZnS1 and CdSe/ZnS2

Sample Name	PLE Wavelength(nm)	Emission wavelength(nm)
Core CdSe4	476	481
ZnS1	333	337, 427, 486
ZnS2	380	385, 422, 445, 486, 529
CdSe/ZnS1	474	487, 531
CdSe/ZnS2	472	484, 532

Table 4.4: Summary of deconvoluted photoluminescence peak positions, corresponding FWHM and relative intensities for core CdSe4, ZnS1 and ZnS2

Sample Name	Spectral position of PL emission					FWHM					Intensity				
	E1	*E2*	*E3*	*E4*	*E5*	*E1*	*E2*	*E3*	*E4*	*E5*	*E1*	*E2*	*E3*	*E4*	*E5*
Core CdSe4	481	529	586			30	56	139			192	72	198		
ZnS1	335	357	417	491		29	45	63	29		276	250	185	91	
ZnS2	384	405	442	487	529	21	39	56	14	38	312	228	217	149	135
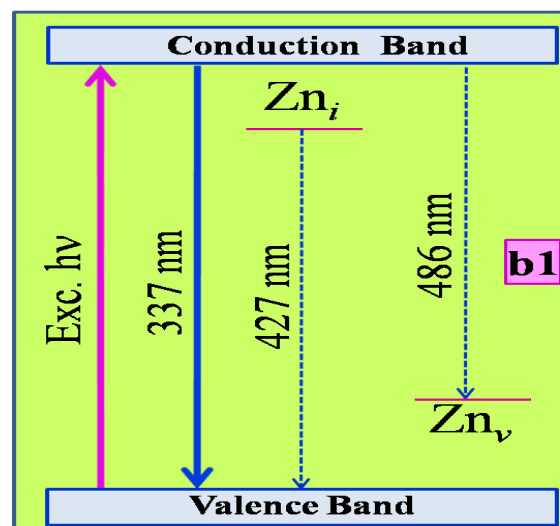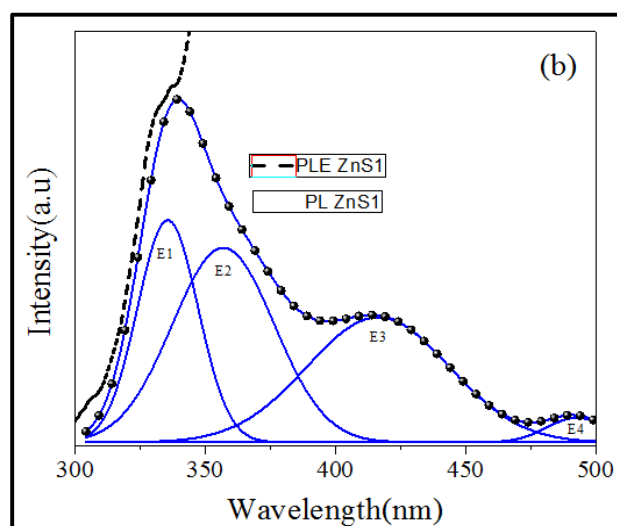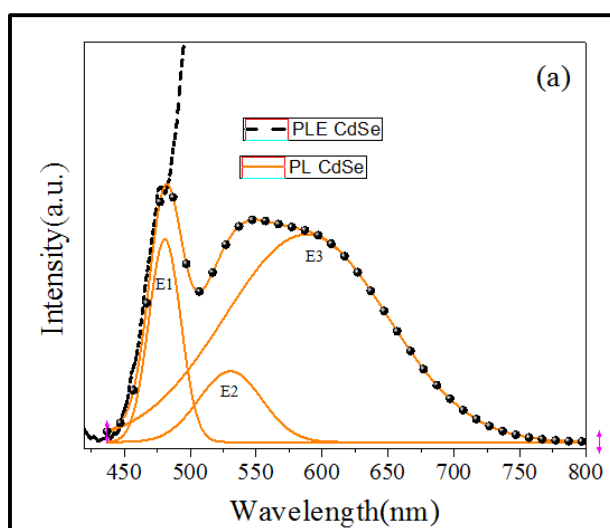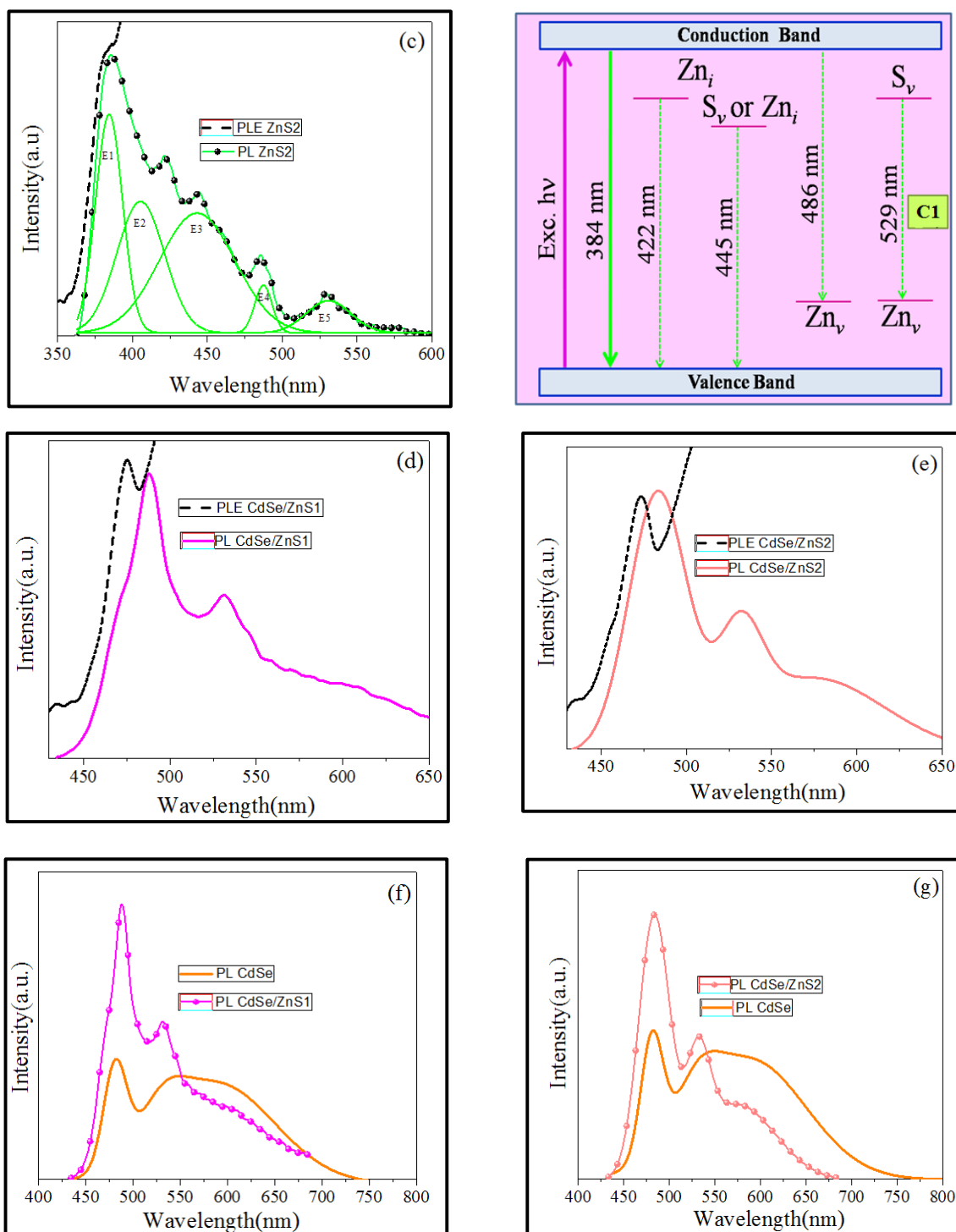
Figure 4.5: Photoluminescence and Photoluminescence excitation spectra for (a) Core CdSe4 QDs (b) ZnS1 (b1) Schematic representation of emission transitions in ZnS1 QDs (c) ZnS2 (c1) Schematic representation of emission transitions in ZnS2 QDs (d) CdSe/ZnS1 (e) CdSe/ZnS2 (f) Comparative PL spectra for CdSe, CdSe/ZnS1and (g) Comparative PL spectra for CdSe and CdSe/ZnS2

4.5 FTIR analysis

FTIR spectra of prepared QDs were recorded for confirmation of functionality present on surface of QDs. In case of core CdSe4 peaks at 1630 cm^{-1} assigned to -NH bending and 1462 cm^{-1} is due to CH$_2$ bending (figure (4.6 (a)).
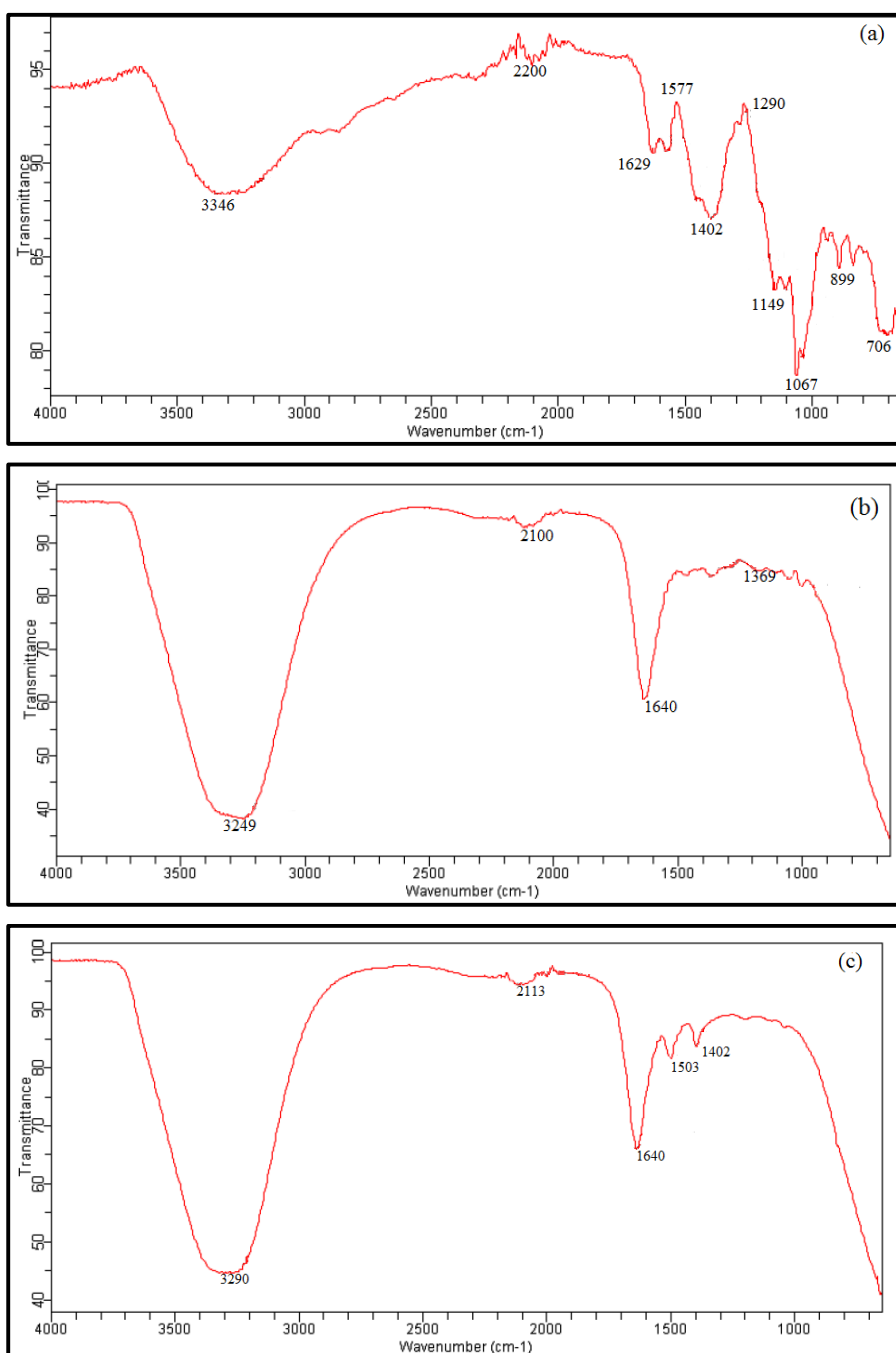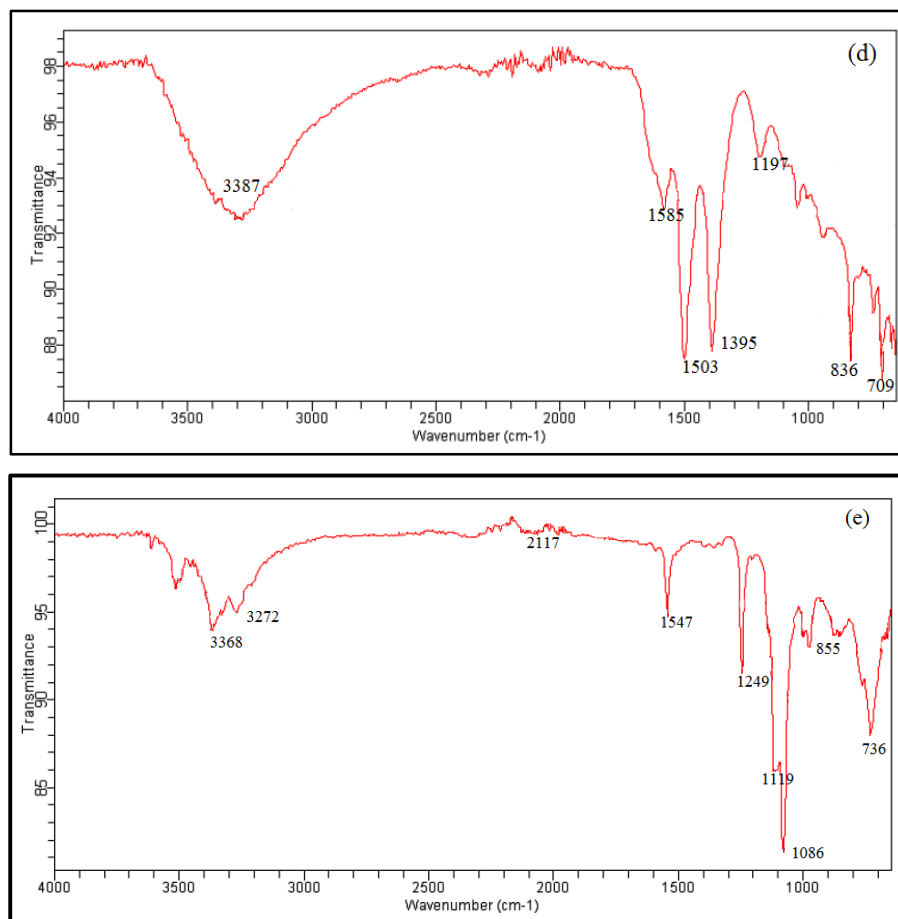
Figure 4.6: FTIR spectra for (a) Core CdSe4 QDs (b) ZnS1 QDs (c) ZnS2 QDs (d) CdSe/ZnS1QDs and (e) CdSe/ZnS2QDs

Intense peak at 3346 cm^{-1} confirms presence of -OH group. Peak approximately at 1100 cm^{-1} is due to CH$_2$ rocking. Weaker band at 2200 cm^{-1} shows presence of thiol group. Peak at 1067-1041 cm^{-1} assigned to C-O stretching. Peak showing C-S band stretching is at 706-899 cm^{-1}. In ZnS1 (figure (4.6 b)) peak at 3249 cm^{-1} is intense and is due to -OH group. Peak at 1640 cm^{-1} and 2100 cm^{-1} are ascribed to -NH bends characteristic vibrations. Peaks at 3290 cm^{-1} and 1640 cm^{-1} in FTIR spectra of ZnS2 (figure (4.6 c)) corresponds to -OH group and -NH bending respectively. Weak peak in the region of the 1503 cm^{-1} and 1402 cm^{-1} are due to C-N vibrations. In CdSe/ZnS1 (figure (4.6 d)) peaks at 3387 cm$^{-1,}$ 1503 cm^{-1} and 1395 cm^{-1} are due to -OH group and C-N vibrations respectively. Peak at 1197 cm^{-1} is because of CH$_2$ rocking. Peak observed at 709-899 cm^{-1} corresponds to C-S stretching. Similarly in case of CdSe/ZnS2 (figure (4.6e)) peaks

at 3368 cm^{-1} for -OH, 2117 cm^{-1} for alkynes and at 1547 cm^{-1} for C-N vibrations, 1119 cm^{-1} due to CH_2 rocking. Presence of -NH and -OH groups in FTIR spectra of these QDs confirms hydrophilic and biocompatible nature of these QDs.

4.6 Conclusion

In this chapter we have evaluated the change in optical characteristics of ZnS and CdSe/ZnS core-shell structures as an effect of ZnS precursor reactivity. Precursor reactivity also affects the size of QDs. From structural analysis of prepared QDs it was confirmed that particle size of ZnS1 was greater than ZnS2. Optical analysis of QDs confirms that precursor used to synthesize ZnS1 and ZnS2 influence the band edge and defect emission positions. In case of ZnS1 band edge emission was found at 337 nm along with few defects at 427 nm, 486 nm. As compared to ZnS1, in case of Zns2 band edge emission was at 384 along with defects at 422 nm, 445 nm, 486 nm and 529 nm. It was concluded from optical studies that ZnS1 synthesized by $ZnSO_4.7H_2O$ shows less defects as compared to ZnS2. From all these studies it has been concluded that reactivity of precursor effect the particle size as well as optical properties. Hence connection was established between reactivity of precursor with optical properties and size of QDs. In case of core-shell structures it is found on comparison of PL spectra of CdSe and CdSe/ZnS that there is improvement in intensity on shell formation with reduction in defect, although these defects were not removed completely on shell formation. In case of bare CdSe QDs intensity of band edge luminescence is almost analogous to defect luminescence. But in core-shell CdSe-QDs structures band edge emission is prominent as compared to defect luminescence and this is due to smoothening and passivation of unsatisfactory bonds on shell formation.

4.7 References

1. Tierno A., Ackemann T., Leburn C.G., Brown C.T.A., *"Saturation of absorption and gain in a quantum dot diode with continuous-wave driving",* Applied Physics Letters, vol. 97(23), pp. 231104, Dec. 2010.

2. Mora-Seró I., Giménez S., Moehl T., Fabregat-Santiago F., Lana-Villareal T., Gómez R., Bisquert J., *"Factors determining the photovoltaic performance of a CdSe quantum dot*

sensitized solar cell: the role of the linker molecule and of the counter electrode", Nanotechnology, vol. 19(42), pp. 424007, Sep. 2008.

3. Wang T., Pang F., Wang K., Zhang R., Liu G., *"Evanescent wave coupled semiconductor quantum dots fiber amplifier based on reverse Micelle method",* In Nanotechnology, IEEE-NANO 2007, pp. 819-822, Aug. 2007.

4. Kim L., Anikeeva P.O., Coe-Sullivan S.A., Steckel J.S., Bawendi M.G., Bulovic V., *"Contact printing of quantum dot light-emitting devices",* Nano letters, vol. 8(12), pp. 4513-4517, Nov. 2008.

5. Delehanty J.B., Medintz I.L., Pons T., Brunel F.M., Dawson P.E., Mattoussi H., *"Self-assembled quantum dot−peptide bioconjugates for selective intracellular delivery*", Bioconjugate chemistry, vol. 17(4), pp. 920-927, July 2006.

6. Kim J., Lee J., Kyhm K., *"Surface-plasmon-assisted modal gain enhancement in Au-hybrid CdSe/ZnS nanocrystal quantum dots",* Applied Physics Letters, vol. 99(21), pp. 213112, Nov. 2011.

7. Nirmal M., Brus, L., *"Luminescence photophysics in semiconductor nanocrystals",* Accounts of chemical research, vol. 32(5), pp. 407-414, May 1999.

8. Mattoussi H., Mauro J.M., Goldman E.R., Anderson G.P., Sundar V.C., Mikulec F.V., Bawendi M.G., "Self-assembly of CdSe− ZnS quantum dot bioconjugates using an engineered recombinant protein", *Journal of the American Chemical Society*, *122*(49), 12142-12150, Dec. 2000.

9. Fu Y., Kim D., Jiang W., Yin W., Ahn T.K., Chae H., *"Excellent stability of thicker shell CdSe@ ZnS/ZnS quantum dots",* RSC Advances, vol. 7(65), pp. 40866-40872, 2017.

10. Nomoev A.V., Bardakhanov S.P., Schreiber M., Bazarova D.G., Romanov N.A., Baldanov B.B., Syzrantsev V.V., *"Structure and mechanism of the formation of core–shell nanoparticles obtained through a one-step gas-phase synthesis by electron beam evaporation",* Beilstein journal of nanotechnology, vol. *6*, pp. 874, 2015.

11. Talapin D.V., Mekis I., Götzinger S., Kornowski A., Benson O., Weller H., *"CdSe/CdS/ZnS and CdSe/ZnSe/ZnS Core− Shell− Shell Nanocrystals"*, The Journal of Physical Chemistry B, vol. 108(49), pp. 18826-18831, Dec. 2004.

12. Dabbousi B.O., Rodriguez-Viejo J., Mikulec F.V., Heine J.R., Mattoussi H., Ober R., Bawendi M.G., *"CdSe) ZnS core− shell quantum dots: synthesis and characterization of a size series of highly luminescent nanocrystallites"*, The Journal of Physical Chemistry B, vol. 101(46), pp. 9463-9475, Nov. 1997.

13. Viswanatha R., Sarma D.D., *"Growth of nanocrystals in solution"*, Nanomaterials chemistry: recent developments and new directions, pp. 139-170, 2007.

14. Rempel J.Y., Bawendi M.G., Jensen K.F., *"Insights into the kinetics of semiconductor nanocrystal nucleation and growth"*, Journal of the American Chemical Society, vol. 131(12), pp. 4479-4489, Mar. 2009.

15. Clark M.D., Kumar S.K., Owen J.S., Chan E.M., *"Focusing nanocrystal size distributions via production control"*, Nano letters, vol. 11(5), pp. 1976-1980, Apr. 2011.

16. Hens Z., Čapek R.K., *"Size tuning at full yield in the synthesis of colloidal semiconductor nanocrystals, reaction simulations and experimental verification"*, Coordination Chemistry Reviews, vol. 263, pp. 217-228, Mar. 2014.

17. Abé S., Capek R., De Geyter B., Hens Z., *"Using the acid concentration and chain length as a tuning strategy in the hot injection synthesis, an experimental and theoretical analysis"*, In *5th Conference on Nanoscience with Nanocrystals (NaNax 5)*, 2012.

18. Sugimoto T., Shiba F., Sekiguchi T., Itoh H., *"Spontaneous nucleation of monodisperse silver halide particles from homogeneous gelatin solution I: silver chloride"*, Colloids and Surfaces A: Physicochemical and Engineering Aspects, vol. 164(2-3), pp. 183-203, May 2000.

19. Hamad S., Catlow C.R.A., Spano E., Matxain J.M., Ugalde J.M., *"Structure and properties of ZnS nanoclusters"*, The Journal of Physical Chemistry B, vol. 109(7), pp. 2703-2709, Feb. 2005.

20. Murugadoss G., Ramasamy V., Kumar M.R., *"Photoluminescence enhancement of hexagonal-phase ZnS: Mn nanostructures using 1-thioglycolic acid",* Applied Nanoscience, vol. 4(4), pp. 449-454, Apr. 2014.

21. Rathore K.S., Patidar D., Janu Y., Saxena N.S., Sharma K., Sharma T.P., "Structural and optical characterization of chemically synthesized ZnS nanoparticles"*, Chalcogenide Letters*, vol. 5(6), pp. 105-110, June 2008.

22. Kumari A., Singh R.R., *"Encapsulation of highly confined CdSe quantum dots for defect free luminescence and improved stability", Physica E: Low-dimensional Systems and Nanostructures*, vol. 89, pp. 77-85, May 2017.

23. Hu P.A., Liu, Y., Fu L., Cao L., Zhu D., *"Self-assembled growth of ZnS nanobelt networks",* The Journal of Physical Chemistry B, vol. 108(3), pp. 936-938, Jan. 2004.

24. Hou L., Gao F., *"Phase and morphology controlled synthesis of high-quality ZnS nanocrystals",* Materials letters, vol. 65(3), pp. 500-503, Feb. 2011.

CHAPTER-5

SYNTHESIS AND CHARACTERIZATION OF NEAR INFRARED CADMIUM TELLURIDE (CdTe) QUANTUM DOTS AND THEIR POLYMER ENCAPSULATED STRUCTURES
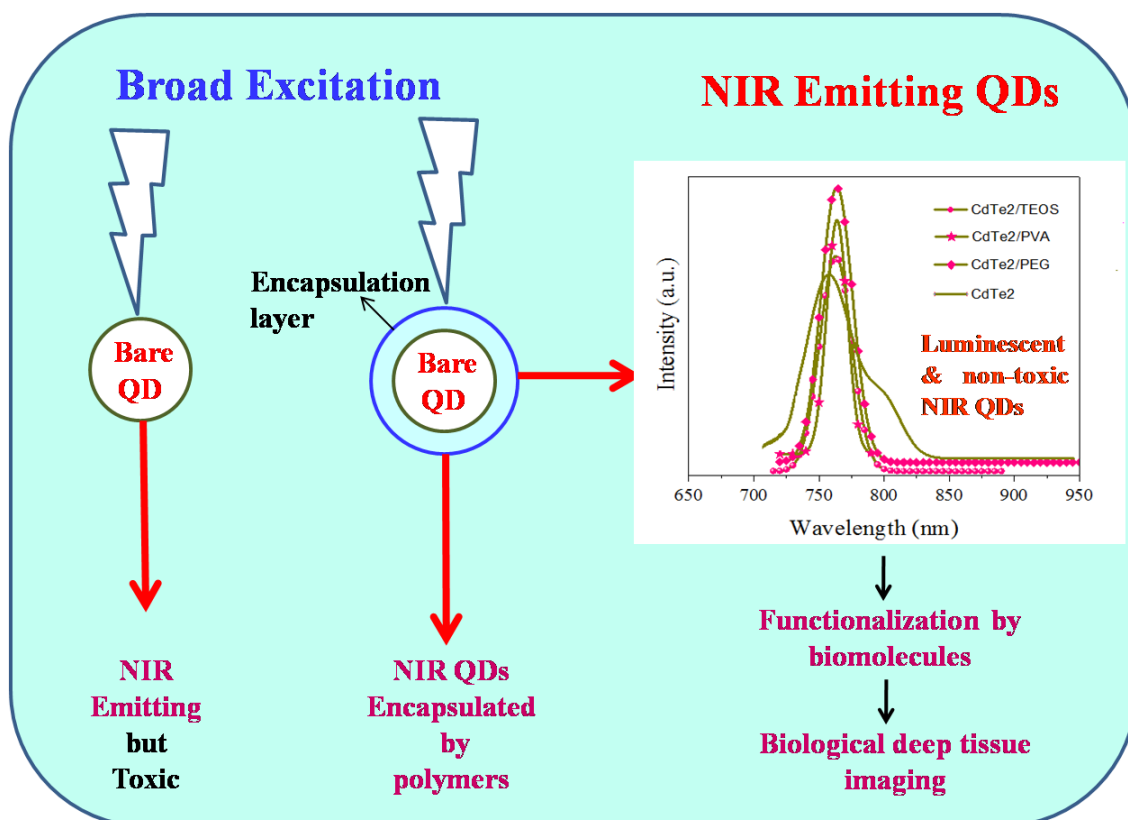
Highlights

- Synthesis of NIR poly CdTe, CdTe1, CdTe2 and CdTe3 QDs, CdTe2/TEOS, CdTe2/PVA and CdTe2/PEG quantum dots by wet chemical aqueous route.
- Studied effect of 3-MPA on optical properties and size of QDs.
- Removal of defect trap states by encapsulation of QDs.
- Improvement in optical properties on encapsulation.

Abstract

This chapter describes the effect of stabilizing agent 3-MPA on optical properties of CdTe NIR QDs. Different sized CdTe NIR QDs were synthesized by wet chemical aqueous route using different concentration of 3-MPA. Addition of high concentration of 3-MPA leads to blue shift in emission position of QDs and indicate quantum confinement. These CdTe QDs provide emission in NIR optical diagnostic window. These kind of NIR emitting QDs can further be used for biomedical application by modifying surface properties of these QDs. Surface modification of these NIR QDs is made to stabilize these QDs and to improve fluorescent behavior of QDs. Photoluminescence spectra of these bare CdTe and polymer, silicate encapsulated QDs confirms that surface modification of these QDs and in turn enhance their optical properties. FTIR analysis of these QDs confirms that polymer encapsulated QDs are more biocompatible as compared to uncovered CdTe QDs.

5.1 Introduction

Most interesting facts about QDs are high surface to volume ratio and quantum confinement effect. Quantum confinement effect of QDs show tunable fluorescent properties within the UV and IR range. NIR QDs have evolved as a novel category of luminous material for biological applications specifically bioimaging. NIR QDs are getting much attention in current years due to their exceptional properties like deep tissue penetration of emitted light [1-5]. These NIR QDs provides emission in diagnostic window (700 nm to 1100 nm). Penetration of NIR QDs avoid scattering of light by tissues because scattering of light and autoflourescence by tissues is negligible in NIR range as compared with UV-visible emitting QDs. Therefore, due to less absorption and minimal autofluorescence these QDs can be utilized for bio-imaging. Till date NIR QDs, like CdHgTe [6-8], CdTe/CdS [9], CdTeSe [10] CdTeS [11], and CulnS2 [12] QDs have been productively synthesized and characterized.

CdTe QDs are smaller band gap QDs as compared to other II-VI group QDs. These QDs experience few drawbacks due to the toxicity produced by heavy metals in living cells and tissues. To achieve biological tissue/organ targeted imaging it is necessary to functionalize QDs by biomolecules like folic acid, enzyme and peptides etc. Surface modification of QDs by Surface coating folic acid, enzyme and peptides is not possible directly. Before modification these QDs must be capped with mercaptopropionic acid (MPA), bovine serum albumin (BSA) and streptavidin etc. It is also requisite to improve optical properties and stability of NIR QDs. Surface coating of NIR QDs has been extensively used for prevention of oxidation of QDs and in this manner surface coating also diminish the cytotoxicity of QDs. There are few reports on the straight use of biomolecules as a stabilizer for nanoparticles [13-18]. For example, in a report glutathione (GSH) was used for coating of QDs. This provides a physical hurdle to release of toxic heavy metals. These, GSH capped QDs were showing slight toxicity toward living cells [19].

Some authors use microwave irradiation method to generate a potent heating system to improve the quantum yield and stability of water-soluble GSH capped QDs [20-22]. By keeping all the point in mind we have selected aqueous wet chemical route for synthesis of CdTe QDs. These CdTe1, CdTe2 and CdTe3 QDs were stabilized by 3-MPA (3-Mercaptopropionic acid).

This route of synthesis is inexpensive and environment friendly. After synthesis these QDs were characterized by XRD, TEM, EDS, PL and FTIR. Out of all these CdTe1, CdTe2 and CdTe3 QDs we have selected CdTe2 for further analysis because CdTe2 shows emission in NIR range. Moreover, as compared to CdTe2, CdTe1 emits at 786 nm but it contains lesser concentration of 3-MPA which leads to its poor stability. Although CdTe1 also shows emission in NIR range but its stability is less as compared to CdTe2, whereas CdTe3 QDs were emitting in UV-Visible range. After the synthesis of CdTe2 QDs we have encapsulated them by polymer and silicates to stabilize and to improve their optical properties. CdTe2 was selected for further studies because of its emission in NIR optical diagnostic window i.e., at 757 nm and its stability.

5.2 Experimental details

Wet chemical aqueous route was employed to synthesize poly CdTe and CdTe QDs. Complete procedure for synthesis of CdTe QDs is presented in chapter2 (section 2.4). Structural, elemental and optical properties of prepared QDs was studied by XRD (Shimadzu powder x-ray diffractometer using Cu Kα1 radiation), TEM (HITACHI (H-7500), EDX (TECNAI G^2 20S-TWIN (FEI Neitherlands)) and PL (Perkin Elmer LS55). Confirmation of functional group on surface of CdTe was carried out by FTIR (Cary 630 spectrophotometer (Agilent technology). These characterization techniques are discussed in detail in chapter 2.

5.3 Results and discussion

5.3.1 Structural analysis of Poly CdTe, CdTe1, CdTe2 and CdTe3 QDs

Figure 5.1 presents the XRD pattern of poly CdTe, CdTe1, CdTe2, and CdTe3 QDs. As clear from the figure 5.1 reflections are present at 2θ = 23°, 26°, 34°, 37°, 42°, 46° and 48°. These reflections corresponds to (100), (101), (102), (110), (103), (200) and (202) planes assigned to hexagonal phase of CdTe. Crystallize size of poly CdTe and CdTe QDs was calculated by most prominent peak (101) using Scherrer's formula. Size obtained for poly CdTe was 26 nm as it contains no stabilizing agent therefore no confinement. On addition of 3-MPA (stabilizer) crystallite size was 7 nm for CdTe1. There was reduction in size on further increasing the concentration of 3-MPA (from 1 ml - 3 ml) 5 nm for CdTe2 and 4.2 nm for CdTe3. This confirms superior control capability of 3-MPA on crystallite size.
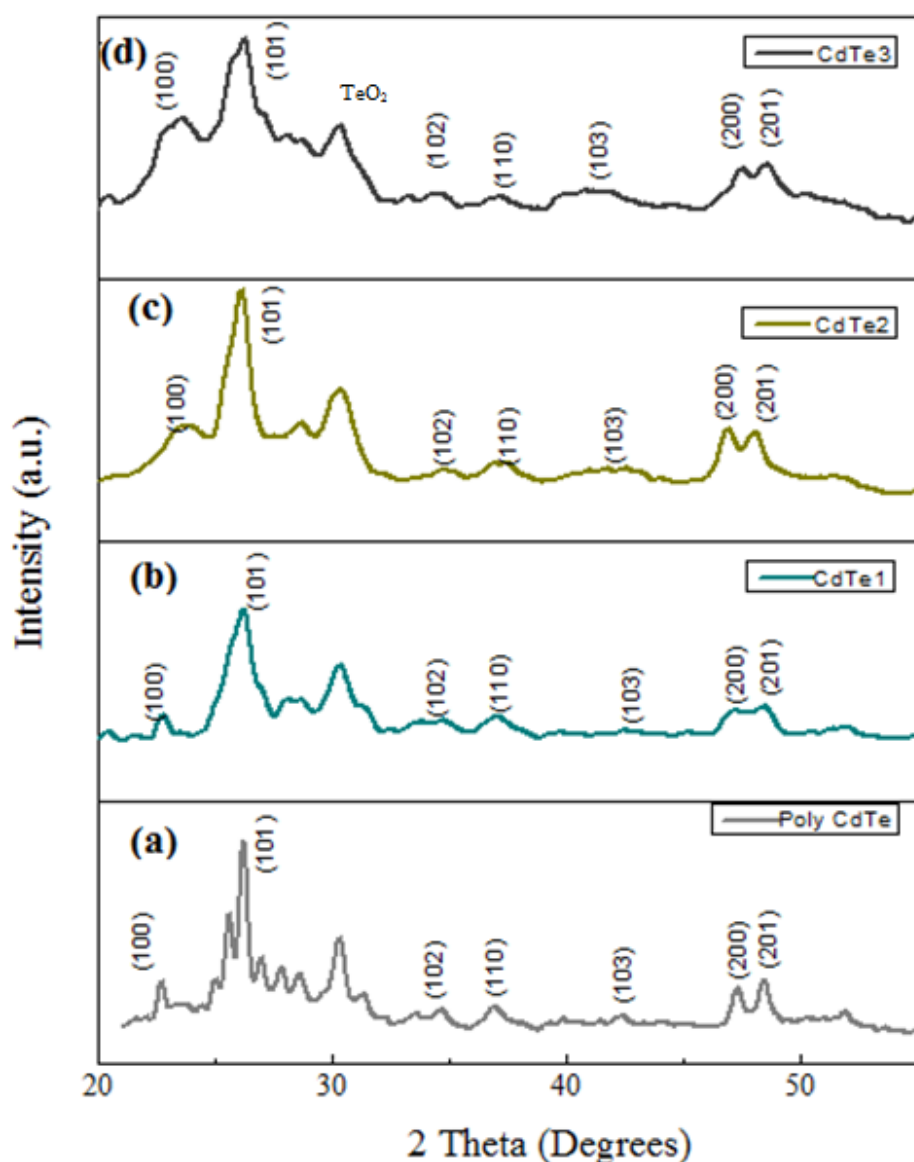
Figure 5.1: XRD spectra of synthesized (a) poly CdTe (b) CdTe1(c) CdTe2 and (d) CdTe3

Table 5.1 also clarifies that there is increase in surface to volume ratio with decrease in size. Strain value was also increasing with decrease in size. Lattice parameters a and c calculated for hexagonal CdTe were found close to standard values. These all parameter confirms formation of hexagonal CdTe. All the calculated structural parameters along with strain and crystallite size of CdTe1, CdTe2, CdTe3 QDs and poly CdTe are presented in the table 5.1.

Table 5.1: Structural parameters of poly CdTe, CdTe1, CdTe2 and CdTe3 QDs

Sample Name	2θ (^{0})	d(Å)	FWHM (^{0})	(hkl)	Size from XRD (nm)	Size from TEM (nm)	Lattice Constant		Surface/ Volume Ratio (nm^{-1})	Strain
							a (Å)	c (Å)		
Poly CdTe	26.22	3.5	0.34	101	26	28	4.62	7.53	0.21	0.36
	42.66	2.13		103			4.62	7.53		
	47.30	1.92		200			4.40	7.16		
CdTe1	26.37	3.5	1.2	101	7	7.2	4.62	7.53	0.83	1.28
	42.56	2.13		103			4.62	7.53		
	47.32	1.92		200			4.40	7.16		
CdTe2	26.22	3.5	1.5	101	5	5.6	4.63	7.53	1.07	1.61
	42.05	2.2		103			4.85	7.90		
	47.17	1.92		200			4.44	7.23		
CdTe3	26.22	3.5	2.1	101	4.2	4.8	4.63	7.53	1.25	2.25
	42.56	2.13		103			4.62	7.53		
	47.32	1.92		200			4.4	7.16		

5.3.2 Transmission electron microscopy

For determination of shape and size TEM images of poly CdTe, CdTe1, CdTe2, CdTe3 were recorded. It was confirmed from figure 5.2 (a, b, c, and d) that all the prepared samples are spherical in shape and agglomeration tendency of particle was found negligible. Particle size for these prepared samples was calculated by using Image J software. Calculated particle size is tabulated in table 5.1. The obtained particle size was found less than the Bohr exciton radius of CdTe that is 10 nm. Size acquired from TEM analysis was close to size that was obtained from X-ray diffraction analysis. As already been presented in previous chapter 3 that TEM analysis of

polymer encapsulated CdSe QDs did not show any special effect on morphology due to polymer encapsulation [23] due to difference in electron density of core and shell material and hence in case of CdTe QDs also.
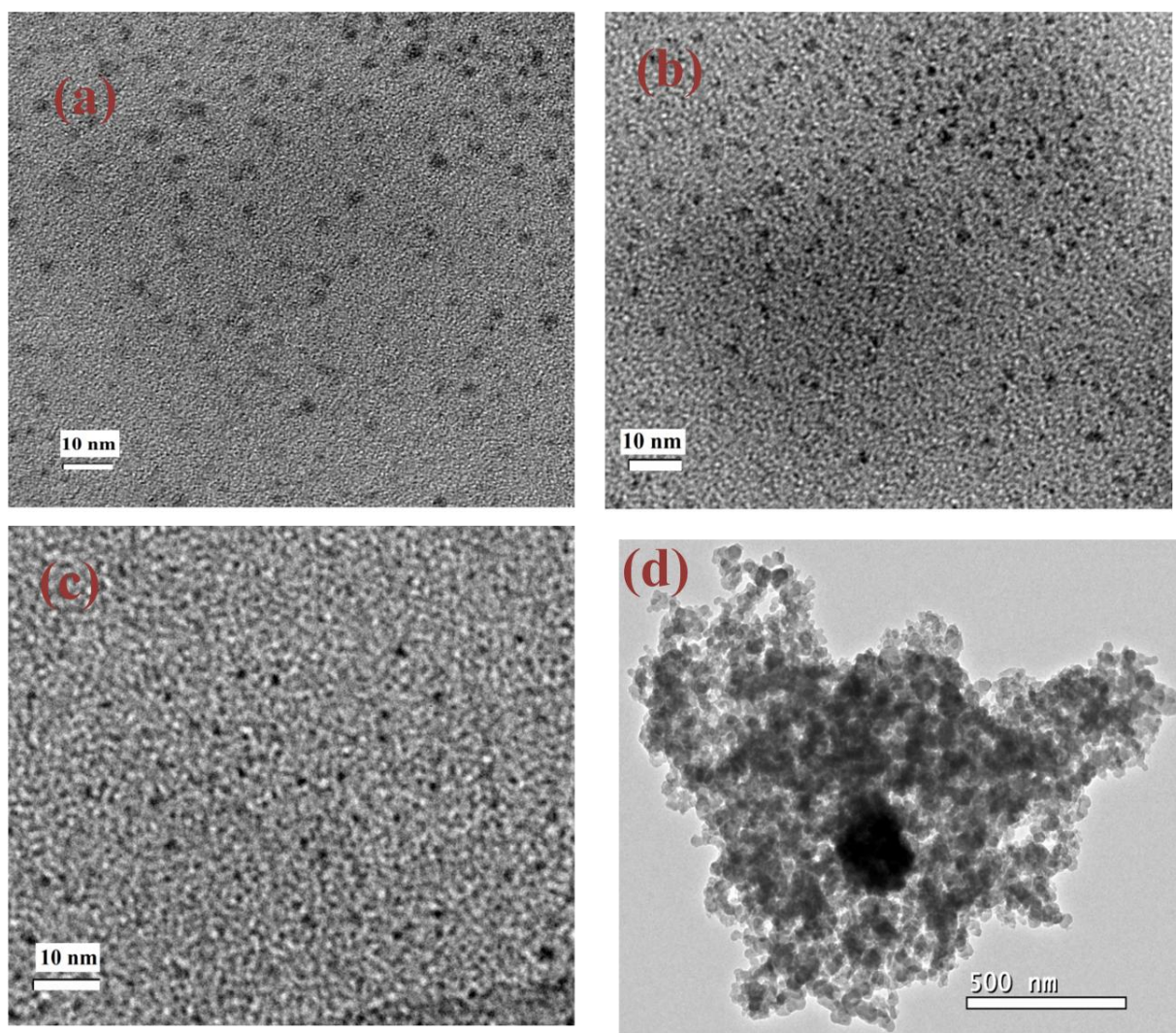
Figure 5.2: TEM images of synthesized (a) CdTe1 (b) CdTe2 (c) CdTe3 and (d) Poly CdTe

5.3.3 Energy-dispersive X-ray spectra

EDX examination of poly CdTe, CdTe1, CdTe2, CdTe3 and their encapsulated structure (figure 5.3 (a-g)) was performed to corroborate elemental composition of samples.
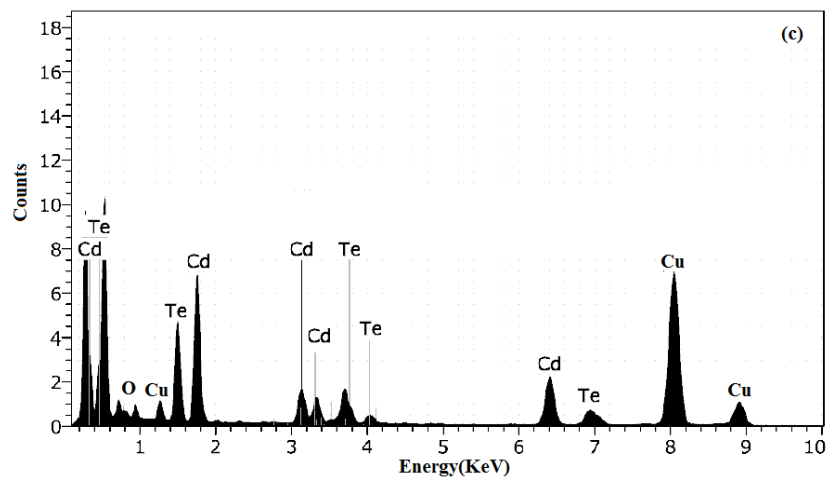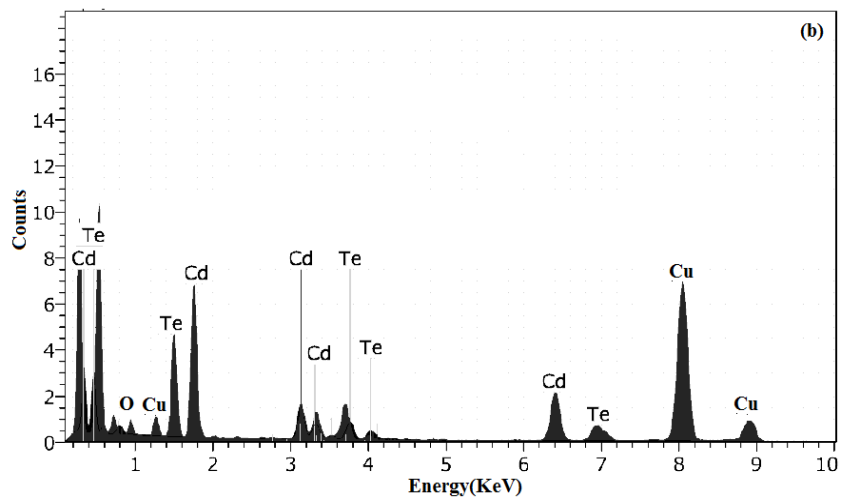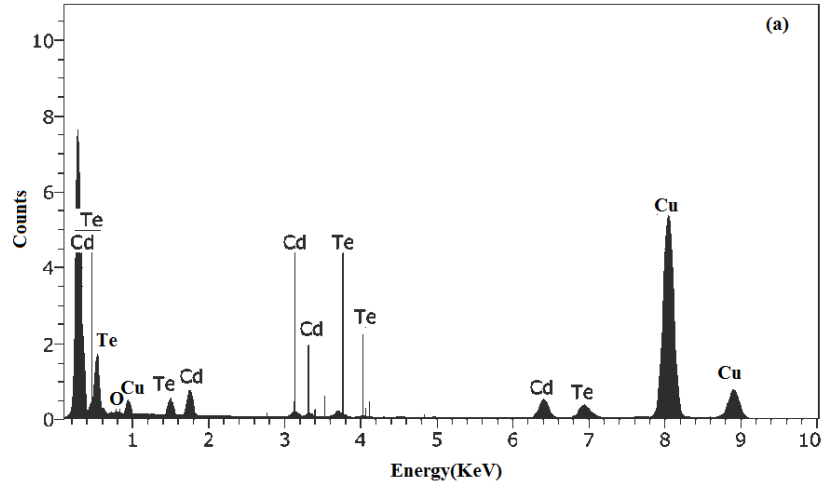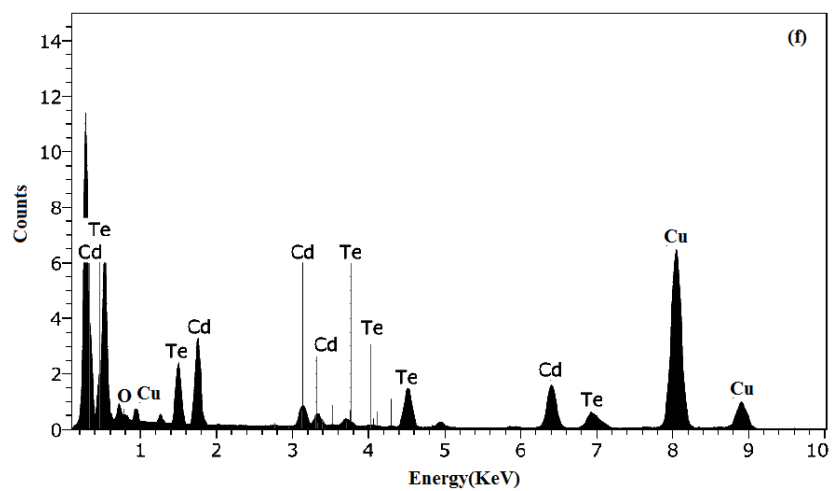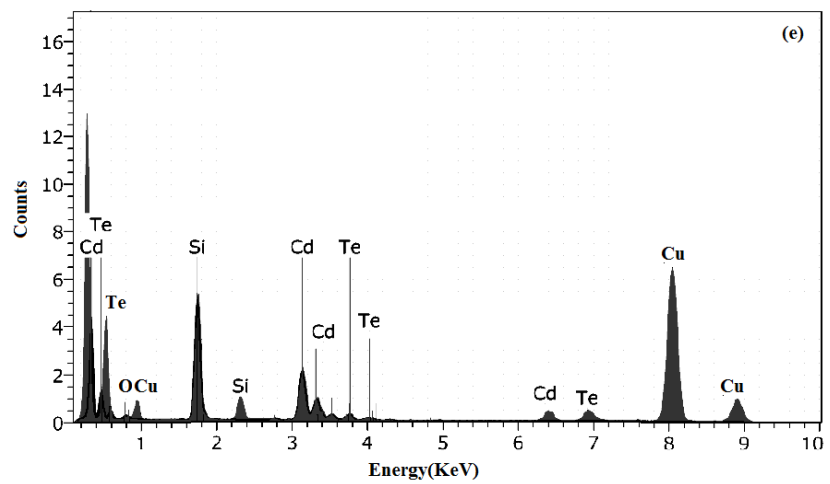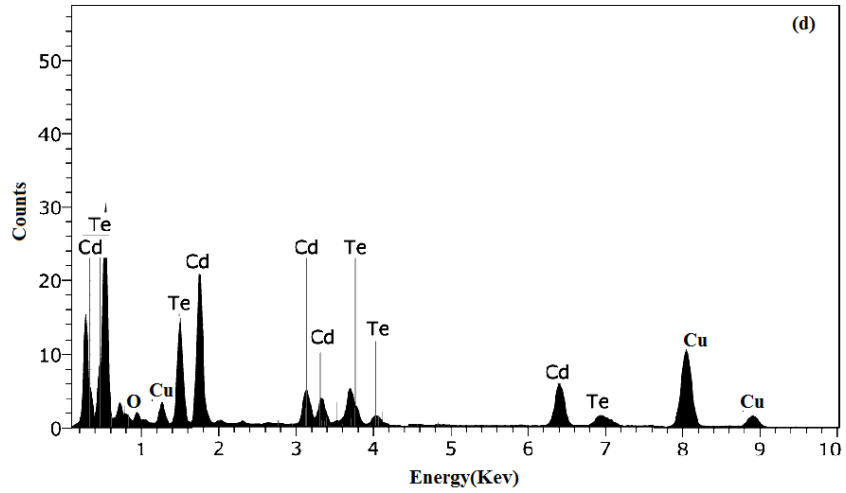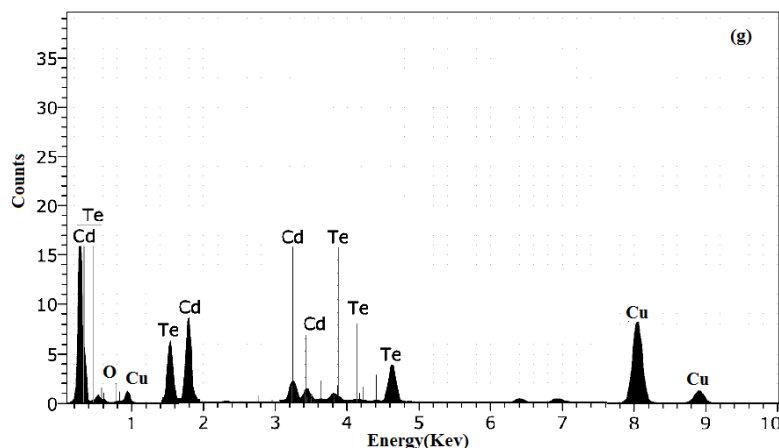
Figure 5.3: EDX spectra of synthesized (a) poly CdTe (b) CdTe1(c) CdTe2 (d) CdTe3 (e) CdTe2/TEOS (f) CdTe2/PVA and (g) CdTe2/PEG

Carbon and copper peaks in EDX spectra of all samples were attributed to carbon coated copper grid used for characterization. Cadmium and telluride peaks in all samples confirm formation of CdTe samples. Presence of silica peak in EDX spectra of CdTe2/TEOS (figure 5.3(e)) confirms the encapsulation of CdTe2 by TEOS. In case of polymer encapsulated CdTe samples no special peak was found which can confirm the presence of polymers. EDX analysis does not give information about polymeric materials [24]. Like CdSe QDs EDX spectrum of CdTe QDs does not show presence of sulphur peak means no hole scavenging group are found here in CdTe which are responsible for defect generation in PL spectra. Obtained value for ratio of atomic percentage of Cd:Te for all samples is tabulated in Table 5.2.

Table 5.2: Value for ratio of atomic percentage of Cd: Te from EDX analysis

Sample	Ratio of Cd:Te	Ratio of Cd:Te:Si
Poly CdTe	1:0.79	-
CdTe1	1:0.76	-
CdTe2	1:0.63	-
CdTe3	1:0.55	-
CdTe2/TEOS	1:0.66	1:0.66:0.78
CdTe2/PVA	1:0.81	-
CdTe2/PEG	1:0.89	-

5.3.4 Optical studies

Photoluminescence and PLE spectra of NIR QDs were recorded by using 0.02 mg/ml of sample in solution. PL spectra of all the prepared CdTe QDs and their encapsulated structures were recorded at different excitation wavelength in order to confirm whether the emission from band edge or from the defect states. PLE spectra have also been recorded for QDs by fixing emission wavelength to study the excitation profile. Figure 5.4 (a) shows effect of concentration of stabilizing agent 3-MPA on PL emission of CdTe1, CdTe2 and CdTe3 where concentration of 3-MPA got increased form CdTe1 to CdTe3. Figure 5.4 (a) clarifies blue shift in band edge emission peak on increasing the concentration of 3-MPA. The emission peak of CdTe3 contains high concentration of 3-MPA get blue shifted as compared to CdTe1 from 778 nm (CdTe1) to 657 nm (CdTe3). This proves superior capping efficiency of 3-MPA. The emission spectra of CdTe1, CdTe2 and CdTe3 show defect emission position along with band emission (Table 5.3).

PLE spectra for CdTe1 is presented in figure 5.4 (b) and this figure clarifies that CdTe1 comprised an excitation peak present at 778 nm which reciprocate band emission at 786 nm and defect emission at 825 nm. Similarly in case of CdTe2 (figure 5.4 (c)) PLE shows excitation peak at 744 nm corresponds to emission at 757 nm and 799 nm. In case of CdTe 3(figure 5.4 (d)) excitation peak was found at 657 nm which corresponds to band edge emission at 672 nm along with defect emission at 720 nm, 758 nm and 862 nm. All the emission peaks and PLE peaks are tabulated in table 5.2. PL spectra of CdTe1 (figure 5.5 (e)), CdTe2 (figure 5.4 (f)) and CdTe3 (figure 5.4 (g)) were deconvulated for better understanding for the peak profiles. PL spectra were fitted to different peaks after deconvulation. E1 peak in each deconvulated spectra presents band edge emission and other additional peaks presents defects.

Defect emission in case of CdTe1, CdTe2 and CdTe3 NIR QDs was attributed to vacancy of cadmium and tellurium. In case of small sized QDs high surface to volume ratio leads to presence of many dangling bonds on surface of QDs. These unsatisfactory bonds and trap states origin due to leakage of Cd, Te results in non radiative recombination. Previously in chapter 3 in case of CdSe QDs, thiol group from 2-ME was also playing an important role in origin of traps as we were increasing the concentration of 2-ME. This was confirmed from PL and EDX analysis. But here in case of CdTe QDs no special effect of 3-MPA on PL emission was found.

Peak position in deconvulated spectra along with FWHM value and intensity are presented in table 5.4.
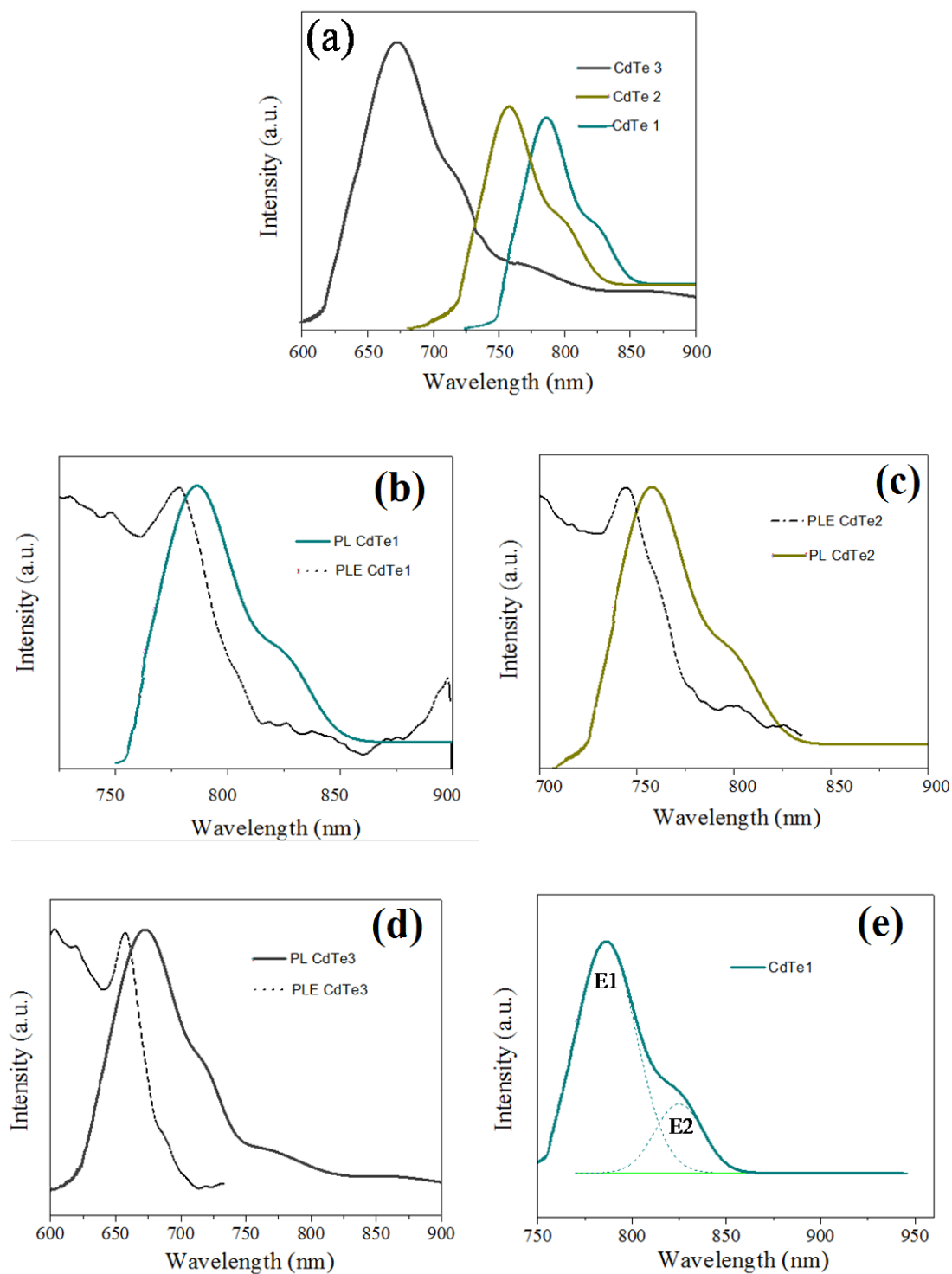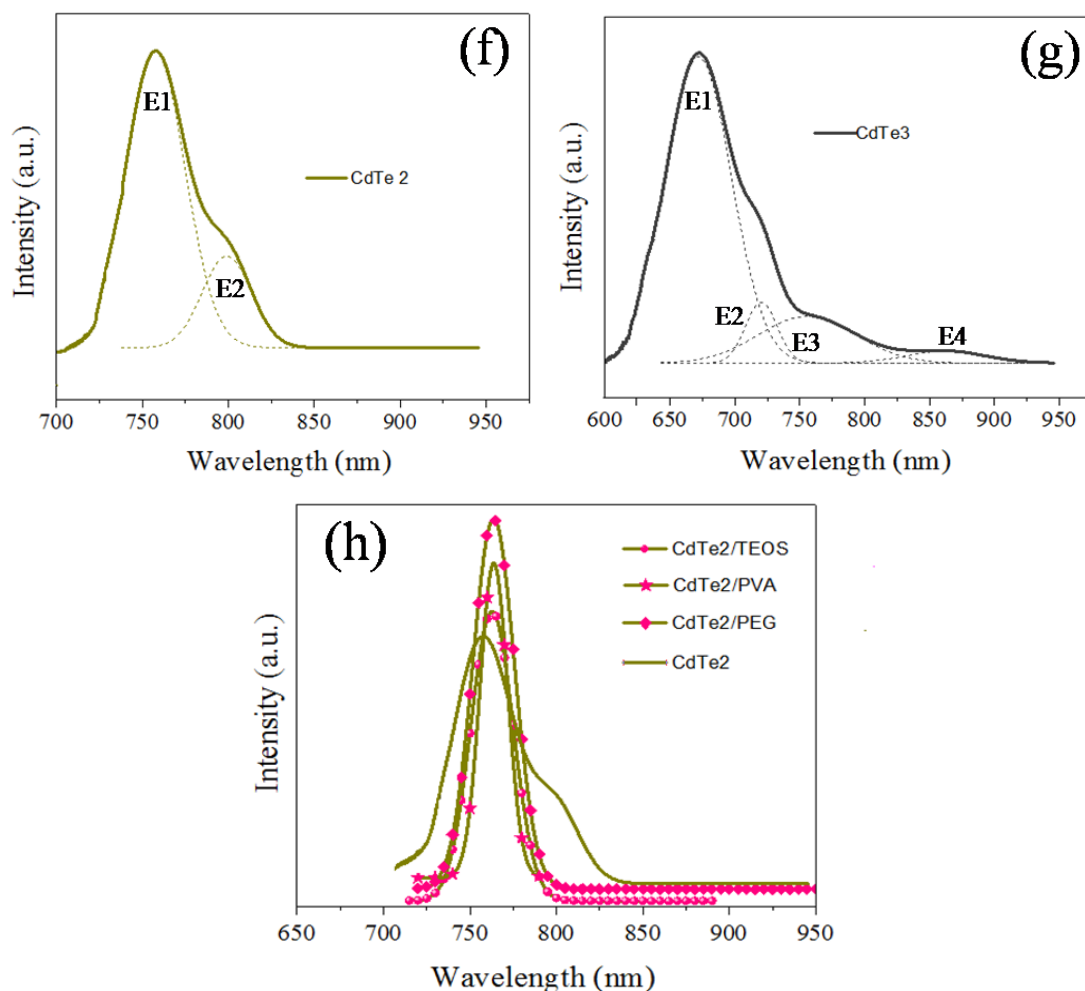
Figure 5.4: (a) Photoluminescence spectra of capped CdTe QDs with different concentration of 3-MPA (b) PL and PLE spectra of CdTe1 (c) PL and PLE spectra of CdTe2 (d) PL and PLE spectra of CdTe3 (e) Deconvulated PL spectra of CdTe1 (f) Deconvulated PL spectra of CdTe2 (g) Deconvulated PL spectra of CdTe3 and (h) Comparative PL spectra of CdTe2 QDs encapsulated with different polymers

Table 5.3: Emission peaks and PLE peaks of CdTe1, CdTe2 and CdTe3

Sample Name	PLE Wavelength(nm)	Emission wavelength (nm)
CdTe1	778	786, 825
CdTe2	744	757, 799
CdTe3	657	672, 720, 758, 862

Table 5.4: Summary of deconvoluted photoluminescence peak positions, corresponding FWHM and relative intensities for CdTe1, CdTe2 and CdTe3

Sample Name	Spectral position of PL emission				FWHM				Intensity			
	E1	*E2*	*E3*	*E4*	*E1*	*E2*	*E3*	*E4*	*E1*	*E2*	*E3*	*E4*
CdTe1	786	825			36	29			76	39		
CdTe2	757	799			40	35			80	40		
CdTe3	672	720	758	862	62	28	83	54	100	34	30	22

Table 5.5: Summary of emission positions, corresponding FWHM and relative %age intensity of CdTe2, CdTe2 /TEOS, CdTe2/PVA and CdTe2/PEG

Sample Name	Spectral position of PL emission	FWHM	%age intensity increase
CdTe2	757	40	1%
CdTe2/TEOS	762	28	10%
CdTe2/PVA	763	20	28%
CdTe2/PEG	764	29	45%

As we have already discussed about the sample selection that is CdTe2 and we had got some defect states in CdTe2 on QD formation. Therefore, to remove the defects we have encapsulated CdTe2 by PEG, PVA and TEOS and tested, we have already discussed the possibilities of using these polymers and silicates for encapsulation purposes for surface modification in chapter 3. Figure 5.4 (h) shows comparative spectra of CdTe2 and their polymer encapsulated structure CdTe2/PEG, CdTe2/PVA and CdTe2/TEOS. This figure shows complete removal of defects from polymer and silicate encapsulated CdTe2 QD structures. It also helps to intensify the intensity of polymer and silicate encapsulated QDs along with defect removal. This increase in intensity on polymer encapsulation is due to reduction in non-radiative transitions which occurs in bare CdTe QDs because of some trap states. This reduction in non-radiative transition reduces the energy loss and leads to increase in intensity of radiative transitions. Emission peak positions with compared intensity for CdTe2 QDs, CdTe2/PEG, CdTe2/PVA and CdTe2/TEOS structures are demonstrated in table 5.5. Results revealed that PL intensity is low in bare CdTe2 however on encapsulation intensity gets improved by two to four folds. This

improvement in fluorescence intensity by encapsulation is because of smoothening of QDs surface. This encapsulation layer on bare CdTe pacifies defect states and dangling bonds on surface of CdTe QDs and stabilizes these QDs.

5.3.5 FTIR analysis

FTIR spectra of poly CdTe, CdTe QDs and encapsulated structures were recorded to know about the presence of possible functional groups on the surface of QDs and presented in figure 5.5.
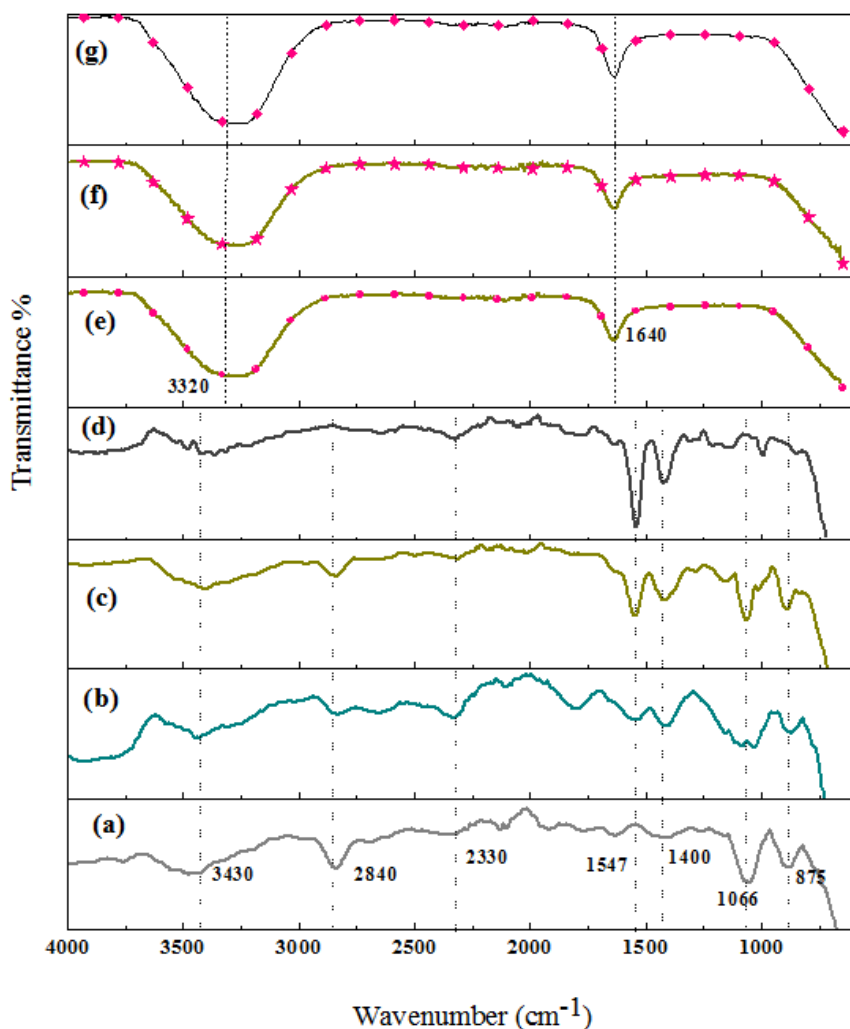
Figure 5.5: (a) FTIR spectra of poly CdTe (b) FTIR spectra of CdTe1 QDs (c) FTIR spectra of CdTe2 QDs (d) FTIR spectra of CdTe3 QDs (e) FTIR spectra of CdTe2/TEOS QDs (f) FTIR spectra of CdTe2/PVA QDs and (g) FTIR spectra of CdTe2/PEG QDs

FTIR results of poly CdTe, CdTe1, CdTe2 and CdTe3 shows peaks at 3430 cm^{-1}, 2840 cm^{-1}, 1400 cm^{-1}, 1066 cm^{-1} and 875 cm^{-1}. The presence of these peaks at particular wavelengths are due to -OH group, -CH stretching,-CH2 bending, C-O stretching and C-S stretching respectively. Peak at 1541 cm^{-1} is characteristic peak of nitro group. Similarly, in FTIR spectra for CdTe2/PVA, CdTe2/PEG and CdTe2/TEOS presence of two intense peaks one at 3320 cm^{-1} was assigned to -OH and at 1640 cm^{-1} be a sign of -NH group. FTIR results of these NIR QDs confirm hydrophilic nature of surface modified QDs. These QDs contain biocompatible functional groups like –NH and -OH on their surface. By using these functional groups these QDs can be easily attached to biomolecules, ligands for further biological applications.

5.4 Conclusion

This work concludes that capping of NIR CdTe QDs by 3-MPA controls the particles size of CdTe. This decrease in particle size leads to shift in PL emission peak position confirms that CdTe QDs are quantum confined. Trap emission position got increased with decrease in size. TEM, XRD, EDX and PL analysis confirms structural, elemental, optical properties of CdTe. From PL analysis of CdTe it was confirmed that CdTe1, CdTe2 shows emission in NIR range. XRD spectra confirm formation of hexagonal phase of CdTe QDs. PL spectra of polymer and silicate encapsulated CdTe QDs confirm enhanced fluorescence intensity. FTIR analysis of these QDs confirm biocompatible and hydrophilic nature of these QDs. Owing to emission of these encapsulated QDs in NIR range these can be utilized for biological applications specifically for deep tissue imaging in future.

5.5 References

1.Park J., Joo J., Kwon S.G., Jang Y., Hyeon T., *"Synthesis of monodisperse spherical nanocrystals",* Angewandte Chemie International Edition, vol. 46(25), pp. 4630-4660, June 2007.

2.Reiss P., Protiere M., Li L., *"Core/shell semiconductor nanocrystals",* small, vol. 5(2), pp. 154-168, Jan.2009.

3.Medintz I.L., Uyeda H.T., Goldman E.R., Mattoussi H., *"Quantum dot bioconjugates for imaging, labelling and sensing"*, Nature materials, vol. 4(6), pp. 435, June 2005.

4.Holder E., Tessler N., Rogach A.L., *"Hybrid nanocomposite materials with organic and inorganic components for opto-electronic devices",* Journal of Materials Chemistry, vol. 18(10), pp. 1064-1078, 2008.

5.Talapin D.V., Lee, J.S., Kovalenko, M.V., Shevchenko E.V., *"Prospects of colloidal nanocrystals for electronic and optoelectronic applications",* Chemical reviews, vol. 110(1), pp. 389-458, Dec. 2009.

6.Chen H., Wang Y., Xu J., Ji J., Zhang J., Hu Y., Gu Y., *"Non-invasive near infrared fluorescence imaging of CdHgTe quantum dots in mouse model",* Journal of fluorescence, vol. 18(5), pp. 801-811, Sep. 2008.

7.Harrison M.T., Kershaw S.V., Burt M.G., Eychmüller A., Weller H., Rogach A.L., *"Wet chemical synthesis and spectroscopic study of CdHgTe nanocrystals with strong near-infrared luminescence",* Materials Science and Engineering: B, vol. 69, pp. 355-360, Jan. 2000.

8.Rogach A.L., Eychmüller A., Hickey S.G., Kershaw S.V., *"Infrared‐emitting colloidal nanocrystals: synthesis, assembly, spectroscopy, and applications",* Small, vol. 3(4), pp. 536-557, Apr. 2007.

9.Zhao D., He Z., Chan W.H., Choi M.M., *"Synthesis and characterization of high-quality water-soluble near-infrared-emitting CdTe/CdS quantum dots capped by N-acetyl-L-cysteine via hydrothermal method",* The Journal of Physical Chemistry C, vol. 113(4), pp. 1293-1300, Dec.2008.

10. Liang G.X., Gu M.M., Zhang J.R., Zhu J.J., *"Preparation and bioapplication of high-quality, water-soluble, biocompatible, and near-infrared-emitting CdSeTe alloyed quantum dots",* Nanotechnology, vol. 20(41), pp. 415103, Sep.2009.

11. Mao W., Guo J., Yang W., Wang C., He J., Chen J., *"Synthesis of high-quality near-infrared-emitting CdTeS alloyed quantum dots via the hydrothermal method",* Nanotechnology, vol. 18(48), pp. 485611, Nov. 2007.

12. Liu S., Zhang H., Qiao Y., Su X., *"One-pot synthesis of ternary CuInS 2 quantum dots with near-infrared fluorescence in aqueous solution",* RSC Advances, vol. 2(3), pp. 819-825, 2012.

13. Yang G., Qin D., Du X., Zhang L., Zhao G., Zhang Q., Wu J., *"Aqueous synthesis and characterization of bovine hemoglobin-conjugated cadmium sulfide nanocrystals"*, Journal of Alloys and Compounds, vol. 604, pp. 181-187, Aug. 2014.

14. Kong Y., Chen J., Gao F., Brydson R., Johnson B., Heath G., Zhou D., *"Near-infrared fluorescent ribonuclease-A-encapsulated gold nanoclusters: preparation, characterization, cancer targeting and imaging"*, Nanoscale, vol. 5(3), pp. 1009-1017, 2013.

15. Chen J., Zhang T., Feng L., Zhang X., Zhang M., Cui D., *"Synthesis of ribonuclease A-conjugated CdS quantum dots and its photocatalytic properties"*, Micro & Nano Letters, vol. 7(10), pp. 1023-1025, Oct. 2012.

16. Samanta A., Deng Z., Liu Y., *"Aqueous synthesis of glutathione-capped CdTe/CdS/ZnS and CdTe/CdSe/ZnS core/shell/shell nanocrystal heterostructures"*, Langmuir, vol. 28(21), pp. 8205-8215, May 2012.

17. Shen Y., Liu S., He Y., *"Fluorescence quenching investigation on the interaction of glutathione‐CdTe/CdS quantum dots with sanguinarine and its analytical application"*, Luminescence, vol. 29(2), pp. 176-182, Mar. 2014.

18. Gui R., An X., *"Layer-by-layer aqueous synthesis, characterization and fluorescence properties of type-II CdTe/CdS core/shell quantum dots with near-infrared emission"*, RSC Advances, vol. 3(43), pp. 20959-20969, 2013.

19. Jing L., Kershaw S.V., Kipp T., Kalytchuk S., Ding K., Zeng J., Gao M., *"Insight into strain effects on band alignment shifts, carrier localization and recombination kinetics in CdTe/CdS core/shell quantum dots"*, Journal of the American Chemical Society, vol. 137(5), pp. 2073-2084, Feb. 2015.

20. He H., Sun X., Wang X., Xu H., *"Synthesis of highly luminescent and biocompatible CdTe/CdS/ZnS quantum dots using microwave irradiation: a comparative study of different ligands"*, Luminescence, vol. 29(7), pp. 837-845, Nov. 2014.

21. Huang L., Han H., *"One-step synthesis of water-soluble ZnSe quantum dots via microwave irradiation"*, Materials Letters, vol. 64(9), pp. 1099-1101, May 2010.

22. Du J., Li X., Wang S., Wu Y., Hao X., Xu C., Zhao X*., "Microwave-assisted synthesis of highly luminescent glutathione-capped Zn 1− x Cd x Te alloyed quantum dots with excellent biocompatibility",* Journal of Materials Chemistry, vol. 22(22), pp. 11390-11395, 2012.

23. Schipper M.L., Iyer G., Koh A.L., Cheng Z., Ebenstein Y., Aharoni A., Chen X., *"Particle size, surface coating, and PEGylation influence the biodistribution of quantum dots in living mice",* Small, vol. 5(1), pp. 126-134, Jan. 2009.

24. Saravanan L., Diwakar S., Mohankumar R., Pandurangan A., Jayavel R., *"Synthesis, structural and optical properties of PVP encapsulated CdS nanoparticles",* Nanomaterials and Nanotechnology, vol. 1:17, Nov. 2011.

CHAPTER -6

COMPREHENSIVE INVESTIGATION OF CYTOTOXIC AND ANTIMICROBIAL BEHAVIOUR OF CdSe AND CdTe BASED NANOSTRUCTURES
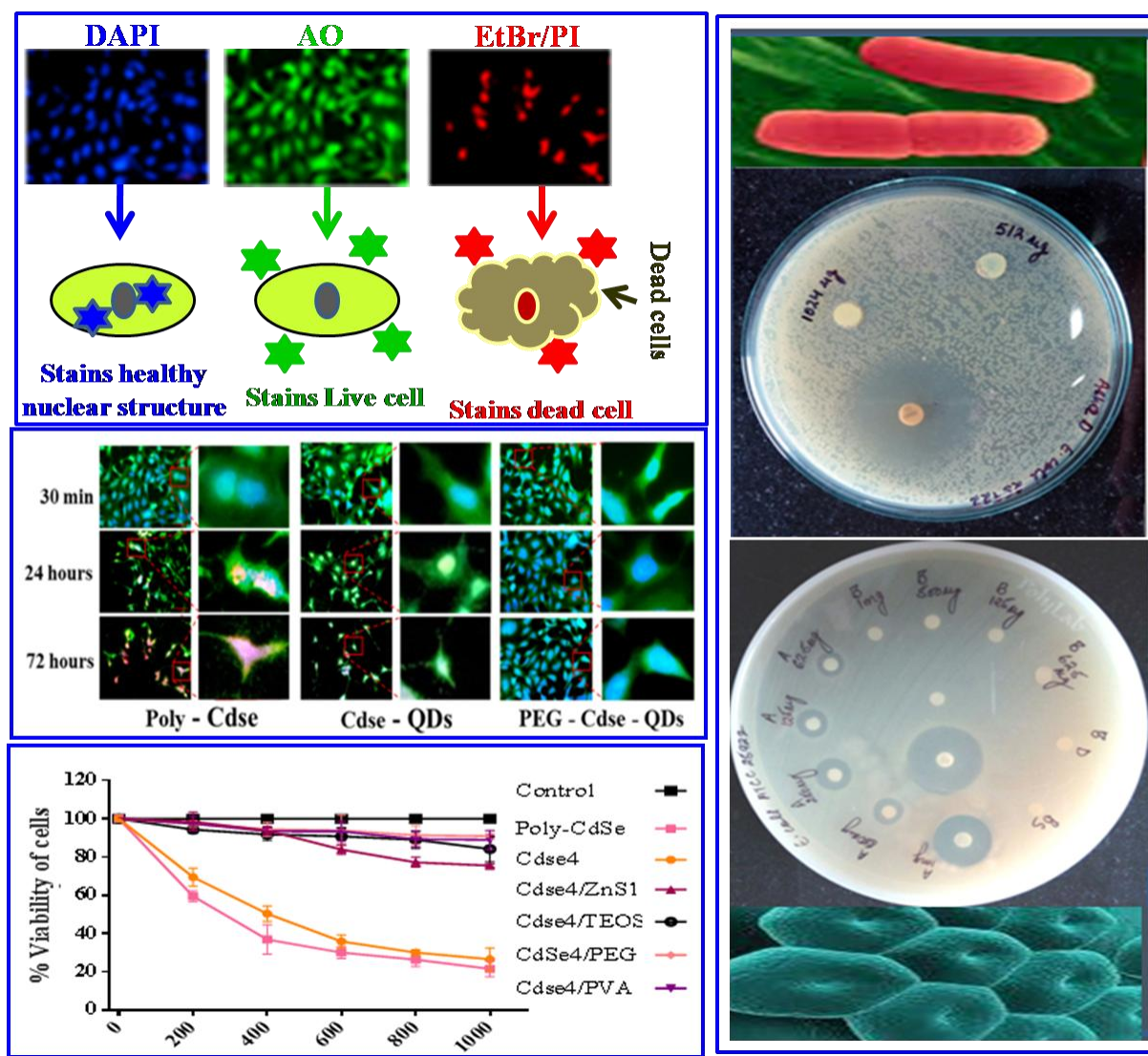
Highlights

- Comparative study of cytotoxic behavior of CdSe quantum dots and their encapsulated structures.

- Toxicity study of CdTe based nanostructures toward HEK 293 cell line.

- Found the relation of origin of defects in CdSe QDs with cytotoxicity.

- Encapsulation engraves toxicity compared to bare CdSe-QDs toward HEK 293 cell line.

- Antimicrobial activity of CdSe and CdTe based nanostructures.

- Effect of shell formation on core quantum dots antimicrobial behavior was studied.

- Non antibacterial core-shell QDs can be used to study the microbial population.

- QDs are antibacterial against multidrug resistant bacteria *A. baumannii.*

Abstract

This chapter focuses on cytotoxicity studies and antimicrobial studies of CdSe and CdTe based nanomaterials. Cytotoxicity of CdSe and CdTe based configurations was carried out toward HEK-293 cells. Cytotoxic effect of these configurations was evaluated by using MTT assay. After confirmation of toxic effects by MTT assay cellular apoptosis caused by QDs was further analyzed for better understanding of the toxicity by DAPI/AO/PI and DAPI/AO/EtBr fluorescent staining on HEK-293 cells for CdSe and CdTe QDs. This chapter also includes study of antimicrobial effect of CdSe4, ZnS1, ZnS2, CdSe4/ZnS1 and CdSe4/ZnS2 QDs by Kirby Bauer's disk diffusion method against potential gram negative pathogens; *Escherichia coli* ATCC 25922 and *Acinetobacter baumannii* ATCC 19606. Antimicrobial behavior of CdTe based nanostructures was tested towards E.coli and *S. aureus.*

6.1 Introduction

QDs are luminescent nanomaterials with improved optical properties owing to this special characteristic of QDs these are preferred as potential materials for biomedical diagnostics like optical labels for the multiplexed investigation of immunocomplexes, light-emitting diodes, sensors and solar cells [1, 2]. QDs can be used as potential luminous marker if they posses some important features like brightness, stability, biocompatibility and non-toxicity. In biological applications like cellular imaging, cell labeling and tracking luminescence technique has extremely broad magnitude. For biological applications these QDs must have broad excitation and narrow emission spectra [3]. The utilization of functionalized luminescent QDs in biology emerge as one of the fast moving and exciting research directions [4, 5]. These QDs have high photobleaching resistance and stability in comparison with standard fluorescent organic dyes [6]. These features of luminescent QDs over organic dyes permit and encourage the use of these QDs in biological processes [7, 8]. Before using these QDs in the field of biology some of the factors are inescapable which hamper their biological applications like luminescence intensity, water solubility and extent of toxicity toward cells. Literature survey recommends that QDs obtained by organometallic route have fine optical properties but these QDs cannot disperse in water which is a major disadvantage for implication of QDs in biological applications [9, 10]. To circumvent this issue we synthesized hydrophilic QDs by using aqueous solvent. It was observed in our work that (chapter 3) QDs prepared by aqueous route have poor luminescence intensity with defect states. Therefore we worked on improvement of luminescence intensity by encapsulating QDs by polymers [11]. Photoluminescence intensity and stability get improved by encapsulation of CdSe QDs which we have already discussed in chapter 3. After these findings about QDs one major aspect remained for study before using these QDs in the bio relevance is cytotoxicity testing.

Literature survey related to toxicity of QDs confirmed that thiol stabilizing agent stabilizes QDs and avert them from surface oxidation [12]. Several research groups disclosed toxicity of these thiol stabilized QDs toward the cells based on metal ion and stabilizer [13-20]. Furthermore, aqueous synthesized and thiol stabilized CdTe QDs and CdSe QDs and these QDs prepared by organic route illustrate the equal cytotoxicity [21]. These two factors one is cytotoxicity and another is luminescence stability are the severe factors which impact their

biological utilization [22-24]. The main reason of toxicity reported in CdSe QDs is leakage of cadmium or other heavy metals [25-27]. These heavy metal ions have been reported to show toxicity toward cell lines under certain circumstances [28-30]. Hence it is easier to choose for aqueous based quantum dots for biological application as to reduce the toxicity of these QDs is much easier in comparison to reduce the toxicity of organically synthesized QDs because of the non water dispersity of later QDs [31]. Much attempt has been dedicated to get better spectral properties of aqueous QDs along with less cytotoxicity [32-35]. In previous chapters we have discussed about the simple aqueous synthesis route of QDs and their encapsulated structures. It was found that optical properties get improved on encapsulation. At this moment essential issue lingering for use of these QDs biologically is to analyze their cytotoxicity. Previously cytotoxicity of CdTe and CdS/CdSe was tested toward K562 and HEK-293T and decrease in cell viability was observed after 24 hour of incubation and after 48 hours cell viability reaches maximum [36, 37]. Here in this current chapter we evaluate comparative cytotoxicity of prepared poly, CdSe QDs, CdSe/ZnS1, CdSe/TEOS, CdSe/PVA, and CdSe/PEG. This also involves cytotoxicity study of CdTe based nanostructures. Antimicrobial behavior of CdSe and CdTe QDs have also been performed and presented in the chapter to conclude about the application of these luminescent QDs for bacterial studies and if found antimicrobial in any case these QDs can be used as antimicrobial agents.

6.2 Results and Discussion

6.2.1 Cell cytotoxicity of CdSe based nanostructures

Cytotoxicity of QDs toward HEK-293 cells was evaluated by using MTT assay. The procedure adopted for cell cytotoxicity or cell viability of CdSe and CdTe based nanostructures is being presented in figure 6.1.

The cells were exposed for 12 h, 24 h and 72 h with increasing concentrations of QDs (0 to 1000 μg/ml). Cell viability was systematically deliberated to explain the toxicity. 24 h of incubation period shows prominent reduction in cell viability for considerable conclusion. It was clear from figure 6.2 that QDs show signs of concentration reliant reduction in cell viability. Out of all the prepared QDs, Poly-CdSe was most toxic with IC_{50} values 440.84 μg/ml at 12 h and 251.19μg/ml at 24 h, similarly CdSe-QDs correspond to IC_{50} values of 529.71 μg/ml and 397.94 μg/ml for 12 h and 24 h respectively.
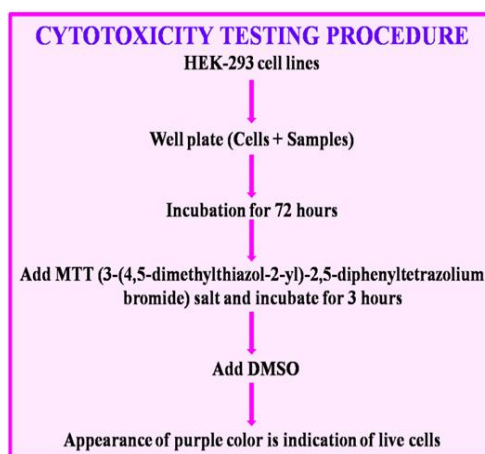
Figure 6.1: Procedure for cell cytotoxicity of CdSe and CdTe based nanostructures

Cytotoxic outcome in case of CdSe/ZnS1 QDs was time and dose dependent but, CdSe/ZnS1 demonstrate less anti-proliferative activity in comparison to Poly-CdSe with increase in IC_{50} value by 3.2 fold, 4.2 fold and 2.3 fold for 12 h, 24 h and 72 h respectively (Table 6.1). In the same way, IC_{50} values for CdSe/TEOS also rise by 3.1 fold, 5.5 fold and 2.3 fold for 12 h, 24 h and 72 h respectively (Table 6.1). CdSe/PVA QDs illustrate 8.8 fold, 15.1 fold and 13.1 fold rise in IC_{50} for 12 h, 24 h and 72 h in comparison to Poly-CdSe. Fascinatingly, CdSe/PEG QDs illustrate 13.7 folds, 23.3 folds and 14.2 folds rise in IC_{50} for 12 h, 24 h and 72 h (Table 6.1). PEG-CdSe-QDs and PVA-CdSe-QDs pursue the same pattern of cell proliferation in the tested time scale of 72 h of cell incubation (Figure 6.2(d)).
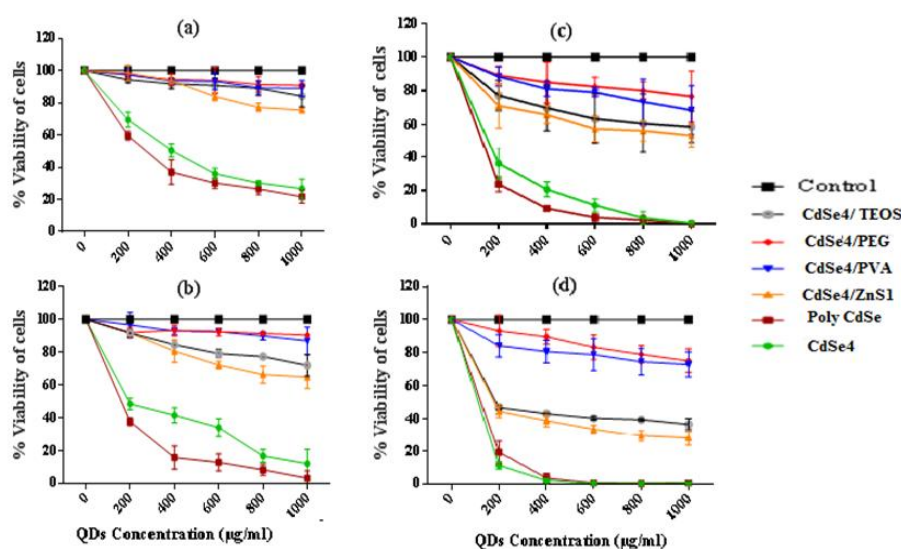
Figure 6.2: Viability of HEK-293 cells after treatment with synthesized QDs at different concentrations upto (a) 12 hrs (b) 24 hrs (c) 48 hrs and (d) 72 hrs. Percentage cell viability was calculated with respect to viability of the un-treated (control) cells and which was taken as 100 %. The results are mean ± SD from three experiments

Table 6.1: Corresponding IC_{50} values and fold change in IC_{50} values of synthesized QDs on HEK-293 cells proliferation at 12 h, 24 h and 72 h with respect to Poly-CdSe

Samples	12 Hours		24 Hours		72 Hours	
	IC_{50} (µg/ml)	Fold Change	IC_{50} (µg/ml)	Fold Change	IC_{50} (µg/ml)	Fold Change
Poly-CdSe	440.84	-	251.19	-	131.19	-
CdSe 4-QD	529.71	0.2	397.94	0.5	92.45	-0.30
CdSe4/ZnS1 QD	1862.84	3.2	1287.85	4.2	427.10	2.3
CdSe4/TEOS	1764.12	3.1	1621.12	5.5	521.99	2.3
CdSe4/PVA	4352.55	8.8	4020.96	15.1	1844.20	13.1
CdSe4/PEG	6518.24	13.7	6124.24	23.3	1989.48	14.2

Biocompatibility of QDs was attained in subsequent order, CdSe 4/PEG QDs > CdSe 4/ PVA QDs> CdSe 4/TEOS QDs > CdSe 4/ZnS1 QDs >CdSe 4 QDs > Poly CdSe. CdSe4 QDs encapsulated by PEG were showing good biocompatibility. This is because of polymer coating which hampered the discharge of cadmium ions. Toxic nature of Poly CdSe was due to absence of stabilizing agent this cause release of toxic ions cadmium and selenium. CdSe4 QDs have high surface to volume ratio thus they contain large number unsatisfactory groups and dangling bond and this was also corroborated from FTIR spectra of CdSe-QDs.

Exposure of CdSe-QDs to oxidative environment for long time causes decomposition. Consequently lead to liberation of toxic ions and cause toxicity towards cells. Encapsulated structures have reduced toxicity and this was attributed to formation of a layer on QDs surface. This layer formation pacify surface dangling bonds, as well reduce the probability of leakage of toxic Cd^{2+}, Se^{2-} from QDs and ultimately trim down toxic effect. On the basis of toxicity studies PEG-CdSe-QDs were found less toxic, highly luminescent and biocompatible for bioimaging purpose.

6.2.2 Fluorescent staining to explore cellular apoptosis in case of CdSe based nanostructures: 4', 6-diamidino-2-phenylindole/ Acridine orange/Propidium iodide (/DAPI/ AO/PI) staining

Cellular apoptosis caused by QDs was further analyzed for better understanding of the toxicity by DAPI/AO/PI (or EtBr in case of CdTe QDs in section 6.2.4) fluorescent staining on HEK-293 cells. Figure 6.3 represent the staining mechanism of cells at different stages.
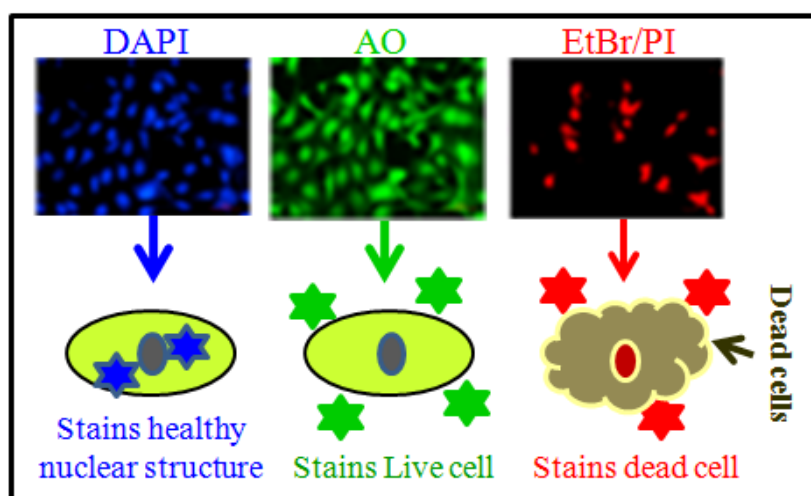
Figure 6.3: Staining mechanism for cells

Healthy normal nuclear structure were stained by DAPI with blue fluorescence while premature apoptotic cells show bright blue fluorescence with nuclear deformity, whereas, AO stains live cell (green fluorescence) (Figure 6.4(a)). PI (or EtBr in case of CdTe QDs in section 6.2.4) stains dead and necrotic cells with condensed chromatin by intense red fluorescence. This fluorescent staining was performed for different time period by taking concentration of QDs equivalent to Poly-CdSe IC_{50} value (approximately 250 µg/ml). Conclusion from this study was obtained by calculating CTCF of all QDs from cells incubated for different time period (figure 6.4 (b)). Poly-CdSe show time dependent cell apoptosis at concentration (250 µg/ml) with highest cytotoxicity. It was also noted that apoptotic cells get increased in CdSe-QDs with prolonged time of incubation. It was justified from CTCF count that CdSe/ZnS, CdSe/TEOS, CdSe/PVA and CdSe/PEG did not show any indication of cell morphological damage for different incubation period. Whereas, minor increase in CTCF is accredited to natural cell death as observed from figure 6.4(b). These observations authenticated that encapsulation of CdSe

QDs prevent the additional reactions and decreases the cytotoxicity as compared with poly-CdSe and bare CdSe-QDs.
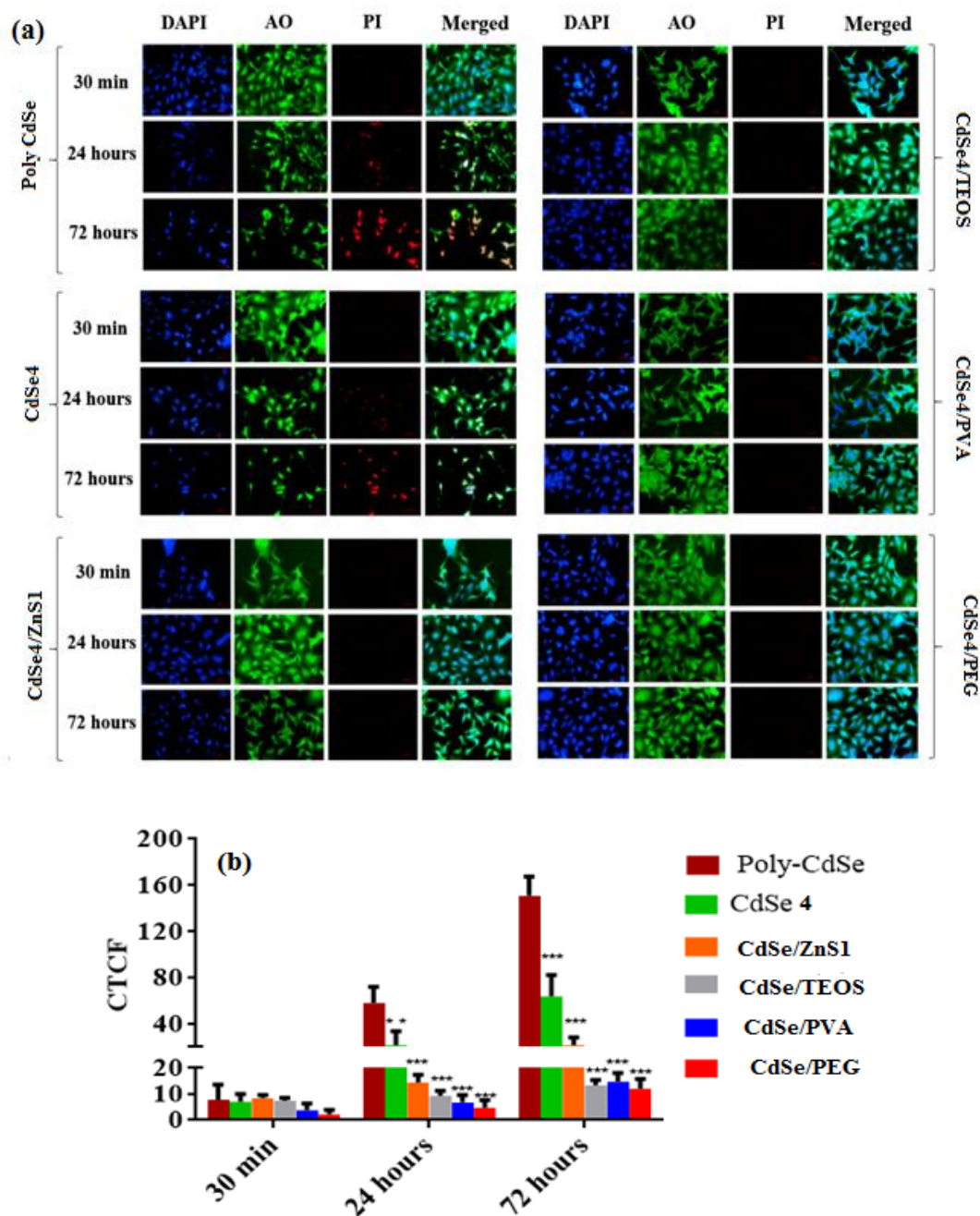
Figure 6.4: (a) Cellular apoptosis as an effect of QDs treatment at different time periods. The scale bar of images corresponds to 50μm (200X) (b) Graph represents the collective total cell fluorescence ratio for red fluorescence indicating dead PI stained cells.* signify $p < 0.05$, ** signify $p < 0.01$ and *** signify $p < 0.001$ when fluorescent intensity compared with Poly-CdSe

6.2.3 Cell cytotoxicity of CdTe based nanostructures

On the basis of results obtained for CdSe based nanostructures we have performed cytotoxicity study of CdTe based nanostructures for 24 hours. Because results for 24 hours of viability studies in case of CdTe based nanostructures were adequate to give enough information based on stupendous reduction in cell viability for CdSe based nanostructures. Therefore, reduction in cell viability was enough prominent at 24 h of incubation for note worthy interpretation in CdTe nanostructures.

As depicted in figure 6.5, QDs showed the concentration dependent decline in the cells viability. Poly/CdTe exhibited most toxic effect on the cells with IC_{50} of 6.95 µg/ml, whereas CdTe2 represented IC_{50} 8.27 µg/ml. After successful mounting of QDs with PVA, PEG and TEOS we witnessed decline in the toxic effects, where, PEG was found to be least toxic (IC_{50} values =548.08µg/ml). PVA and TEOS have IC_{50} values of 306.55 µg/ml and 129.30 µg/ml respectively (Table 6.2). Cytotoxicity studies of CdTe based nanostructures clarify that Poly CdTe and CdTe QDs are showing toxic effect due to leakage of toxic Cd^{2+} and Se^{2-} while encapsulation of CdTe QDs by polymers and silicates thwarts the leakage of these toxic heavy metals. This surface interaction play important role in trim down the toxic effect of CdTe based nanostructures.

Table 6.2: Showing individual IC_{50} value for poly CdTe, CdTe and encapsulated structures

Sr.No	Sample	IC_{50} Value
1	Poly CdTe	6.95
2	CdTe2	8.27
3	CdTe2/ PVA	306.55
4	CdTe2/PEG	548.08
5	CdTe2/TEOS	129.30
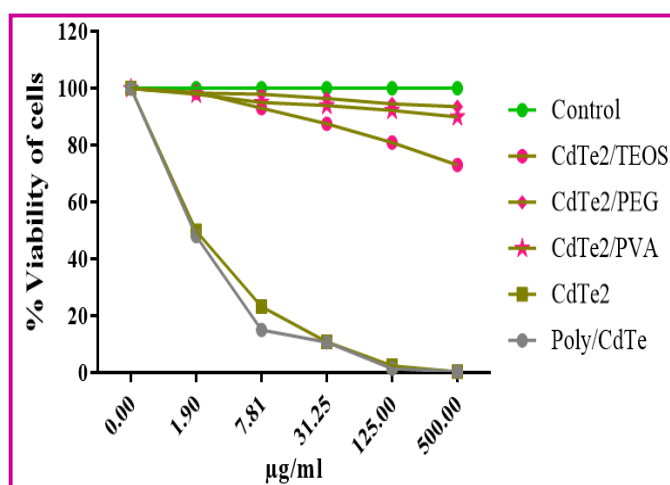
Figure 6.5: Viability of HEK-293 cells after treatment with synthesized CdTe QDs at different concentrations for 24 hrs

6.2.4 Fluorescent staining to explore cellular apoptosis in case of CdTe based nanostructures: Acridine orange and Ethidium bromide (AO/EtBr) staining

Cellular apoptosis caused by CdTe QDs was further investigated for worthier understanding of the toxicity by AO/EtBr fluorescent staining on HEK-293 cells. AO stains live as well as dead cells (green fluorescence). EtBr stains specifically necrotic and dead cells with condensed chromatin exhibiting bright red fluorescence (Figure 6.6). To perform this study, concentration of the QDs were taken equivalent to poly CdTe IC_{50} value (approximately 7 µg/ml). As presented in Figure 6.6. Poly/CdTe exhibited cell apoptosis at the selected concentration (7 µg/ml) with maximum cytotoxic followed by CdTe2. In contrast, other synthesized QDs did not showed any sign of cell morphological damage.
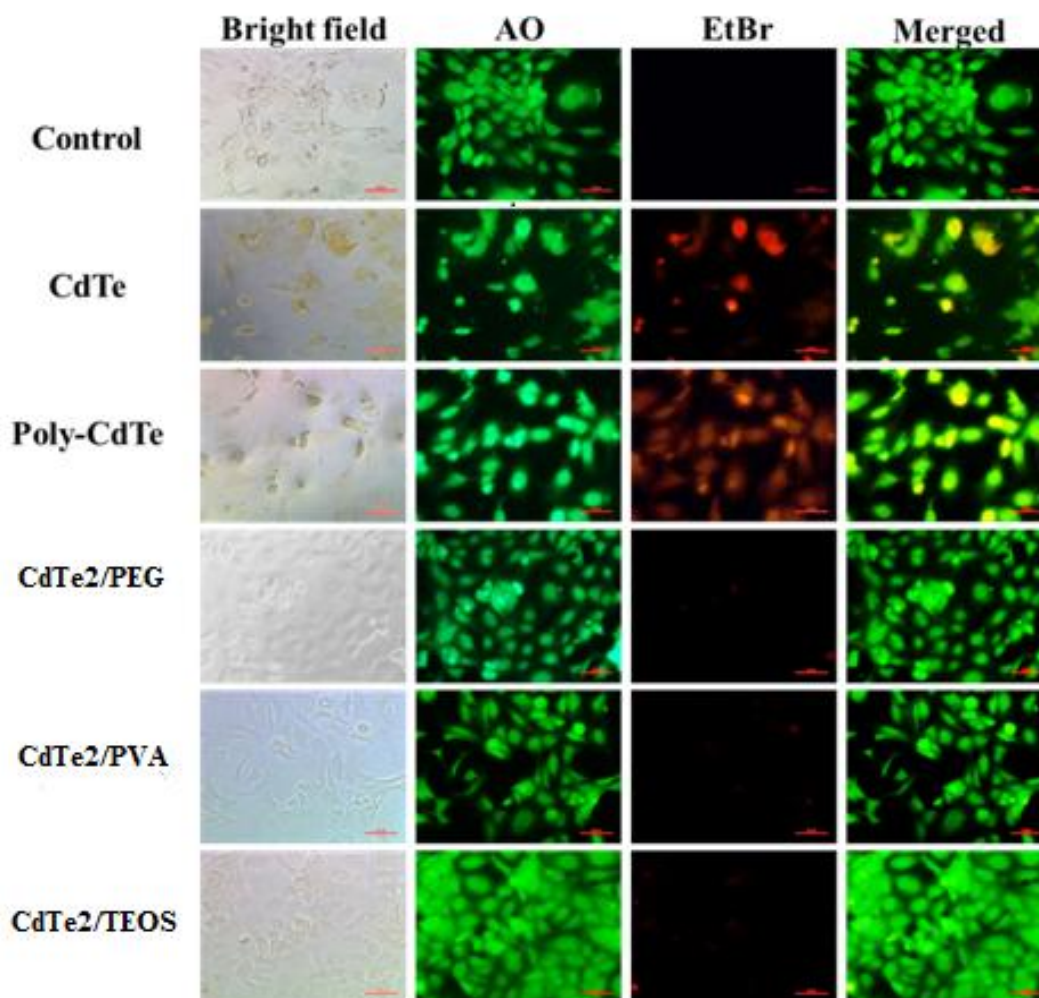
Figure 6.6: Showing cellular apoptosis as an effect of QDs treatment and staining assay on HEK-293 cell line

6.3 Introduction to antimicrobial behavior

Quantum dots are considered as fine applicant to replace traditional irritant and toxic organic antimicrobial agents because of their large surface area and small size [38, 39]. Previously use of metal nanoparticles has been well described to show good antimicrobial activity toward Gram-positive and Gram-negative bacteria stains [40]. However QDs have stunning photostability, brilliant photoluminescence, narrow emission, and broad absorption spectra in addition to antimicrobial activity [41]. Owing to these exceptional features QDs could be applied in lots of biological applications like in cell imaging, biosensors [42]. Luminescent behavior of QDs plays significant role in studying complex microbial populations and recognition of bacteria. Single bacterial imaging through probe-conjugated QDs is one of the main practicable research areas in biological applications [43]. Due to broad probable applications of QDs, they were planned for antimicrobial activities. QDs mostly contain Pb, Cd, Te, Se etc heavy metal and release of these heavy metals cause toxicity to bacteria [44]. In earlier reports different rationale for antimicrobial behavior of QDs was elucidated by different research groups. Prior studies have accredited the free radicals formation to play chief role in antibacterial activity [45-47]. Sunlight generated photo-toxicity and high intensity lamps release toxic metal ions (Cd^{2+}) which show toxicity to the bacteria [48, 49].

6.3.1 Antimicrobial activity of compounds of CdSe based core shell material

Present section is focused on studies for antimicrobial activity of prepared poly CdSe, CdSe4 QDs and their core-shell structures against different pathogen bacteria to state the utilization of these fluorescent probes in bacterial studies. Kirby Bauer's disk diffusion method was used to confirm antimicrobial behavior for compounds A and F which are having effective antibacterial activity against gram negative pathogens (Table3). QDs whose antimicrobial study was carried out were referred as compound A-CdSe4, Compound B-ZnS1, Compound C-ZnS2, Compound D-CdSe4/ZnS1, compound E-CdSe4/ZnS2 and compound F-poly CdSe respectively. *E. coli* strains cause intestinal as well as extra-intestinal infectivity [50]. Another pathogen which we use in our study is *Acinetobacter baumannii* which is regarded as foremost cause of nosocomial pathogen, these results in wide range of blood, respiratory, skin and soft tissue infections. In recent times, *A. baumannii* has been listed as the chief multidrug resistant bacteria among hospital settings by World Health Organization.

There was clear formation of circular zones of lysis for compound A and control antibiotics against reference strains against *E.coli* in figure 6.7 (a). Antimicrobial activity of compound A against *Acinetobacter baumannii* is shown in figure 6.7 (b). Both of these figures clarify that compound A have good antimicrobial activity against *E.coli* but no antimicrobial activity was observed against *Acinetobacter baumannii*. Similarly figure 6.7 (f) and (g) displays zone of lysis for compound F against *E.coli* and *Acinetobacter baumannii* respectively. Observed zones of inhibition for all compounds in mm are presented in Table 6.3 and it was concluded from this Table 6.3 that compound A and F show good antimicrobial activity. On the other hand no zone lysis values were attained for compounds B, C, D and E demonstrate that these compounds does not inhibit growth of E.coli and *Acinetobacter baumannii*. Figure 6.7 (c, d and e) clarify that there was no formation of zone of lysis in compound B and compound D for *Acinetobacter baumannii* and for *E.coli* respectively. The difference in size of zone of inhibition between all QDs could be linked to elemental composition, surface modification, particles size and different diffusion tendency of QDs with cell wall. Difference in the size and binding tendency of QDs to cell wall is also responsible for this kind of observations.

Table 6.3: Antimicrobial susceptibility tests of compounds against gram negative pathogens

Concentration of compounds in μg/ml	Zone of lysis in mm											
	Compound CdSe4		Compound ZnS1		Compound ZnS2		Compound CdSe4/ZnS 1		Compound CdSe4/ZnS 2		Compound Poly CdSe	
	E. coli	*A. baumannii*	*E. coli*	*A. baumannii*	*E. coli*	*A. baumannii*	*E. coli*	*A. baumannii*	*E. coli*	*A. baumannii*	*E. coli*	*A. baumannii*
1024	29	-	-	-	-	-	-	-	-	-	20	25
512	16	-	-	-	-	-	-	-	-	-	17	23
256	13	-	-	-	-	-	-	-	-	-	15	21
128	12	-	-	-	-	-	-	-	-	-	12	19
64	10	-	-	-	-	-	-	-	-	-	-	17
32	-	-	-	-	-	-	-	-	-	-	-	16

Elemental composition of CdSe4 QDs and poly CdSe was very toxic due to heavy metals which were confirmed from EDX. Because of this toxic composition of CdSe4 QDs they show good antimicrobial activity. As compare to CdSe4 and poly CdSe, ZnS1 and ZnS2 QDs do not show any sign of antimicrobial activity means no formation of zone of inhibition in ZnS1 and ZnS2 (Table 6.3). Bactericidal performance of CdSe4 QDs has also been accredited to their small size in contrast to ZnS1 and ZnS2. Smaller size of CdSe4 QDs has been confirmed from XRD and TEM analysis as compare to ZnS1 and ZnS2.

Likewise CdSe/ZnS1 and CdSe/ZnS2 do not confirms any antimicrobial activity because of increase in size on shell formation. This shell creation on core CdSe4 also stops leakage of heavy toxic metal and prevent photo oxidation of core material. Beside with all these reasons difference in size of zone of inhibition between QDs was linked to diffusion tendency of QDs with cell wall. Luminescent QDs which are not having antimicrobial activity are biocompatible includes compound B-ZnS1, Compound C-ZnS2, Compound D-CdSe/ZnS1, compound E-CdSe/ZnS2 and these can be employed to study the microbial population and for recognition of bacteria by conjugating with a probe. This bacterial imaging by probe-conjugated QDs is one of the most feasible study areas in biological applications.
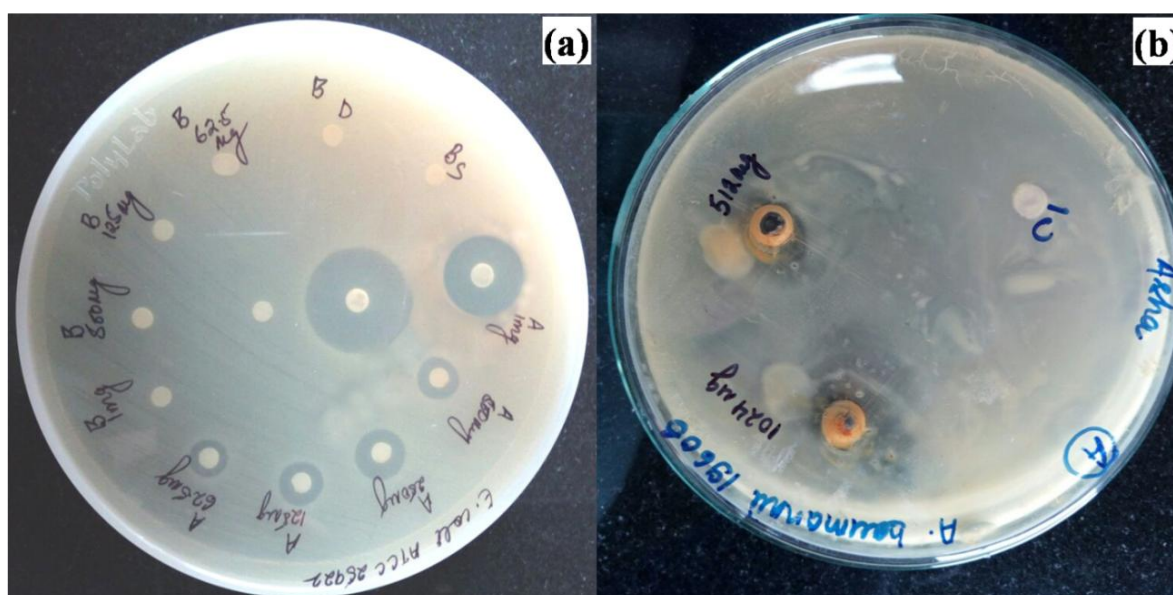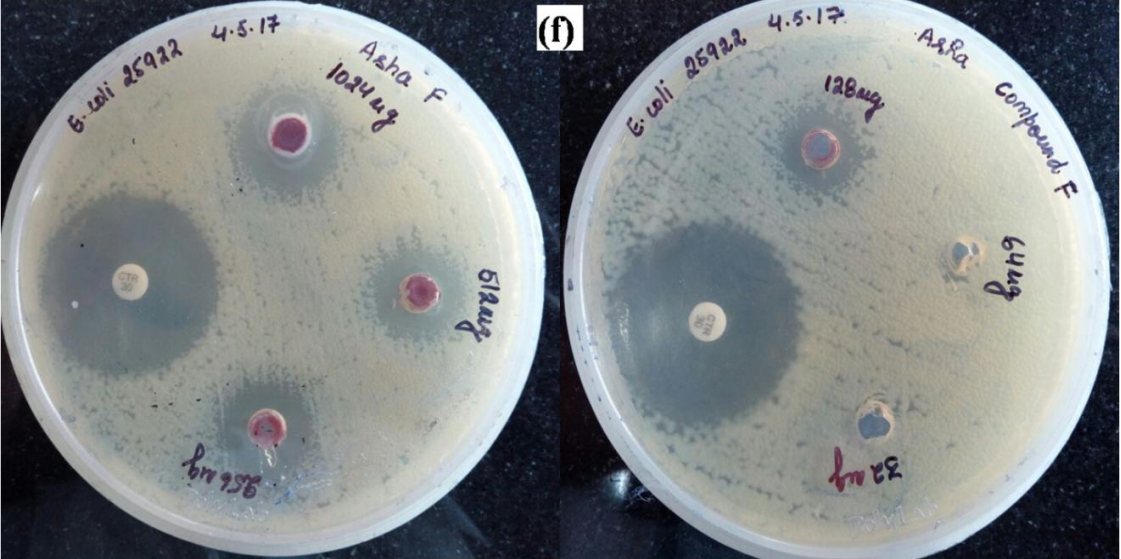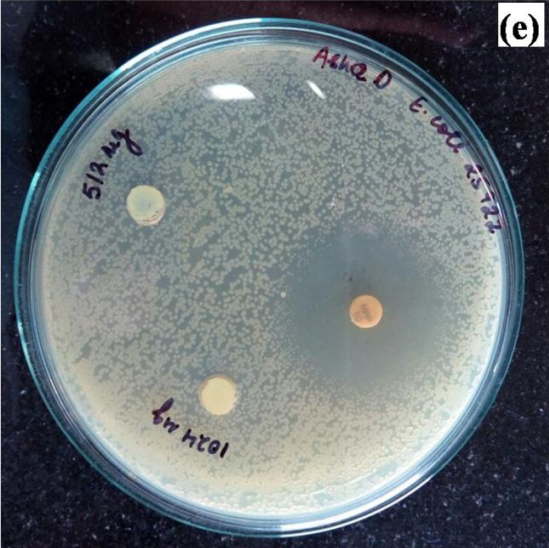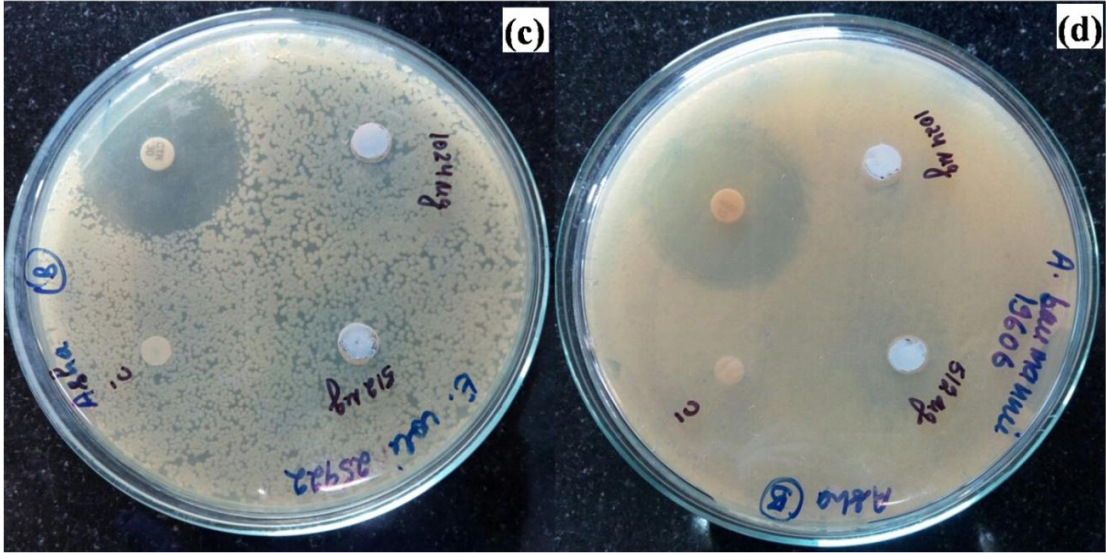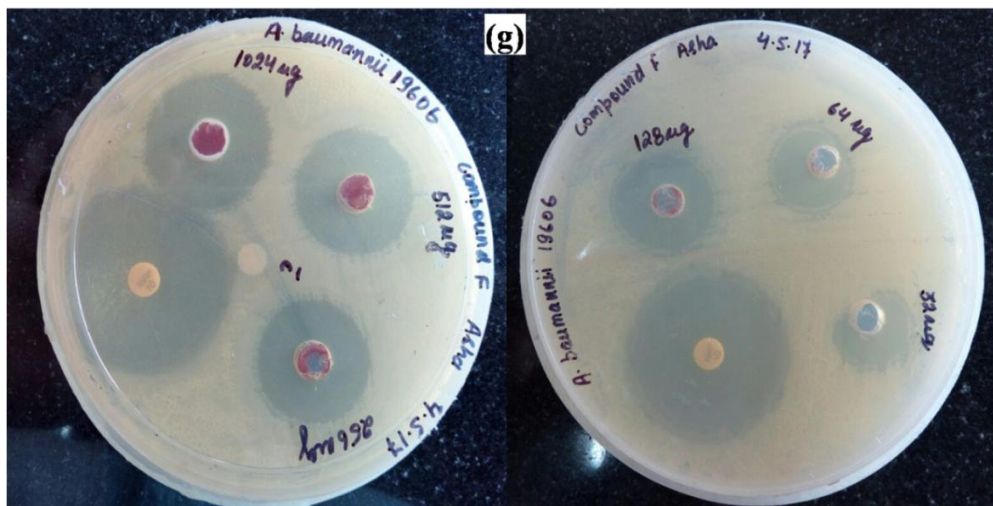
Figure 6.7 : Antimicrobial results for synthesized compound A against (a) *E. coli* (b) *A.baumannii* (c) *Compound* B against *E. coli* (d) Compound D against *A.baumannii* (e) Compound D against *E. coli* (f) Compound F against *E. coli and* (g) Compound F against *A.baumannii.* 1= Meropenem (10 mcg), 2= Cotrimoxazole (25 mcg)

6.3.2 Antimicrobial activity of compounds of CdTe based materials

Present section includes antimicrobial results of prepared poly CdTe, CdTe2, CdTe2/PEG, CdTe2/PVA and CdTe2/TEOS against *E.coli* and *S. aureus*. *S. aureus* cause skin and soft tissue infections and *E.coli* is responsible for intestinal infections.

Figure 6.8 (a) clarifies that there was no zone of lysis for *E.coli* in case of all the compounds. These all compounds were also not showing any zone of lysis for *S.aureus* (Figure 6.8 (b)). It is possible to get antimicrobial activity of these CdTe based compounds by varying concentrations. But unlike CdSe these CdTe based compound are not showing antimicrobial activity this may be due to the different stabilizers have been used for synthesis of CdSe and CdTe based compounds. As CdSe was synthesized by using 2-mercaptoethanol (2-ME) contains two carbon chains while CdTe is synthesized by using 3-mercaptopropionic acid contains 3 carbon chains. This 3-MPA in case of CdTe may be sufficiently preventing leakage of cadmium and tellurium by strengthening the bonding between Cd and Te. One more possible reason as we have already discussed that this may be due to difference in interaction of these compounds with bacterial cell wall. This antimicrobial behavior previously also has been related to shape and size of nanomaterials. But these CdTe based compounds are fluorescent in nature and due to this they can be used for bacterial imaging by probe-conjugated QDs.

Figure 6.8: (a) Representing image suggesting the effect of formulated QDs on gram-negative bacteria

(b) Representing image suggesting the effect of formulated QDs on gram-positive bacteria

6.4 Conclusion

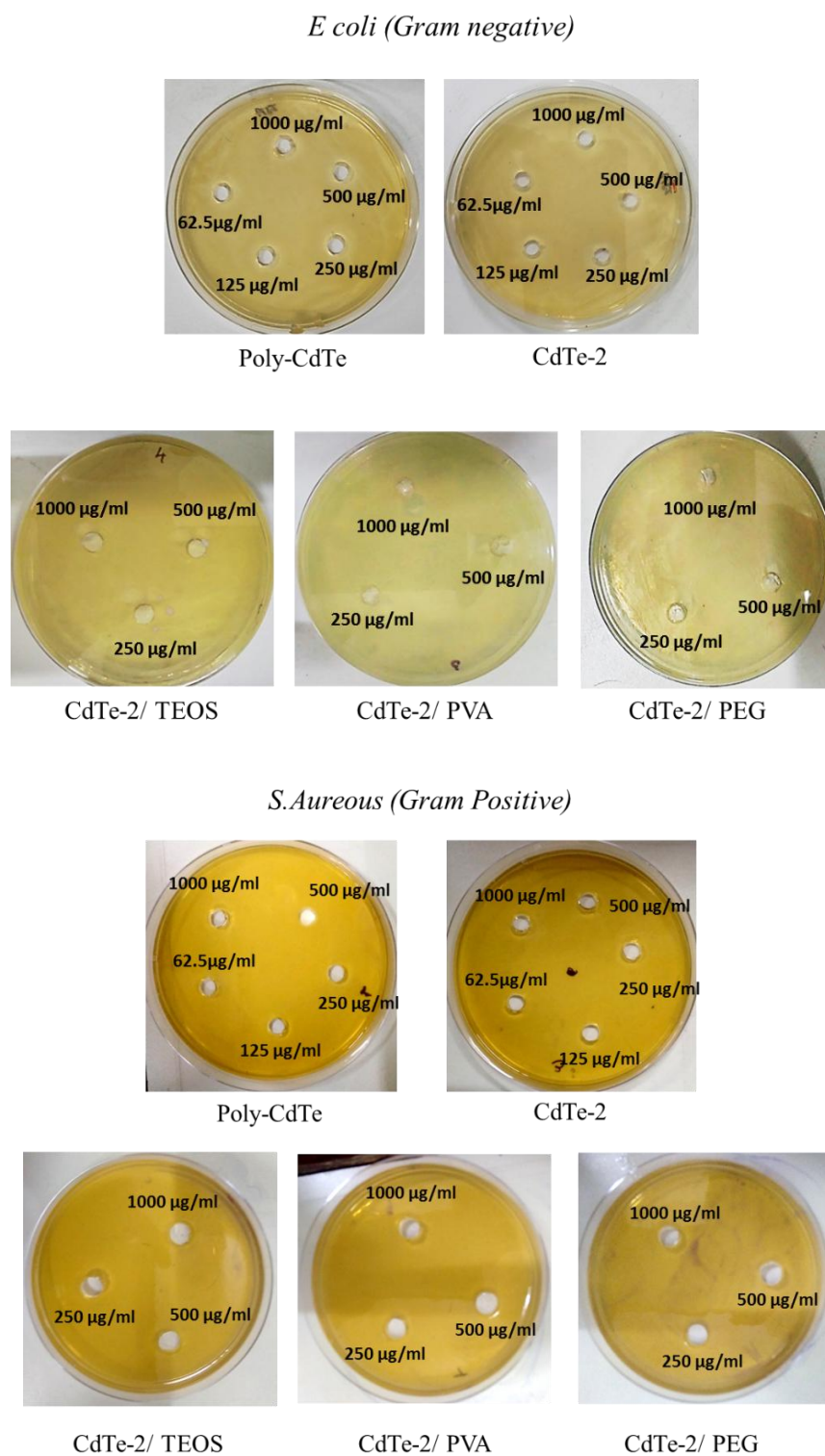Cytotoxicity concern of CdSe based and CdTe based nanostructure was systematically studied and assessed. For CdSe based nanostructures poly CdSe and CdSe4 QDs were found highly toxic. High toxicity of poly CdSe and CdSe4 QDs was because of release of toxic ions. In comparison with encapsulated QDs, encapsulated CdSe based QDs are nontoxic still at very high concentrations and long incubation time of 24 hours and even up to 72 hours of incubation. Non toxic nature of encapsulated CdSe QDs is probably due to occurrence of layer on CdSe QDs. This layer prevents degradation of QDs and release of toxic ions. CdSe QDs encapsulated with polymers did not show any sign of cell morphological injure which was defensible through CTCF count at different time periods of incubation. Out of all synthesized QDs, QDs which are capped with PVA and PEG are highly biocompatible. As we intended to make exceedingly luminescent and defect free biocompatible CdSe QDs the results attained for CdSe4/PEG-QD are best for both and these can be used as luminescent probes for bioimaging applications. In case of CdTe QDs reduction in cell viability was enough prominent at 24 h of incubation. These QDs like CdSe also showed the concentration dependent decline in the cells viability. Poly CdTe exhibited most toxic effect on the cells with IC50 of 6.95 µg/ml, whereas CdTe2 represented IC_{50} 8.27 µg/ml. After successful encapsulation of QDs with PVA, PEG and TEOS we witnessed decline in the toxic effects, where, PEG was found to be least toxic (IC_{50} values =548.08µg/ml). PVA and TEOS exhibited IC_{50} values of 306.55µg/ml and 129.30 µg/ml respectively.

Kirby Bauer's disk diffusion method was used to study antimicrobial behavior of prepared QDs against *Escherichia coli* ATCC 25922 and *Acinetobacter baumannii* ATCC 19606. Out of all these samples because of toxic composition Poly CdSe and CdSe QDs were showing fine antimicrobial activity. *A. baumannii* is multidrug resistant bacteria the antimicrobial activity of poly CdSe can be a breach. While other compounds like ZnS1 and ZnS2 QDs do not show any antimicrobial activity. This has been credited to small size of CdSe in contrast to ZnS1 and ZnS2. CdSe/ZnS1 and CdSe/ZnS2 were also found non-antimicrobial and this happens because of shell formation. This shell prevents seepage of toxic metal from CdSe. PL spectra of these samples reported in previous chapters confirmed the fluorescent behavior of these QDs. Similarly antimicrobial behavior of CdTe based compounds was studied by agar well diffusion method. These CdTe based compounds are not showing any zone of lysis although

these are fluorescent in nature. So these fluorescent QDs which have no antimicrobial activity, these are biocompatible confirmed from FTIR. These can be utilized for bacterial imaging by probe-conjugated QDs.

6.5 References

1. Gill R., Zayats M., Willner I., *"Semiconductor quantum dots for bioanalysis",* Angewandte Chemie International Edition, vol. 47(40), pp. 7602-7625, Sep. 2008.

2. Kamat P.V., *"Quantum dot solar cells. The next big thing in photovoltaics",* The Journal of Physical Chemistry Letters, vol. 4(6), pp. 908-918, Mar. 2013.

3. Walling M.A., Novak J.A., Shepard J.R., *"Quantum dots for live cell and in vivo imaging",* International journal of molecular sciences, vol. 10(2), pp. 441-491, Feb. 2009.

4. Rothenfluh D.A., Bermudez H., O'Neil C.P., Hubbell J.A., *"Biofunctional polymer nanoparticles for intra-articular targeting and retention in cartilage",* Nature materials, vol. 7(3), pp. 248, Mar. 2008.

5. Kostarelos K., Bianco A., Prato M., *"Promises, facts and challenges for carbon nanotubes in imaging and therapeutics",* Nature nanotechnology, vol. 4(10), pp. 627, Oct. 2009.

6. Resch-Genger U., Grabolle M., Cavaliere-Jaricot S., Nitschke R., Nann T., *"Quantum dots versus organic dyes as fluorescent labels",* Nature methods, vol. 5(9), pp. 763, Sep. 2008.

7. Rockenberger J., Tröger L., Rogach A.L., Tischer M., Grundmann M., Eychmüller A.,Weller H., *"The contribution of particle core and surface to strain, disorder and vibrations in thiolcapped CdTe nanocrystals",* The Journal of chemical physics, vol. 108(18), pp. 7807-7815, May 1998

8. Borchert H., Talapin D.V., Gaponik N., McGinley C., Adam S., Lobo A., Weller H., *"Relations between the photoluminescence efficiency of CdTe nanocrystals and their surface properties revealed by synchrotron XPS",* The Journal of Physical Chemistry B, vol. 107(36), pp. 9662-9668, Sep. 2003.

9. Murray C.B., Nirmal M., Norris D.J., Bawendi M.G., *"Synthesis and structural characterization of II–VI semiconductor nanocrystallites (quantum dots)",* Zeitschrift für Physik D Atoms, Molecules and Clusters, vol. 26(1), pp. 231-233, Mar. 1993.

10. Chen N., He Y., Su Y., Li X., Huang Q., Wang H., Fan C., *"The cytotoxicity of cadmium-based quantum dots",* Biomaterials, vol. 33(5), pp. 1238-1244, Feb. 2012.

11. Kumari A., Singh R.R., *"Encapsulation of highly confined CdSe quantum dots for defect free luminescence and improved stability",* Physica E: Low-dimensional Systems and Nanostructures, vol. *89*, pp. 77-85, May 2017.

12. Owens S.A., Carpenter M.C., Sonne J.W., Miller C.A., Renehan J.R., Odonkor C.A., Miles D.T., *"Reversed-phase HPLC separation of water-soluble, monolayer-protected quantum dots",* The Journal of Physical Chemistry C, vol. 115(39), pp. 18952-18957, Sep. 2011.

13. Su Y., Hu M., Fan C., He Y., Li Q., Li W., Huang Q., *"The cytotoxicity of CdTe quantum dots and the relative contributions from released cadmium ions and nanoparticle properties",* Biomaterials, vol. 31(18), pp. 4829-4834, June 2010.

14. Hoshino A., Fujioka K., Oku T., Suga M., Sasaki Y.F., Ohta T., Yamamoto K., *"Physicochemical properties and cellular toxicity of nanocrystal quantum dots depend on their surface modification",* Nano Letters, vol. 4(11), pp. 2163-2169, 2004.

15. Hoshino A., Hanada S., Yamamoto K., *"Toxicity of nanocrystal quantum dots: the relevance of surface modifications",* Archives of toxicology, vol. 85(7), pp. 707, July 2011.

16. Tan S.J., Jana N.R., Gao S., Patra P.K., Ying J.Y., *"Surface-ligand-dependent cellular interaction, subcellular localization, and cytotoxicity of polymer-coated quantum dots",* Chemistry of Materials, vol. 22(7), pp. 2239-2247, Feb. 2011.

17. Rzigalinski B.A., Strobl J.S., *"Cadmium-containing nanoparticles: perspectives on pharmacology and toxicology of quantum dots",* Toxicology and applied pharmacology, vol. 238(3), pp. 280-288, Aug. 2009.

18. Contreras E.Q., Cho M., Zhu H., Puppala H.L., Escalera G., Zhong W., Colvin V.L., *"Toxicity of quantum dots and cadmium salt to Caenorhabditis elegans after multigenerational exposure",* Environmental science & technology, vol. 47(2), pp. 1148-1154, Dec. 2012.

19. Wang L., Zheng H., Long Y., Gao M., Hao J., Du J., Zhou D., *"Rapid determination of the toxicity of quantum dots with luminous bacteria",* Journal of hazardous materials, vol. 177(1-3), pp. 1134-1137, May 2010.

20. Kim J., Sakthivel K., Choi H.J., Joo W.H., Shin S.K., Lee, M.J., Lee, Y.I., *"Highly fluorescent CdTe quantum dots with reduced cytotoxicity-A Robust biomarker",* Sensing and Bio-Sensing Research, vol. 3, pp. 46-52, Mar. 2015.

21. Kirchner C., Javier A.M., Susha A.S., Rogach A.L., Kreft O., Sukhorukov G.B., Parak W.J., *"Cytotoxicity of nanoparticle-loaded polymer capsules",* Talanta, vol. 67(3), pp. 486-491, Sep. 2005.

22. Bruchez M., Moronne M., Gin P., Weiss, S., Alivisatos A.P., *"Semiconductor nanocrystals as fluorescent biological labels",* Science, vol. 281(5385), pp. 2013-2016, Sep. 1998.

23. Chan W.C., Nie S., *"Quantum dot bioconjugates for ultrasensitive nonisotopic detection",* Science, vol. 281(5385), pp. 2016-2018, Sep.1998.

24. Manzoor K., Johny S., Thomas D., Setua S., Menon D., Nair S., *"Bio-conjugated luminescent quantum dots of doped ZnS: a cyto-friendly system for targeted cancer imaging",* Nanotechnology, vol. 20(6), pp. 065102, Jan. 2009.

25. Shiohara A., Hoshino A., Hanaki K.I., Suzuki K., Yamamoto K., *"On the cyto-toxicity caused by quantum dots Microbiology and immunology",* vol. 48(9), pp. 669-675, Sep. 2004.

26. Lovrić J., Bazzi H.S., Cuie Y., Fortin G.R., Winnik F.M., Maysinger D., *"Differences in subcellular distribution and toxicity of green and red emitting CdTe quantum dots",* Journal of Molecular Medicine, vol. 83(5), pp. 377-385, May 2005.

27. Hoshino A., Fujioka K., Oku T., Suga M., Sasaki Y.F., Ohta T., Yamamoto K., *"Physicochemical properties and cellular toxicity of nanocrystal quantum dots depend on their surface modification",* Nano Letters, vol. 4(11), pp. 2163-2169, Nov. 2004.

28. Derfus A.M., Chan W.C., Bhatia S.N., *"Probing the cytotoxicity of semiconductor quantum dots",* Nano letters, vol. 4(1), pp. 11-18, Jan. 2004.

29. Kirchner C., Liedl T., Kudera S., Pellegrino T., Muñoz Javier A., Gaub H.E., Parak W.J., *"Cytotoxicity of colloidal CdSe and CdSe/ZnS nanoparticles Nano letters",* vol. 5(2), pp. 331-338, Feb. 2005.

30. Ray P.C., Yu H., Fu P.P., *"Toxicity and environmental risks of nanomaterials: challenges and future needs"* Journal of Environmental Science and Health Part C, vol. 27(1), pp. 1-35, Feb. 2009.

31. Soenen S.J., Manshian B., Montenegro J.M., Amin F., Meermann B., Thiron T., De Smedt S., *"Cytotoxic effects of gold nanoparticles: a multiparametric study",* ACS nano, vol. 6(7), pp. 5767-5783, June 2012.

32. Gerbec J.A., Magana D., Washington A., Strouse G.F., *"Microwave-enhanced reaction rates for nanoparticle synthesis",* Journal of the American Chemical Society, vol. 127(45), pp. 15791-15800, Nov. 2005.

33. Li L., Qian H., Ren J., *"Rapid synthesis of highly luminescent CdTe nanocrystals in the aqueous phase by microwave irradiation with controllable temperature",* Chemical Communications, vol. (4), pp. 528-530 2005.

34. He H., Qian H., Dong C., Wang K., Ren J., *"Single nonblinking CdTe quantum dots synthesized in aqueous thiopropionic acid",* Angewandte Chemie, vol. 118(45), pp. 7750-7753, Nov. 2006.

35. Rogach A.L., Franzl T., Klar T.A., Feldmann J., Gaponik N., Lesnyak V., Donegan J. F., *"Aqueous synthesis of thiol-capped CdTe nanocrystals: state-of-the-art",* The Journal of Physical Chemistry C, vol. 111(40), pp. 14628-14637, Oct. 2007.

36. Su Y., He Y., Lu H., Sai L., Li Q., Li W., Fan C., *"The cytotoxicity of cadmium based, aqueous phase–synthesized, quantum dots and its modulation by surface coating",* Biomaterials, vol. 30(1), pp. 19-25.Jan. 2009.

37. Bhanoth S., Kshirsagar A.S., Khanna P.K., Tyagi A., Verma A.K., "Biotoxicity of CdS/CdSe Core-Shell Nano-Structures", Advances in Nanoparticles, vol. 5(01), pp. 1, Feb. 2016.

38. Klaine S.J., Alvarez P.J., Batley G.E., Fernandes T.F., Handy R.D., Lyon D.Y., Lead J.R. *"Nanomaterials in the environment: behavior, fate, bioavailability, and effects"*, Environmental toxicology and chemistry*", vol. 27(9), pp. 1825-1851, Sep. 2008.

39. Lee D., Cohen R.E., Rubner M.F., *"Antibacterial properties of Ag nanoparticle loaded multilayers and formation of magnetically directed antibacterial microparticles"*, Langmuir, vol. 21(21), pp. 9651-9659, Oct. 2005.

40. Adams L.K., Lyon D.Y., Alvarez P.J., *"Comparative eco-toxicity of nanoscale TiO2, SiO2, and ZnO water suspensions"*, Water research, vol. 40(19), pp. 3527-3532, Nov. 2006.

41. Constantine C.A., Gattás-Asfura K.M., Mello S.V., Crespo G., Rastogi V., Cheng T.C., Leblanc R.M., *"Layer-by-layer biosensor assembly incorporating functionalized quantum dots"*, Langmuir, vol. 19(23), pp. 9863-9867, Nov.2003.

42. Biju V., Muraleedharan D., Nakayama K.I., Shinohara Y., Itoh T., Baba Y., Ishikawa M., *"Quantum dot-insect neuropeptide conjugates for fluorescence imaging, transfection, and nucleus targeting of living cells"*, Langmuir, vol. 23(20), pp.10254-10261, Sep. 2007.

43. Voura E.B., Jaiswal J.K., Mattoussi H., Simon S.M., *"Tracking metastatic tumor cell extravasation with quantum dot nanocrystals and fluorescence emission-scanning microscopy"*, Nature medicine, vol. 10(9), pp. 993, Sep. 2004.

44. Park S., Chibli H., Wong J., Nadeau J.L., *"Antimicrobial activity and cellular toxicity of nanoparticle–polymyxin B conjugates"*, Nanotechnology, vol. 22(18), pp. 185101, Mar. 2011.

45. Wei C., Lin W.Y., Zainal Z., Williams N.E., Zhu K., Kruzic A.P., Rajeshwar K., *"Bactericidal activity of TiO2 photocatalyst in aqueous media: toward a solar-assisted water disinfection system"*, Environmental science & technology, vol. 28(5), pp. 934-938, May 1994.

46. Hajkova P., Patenka P.S., Horsky J., Horska I., Kolouch A., *"Antiviral and antibacterial effect of photocatalytic TiO2 films"*, In Tissue Engineering, vol. 13, pp. 908-908, Apr. 2007.

47. Ipe B.I., Lehnig M., Niemeyer C.M., *"On the generation of free radical species from quantum dots"*, Small, vol. 1(7), pp. 706-709, July 2005.

48. Dumas E.M., Ozenne V., Mielke R.E., Nadeau J.L., *"Toxicity of CdTe quantum dots in bacterial strains",* IEEE transactions on nanobioscience, vol. 8(1), ;pp. 58-64, Mar. 2009.

49. Dumas E., Gao C., Suffern D., Bradforth S.E., Dimitrijevic N.M., Nadeau J.L., *"Interfacial charge transfer between CdTe quantum dots and gram negative vs gram positive bacteria",* Environmental science & technology, vol. 44(4), pp. 1464-1470, Jan. 2010.

50. Nataro J.P., Kaper J.B., *"Diarrheagenic escherichia coli.",* Clinical microbiology reviews, vol. 11(1), pp. 142-201, Jan. 1998.

CHAPTER-7

SUMMARY AND FUTURE SCOPE

7.1 Summary

Aim of our thesis was to synthesize visible and NIR QDs for imaging purpose and processing of the surface of these QDs to make them biocompatible and nontoxic. So in conclusion Visible and NIR emitting QDs have been synthesized successfully by wet chemical aqueous route. These synthesized QDs are CdSe1, CdSe2, CdSe4, ZnS1, ZnS2, CdSe/ZnS1, CdSe/Zns2, CdTe1, CdTe2, CdTe3 and polymer encapsulated structures like CdSe4/PEG, CdSe4/PVA, CdSe4/TEOS and CdTe2/PEG, CdTe2/PVA and CdTe2/TEOS. Introduction to the visible QDs and NIR QDs and other important concepts were briefly presented in Chapter1. Chapter2 stepwise described the synthesis procedure and characterization techniques. It is concluded from chapter 2 that all the visible and NIR QDs are successfully synthesized by wet chemical aqueous route. After this chapter 3, 4, 5 and 6 presents the results obtained for these QDs.

It is concluded from chapter 3 that concentration of stabilizing agent i.e., 2-ME playing an important role in controlling the particle size of CdSe QDs. High concentration of 2-ME reduces size of CdSe and directly related to trap states. Origin of trap states in small CdSe QDs originated due to hole scavenging property of thiol group of 2-ME. Surface encapsulation of CdSe QDs by polymer and silicates improve optical properties of CdSe QDs confirmed from PL spectra of these QDs. The all set QDs were characterized by XRD, TEM, EDX, absorbance spectroscopy, photoluminescence spectroscopy and FTIR. Photoluminescence spectroscopy reveals that CdSe QDs are of very small size having band edge emission at 480 nm along with defect emission. This study confirms that thiol content is responsible for trap emission afar a particular concentration of 2-ME. These results have been also supported by from EDX analysis. Other possible reason of trap emission was occurrence of dangling bonds, high surface/volume ratio or furthermore may be due to selenium vacancies. PL studies conspicuously exposed that QDs encapsulated with polymers show dazzling emission intensity with whole removal of trap emission. Polymer encapsulated QDs were found to posses stupendous aqueous dispersibility better trap free band edge emission intensity and superior fluorescence stability. After this

conclusion we have tried ZnS shell over CdSe QDs. So firstly we synthesized ZnS1 and ZnS2 by different precursor. On the basis of these results we formed shell over CdSe. Results obtained for these QDs and core-shell structures are presented in chapter 4.

Chapter 4 concludes changed optical properties of ZnS and CdSe/ZnS core-shell structures on the basis of reactivity of precursor. Size of these QDs also gets affected based on precursor reactivity. XRD confirmed that particle size of ZnS1 was larger than ZnS2. Optical investigation of QDs verify that precursor used to synthesize ZnS1 and ZnS2 affect the band edge and defect emission positions. Band edge emission for ZnS1was found at 337 nm alongside with few defects at 427, 486 nm, while in Zns2 band edge emission was at 384 along with defects at 422, 445, 486 nm and 529 nm. Optical studies concludes that ZnS1 synthesized by $ZnSO_4.7H_2O$ have less defects as compared to ZnS2. From all these studies it has been concluded that reactivity of precursor effect the particle size as well as optical properties. In case of core-shell structures it is found on comparison of PL spectra of CdSe and CdSe/ZnS that there is improvement in intensity on shell formation with reduction in defect, although these defects were not removed completely on shell formation. In case of bare CdSe QDs intensity of band edge luminescence is almost analogous to defect luminescence. But in core-shell CdSe-QDs structures band edge emission is prominent as compared to defect luminescence and this is due to smoothening and passivation of unsatisfactory bonds on shell formation. After studying fluorescent behavior of these QDs we have worked on CdTe QDs. These QDs are NIR emitting and in future can be utilized for deep tissue imaging.

Results of CdTe base QDs are presented in chapter 5 and this concludes that capping of NIR CdTe QDs by 3-MPA controls the particles size of CdTe. This decrease in particle size leads to shift in PL emission peak position confirms that CdTe QDs are quantum confined. Trap emission position got increased with decrease in size. TEM, XRD, EDX and PL analysis confirms structural, elemental, optical properties of CdTe. From PL analysis of CdTe it was confirmed that CdTe1, CdTe 2 shows emission in NIR range. XRD spectra confirm formation of hexagonal phase of CdTe QDs. PL spectra of polymer and silicate encapsulated CdTe QDs confirm enhanced fluorescence intensity. FTIR analysis of these QDs confirm biocompatible and hydrophilic nature of these QDs. Owing to emission of these encapsulated QDs in NIR range these can be utilized for biological applications in future. After confirmation of fluorescent,

hydrophilic and biocompatible nature of QDs it was necessary to study toxic behavior of these QDs.

Chapter 6 includes the detail about toxic behavior of QDs. It is concluded from chapter 6 that CdSe based nanostructures poly CdSe and CdSe4-QDs were highly toxic. High toxicity of poly CdSe and CdSe-4 QDs was due to release of toxic ions. In comparison with encapsulated QDs, encapsulated CdSe based QDs are nontoxic still at very high concentrations and long incubation time of 24 hours and even up to 72 hours of incubation. Non toxic nature of encapsulated CdSe QDs is probably due to occurrence of layer on CdSe-QDs. This layer prevents degradation and release of toxic ions. CdSe QDs encapsulated with polymers did not show any sign of cell morphological injure which was defensible through CTCF count at different time periods of incubation. Out of all synthesized QDs, QDs which are capped with PVA and PEG are highly biocompatible. As we intended to make exceedingly luminescent and defect free biocompatible CdSe QDs the results attained for CdSe4/PEG-QD are best for both and these can be used as luminescent probes for bioimaging applications. In case of CdTe QDs reduction in cell viability was enough prominent at 24 h of incubation. These QDs like CdSe also showed the concentration dependent decline in the cells viability. Poly CdTe exhibited most toxic effect on the cells with IC_{50} of 6.95 µg/ml, whereas CdTe2 represented IC_{50} 8.27 µg/ml. After successful encapsulation of QDs with PVA, PEG and TEOS we witnessed decline in the toxic effects, where, PEG was found to be least toxic (IC_{50} values $=548.08$µg/ml). PVA and TEOS exhibited IC_{50} values of 306.55µg/ml and 129.30 µg/ml respectively.

After this we have also studied antimicrobial activity of these QDs from application point of view. Kirby Bauer's disk diffusion method was used to study antimicrobial behavior of prepared QDs against *Escherichia coli* ATCC 25922 and *Acinetobacter baumannii* ATCC 19606. Out of all these samples because of toxic composition Poly CdSe and CdSe QDs were showing fine antimicrobial activity. *A. baumannii* is multidrug resistant bacteria the antimicrobial activity of poly CdSe can be a breach. While other compounds like ZnS1 and ZnS2 QDs do not show any antimicrobial activity. This has been credited to small size of CdSe in contrast to ZnS1 and ZnS2. CdSe/ZnS1 and CdSe/ZnS2 were also found non-antimicrobial and this happens because of shell formation. This shell prevents seepage of toxic metal from CdSe. PL spectra of these samples reported in previous chapters confirmed the fluorescent behavior of

these QDs. So these fluorescent QDs which have no antimicrobial activity, these are biocompatible confirmed from FTIR. These can be utilized for bacterial imaging by probe-conjugated QDs. This work concludes that our prepared bare QDs and their encapsulated structures are fluorescent in nature. Fluorescence intensity gets improved on encapsulation. Cytotoxicity results conclude that these bare QDs are toxic while encapsulated structures are nontoxic in nature. Polymer encapsulated QDs were found hydrophilic, biocompatible and nontoxic as compare to bare QDs.

7.2 Future scope

Main points that can be incorporated to this research topic in future are:

- Encapsulation of these QDs by peptides and other biocompatible groups.
- As non toxic nature of these QDs is confirmed from *cytotoxicity* studies.
- In future these non-toxic QDs can be attached to specific biomolecule to study particular kind of cell *In-vitro.*
- Pharmaco-kinetics and pharmaco-dynamic studies of these QDs. On the basis of results of Pharmaco-kinetics and pharmaco-dynamic studies these QDs can be used in-vivo studies of cell, tumors.
- In future these QDs can be used for pathogenic detection.